Preface

Age and treachery will always overcome youth and skill. –anonymous

The electronic version of this book as well as my four earlier books are freely available at my web site[1]. At that web site, find (1) two versions, one for classroom use, the other with many unfinished loose ends; and (2) videos of me narrating this book for use in my newly "flipped" class. If you have this book in print in your hands, you have the free limited edition version of it. A final version will be sold by Some University Press.

I have had the good fortune of having excellent computer access all my professional life and the further good fortune of 47 years of continuous close association with a stream of excellent graduate students, typically a dozen at any time. From this I have prepared five textbooks, this to be the last, on the topic of geophysical data analysis. I tell the students, "We get paid to add value to data that has been collected at great expense. We do theoretical work based on the data we see; and from that theory and data we try to coax value."

In this book I have mostly avoided examples from my own field of specialization, reflection seismology, as they are covered in my earlier books, and they tend to be complicated, a competitive activity feeding an aggressive industry, the construction of 3-D subsurface landform images, an activity where it is not easy to build yourself a niche. See a touch of it here in the final chapter.

Instead, here find basic examples from wide ranging applications chosen for their diversity and for their lack of application-specific complexity, thus leading us soon to the kind of complications likely to turn up wherever you go. Young people new to building images from complicated models of data wishing to join the forefront of an established field, need help overcoming frustrations long since overcome by oldsters like me. Before jumping into the fray, they could use experience with the simpler examples in this book.

[1] http://sep.stanford.edu/sep/prof/

Acknowledgements

In this book, as in my previous books, I owe a great deal to many former students at the Stanford Exploration Project. You, my readers, are not prepared for a lengthy explication of the contributions of each of those ex-students, now colleagues. Alternately, it is not fair to show a giant list of names with no distinction between major and minor contributors. So I list them in non-alphabetical order.

Sergey Fomel converted my early F77 draft to F90 and did all the helix coding. Antoine Guitton coded and produced most of the results in Chapter 6. Otherwise I made most the illustrations in this book myself, but over time I was assisted by many other students and ex-students. These were: Bob Clapp, Morgan Brown, Jesse Lomask, Ray Abma, James Rickett, Christine Ecker, Elita (Yunyue) Li, Xukai Shen, Yang Zhang, and Daniel Rosales.

My second list of credits goes to those who substantially contributed to the infrastructure that I have depended on: Bob Clapp, Joe Dellinger, Sergey Fomel, Matthias Schwab, Stew Levin, Paul Sava, Kamal Al-Yahya, Steve Cole, Dave Nichols, Martin Karrenbach, Jenny Etgen, and Ali Almomen.

My third list of credits is to those who generously supplied data: David Sandwell (UCSD), Zvi ben Avraham (Tel Aviv), Umberto Spagnolini (Milan), Alexander Kosovichev (Stanford), Alistair Harding (UCSD), Oz Yilmaz (Western Geophysical), James Rickett (Chevron), John Toldi (Chevron), and Sheldon Breiner.

Finally, my unbounded gratitude goes to my beloved wife Diane who accepted to live with a kind of an alien. Without her continuous love and support during half a century none of my books could have existed.

July 4, 2014

Comments:

(1) - first usage of wording that can be an acronym/abbrev. should be followed by the acronym/abbrev. in paren.

(2) - hyphenation not used in prefixes with different connecting letter - only when connecting identical letters like "re-emerge"

(3) - "these" (like "this") needs a referent

Overview

The difference between theory and practice is smaller in theory than it is in practice. –folklore

This book is about the estimation and construction of geophysical images. Geophysical images are used to visualize petroleum and mineral resource prospects, for subsurface water, contaminent transport (environmental pollution), archeology, lost treasure, graves, and for simple curiosity. What does it look like inside the earth? Here we follow physical measurements from a wide variety of geophysical sounding devices to a geophysical image, a 1-, 2-, or 3-dimensional Cartesian mesh that is easily transformed to a graph, map image, or computer movie.

Beyond "simulation" the fields of geophysics, engineering, statistics, and applied mathematics include a topic called "inverse theory" which concerns the reverse — fitting models to data. The bulk of this theory is based on the idea that data contains noise. Our data is good data. Reality in science, geophysics, and research engineering is that misfit means the data contains information the model is not cognizant of. Identifying its meaning is the real prize. This book aspires to lead you there. With such a grandiose ambition, the best route I can see is an excursion past many examples, each by necessity of minimal complexity.

Geophysical sounding data used in this book comes from acoustics, radar, seismology, and even bits of astrophysics and biology. Sounders are operated along tracks on the earth surface (or tracks in the ocean, air, or earth orbit). A basic goal of data processing is an image that shows the earth itself, not an image of our data-acquisition tracks. We want to hide our data acquisition footprint.

To enable this book to move rapidly along from one application to another, we avoid applications where the transform from model to data is mathematically complicated; but we include the central techniques of constructing the adjoint of any such complicated transformation. By setting aside application-specific complications, we soon uncover and deal with universal difficulties such as: (1) irregular geometry of recording, (2) locations where no recording took place and, (3) locations where crossing tracks made inconsistent measurements, (4) merging the data of various illumination directions. Noise itself comes in four flavors: (1) drift (zero to low frequency), (2) white or steady and stationary broad band, and (3) bursty, i.e., occasional but large and erratic, and (4) all at once (aaack!). This book has all four kinds.

Missing data and inconsistent data are two humble, though universal problems. Because they are universal problems, science and engineering have produced a cornucopia of ideas ranging from mathematics (Hilbert adjoint) to statistics (stationary, inverse covariance)

to physics (multi-dimensional spectral, scale-invariant) to numerical analysis (conjugate direction, preconditioner) to computer science (object oriented) to simple common sense. Besides geophysical imaging, a journey through this maze is good preparation for many other fields! A course in applied mathematics might often turn out to be more narrowly focused. Our guide through this maze of opportunities, digressions, and misconceptions is the test of what works on real data, what will make a better image.

Inverse theory is too theoretical.

We make discoveries about reality by examining the discrepancy between theory and practice. There is a well-developed *theory* about the difference between theory and practice and it is called "geophysical inverse theory." In this book we investigate the *practice* of the difference between theory and practice. As the folklore tells us, there is a big difference. Inverse theory provides a logical basis for learning from geophysical data. But in practice it often fails. Inverse theory says data is noisy. Practice tells us to find aspects of the data that are missing in the theory. As with computer coding, our first attempts nearly always fail. Inverse theory is the fine art of dividing by zero (inverting a singular matrix).

The first problem with all mathematical theory is that it is based on assumptions. Mathematicians are very good at stating exactly what the assumptions are. But the practitioner often fails to recognize the significance of all the assumptions. For example in 2009 we were in a financial crisis. America's biggest financial institutions were in a state of collapse. People who had been fabulously wealthy were no longer. A major contributing reason is that Nobel prize winning economists have propagated theories dependent on the "stationarity assumption," an assumption ignored by financial leaders because they never saw so many examples of its failures as we are going to see here!

Closer to home, academics often take the world to be homogeneous, one dimensional, or two dimensional when in reality it is three dimensional, heterogeneous, and sometimes time variable as well. My colleagues in exploration seismology for example, often adopt the doubtful assumptions that they have an impulsive point source, that they can neglect multiple reflections, shear waves, anisotropy, and that they already have an adequate velocity model.

Synthetic data is often used as a test of new software. That's fine, as far as it goes, but the real opportunities lie just beyond, when the real data fits a model somewhat different from what we have planned. That's where this book fills a need. I have chosen a wide collection of geophysical data types from among those areas where the basic theory is dirt simple. Then when theory fails (as it always does when we are starting out), it is not so hard to recognize what is happening.

Another big problem with inverse theory in geophysics is the problem of dimensionality. In geophysics we often construct a map or an image which is a specialized form of data display. Your computer screen has about 1000×1000 pixels. Currently, high definition television is about 2000×1000 pixels. A low resolution geophysical image would be 100×100 pixels. For each pixel in such a small image we must find its value by something like inverse theory. Basic application of inverse theory implies a calculation like $\mathbf{m} = (\mathbf{F}^*\mathbf{F})^{-1}\mathbf{F}^*\mathbf{d}$. But for that, even the small image $\mathbf{m}$ has $10,000 = 10^4$ unknowns so the matrix $\mathbf{F}^*\mathbf{F}$ has 10^8 elements. Even with such a tiny image, the matrix is too big to invert on today's computers.

The cost rises with the third power of the number of pixels which is the sixth power of the resolution. Clearly, most geophysical tasks present computational challenges too steep for straightforward application of inverse theory.

Weights, filters, and theory we don't need

We find here many applications that have a great deal in common with one another. First, many applications draw our attention to the importance of two weighting functions (one required for data space and the other for model space). Solutions depend strongly on these weighting functions (eigenvalues do too!). Where do these functions come from, from what rationale or estimation procedure? We'll see many examples here, and find that these functions are not merely weights but filters. Even deeper, they are generally a combination of weights and filters. We do some tricky bookkeeping and bootstrapping when we filter the multidimensional neighborhood of missing and/or suspicious data.

Prior knowledge exploited here is that unknowns are functions of time and space (so the covariance matrix has known structure). This structure gives them predictability. Predictable functions in 1-D are tides, in 2-D are lines on images (linements), in 3-D are sedimentary layers, and in 4-D are wavefronts. The tool we need to best handle this predictability is the multidimensional "prediction-error filter" (PEF), one theme of this book.

Books on geophysical inverse theory tend to address theoretical topics that are little used in practice. Foremost is probability theory. In practice, probabilities are neither observed nor derived from observations. For more than a handful of variables, it would not be practical to display joint probabilities, even if we had them. If you are data poor, you might turn to probabilities. If you are data rich, you have far too many more rewarding things to do. When you estimate a few values, you ask about their standard deviations. When you have an image-making machine, you turn the knobs and make new images (and invent new knobs). Singular-value (eigenvalue) theory is also a valuable intellectual tool, but it is not used here.

A clever friend asked me why my book had no eigenfunctions? A good question. He's the kind of friend who digs into deep problems and comes up with hair-raising integral operators. After calculating potential data everywhere on the surface of the earth we need the linear operator that selects from his ideal data the subset where we record real data. This is nasty. On the earth surface we may often find a nice long survey line of uniformly sampled geophysical data. Widening our eyes from the line to the surface plane we find a mess of too-sparse instrument spacing interrupted by surface obstacles. Unfortunately there is little money to be made these days with single survey lines. My ugly data selection operator multiplies his elegant integral operator. Those beautiful eigenfunctions are ruined.

Going to work

Are you aged 23? If so, this book is designed for you. Life has its discontinuities: when you enter school at age 5, when you leave university, when you marry, when you retire. The discontinuity at age 23, mid graduate school, is when the world loses interest in your potential to learn. Instead the world wants to know what you are accomplishing right now!

This book is about how to make images. It is theory and programs that you can use right now.

This book is not devoid of theory and abstraction. Indeed it makes an important new contribution to the theory (and practice) of data analysis: multidimensional autoregression via the helical coordinate system.

The biggest chore in the study of "the practice of the difference between theory and practice" is that we must look at algorithms. Some of them are short and sweet, but other important algorithms are complicated and ugly in any language. This book can be printed without the computer programs and their surrounding paragraphs, or you can read it without them. I suggest, however, you take a few moments to try to read each program. If you can *write* in any computer language, you should be able to *read* these programs well enough to grasp the concept of each, to understand what goes in and what should come out. I have chosen the computer language (more on this later) that I believe is best suited for our journey through the "elementary" examples in geophysical image estimation.

Besides the tutorial value of the programs, if you can read them, you will know exactly how the many interesting illustrations in this book were computed so you will be well equipped to move forward in your own direction.

Scaling up to big problems

Although most the examples in this book are presented as toys, where results are obtained in a few minutes on a home computer, we have serious industrial-scale jobs always in the backs of our minds. This forces us to avoid representing operators as matrices. Instead we represent operators as a pair of subroutines, one to apply the operator and one to apply the adjoint (transpose matrix). (This will be more clear when you reach the middle of chapter 2.

By taking a function-pair approach to operators instead of a matrix approach, this book becomes a guide to practical work on realistic-sized data sets. By realistic, I mean as large and larger than those here; i.e., data ranging over two or more dimensions, and the data space and model space sizes being larger than about a $300 \times 300 \approx 100,000 = 10^5$ element image. Even for these, the world's biggest computer would be required to hold in random access memory the $10^5 \times 10^5$ matrix linking data and image. Mathematica, Matlab, kriging, etc. are nice tools but[2] it was no surprise when a curious student tried to apply one to an example from this book and discovered that he needed to abandon 99.6% of the data to make it work. Matrix methods are limited not only by the size of the matrices but also by the fact that the cost to multiply or invert is proportional to the third power of the size. For simple experimental work, this limits the matrix approach to data and images of about 4000 elements, a low-resolution 64×64 image.

[2] I do not mean to imply that these tools cannot be used in the function-pair style of this book, only that beginners tend to use a matrix approach.

Computer Languages

One feature of this book is that it introduces and uses "object programming". Older languages like Fortran 77, Matlab, C, and Visual Basic, are not object-oriented languages. The introduction of object-oriented languages like C++, Java, and Fortran 90 a couple decades back greatly simplified many application programs. An earlier version of this book used Fortran 77. I had the regrettable experience that issues of Geophysics were constantly being mixed in the same program as issues of Mathematics. This is easily avoided in object-based languages. For ease of debugging and for ease of understanding, we want to keep the mathematical technicalities away from the geophysical technicalities. This is called "information hiding". We geophysicists can work with numerical analysts without either of us needing to know many details of the other's work.

In the older languages it is easy for a geophysical application program to call a mathematical subroutine. That is new code calling old code. The applications we encounter in this book require the opposite, old optimization code written by someone with a mathematical hat calling linear operator code written by someone with a geophysical hat. The older code must handle objects of considerable complexity only now being built by the newer code. It must handle them as objects without knowing what is inside them. Linear operators are conceptually just matrix multiply (and its transpose), but concretely they are not simply matrices. While a matrix is simply a two-dimensional array, a sparse matrix may be specified by many complicated arrangements.

The newer languages allow information hiding; but a price paid, from my view as a textbook author, is that the codes are now more verbose, hence make the book uglier. Many initial lines of code are taken up by definitions and declarations making my simple textbook codes about twice as lengthy as in old F77 (or pseudocode). This is not a disadvantage for the reader who can rapidly skim over what soon become familiar definitions.

Of the three object-based languages available, I chose Fortran because, as its name implies, it looks most like mathematics. Fortran has excellent primary support for multi-dimensional cartesian arrays and complex numbers, unlike Java and C++. Fortran, while looked down upon by the computer science community, is the language of choice among physicists, mechanical engineers, and numerical analysts. While our work is certainly complex, in computer science their complexity is more diverse.

The Loptran computer dialect

Along with theory, illustrations, and discussion, I display the programs that created the illustrations. To reduce verbosity in these programs, my colleagues and I have invented a little language called Loptran that is readily translated to Fortran 90. I believe readers without Fortran experience will comfortably be able to *read* Loptran, but they should consult a Fortran book if they plan to *write* it. Loptran is not a new language compiler but a simple text processor that expands concise scientific language into the more verbose expressions required by Fortran 90. The name Loptran denotes Linear OPerator TRANslator.

Fortran is the original language shared by scientific computer applications. The people who invented C and UNIX also made Fortran more readable by their invention of Ratfor[3].

[3] http://sepww.stanford.edu/sep/bob/src/ratfor90.html

Sergey Fomel, Bob Clapp, and I have taken the good ideas from original Ratfor and merged them with concepts of linear operators to make Loptran, a language with much the syntax of modern languages like C++ and Java. Loptran is a small and simple adaptation of well-tested languages, and translates to F90. On the web[4] you should be able to find the codes used in this book in both Fortran 90 and Loptran.

Reproducibility

We have long held the goal of delivering reproducible research by which we mean we wish you could find yourself in an environment where you could replicate the calculation we did for each illustration in a document. I still try, but reality has intruded in many ways. Is this the place to cite them all? Most likely not, but here are a few. We build upon many software tools of others. All software has "the versioning problem". Besides our own SEP libraries, I can cite Fortran, C, shell, make, LaTeX, postscript, PDF, Xwindow as software that over the long haul has changed in various ways.

Another problem is that geophysical data is expensive to collect, so when we receive it we are ordinarily not free to pass it along to others. (But if some particular data set catches your heart strings, don't be afraid to ask.)

Internally, our idea of reproducible research is that each computed illustration in a document has in its caption a key to a menu allowing us to burn and rebuild that illustration (or movie) from its code and data sources.

Hopefully, as computers mature, these obstacles will be less formidable. Anyway, our SEP libraries are also offered free on the SEP web site. Our software is developed in LINUX, works also on Mac, but has not been adapted to the Microsoft environment.

[4] http://sepww.stanford.edu/sep/prof/gee/Lib/

Chapter 1

Basic operators and adjoints

A great many of the calculations we do in science and engineering are really matrix multiplication in disguise. The first goal of this chapter is to unmask the disguise by showing many examples. Second, we see how the **adjoint** operator (matrix transpose) back projects information from data to the underlying model.

Geophysical modeling calculations generally use linear operators that predict data from models. Our usual task is to find the inverse of these calculations; i.e., to find models (or make images) from the data. Logically, the adjoint is the first step and a part of all subsequent steps in this **inversion** process. Surprisingly, in practice the adjoint sometimes does a better job than the inverse! This is because the adjoint operator tolerates imperfections in the data and does not demand that the data provide full information.

Using the methods of this chapter, you will find that once you grasp the relationship between operators in general and their adjoints, you can obtain the adjoint just as soon as you have learned how to code the modeling operator.

If you will permit me a poet's license with words, I will offer you the following table of **operator**s and their **adjoint**s:

matrix multiply	conjugate-transpose matrix multiply
convolve	crosscorrelate
truncate	zero pad
replicate, scatter, spray	sum or stack
spray into neighborhoods	sum within bins
derivative (slope)	negative derivative
causal integration	anticausal integration
add functions	do integrals
assignment statements	added terms
plane-wave superposition	slant stack / beam form
spread on a curve	sum along a curve
stretch	squeeze
scalar field gradient	negative of vector field divergence
upward continue	downward continue
diffraction modeling	imaging by migration
hyperbola modeling	stacking for image or velocity

chop image into overlapping patches	merge the patches
ray tracing	**tomography**

The left column above is often called "**modeling**," and the adjoint operators on the right are often used in "data **processing**."

When the adjoint operator is *not* an adequate approximation to the inverse, then you apply the techniques of fitting and optimization explained in Chapter 2. These techniques require iterative use of the modeling operator and its adjoint.

The adjoint operator is sometimes called the "**back projection**" operator because information propagated in one direction (earth to data) is projected backward (data to earth model). Using complex-valued operators, the transpose and complex conjugate go together; and in **Fourier analysis**, taking the complex conjugate of $\exp(i\omega t)$ reverses the sense of time. With more poetic license, I say that adjoint operators *undo* the time and phase shifts of modeling operators. The inverse operator does this too, but it also divides out the color. For example, when linear interpolation is done, then high frequencies are smoothed out; so inverse interpolation must restore them. You can imagine the possibilities for noise amplification. That is why adjoints are safer than inverses. But nature determines in each application what is the best operator to use, and whether to stop after the adjoint, to go the whole way to the inverse, or to stop partway.

The operators and adjoints above transform vectors to other vectors. They also transform data planes to model planes, volumes, etc. A mathematical operator transforms an "abstract vector" which might be packed full of volumes of information like television signals (time series) can pack together a movie, a sequence of frames. We can always think of the operator as being a matrix but the matrix can be truly huge (and nearly empty). When the vectors transformed by the matrices are large like geophysical data set sizes then the matrix sizes are "large squared," far too big for computers. Thus although we can always think of an operator as a matrix, in practice, we handle an operator differently. Each practical application requires the practitioner to prepare two computer programs. One performs the matrix multiply $\mathbf{y} = \mathbf{B}\mathbf{x}$ and another multiplys by the transpose $\tilde{\mathbf{x}} = \mathbf{B}^*\mathbf{y}$ (without ever having the matrix itself in memory). It is always easy to transpose a matrix. It is less easy to take a computer program that does $\mathbf{y} = \mathbf{B}\mathbf{x}$ and convert it to another to do $\tilde{\mathbf{x}} = \mathbf{B}^*\mathbf{y}$. In this chapter are many examples of increasing complexity. At the end of the chapter we will see a test for any program pair to see whether the operators $\mathbf{B}$ and $\mathbf{B}^*$ are mutually adjoint as they should be. Doing the job correctly (coding adjoints without making approximations) will reward us later when we tackle model and image estimation applications.

Mathematicians often denote the transpose of a matrix $\mathbf{B}$ by $\mathbf{B}^{\mathrm{T}}$. In physics and engineering we often encounter complex numbers. There the adjoint is the complex-conjugate transposed matrix denoted $\mathbf{B}^*$. What this book calls the adjoint is more properly called the Hilbert adjoint.

1.0.1 Programming linear operators

The operation $y_i = \sum_j b_{ij} x_j$ is the multiplication of a matrix $\mathbf{B}$ by a vector $\mathbf{x}$. The adjoint operation is $\tilde{x}_j = \sum_i b_{ij} y_i$. The operation adjoint to multiplication by a matrix is multiplication by the transposed matrix (unless the matrix has complex elements, in which case we need the complex-conjugated transpose). The following **pseudocode** does matrix multiplication $\mathbf{y} = \mathbf{B}\mathbf{x}$ and multiplication by the transpose $\tilde{\mathbf{x}} = \mathbf{B}^*\mathbf{y}$:

```
if adjoint
        then erase x
if operator itself
        then erase y
do iy = 1, ny {
do ix = 1, nx {
        if adjoint
                x(ix) = x(ix) + b(iy,ix) × y(iy)
        if operator itself
                y(iy) = y(iy) + b(iy,ix) × x(ix)
        }}
```

Notice that the "bottom line" in the program is that x and y are simply interchanged. The above example is a prototype of many to follow; so observe carefully the similarities and differences between the adjoint and the operator itself.

Next we restate the matrix-multiply pseudo code in real code, in a language called **Loptran**[1], a language designed for exposition and research in model fitting and optimization in physical sciences.

The module `matmult` for matrix multiply and its adjoint exhibits the style that we will use repeatedly. At last count there were 53 such routines (operator with adjoint) in this book alone.

matrix multiply.lop

```
module matmult {   # matrix multiply and its adjoint
real, dimension (:,:), pointer :: bb
#%  _init( bb)
#%  _lop(  x, y)
integer ix, iy
do ix= 1, size(x) {
do iy= 1, size(y) {
        if( adj)
                x(ix) = x(ix) + bb(iy,ix) * y(iy)
        else
                y(iy) = y(iy) + bb(iy,ix) * x(ix)
        }}
}
```

Notice that the module `matmult` does not explicitly erase its output before it begins, as

[1] The programming language, Loptran, is based on a dialect of Fortran called Ratfor. For more details, see Appendix A.

does the pseudo code. That is because Loptran will always erase for you the space required for the operator's output. Loptran also defines a logical variable `adj` for you to distinguish your computation of the adjoint $\mathbf{x} = \mathbf{x} + \mathbf{B}^*\mathbf{y}$ from the forward operation $\mathbf{y} = \mathbf{y} + \mathbf{Bx}$. In computerese, the two lines beginning #% are macro expansions that take compact bits of information which expand into the verbose boilerplate that Fortran requires. Loptran is Fortran with these macro expansions. You can always see how they expand by looking at `http://sep.stanford.edu/sep/prof/`.

What is new in Fortran 90, and will be a big help to us, is that instead of a subroutine with a single entry, we now have a module with two entries, one named `_init` for the physical scientist who defines the physical problem by defining the matrix, and another named `_lop` for the least-squares problem solver, the computer scientist who will not be interested in how we specify $\mathbf{B}$, but who will be iteratively computing $\mathbf{Bx}$ and $\mathbf{B}^*\mathbf{y}$ to optimize the model fitting. The lines beginning with `#%` are expanded by Loptran into more verbose and distracting Fortran 90 code. The second line in the module `matmult`, however, is pure Fortran syntax saying that `bb` is a pointer to a real-valued matrix.

To use `matmult`, two calls must be made, the first one

```
call matmult_init( bb)
```

is done by the physical scientist after he or she has prepared the matrix. Here memory is allocated, often later released by `call matmult_close()`. Most later calls are done by numerical analysts in solving code like in Chapter 2. These calls look like

```
stat = matmult_lop( adj, add, x, y)
```

where `adj` is the logical variable saying whether we desire the adjoint or the operator itself, and where `add` is a logical variable saying whether we want to accumulate like $\mathbf{y} \leftarrow \mathbf{y} + \mathbf{Bx}$ or whether we want to erase first and thus do $\mathbf{y} \leftarrow \mathbf{Bx}$. The return value `stat` is an integer parameter, mostly useless (unless you want to use it for error codes).

We split operators into two independent processes, the first is used for geophysical set up while the second is invoked by mathematical library code (introduced in the next chapter) to find the model that best fits the data. Here is why we do so. It is important that the math code contain nothing about the geophysical particulars. This enables us to use the same math code on many different geophysical applications. This concept of "information hiding" arrived late in human understanding of what is desirable in a computer language. This feature alone is valuable enough to warrant upgrading from Fortran 77 to Fortran 90, and likewise from C to C++. Subroutines and functions are the way that new programs use old ones. Object modules are the way that old programs (math solvers) are able to use new ones (geophysical operators).

1.1 FAMILIAR OPERATORS

The simplest and most fundamental linear operators arise when a matrix operator reduces to a simple row or a column.

A **row** is a summation operation.

A **column** is an impulse response.

If the inner loop of a matrix multiply ranges within a

row, the operator is called *sum* or *pull.*

column, the operator is called *spray* or *push.*

Generally, inputs and outputs will be high dimensional such as signals or images. Push gives ugly outputs. Some output locations will be empty, each having an erratic number of contributions to it. Consequently, most data processing (adjoint) is done by *pull.*

A basic aspect of adjointness is that the adjoint of a row matrix operator is a column matrix operator. For example, the row operator $[a, b]$

$$y = [\, a \; b \,] \begin{bmatrix} x_1 \\ x_2 \end{bmatrix} = ax_1 + bx_2 \tag{1.1}$$

has an adjoint that is two assignments:

$$\begin{bmatrix} \hat{x}_1 \\ \hat{x}_2 \end{bmatrix} = \begin{bmatrix} a \\ b \end{bmatrix} y \tag{1.2}$$

The adjoint of a sum of N terms is a collection of N assignments.

1.1.1 Adjoint derivative

In numerical analysis we represent the derivative of a time function by a finite difference. We do this by subtracting each two neighboring time points and then dividing by the sample interval Δt. This amounts to convolution with the filter $(1, -1)/\Delta t$. Omitting the Δt we express this concept as:

$$\begin{bmatrix} y_1 \\ y_2 \\ y_3 \\ y_4 \\ y_5 \\ y_6 \end{bmatrix} = \begin{bmatrix} -1 & 1 & . & . & . & . \\ . & -1 & 1 & . & . & . \\ . & . & -1 & 1 & . & . \\ . & . & . & -1 & 1 & . \\ . & . & . & . & -1 & 1 \\ . & . & . & . & . & 0 \end{bmatrix} \begin{bmatrix} x_1 \\ x_2 \\ x_3 \\ x_4 \\ x_5 \\ x_6 \end{bmatrix} \tag{1.3}$$

The is seen in any column in the middle of the matrix, namely $(1, -1)$. In the transposed matrix, the filter-impulse response is time-reversed to $(-1, 1)$. So, mathematically, we can say that the adjoint of the time derivative operation is the negative time derivative. This corresponds also to the fact that the complex conjugate of $-i\omega$ is $i\omega$. We can also speak of the adjoint of the boundary conditions: we might say that the adjoint of "no boundary condition" is a "specified value" boundary condition. The last row in equation (1.3) is

optional. It may seem unnatural to append a null row, but it can be a small convenience (when plotting) to have the input and output be the same size.

Equation (1.3) is implemented by the code in module `igrad1` which does the operator itself (the forward operator) and its adjoint.

first difference.lop

```
module igrad1 {                                    # gradient in one dimension
#%  _lop( xx,  yy)
integer i
do i= 1, size(xx)-1 {
        if( adj) {
                xx(i+1) = xx(i+1) + yy(i)          # resembles equation (1.2)
                xx(i  ) = xx(i  ) - yy(i)
                }
        else
                yy(i) = yy(i) + xx(i+1) - xx(i)    # resembles equation (1.1)
        }
}
```

The adjoint code may seem strange. It might seem more natural to code the adjoint to be the negative of the operator itself and then make the special adjustments for the boundaries. The code given, however, is correct and requires no adjustments at the ends. To see why, notice for each value of `i`, the operator itself handles one row of equation (1.3), while for each `i` the adjoint handles one column. That's why coding the adjoint in this way does not require any special work on the ends. The present method of coding reminds us that the adjoint of a sum of N terms is a collection of N assignments. Think of the meaning of $y_i = y_i + a_{i,j} x_j$ for any particular i and j. The adjoint simply accumulates that same value of $a_{i,j}$ going the other direction $x_j = x_j + a_{i,j} y_i$.

The Ratfor90 dialect of Fortran allows us to write the inner code of the `igrad1` module more simply and symmetrically using the syntax of modern languages such as C, C++, Java, Python, and Perl. Expressions like `a=a+b` can be written more tersely as `a+=b`. With this, the heart of module `igrad1` becomes

```
if( adj) {   xx(i+1) += yy(i)
             xx(i)   -= yy(i)
           }
else {       yy(i)   += xx(i+1)
             yy(i)   -= xx(i)
           }
```

where we see that each component of the matrix is handled both by the operator and the adjoint. With the forward operator a single value `yy(i)` is "pulled" from all the values in `x()`-space. With the adjoint operator the single value `yy(i)` is "pushed" to all the values in `x()`-space.

```
do iy=1,ny      # north-south derivative on 1-axis
      stat = igrad1_lop( adj, add, map(:,iy), ruf(:,iy))
do ix=1,nx       # east-west derivative on 2-axis
      stat = igrad1_lop( adj, add, map(ix,:), ruf(ix,:))
```

Figure 1.1 illustrates the use of module `igrad1` for each north-south line of a topographic map. We observe that the gradient gives an impression of illumination from a low sun angle.

1.1.2 Transient convolution

The next operator we examine is convolution. It arises in many applications; and it could be derived in many ways. A basic derivation is from the multiplication of two polynomials, say $X(Z) = x_1 + x_2 Z + x_3 Z^2 + x_4 Z^3 + x_5 Z^4 + x_6 Z^5$ times $B(Z) = b_1 + b_2 Z + b_3 Z^2 + b_4 Z^3$.[2] Identifying the k-th power of Z in the product $Y(Z) = B(Z)X(Z)$ gives the k-th row of the convolution transformation (1.4).

$$\mathbf{y} = \begin{bmatrix} y_1 \\ y_2 \\ y_3 \\ y_4 \\ y_5 \\ y_6 \\ y_7 \\ y_8 \end{bmatrix} = \begin{bmatrix} b_1 & 0 & 0 & 0 & 0 & 0 \\ b_2 & b_1 & 0 & 0 & 0 & 0 \\ b_3 & b_2 & b_1 & 0 & 0 & 0 \\ 0 & b_3 & b_2 & b_1 & 0 & 0 \\ 0 & 0 & b_3 & b_2 & b_1 & 0 \\ 0 & 0 & 0 & b_3 & b_2 & b_1 \\ 0 & 0 & 0 & 0 & b_3 & b_2 \\ 0 & 0 & 0 & 0 & 0 & b_3 \end{bmatrix} \begin{bmatrix} x_1 \\ x_2 \\ x_3 \\ x_4 \\ x_5 \\ x_6 \end{bmatrix} = \mathbf{Bx} \tag{1.4}$$

Notice that columns of equation (1.4) all contain the same signal but with different shifts. This signal is called the filter's impulse response.

Equation (1.4) could be rewritten as

$$\mathbf{y} = \begin{bmatrix} y_1 \\ y_2 \\ y_3 \\ y_4 \\ y_5 \\ y_6 \\ y_7 \\ y_8 \end{bmatrix} = \begin{bmatrix} x_1 & 0 & 0 \\ x_2 & x_1 & 0 \\ x_3 & x_2 & x_1 \\ x_4 & x_3 & x_2 \\ x_5 & x_4 & x_3 \\ x_6 & x_5 & x_4 \\ 0 & x_6 & x_5 \\ 0 & 0 & x_6 \end{bmatrix} \begin{bmatrix} b_1 \\ b_2 \\ b_3 \end{bmatrix} = \mathbf{Xb} \tag{1.5}$$

In applications we can choose between $\mathbf{y} = \mathbf{Xb}$ and $\mathbf{y} = \mathbf{Bx}$. In one case the output $\mathbf{y}$ is dual to the filter $\mathbf{b}$; and in the other case the output $\mathbf{y}$ is dual to the input $\mathbf{x}$. Sometimes we must solve for $\mathbf{b}$ and sometimes for $\mathbf{x}$; so sometimes we use equation (1.5) and sometimes (1.4). Such solutions begin from the adjoints. The adjoint of (1.4) is

$$\begin{bmatrix} \hat{x}_1 \\ \hat{x}_2 \\ \hat{x}_3 \\ \hat{x}_4 \\ \hat{x}_5 \\ \hat{x}_6 \end{bmatrix} = \begin{bmatrix} b_1 & b_2 & b_3 & 0 & 0 & 0 & 0 & 0 \\ 0 & b_1 & b_2 & b_3 & 0 & 0 & 0 & 0 \\ 0 & 0 & b_1 & b_2 & b_3 & 0 & 0 & 0 \\ 0 & 0 & 0 & b_1 & b_2 & b_3 & 0 & 0 \\ 0 & 0 & 0 & 0 & b_1 & b_2 & b_3 & 0 \\ 0 & 0 & 0 & 0 & 0 & b_1 & b_2 & b_3 \end{bmatrix} \begin{bmatrix} y_1 \\ y_2 \\ y_3 \\ y_4 \\ y_5 \\ y_6 \\ y_7 \\ y_8 \end{bmatrix} \tag{1.6}$$

[2] This book is more involved with matrices than with Fourier analysis. If it were more Fourier analysis we would choose notation to begin subscripts from zero like this: $B(Z) = b_0 + b_1 Z + b_2 Z^2 + b_3 Z^3$.

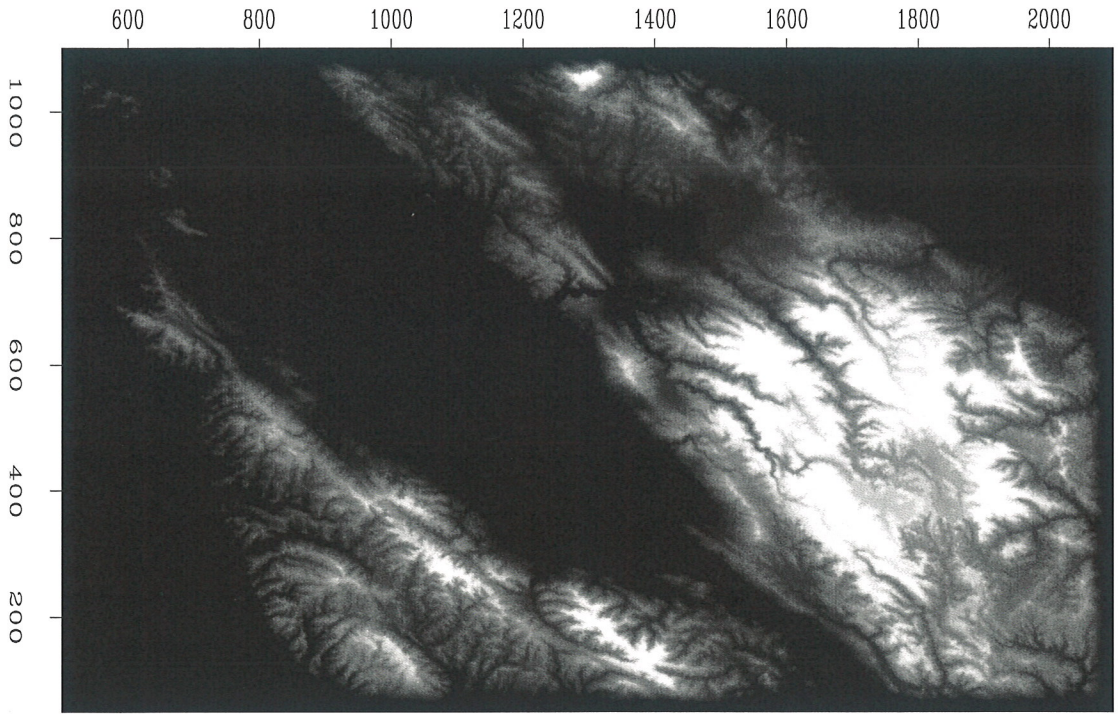

Topographic map, Stanford area

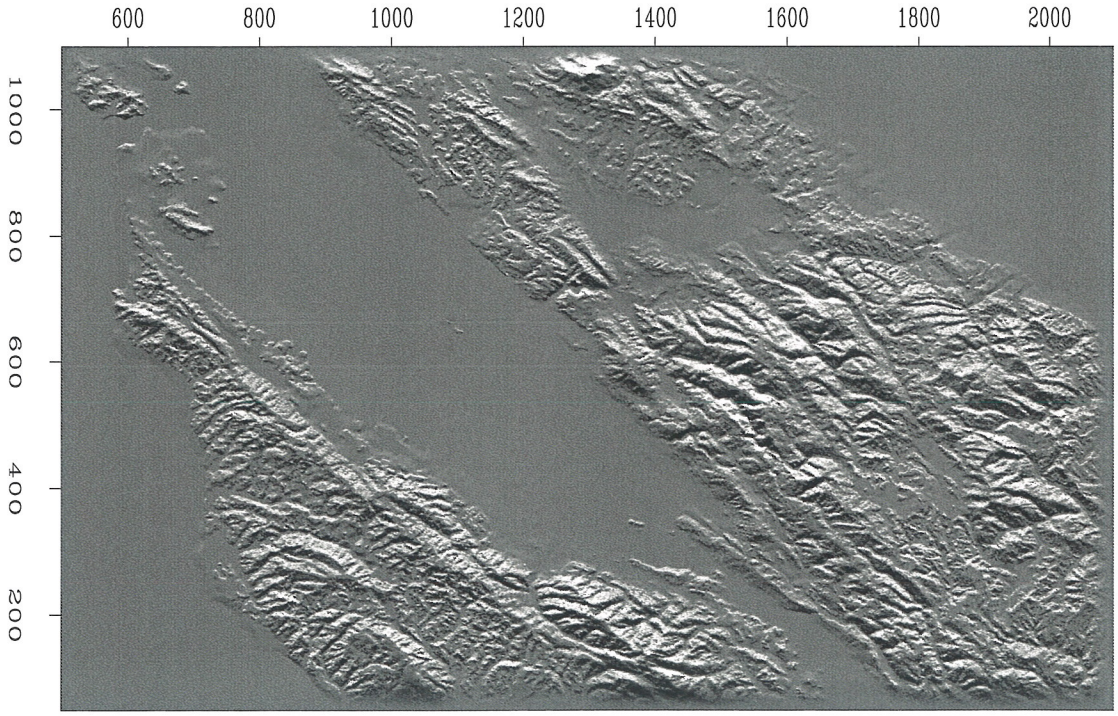

Southward slope

Figure 1.1: Topography near Stanford (top) southward slope (bottom). VIEW ajt/. stangrad90

The adjoint ***crosscorrelates*** with the filter instead of convolving with it (because the filter is backwards). Notice that each row in equation (1.6) contains all the filter coefficients and there are no rows where the filter somehow uses zero values off the ends of the data as we saw earlier. In some applications it is important not to assume zero values beyond the interval where inputs are given.

The adjoint of (1.5) crosscorrelates a fixed portion of filter input across a variable portion of filter output.

$$\begin{bmatrix} \hat{b}_1 \\ \hat{b}_2 \\ \hat{b}_3 \end{bmatrix} = \begin{bmatrix} x_1 & x_2 & x_3 & x_4 & x_5 & x_6 & 0 & 0 \\ 0 & x_1 & x_2 & x_3 & x_4 & x_5 & x_6 & 0 \\ 0 & 0 & x_1 & x_2 & x_3 & x_4 & x_5 & x_6 \end{bmatrix} \begin{bmatrix} y_1 \\ y_2 \\ y_3 \\ y_4 \\ y_5 \\ y_6 \\ y_7 \\ y_8 \end{bmatrix} \tag{1.7}$$

Module `tcai1` is used for $\mathbf{y} = \mathbf{B}\mathbf{x}$ and module `tcaf1` is used for $\mathbf{y} = \mathbf{X}\mathbf{b}$.

transient convolution.lop

```
module tcai1 {              # Transient Convolution Adjoint Input 1-D. yy(m1+n1)
real, dimension (:), pointer :: bb
#%  _init( bb)
#%  _lop ( xx, yy)
integer b, x, y
if( size(yy) < size (xx) + size(bb) - 1 ) call erexit('tcai')
do b= 1, size(bb) {
do x= 1, size(xx) {                    y = x + b - 1
        if( adj)          xx(x) +=  yy(y) * bb(b)
        else              yy(y) +=  xx(x) * bb(b)
        }}
}
```

transient convolution.lop

```
module tcaf1 {                # Transient Convolution, Adjoint is the Filter, 1-D
real, dimension (:), pointer :: xx
#%  _init( xx)
#%  _lop ( bb,  yy)
integer         x,    b,    y
if( size(yy) < size(xx) + size(bb) - 1 )    call erexit('tcaf')
do b= 1, size(bb) {
do x= 1, size(xx) {                    y = x + b - 1
        if( adj)          bb(b) +=  yy(y) * xx(x)
        else              yy(y) +=  bb(b) * xx(x)
        } }
}
```

The polynomials $X(Z)$, $B(Z)$, and $Y(Z)$ are called Z transforms. An important fact in real life (but not important here) is that the Z transforms are Fourier transforms in disguise. Each polynomial is a sum of terms and the sum amounts to a Fourier sum when we take $Z = e^{i\omega\Delta t}$. The very expression $Y(Z) = B(Z)X(Z)$ says that a product in the frequency domain (Z has a numerical value) is a convolution in the time domain (that's how we multipy polynomials, convolve their coefficients).

1.1.3 Internal convolution

Convolution is the computational equivalent of ordinary linear differential operators (with constant coefficients). Applications are vast, and end effects are important. Another choice of data handling at ends is that zero data not be assumed beyond the interval where the data is given. This is important in data where the crosscorrelation changes with time. Then it is sometimes handled as constant in short time windows. Care must be taken that zero signal values not be presumed off the ends of those short time windows; otherwise, the many ends of the many short segments can overwhelm the results.

In the sets (1.4) and (1.5), the top two equations explicitly assume that the input data vanishes before the interval on which it is given, and likewise at the bottom. Abandoning the top two and bottom two equations in (1.5) we get:

$$\begin{bmatrix} y_3 \\ y_4 \\ y_5 \\ y_6 \end{bmatrix} = \begin{bmatrix} x_3 & x_2 & x_1 \\ x_4 & x_3 & x_2 \\ x_5 & x_4 & x_3 \\ x_6 & x_5 & x_4 \end{bmatrix} \begin{bmatrix} b_1 \\ b_2 \\ b_3 \end{bmatrix} \tag{1.8}$$

The adjoint is

$$\begin{bmatrix} \hat{b}_1 \\ \hat{b}_2 \\ \hat{b}_3 \end{bmatrix} = \begin{bmatrix} x_3 & x_4 & x_5 & x_6 \\ x_2 & x_3 & x_4 & x_5 \\ x_1 & x_2 & x_3 & x_4 \end{bmatrix} \begin{bmatrix} y_3 \\ y_4 \\ y_5 \\ y_6 \end{bmatrix} \tag{1.9}$$

The difference between (1.9) and (1.7) is that here the adjoint crosscorrelates a fixed portion of *output* across a variable portion of *input*, whereas with (1.7) the adjoint crosscorrelates a fixed portion of *input* across a variable portion of *output*.

In practice we typically allocate equal space for input and output. Because the output is shorter than the input, it could slide around in its allocated space, so its location is specified by an additional parameter called its `lag`.

convolve internal.lop

```
module icaf1 {                  # Internal Convolution, Adjoint is Filter. 1-D
integer :: lag
real, dimension (:), pointer :: xx
#%  _init ( xx, lag)
#%  _lop  ( bb,  yy)
integer   x,  b,   y
do b= 1, size(bb) {
        do y= 1+size(bb)-lag, size(yy)-lag+1 {     x= y - b + lag
                if( adj)          bb(b) +=  yy(y) * xx(x)
                else              yy(y) +=  bb(b) * xx(x)
                }
        }
}
```

The value of `lag` always used in this book is `lag=1`. For `lag=1` the module `icaf1` implements

not equation (1.8) but (1.10):

$$\begin{bmatrix} y_1 \\ y_2 \\ y_3 \\ y_4 \\ y_5 \\ y_6 \end{bmatrix} = \begin{bmatrix} 0 & 0 & 0 \\ 0 & 0 & 0 \\ x_3 & x_2 & x_1 \\ x_4 & x_3 & x_2 \\ x_5 & x_4 & x_3 \\ x_6 & x_5 & x_4 \end{bmatrix} \begin{bmatrix} b_1 \\ b_2 \\ b_3 \end{bmatrix} \tag{1.10}$$

It may seem a little odd to put the required zeros at the beginning of the output, but filters are generally designed so that their strongest coefficient is the first, namely `bb(1)` so the alignment of input and output in equation (1.10) is the most common one.

The **end effect**s of the convolution modules are summarized in Figure 1.2.

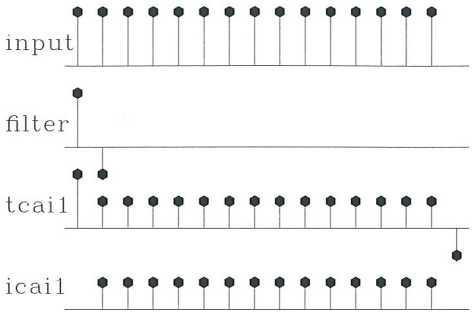

Figure 1.2: Example of convolution end-effects. From top to bottom: input; filter; output of `tcai1()`; output of `icaf1()` also with (`lag=1`). VIEW ajt/. conv90

1.1.4 Zero padding is the transpose of truncation

Surrounding a dataset by zeros (**zero padd**ing) is adjoint to throwing away the extended data (**truncation**). Let us see why this is so. Set a signal in a vector $\mathbf{x}$, and then to make a longer vector $\mathbf{y}$, add some zeros at the end of $\mathbf{x}$. This zero padding can be regarded as the matrix multiplication

$$\mathbf{y} = \begin{bmatrix} \mathbf{I} \\ \mathbf{0} \end{bmatrix} \mathbf{x} \tag{1.11}$$

The matrix is simply an identity matrix $\mathbf{I}$ above a zero matrix $\mathbf{0}$. To find the transpose to zero-padding, we now transpose the matrix and do another matrix multiply:

$$\tilde{\mathbf{x}} = \begin{bmatrix} \mathbf{I} & \mathbf{0} \end{bmatrix} \mathbf{y} \tag{1.12}$$

So the transpose operation to zero padding data is simply *truncating* the data back to its original length. Module `zpad1` below pads zeros on both ends of its input. Modules for two- and three-dimensional padding are in the library named `zpad2()` and `zpad3()`.

zero pad 1-D.lop

```
module zpad1 {
#%  _lop( data,  padd)
integer
do d= 1, size(data) {
        if( adj)
                data(d) = data(d) + padd(p)
        # Zero pad.  Surround data by zeros. 1-D
        p, d
        p = d + (size(padd)-size(data))/2
```

```
        else
                        padd(p) = padd(p) + data(d)
        }
}
```

1.1.5 Adjoints of products are reverse-ordered products of adjoints

Here we examine an example of the general idea that adjoints of products are reverse-ordered products of adjoints. For this example we use the Fourier transformation. No details of **Fourier transformation** are given here and we merely use it as an example of a square matrix $\mathbf{F}$. We denote the complex-conjugate transpose (or **adjoint**) matrix with a prime, i.e., $\mathbf{F}'$. The adjoint arises naturally whenever we consider energy. The statement that Fourier transforms conserve energy is $\mathbf{y}'\mathbf{y} = \mathbf{x}'\mathbf{x}$ where $\mathbf{y} = \mathbf{F}\mathbf{x}$. Substituting gives $\mathbf{F}'\mathbf{F} = \mathbf{I}$, which shows that the inverse matrix to Fourier transform happens to be the complex conjugate of the transpose of $\mathbf{F}$.

With Fourier transforms, **zero padding** and **truncation** are especially prevalent. Most modules transform a dataset of length of 2^n, whereas dataset lengths are often of length $m \times 100$. The practical approach is therefore to pad given data with zeros. Padding followed by Fourier transformation $\mathbf{F}$ can be expressed in matrix algebra as

$$\text{Program} \quad = \quad \mathbf{F} \begin{bmatrix} \mathbf{I} \\ \mathbf{0} \end{bmatrix} \tag{1.13}$$

According to matrix algebra, the transpose of a product, say $\mathbf{AB} = \mathbf{C}$, is the product $\mathbf{C}' = \mathbf{B}'\mathbf{A}'$ in reverse order. So the adjoint routine is given by

$$\text{Program}' \quad = \quad \begin{bmatrix} \mathbf{I} & \mathbf{0} \end{bmatrix} \mathbf{F}' \tag{1.14}$$

Thus the adjoint routine *truncates* the data *after* the inverse Fourier transform. This concrete example illustrates that common sense often represents the mathematical abstraction that adjoints of products are reverse-ordered products of adjoints. It is also nice to see a formal mathematical notation for a practical necessity. Making an approximation need not lead to collapse of all precise analysis.

1.1.6 Nearest-neighbor coordinates

In describing physical processes, we often either specify models as values given on a uniform mesh or we record data on a uniform mesh. Typically we have a function f of time t or depth z and we represent it by `f(iz)` corresponding to $f(z_i)$ for $i = 1, 2, 3, \ldots, n_z$ where $z_i = z_0 + (i-1)\Delta z$. We sometimes need to handle depth as an integer counting variable i and we sometimes need to handle it as a floating-point variable z. Conversion from the counting variable to the floating-point variable is exact and is often seen in a computer idiom such as either of

```
do iz= 1, nz {   z = z0 + (iz-1) * dz
do i3= 1, n3 {  x3 = o3 + (i3-1) * d3
```

The reverse conversion from the floating-point variable to the counting variable is inexact. The easiest thing is to place it at the nearest neighbor. This is done by solving for iz, then adding one half, and then rounding down to the nearest integer. The familiar computer idioms are:

```
iz =  .5 + 1 + ( z - z0) / dz
iz = 1.5 +     ( z - z0) / dz
i3 = 1.5 +     (x3 - o3) / d3
```

A small warning is in order: People generally use positive counting variables. If you also include negative ones, then to get the nearest integer, you should do your rounding with the Fortran function NINT().

1.1.7 Data-push binning

A most basic data modeling operation is to copy a number from an (x, y)-location on a map to a 1-D survey data track $d(s)$, where s is a coordinate running along a survey track. This copying proceeds for all s. The track could be along a straight, curved, or arbitrary line. Let the coordinate s take on integral values. Then along with the elements $d(s)$ are the coordinates $(x(s), y(s))$ where on the map the data value $d(s)$ would be recorded.

Code for the operator is shown in module bin2.

push data into bin.lop

```
module bin2 {
# Data-push binning in 2-D.
integer :: m1, m2
real    ::  o1,d1,o2,d2
real, dimension (:,:), pointer :: xy
#% _init(     m1,m2, o1,d1,o2,d2,xy)
#% _lop ( mm (m1,m2),  dd (:))
integer    i1,i2, id
do id=1,size(dd) {
        i1 = 1.5 + (xy(id,1)-o1)/d1
        i2 = 1.5 + (xy(id,2)-o2)/d2
        if( 1<=i1 && i1<=m1 &&
            1<=i2 && i2<=m2    )
                if( adj)
                        mm(i1,i2) = mm(i1,i2) +  dd( id)
                else
                        dd( id)   = dd( id)   +  mm(i1,i2)
        }
}
```

To invert this data modeling operation, to go from $d(s)$ to $(x(s), y(s))$ requires more than the adjoint operator. Since each bin contains a different number of data values. After the adjoint operation is performed, the inverse operator needs to divide the bin sum by the number of data values that landed in the bin. It is this inversion operator that is generally called binning (although we will use that name here for the modeling operator). To find the number of data points in a bin, we can simply apply the adjoint of bin2 to pseudo data of all ones. To capture this idea in an equation, let $\mathbf{B}$ denote the linear operator in which the

bin value is sprayed to the data values. The inverse operation, in which the data values in the bin are summed and divided by the number in the bin, is represented by

$$\mathbf{m} = \mathbf{diag}(\mathbf{B}^*\mathbf{1})^{-1}\mathbf{B}^*\mathbf{d} \tag{1.15}$$

Empty bins, of course, leave us a problem since we dare not divide by the zero sum they contain. That we'll address in chapter 3. In Figure 1.3, the empty bins contain zero values.

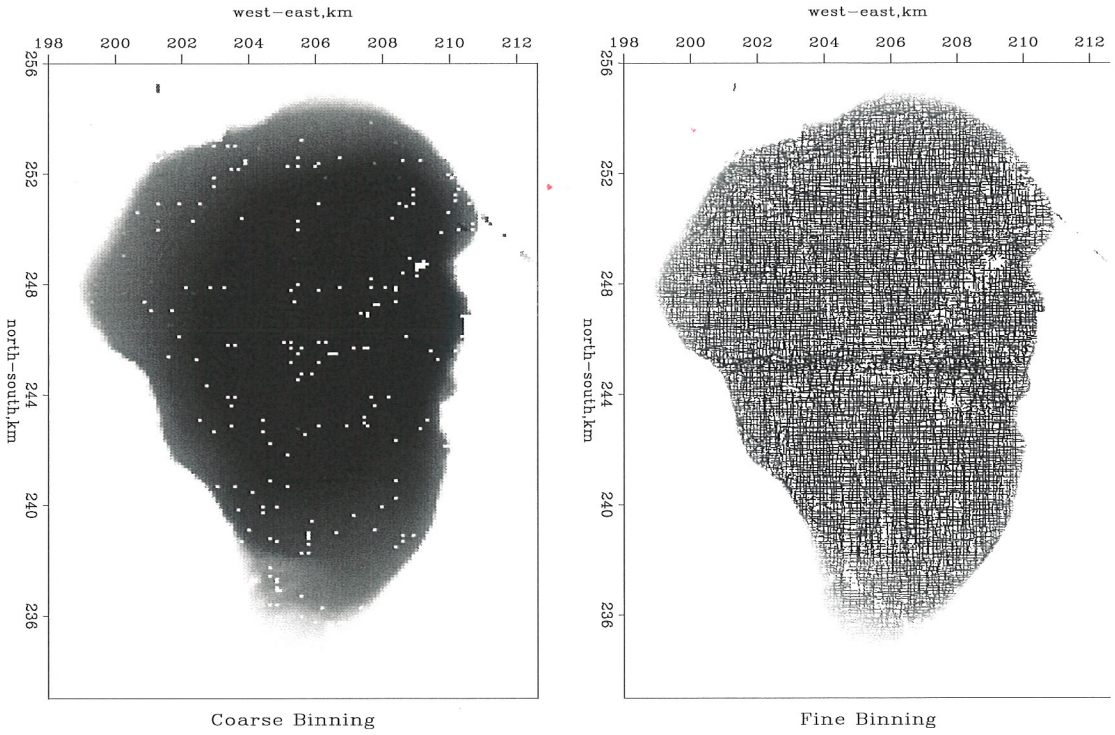

Figure 1.3: Binned depths of the Sea of **Galilee**. VIEW ajt/. galbin90

1.1.8 Linear interpolation

The **linear interpolation** operator is much like the binning operator but a little fancier. When we perform the forward operation, we take each data coordinate and see which two model bin centers bracket it. Then we pick up the two bracketing model values and weight each of them in proportion to their nearness to the data coordinate, and add them to get the data value (ordinate). The adjoint operation is adding a data value back into the model vector; using the same two weights, the adjoint distributes the data ordinate value between the two nearest bins in the model vector. For example, suppose we have a data point near each end of the model and a third data point exactly in the middle. Then for a model space 6 points long, as shown in Figure 1.4, we have the operator in (1.16).

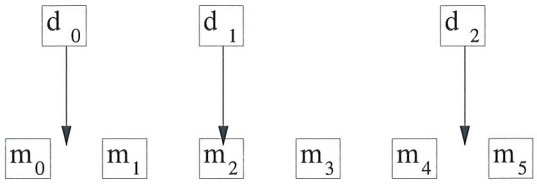

Figure 1.4: Uniformly sampled model space and irregularly sampled data space corresponding to (1.16).
VIEW ajt/. helgerud

$$\begin{bmatrix} d_0 \\ d_1 \\ d_2 \end{bmatrix} \approx \begin{bmatrix} .7 & .3 & . & . & . & . \\ . & . & 1 & . & . & . \\ . & . & . & . & .5 & .5 \end{bmatrix} \begin{bmatrix} m_0 \\ m_1 \\ m_2 \\ m_3 \\ m_4 \\ m_5 \end{bmatrix} \tag{1.16}$$

The two weights in each row sum to unity. If a binning operator were used for the same data and model, the binning operator would contain a "1." in each row. In one dimension (as here), data coordinates are often sorted into sequence, so that the matrix is crudely a diagonal matrix like equation (1.16). If the data coordinates covered the model space uniformly, the adjoint would roughly be the inverse. Otherwise, when data values pile up in some places and gaps remain elsewhere, the adjoint would be far from the inverse.

Module `lint1` does linear interpolation and its adjoint. In chapters 3 and 7 we build inverse operators.

linear interp.lop

```
# Nearest-neighbor interpolation would do this:  data = model( 1.5 + (t-t0)/dt)
#                                This is likewise but with _linear_ interpolation.
module lint1 {
real :: o1,d1
real, dimension (:), pointer :: coordinate
#%  _init ( o1,d1, coordinate)
#%  _lop  ( mm, dd)
integer i, im,  id
real    f, fx,gx
do id= 1, size(dd) {
        f = (coordinate(id)-o1)/d1;      i=f  ;   im= 1+i
        if( 1<=im && im< size(mm)) {   fx=f-i;   gx= 1.-fx
                if( adj) {
                        mm(im  ) +=  gx * dd(id)
                        mm(im+1) +=  fx * dd(id)
                        }
                else
                        dd(id)   +=  gx * mm(im)  +  fx * mm(im+1)
                }
        }
}
```

1.1.9 Spray and sum : scatter and gather

Perhaps the most common operation is the summing of many values to get one value. Its adjoint operation takes a single input value and throws it out to a space of many values. The **summation operator** is a row vector of ones. Its adjoint is a column vector of

ones. In one dimension this operator is almost too easy for us to bother showing a routine. But it is more interesting in three dimensions, where we could be summing or spraying on any of three subscripts, or even summing on some and spraying on others. In module `spraysum`, both input and output are taken to be three-dimensional arrays. Externally, however, either could be a scalar, vector, plane, or cube. For example, the internal array `xx(n1,1,n3)` could be externally the matrix `map(n1,n3)`. When module `spraysum` is given the input dimensions and output dimensions stated below, the operations stated alongside are implied.

`(n1,n2,n3)`	`(1,1,1)`	Sum a cube into a value.
`(1,1,1)`	`(n1,n2,n3)`	Spray a value into a cube.
`(n1,1,1)`	`(n1,n2,1)`	Spray a column into a matrix.
`(1,n2,1)`	`(n1,n2,1)`	Spray a row into a matrix.
`(n1,n2,1)`	`(n1,n2,n3)`	Spray a plane into a cube.
`(n1,n2,1)`	`(n1,1,1)`	Sum rows of a matrix into a column.
`(n1,n2,1)`	`(1,n2,1)`	Sum columns of a matrix into a row.
`(n1,n2,n3)`	`(n1,n2,n3)`	Copy and add the whole cube.

If an axis is not of unit length on either input or output, then both lengths must be the same; otherwise, there is an error. Normally, after (possibly) erasing the output, we simply loop over all points on each axis, adding the input to the output. This implements either a copy or an add, depending on the `add` parameter. It is either a spray, a sum, or a copy, according to the specified axis lengths.

sum and spray.lop

```
module spraysum {                       # Spray or sum over 1, 2, and/or 3-axis.
integer ::    n1,n2,n3,      m1,m2,m3
#%  _init(    n1,n2,n3,      m1,m2,m3)
#%  _lop( xx(n1,n2,n3), yy(m1,m2,m3))
integer i1,i2,i3,  x1,x2,x3, y1,y2,y3
        if( n1 != 1  &&  m1 != 1  &&  n1 != m1)   call erexit('spraysum: n1,m1')
        if( n2 != 1  &&  m2 != 1  &&  n2 != m2)   call erexit('spraysum: n2,m2')
        if( n3 != 1  &&  m3 != 1  &&  n3 != m3)   call erexit('spraysum: n3,m3')
do i3= 1, max0(n3,m3) {   x3= min0(i3,n3);   y3= min0(i3,m3)
do i2= 1, max0(n2,m2) {   x2= min0(i2,n2);   y2= min0(i2,m2)
do i1= 1, max0(n1,m1) {   x1= min0(i1,n1);   y1= min0(i1,m1)
        if( adj)  xx(x1,x2,x3)  +=  yy(y1,y2,y3)
        else      yy(y1,y2,y3)  +=  xx(x1,x2,x3)
        }}}
}
```

1.1.10 Causal and leaky integration

Causal integration is defined as

$$y(t) \quad = \quad \int_{-\infty}^{t} x(\tau)\, d\tau \tag{1.17}$$

Leaky integration is defined as

$$y(t) \quad = \quad \int_{0}^{\infty} x(t-\tau)\, e^{-\alpha\tau}\, d\tau \tag{1.18}$$

As $\alpha \to 0$, leaky integration becomes causal integration. The word "leaky" comes from electrical circuit theory where the voltage on a capacitor would be the integral of the current if the capacitor did not leak electrons.

Sampling the time axis gives a matrix equation that we should call causal summation, but we often call it causal integration. Equation (1.19) represents causal integration for $\rho = 1$ and leaky integration for $0 < \rho < 1$.

$$\mathbf{y} = \begin{bmatrix} y_0 \\ y_1 \\ y_2 \\ y_3 \\ y_4 \\ y_5 \\ y_6 \end{bmatrix} = \begin{bmatrix} 1 & 0 & 0 & 0 & 0 & 0 & 0 \\ \rho & 1 & 0 & 0 & 0 & 0 & 0 \\ \rho^2 & \rho & 1 & 0 & 0 & 0 & 0 \\ \rho^3 & \rho^2 & \rho & 1 & 0 & 0 & 0 \\ \rho^4 & \rho^3 & \rho^2 & \rho & 1 & 0 & 0 \\ \rho^5 & \rho^4 & \rho^3 & \rho^2 & \rho & 1 & 0 \\ \rho^6 & \rho^5 & \rho^4 & \rho^3 & \rho^2 & \rho & 1 \end{bmatrix} \begin{bmatrix} x_0 \\ x_1 \\ x_2 \\ x_3 \\ x_4 \\ x_5 \\ x_6 \end{bmatrix} = \mathbf{C}\mathbf{x} \tag{1.19}$$

(The discrete world is related to the continuous by $\rho = e^{-\alpha \Delta \tau}$ and in some applications, the diagonal is 1/2 instead of 1.) Causal integration is the simplest prototype of a recursive operator. The coding is trickier than that for the operators we considered earlier. Notice when you compute y_5 that it is the sum of 6 terms, but that this sum is more quickly computed as $y_5 = \rho y_4 + x_5$. Thus equation (1.19) is more efficiently thought of as the recursion

$$y_t = \rho\, y_{t-1} + x_t \qquad t \text{ increasing} \tag{1.20}$$

(which may also be regarded as a numerical representation of the **differential equation** $dy/dt + y(1-\rho)/\Delta t = x(t)$.)

When it comes time to think about the adjoint, however, it is easier to think of equation (1.19) than of (1.20). Let the matrix of equation (1.19) be called $\mathbf{C}$. Transposing to get $\mathbf{C}^*$ and applying it to $\mathbf{y}$ gives us something back in the space of $\mathbf{x}$, namely $\tilde{\mathbf{x}} = \mathbf{C}^*\mathbf{y}$. From it we see that the adjoint calculation, if done recursively, needs to be done backwards, as in

$$\tilde{x}_{t-1} = \rho \tilde{x}_t + y_{t-1} \qquad t \text{ decreasing} \tag{1.21}$$

Thus the adjoint of causal integration is **anticausal integration**.

A module to do these jobs is `leakint`. The code for anticausal integration is not obvious from the code for integration and the adjoint coding tricks we learned earlier. To understand the adjoint, you need to inspect the detailed form of the expression $\tilde{\mathbf{x}} = \mathbf{C}^*\mathbf{y}$ and take care to get the ends correct. Figure 1.5 illustrates the program for $\rho = 1$.

leaky integral.lop

```
module leakint {                                        # leaky integration
real ::     rho
#%  _init( rho)
#%  _lop ( xx,  yy)
integer i, n
real tt
n = size (xx); tt = 0.
if( adj)
        do i= n, 1, -1 {    tt = rho*tt + yy(i)
```

```
                xx(i)  +=  tt
                }
else
        do i= 1, n {        tt  = rho*tt + xx(i)
                yy(i)  +=  tt
                }
}
```

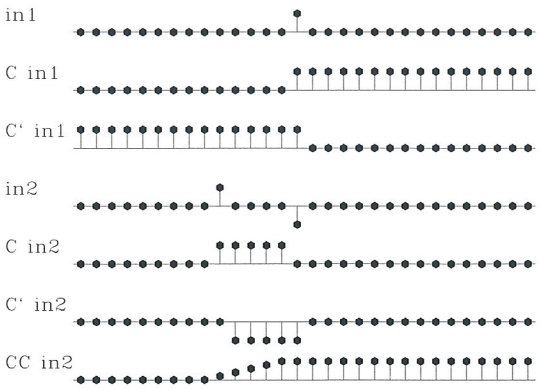

Figure 1.5: `in1` is an input pulse. `C in1` is its causal integral. `C' in1` is the anticausal integral of the pulse. `in2` is a separated doublet. Its causal integration is a box, and its anticausal integration is a negative box. `CC in2` is the double causal integral of `in2`. How can an equilateral triangle be built? VIEW ajt/. causint90

The adjoint has a meaning which is nonphysical. The leaky integration damps both going forward in time and it damps going backward in time, whereas the inverse of leaky integration would grow going backward in time.

Later we will consider equations to march wavefields up towards the earth surface, a layer at a time, an operator for each layer. Then the adjoint will start from the earth surface and march down, a layer at a time, into the earth.

1.1.11 Backsolving, polynomial division and deconvolution

Ordinary differential equations often lead us to the backsolving operator. For example, the damped harmonic oscillator leads to a special case of equation (1.22) where $(a_3, a_4, \cdots) = 0$. There is a huge literature on finite-difference solutions of ordinary differential equations that lead to equations of this type. Rather than derive such an equation on the basis of many possible physical arrangements, we can begin from the filter transformation in (1.4) but put the top square of the matrix on the other side of the equation so our transformation can be called one of inversion or backsubstitution. To link up with applications in later chapters, I specialize to 1's on the main diagonal and insert some bands of zeros.

$$\mathbf{Ay} = \begin{bmatrix} 1 & 0 & 0 & 0 & 0 & 0 & 0 \\ a_1 & 1 & 0 & 0 & 0 & 0 & 0 \\ a_2 & a_1 & 1 & 0 & 0 & 0 & 0 \\ 0 & a_2 & a_1 & 1 & 0 & 0 & 0 \\ 0 & 0 & a_2 & a_1 & 1 & 0 & 0 \\ a_5 & 0 & 0 & a_2 & a_1 & 1 & 0 \\ 0 & a_5 & 0 & 0 & a_2 & a_1 & 1 \end{bmatrix} \begin{bmatrix} y_0 \\ y_1 \\ y_2 \\ y_3 \\ y_4 \\ y_5 \\ y_6 \end{bmatrix} = \begin{bmatrix} x_0 \\ x_1 \\ x_2 \\ x_3 \\ x_4 \\ x_5 \\ x_6 \end{bmatrix} = \mathbf{x} \qquad (1.22)$$

Algebraically, this operator goes under the various names, "**backsolving**", "**polynomial division**", and "**deconvolution**". The **leaky integration** transformation (1.19) is a sim-

ple example of backsolving when $a_1 = -\rho$ and $a_2 = a_5 = 0$. To confirm this, you need to verify that the matrices in (1.22) and (1.19) are mutually inverse.

A typical row in equation (1.22) says

$$x_t = y_t + \sum_{\tau>0} a_\tau \, y_{t-\tau} \tag{1.23}$$

Change the signs of all terms in equation (1.23) and move some terms to the opposite side

$$y_t = x_t - \sum_{\tau>0} a_\tau \, y_{t-\tau} \tag{1.24}$$

Equation (1.24) is a recursion to find y_t from the values of y at earlier times.

In the same way that equation (1.4) can be interpreted as $Y(Z) = B(Z)X(Z)$, equation (1.22) can be interpreted as $A(Z)Y(Z) = X(Z)$ which amounts to $Y(Z) = X(Z)/A(Z)$. Thus, convolution is amounts to polynomial multiplication while the backsubstitution we are doing here is called deconvolution, and it amounts to polynomial division.

A causal operator is one that uses its present and past inputs to make its current output. Anticausal operators use the future but not the past. Causal operators are generally associated with lower triangular matrices and positive powers of Z, whereas **anticausal operators** are associated with upper triangular matrices and negative powers of Z. A transformation like equation (1.22) but with the transposed matrix would require us to run the recursive solution the opposite direction in time, as we did with leaky integration.

A module to backsolve equation 1.22 is `polydiv1`.

deconvolve.lop

```
module polydiv1 {                       # Polynomial division (recursive filtering)
real, dimension (:), pointer :: aa
#%  _init ( aa)
#%  _lop  ( xx, yy)
integer  ia, ix, iy
real     tt
if( adj)
        do ix= size(xx), 1, -1 {
                tt = yy( ix)
                do ia = 1, min( size(aa), size (xx) - ix) {
                        iy = ix + ia
                        tt -=  aa( ia) * xx( iy)
                        }
                xx( ix) = xx( ix) + tt
                }
else
        do iy= 1, size(xx) {
                tt = xx( iy)
                do ia = 1, min( size(aa), iy-1) {
                        ix = iy - ia
                        tt -=  aa( ia) * yy( ix)
                        }
                yy( iy) =  yy( iy) + tt
                }
}
```

We may wonder why the adjoint of $\mathbf{A}\mathbf{y} = \mathbf{x}$ actually is $\mathbf{A}^*\hat{\mathbf{x}} = \mathbf{y}$. With the well known fact that the inverse of a transpose is the transpose of the inverse we have

$$\begin{aligned} \mathbf{y} &= \mathbf{A}^{-1}\mathbf{x} && (1.25)\\ \hat{\mathbf{x}} &= (\mathbf{A}^{-1})^*\mathbf{y} && (1.26)\\ \hat{\mathbf{x}} &= (\mathbf{A}^*)^{-1}\mathbf{y} && (1.27)\\ \mathbf{A}^*\hat{\mathbf{x}} &= \mathbf{y} && (1.28) \end{aligned}$$

1.1.12 The basic low-cut filter

Many geophysical measurements contain very low-frequency noise called "**drift**." For example, it might take some months to survey the depth of a lake. Meanwhile, rainfall or evaporation could change the lake level so that new survey lines become inconsistent with old ones. Likewise, gravimeters are sensitive to atmospheric pressure, which changes with the weather. A magnetic survey of an archeological site would need to contend with the fact that the earth's main magnetic field is changing randomly through time while the survey is being done. Such noises are sometimes called "**secular noise**."

The simplest way to eliminate low frequency noise is to take a time derivative. A disadvantage is that the derivative changes the waveform from a pulse to a doublet (finite difference). Here we examine the most basic low-cut filter. It preserves the waveform at high frequencies, it has an adjustable parameter for choosing the bandwidth of the low cut, and it is causal (uses the past but not the future).

We make a causal lowcut filter (highpass filter) by two stages which can be done in either order.

1. Apply a time derivative, actually a finite difference, convolving the data with $(1, -1)$.
2. Integrate, actually to do a leaky integration, to deconvolve with $(1, -\rho)$ where numerically, ρ is slightly less than unity.

The convolution with $(1, -1)$ ensures that the zero frequency is removed. The leaky integration almost undoes the differentiation but cannot restore the zero frequency. Adjusting the numerical value of ρ has interesting effects in the time domain and in the frequency domain. Convolving the finite difference $(1, -1)$ with the leaky integration $(1, \rho, \rho^2, \rho^3, \rho^4, \cdots)$ gives the result

$$\begin{array}{rl} & (1, \quad \rho, \rho^2, \rho^3, \rho^4, \cdots) \\ - & (0, \quad 1, \rho, \rho^2, \rho^3, \cdots). \end{array}$$

Rearranging, it becomes

$$\begin{array}{rl} & (1, \quad 0, 0, 0, 0, \cdots) \; + \\ (\rho - 1) & (0, \quad 1, \rho, \rho^2, \rho^3, \cdots). \end{array}$$

Since ρ is a tiny bit less than one, $(1 - \rho)$ is a small number. Thus our filter is an impulse followed by the negative of a weak decaying exponential ρ^t. If you prefer a time-symmetric (phaseless) filter, you could follow this one by its time reverse.

Roughly speaking, the cutoff frequency of the filter corresponds to matching one wavelength to the exponential decay time. More formally, the Fourier domain representation of this filter is $H(Z) = (1 - Z)/(1 - \rho Z)$, where Z is the unit-delay operator is $Z = e^{i\omega\Delta t}$ and where ω is the frequency. The spectral response of the filter is $|H(\omega)|$. Were we to plot this function we would see it is nearly 1 everywhere except in a small region near $\omega = 0$ where it becomes tiny. It is called a "low-cut" filter. Figure 1.6 compares a low-cut filter to a finite difference.

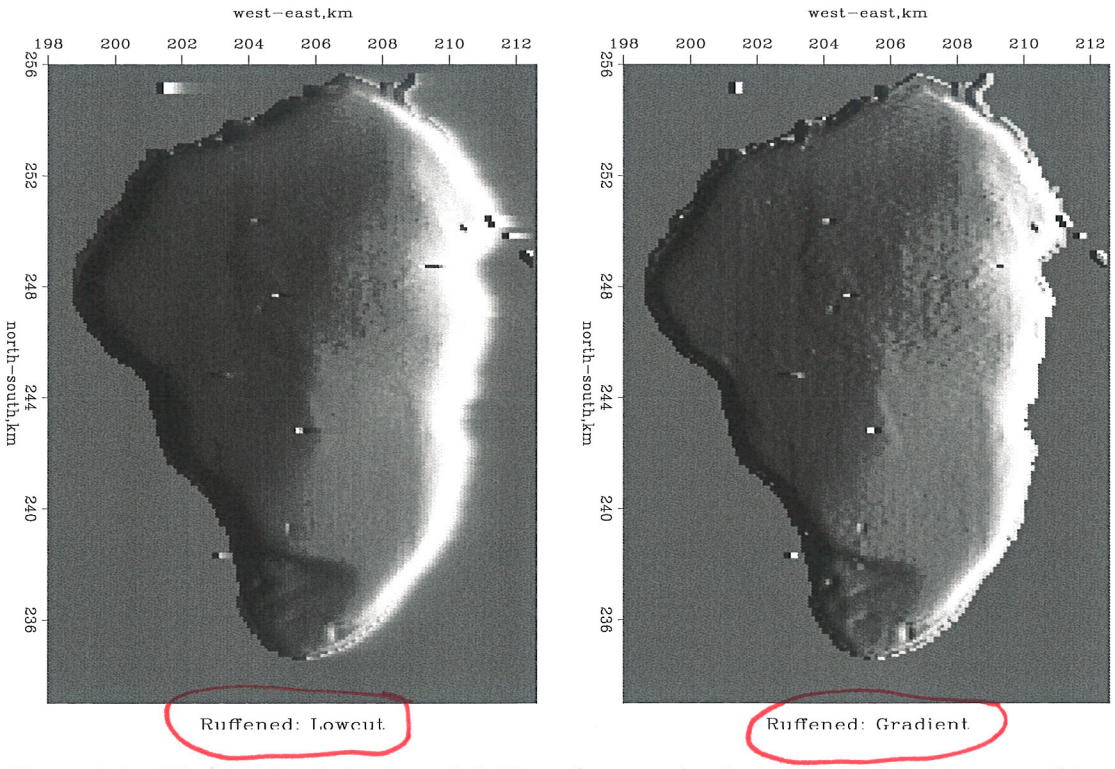

Figure 1.6: The depth of the Sea of Galilee after roughening. On the left, the smoothing is done by low-cut filtering on the horizontal axis. On the right it is a finite difference. We know this because of a few scattered impulses (navigation failure) outside the lake. Both results solve the problem of Figure 1.3 which is too smooth to see interesting features.
ajt/. galocut90

1.1.13 Smoothing with box and triangle

Simple "**smoothing**" is a common application of filtering. A smoothing filter is one with all positive coefficients. On the time axis, smoothing is often done with a single-pole damped exponential function. On space axes, however, people generally prefer a symmetrical function. We will begin with rectangle and triangle functions. When the function width is chosen to be long, then the computation time can be large, but recursion can shorten it immensely.

The inverse of any polynomial reverberates forever, although it might drop off fast enough for any practical need. On the other hand, a rational filter can suddenly drop to

zero and stay there. Let us look at a popular rational filter, the rectangle or "**box car**":

$$\frac{1-Z^5}{1-Z} \quad = \quad 1+Z+Z^2+Z^3+Z^4 \tag{1.29}$$

The filter (1.29) gives a moving average under a *rectangular* window. This is a basic smoothing filter. A clever way to apply it is to move the rectangle by adding a new value at one end while dropping an old value from the other end. This approach is formalized by the polynomial division algorithm, which can be simplified because so many coefficients are either one or zero. To find the recursion associated with $Y(Z) = X(Z)(1-Z^5)/(1-Z)$, we identify the coefficient of Z^t in $(1-Z)Y(Z) = X(Z)(1-Z^5)$. The result is

$$y_t \quad = \quad y_{t-1} + x_t - x_{t-5}. \tag{1.30}$$

This approach boils down to the program `boxconv()` which is so fast it is almost free!

box like smoothing.r90

```
module boxsmooth {
  contains
  subroutine boxconv( nbox, nx, xx, yy) {
    integer,       intent(in)          ::nx,nbox
    integer                            ::i,ny
    real, dimension (:), intent (in) ::xx
    real, dimension (:), intent (out)::yy
    real, dimension (:), allocatable ::bb
    allocate(bb(nx+nbox))
    if( nbox < 1 || nbox > nx)  call erexit('boxconv')  # "||" means .OR.
    ny = nx+nbox-1
    bb(1) = xx(1)
    do i= 2, nx     { bb(i) = bb(i-1) + xx(i) } # B(Z) = X(Z)/(1-Z)
    do i= nx+1, ny { bb(i) = bb(i-1)          }
    do i= 1, nbox     { yy(i) = bb(i)          }
    do i= nbox+1, ny { yy(i) = bb(i) - bb(i-nbox)} # Y(Z) = B(Z)*(1-Z**nbox)
    do i= 1, ny     { yy(i) = yy(i) / nbox     }
    deallocate(bb)
  }
}
```

Its last line scales the output by dividing by the rectangle length. With this scaling, the zero-frequency component of the input is unchanged, while other frequencies are suppressed.

Triangle smoothing is rectangle smoothing done twice. For a mathematical description of the triangle filter, we simply square equation (1.29). Convolving a rectangle function with itself many times yields a result that mathematically tends towards a **Gaussian** function. Despite the sharp corner on the top of the triangle function, it has a shape that is remarkably similar to a Gaussian. Convolve a triangle with itself and you will see a very nice approximation to a Gaussian (the central limit theorem).

With filtering, **end effects** can be a nuisance. Filtering increases the length of the data, but people generally want to keep input and output the same length (for various practical reasons). This is particularly true when filtering a space axis. Suppose the five-point signal $(1,1,1,1,1)$ is smoothed using the `boxconv()` program with the three-point smoothing filter $(1,1,1)/3$. The output is $5+3-1$ points long, namely, $(1,2,3,3,3,2,1)/3$. We could simply abandon the points off the ends, but I like to **fold** them back in, getting

instead $(1+2, 3, 3, 3, 1+2)$. An advantage of the folding is that a constant-valued signal is unchanged by the smoothing. This is desirable since a smoothing filter is a low-pass filter which naturally should pass the lowest frequency $\omega = 0$ without distortion. The result is like a wave reflected by a **zero-slope** end condition. Impulses are smoothed into triangles except near the boundaries. What happens near the boundaries is shown in Figure 1.7. Note that at the boundary, there is necessarily only half a triangle, but it is twice as tall.

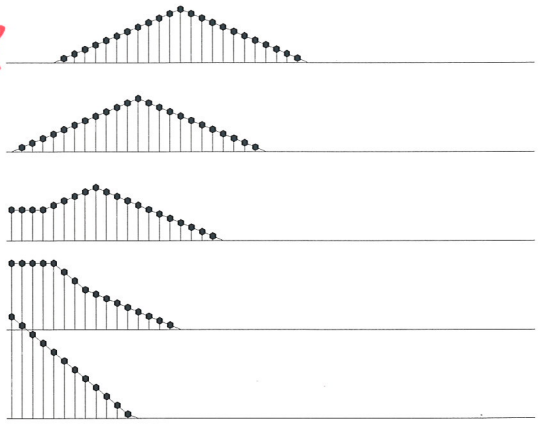

Figure 1.7: Edge effects when smoothing an impulse with a triangle function. Inputs are spikes at various distances from the edge. VIEW ajt/. triend

Why might this be useful? Consider a survey of water depth in an area of the deep ocean. All the depths are strongly positive with interesting but small variations on them. Ordinarily we can enhance high frequency fluctuations by one minus a low pass filter, say $H = 1 - L$. If this is to work, however, it is important that the L truly cancel the 1 near zero frequency.

Figure 1.7 was derived from the routine `triangle()`.

1D triangle smoothing.r90

```
module trianglesmooth { # Convolve with triangle
  use boxsmooth
  contains
  subroutine triangle( nbox, nd, xx, yy) {
    integer,        intent(in)       ::nbox,nd
    integer                          ::i,np,nq
    real, dimension (:), intent (in) ::xx
    real, dimension (:), intent (out)::yy
    real, dimension (:), allocatable ::pp,qq
    allocate(pp(nd+nbox-1), qq(nd+nbox+nbox-2))
    call boxconv( nbox, nd, xx, pp);     np = nbox+nd-1
    call boxconv( nbox, np, pp, qq);     nq = nbox+np-1
    do i=1,nd      { yy(i)      =              qq(i+nbox-1)      }
    do i=1,nbox-1 { yy(i)      =yy(i)       + qq(nbox-i   )      } # fold back
    do i=1,nbox-1 { yy(nd-i+1)=yy(nd-i+1) + qq(nd+(nbox-1)+i)} # fold back
    deallocate(pp,qq)
  }}
```

1.1.14 Nearest-neighbor normal moveout (NMO)

Normal-moveout correction (**NMO**) is a geometrical correction of reflection seismic data that stretches the time axis so that data recorded at nonzero separation x_0 of shot and

receiver, after stretching, appears to be at $x_0 = 0$. NMO correction is roughly like time-to-depth conversion with the equation $v^2t^2 = z^2 + x_0^2$. After the data at x_0 is stretched from t to z, it should look like stretched data from any other x (assuming these are plane horizontal reflectors, etc.). In practice, z is not used; rather, **traveltime depth** τ is used, where $\tau = z/v$; so $t^2 = \tau^2 + x_0^2/v^2$. (Because of the limited alphabet of programming languages, I often use the keystroke `z` to denote τ.)

Typically, many receivers record each shot. Each seismogram can be transformed by NMO and the results all added. This is called "**stacking**" or "**NMO stacking.**" The adjoint to this operation is to begin from a model which ideally is the zero-offset trace and spray this model to all offsets. From a matrix viewpoint, stacking is like a *row* vector of normal moveout operators and modeling is like a *column*. An example is shown in Figure 1.8.

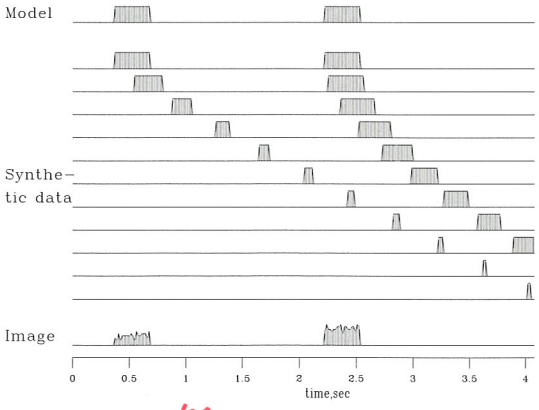

Figure 1.8: Hypothetical model, synthetic data, and model image. VIEW ajt/. cunha

We'll be making operators from other operators. Given operators **A** and **B**, another operator is the is the product **AB**. Still another is the row matrix [**A B**]. We'll consider those soon. Even more tricky than a matrix containing operators is an operator containing operators. This situation gave me a programming bug that took me quite a while to digest, and even longer to explain to others. The essential feature to keep in mind is that the external world will pass your operator module an `adj,add` pair. Likewise, internal to your module will be your own `adj,add` pair that you are feeding to the operator you are calling. Don't confuse the different pairs! Our habit that physical modeling is done without adjoint likely means both pairs have the same `adj`, but there is no reason to predict the two pairs will have the same `add`.

A module that does reverse moveout is `hypotenusei`. Given a zero-offset trace, it makes another at non-zero offset. The adjoint does the usual normal moveout correction.

inverse moveout.lop

```
module hypotenusei {                                    # Inverse normal moveout
integer :: nt
integer, dimension (nt), allocatable :: iz
#%  _init( nt, t0, dt, xs)
integer it
real t0, dt, xs, t, zsquared
do it= 1, nt {  t = t0 + dt*(it-1)
        zsquared =  t * t - xs * xs
        if ( zsquared >= 0.)
```

```
                iz (it) = 1.5 + (sqrt( zsquared) - t0) /dt
        else
                iz (it) = 0
        }
#% _lop(   zz, tt)
integer   it
do it= 1, nt {
        if ( iz (it) > 0 ) {
                        if( adj)   zz( iz(it))  += tt(    it )
                        else       tt(it)       += zz( iz(it))
                }
        }
}
```

(My 1992 textbook (PVI) illustrates many additional features of normal moveout.) A companion routine `imospray` loops over offsets and makes a trace for each. The adjoint of `imospray` is the industrial process of moveout and stack.

inverse NMO spray.lop

```
module imospray {                       # inverse moveout and spray into a gather.
use hypotenusei
real :: x0,dx, t0,dt
integer :: nx,nt
#% _init (slow, x0,dx, t0,dt, nt,nx)
                real slow
                x0 = x0*slow
                dx = dx*slow
#% _lop(  stack(nt),    gather(nt,nx))
integer ix, stat
do ix= 1, nx {
        call hypotenusei_init ( nt, t0, dt, x0 + dx*(ix-1))
        stat = hypotenusei_lop ( adj, .true., stack, gather(:,ix))
        }
call hypotenusei_close ()
}
```

1.1.15 Coding chains and arrays

With a collection of operators, we can build more elaborate operators. An amazing thing about matrices is that their elements may themselves be matrices. A row is a matrix containing two matrices. This is done by subroutine `row0` also in module `smallchain3`. An operator product $\mathbf{A} = \mathbf{BC}$ is represented in the subroutine `chain2( op1, op2, ...)`. As you read these codes, please remember the output is the last argument only when the output is $\mathbf{d}$. When the output is $\mathbf{m}$, the output is the second from last.

operator chain and array.r90

```
module smallchain3 {
  logical , parameter, private :: AJ = .true., FW = .false.
  logical , parameter, private :: AD = .true., ZP = .false.
  interface chain0{
     module procedure column0
     module procedure row0
     module procedure chain20
     module procedure chain30
```

```
  }
contains

  subroutine column0(op1,op2, adj,add, m,d1,d2) { # COLUMN  d1 = Am, d2 = Bm
    interface {
       integer function op1(adj,add,m,d){real::m(:),d(:);logical::adj,add}
       integer function op2(adj,add,m,d){real::m(:),d(:);logical::adj,add}
    }
    logical, intent(in) :: adj, add
    real, dimension(:)  :: m,d1,d2
    integer             :: st

    if(adj) {  st = op1(AJ, add, m, d1)          # m = m0 + A' d1
               st = op2(AJ,  AD, m, d2)          # m = m  + B' d2
    }
    else    {  st = op1(FW, add, m, d1)          # d1 = d1 + A  m
               st = op2(FW, add, m, d2)          # d2 = d2 + B  m
    }
  }

  subroutine row0(op1,op2, adj,add, m1, m2, d) { # ROW  d = Am1+Bm2
    interface {
       integer function op1(adj,add,m,d){real::m(:),d(:);logical::adj,add}
       integer function op2(adj,add,m,d){real::m(:),d(:);logical::adj,add}
    }
    logical, intent (in) :: adj, add
    real, dimension (:)  :: m1,m2,d
    integer              :: st

    if (adj) { st = op1 (AJ, add, m1, d)         # m1 = A'd
               st = op2 (AJ, add, m2, d)         # m2 = B'd
    }
    else {     st = op2 (FW, add, m2, d)    # d = Bm2
               st = op1 (FW,  AD, m1, d)    # d = Am1+Bm2
    }
  }

  subroutine chain20(op1,op2, adj,add, m,d,t1) { # CHAIN 2  d = ABm
    interface {
       integer function op1(adj,add,m,d){real::m(:),d(:);logical::adj,add}
       integer function op2(adj,add,m,d){real::m(:),d(:);logical::adj,add}
    }
    logical, intent(in) :: adj, add
    real, dimension(:)  :: m,d, t1
    integer             :: st
    if(adj) {  st = op1(AJ,  ZP, t1, d)          #        t =    A' d
               st = op2(AJ, add, m, t1)          # m = B' t = B' A' d
    }
    else    {  st = op2(FW,  ZP, m, t1)          #        t =    B  m
               st = op1(FW, add, t1, d)          # d = A  t = A  B  m
    }
  }

  subroutine chain30(op1,op2,op3, adj,add, m,d,t1,t2) { # CHAIN 3  d = ABCm
    interface {
       integer function op1(adj,add,m,d){real::m(:),d(:);logical::adj,add}
       integer function op2(adj,add,m,d){real::m(:),d(:);logical::adj,add}
       integer function op3(adj,add,m,d){real::m(:),d(:);logical::adj,add}
    }
```

```
    logical , intent(in) :: adj, add
    real , dimension(:)  :: m,d, t1,t2
    integer              :: st
    if(adj) {  st = op1(AJ,  ZP, t2, d )  #                t1 =      A' d
               st = op2(AJ,  ZP, t1, t2)  #          t2 = B' t1 =   B' A' d
               st = op3(AJ, add, m , t1)  # m  = C' t2 =       C' B' A' d
    }
    else    {  st = op3(FW,  ZP, m , t1)  #                t1 =      C  m
               st = op2(FW,  ZP, t1, t2)  #          t2 = B  t1 =   B  C  m
               st = op1(FW, add, t2, d )  # d  = A  t2 =       A  B  C  m
    }
  }

}
```

1.2 ADJOINT DEFINED: DOT-PRODUCT TEST

Having seen many examples of **spaces**, operators, and adjoints, we should now see more formal definitions because abstraction helps us push these concepts to their limits.

1.2.1 Definition of a vector space

An operator transforms a **space** to another space. Examples of spaces are model space $\mathbf{m}$ and data space $\mathbf{d}$. We think of these spaces as vectors whose components are packed with numbers, either real or complex numbers. The important practical concept is that not only does this packing include one-dimensional spaces like signals, two-dimensional spaces like images, 3-D movie cubes, and zero-dimensional spaces like a data mean, etc, but spaces can be sets of all the above. One space that is a set of three cubes is the earth's magnetic field, which has three components; and each component is a function of a three-dimensional space. (The 3-D *physical space* we live in is not the abstract ***vector space*** of models and data so abundant in this book. Here the word "space" without an adjective means the vector space.)

A more heterogeneous example of a vector space is **data tracks**. A depth-sounding survey of a lake can make a vector space that is a collection of tracks, a vector of vectors (each vector having a different number of components, because lakes are not square). This vector space of depths along tracks in a lake contains the depth values only. The (x, y)-coordinate information locating each measured depth value is (normally) something outside the vector space. A data space could also be a collection of echo soundings, waveforms recorded along tracks.

We briefly recall information about vector spaces found in elementary books: Let α be any scalar. Then if $\mathbf{d}_1$ is a vector and $\mathbf{d}_2$ is conformable with it, then other vectors are $\alpha\mathbf{d}_1$ and $\mathbf{d}_1 + \mathbf{d}_2$. The size measure of a vector is a positive value called a norm. The norm is usually defined to be the **dot product** (also called the L_2 **norm**), say $\mathbf{d} \cdot \mathbf{d}$. For complex data it is $\bar{\mathbf{d}} \cdot \mathbf{d}$ where $\bar{\mathbf{d}}$ is the complex conjugate of $\mathbf{d}$. A notation that does transpose and complex conjugate at the same time is $\mathbf{d}^* \mathbf{d}$. In theoretical work the "size of a vector" means the vector's norm. In computational work the "size of a vector" means the number of components in the vector.

Norms generally include a **weighting function**. In physics, the norm generally measures a conserved quantity like energy or momentum; so, for example, a weighting function for magnetic flux is permittivity. In data analysis, the proper choice of the weighting function is a practical statistical issue, discussed repeatedly throughout this book. The algebraic view of a weighting function is that it is a diagonal matrix with positive values $w(i) \geq 0$ spread along the diagonal, and it is denoted $\mathbf{W} = \mathbf{diag}[w(i)]$. With this weighting function the L_2 norm of a data space is denoted $\mathbf{d}^*\mathbf{W}\mathbf{d}$. Standard notation for norms uses a double absolute value, where $||\mathbf{d}|| = \mathbf{d}^*\mathbf{W}\mathbf{d}$. A central concept with norms is the triangle inequality, $||\mathbf{d}_1 + \mathbf{d}_2|| \leq ||\mathbf{d}_1|| + ||\mathbf{d}_2||$ whose proof you might recall (or reproduce with the use of dot products).

1.2.2 Dot-product test for validity of an adjoint

There is a huge gap between the conception of an idea and putting it into practice. During development, things fail far more often than not. Often, when something fails, many tests are needed to track down the cause of failure. Maybe the cause cannot even be found. More insidiously, failure may be below the threshold of detection and poor performance suffered for years. The **dot-product test** enables us to ascertain whether the program for the adjoint of an operator is precisely consistent with the operator itself. It can be, and it should be.

Conceptually, the idea of matrix transposition is simply $a'_{ij} = a_{ji}$. In practice, however, we often encounter matrices far too large to fit in the memory of any computer. Sometimes it is also not obvious how to formulate the process at hand as a matrix multiplication. (Examples are differential equations and fast Fourier transforms.) What we find in practice is that an operator and its adjoint are two routines. The first amounts to the matrix multiplication $\mathbf{F}\mathbf{m}$. The adjoint routine computes $\mathbf{F}^*\mathbf{d}$, where $\mathbf{F}^*$ is the **conjugate-transpose** matrix. In later chapters we will be solving huge sets of simultaneous equations in which both routines are required. If the pair of routines are inconsistent, we may be doomed from the start. The dot-product test is a simple test for verifying that the two routines are adjoint to each other.

I'll tell you first what the dot-product test is, and then explain how it works. Take a model space vector $\mathbf{m}$ filled with random numbers, and likewise a data space vector $\mathbf{d}$ filled with random numbers. Use your forward modeling code to compute:

$$\mathbf{m} \Leftarrow \text{random} \tag{1.31}$$
$$\mathbf{d} \Leftarrow \text{random} \tag{1.32}$$
$$\hat{\mathbf{d}} = \mathbf{F}\mathbf{m} \tag{1.33}$$
$$\hat{\mathbf{m}} = \mathbf{F}^*\mathbf{d} \tag{1.34}$$

You should find these two inner products equal:

$$\hat{\mathbf{m}} \cdot \mathbf{m} = \hat{\mathbf{d}} \cdot \mathbf{d} \tag{1.35}$$

If they are, it means what you coded for $\mathbf{F}^*$ is indeed the adjoint of $\mathbf{F}$. There is a glib way of saying why this must be so:

$$\mathbf{d}^*(\mathbf{F}\mathbf{m}) = (\mathbf{d}^*\mathbf{F})\mathbf{m} \tag{1.36}$$
$$\mathbf{d}^*(\mathbf{F}\mathbf{m}) = (\mathbf{F}^*\mathbf{d})^*\mathbf{m} \tag{1.37}$$

This glib way is easily made concrete with explicit summation. We may express $\sum_i \sum_j d_i F_{ij} m_j$ in two different ways:

$$\sum_i d_i (\sum_j F_{ij} m_m) = \sum_j (\sum_i d_i F_{ij}) m_j \tag{1.38}$$

$$= \sum_j (\sum_i F_{ij} d_i) m_j \tag{1.39}$$

$$\mathbf{d}^* \cdot (\mathbf{F}\mathbf{m}) = (\mathbf{F}^* \mathbf{d}) \cdot \mathbf{m} \tag{1.40}$$

$$\mathbf{d}^* \cdot \hat{\mathbf{d}} = \hat{\mathbf{m}} \cdot \mathbf{m} \tag{1.41}$$

Should $\mathbf{F}$ contain complex numbers, the dot-product test is a comparison for both real parts and for imaginary parts.

The program for applying the dot product test is `dot_test`. The Fortran way of passing a linear operator as an argument is to specify the function interface. Fortunately, we have already defined the interface for a generic linear operator. To use the `dot_test` program, you need to initialize an operator with specific arguments (the `_init` subroutine) and then pass the operator itself (the `_lop` function) to the test program. You also need to specify the sizes of the model and data vectors so that temporary arrays can be constructed. The program runs the dot product test twice, second time with `add = .true.` to test if the operator can be used properly for accumulating results, for example. $\mathbf{d} \leftarrow \mathbf{d} + \mathbf{F}\mathbf{m}$.

I ran the dot product test on many operators and was surprised and delighted to find that for small operators it is generally satisfied to an accuracy near the computing precision. For large operators, precision can become and issue. Every time I encountered a relative discrepancy of 10^{-5} or more on a small operator (small data and model spaces) I was later able to uncover a conceptual or programming error. Naturally, when I run dot-product tests, I scale the implied matrix to a small size both to speed things along and to be sure that boundaries are not overwhelmed by the much larger interior.

Do not be alarmed if the operator you have defined has **truncation** errors. Such errors in the definition of the original operator should be matched by like errors in the adjoint operator. If your code passes the **dot-product test**, then you really have coded the adjoint operator. In that case, to obtain inverse operators, you can take advantage of the standard methods of mathematics.

We can speak of a **continuous function** $f(t)$ or a **discrete function** f_t. For continuous functions we use integration, and for discrete ones we use summation. In formal mathematics, the dot-product test *defines* the adjoint operator, except that the summation in the dot product may need to be changed to an integral. The input or the output or both can be given either on a continuum or in a discrete domain. So the dot-product test $\hat{\mathbf{m}} \cdot \mathbf{m} = \hat{\mathbf{d}} \cdot \mathbf{d}$ could have an integration on one side of the equal sign and a summation on the other. Linear-operator theory is rich with concepts not developed here.

1.2.3 Automatic adjoints

Computers are not only able to perform computations; they can do mathematics. Well known software is Mathematica and Maple. Adjoints can also be done by symbol manipulation. For example Ralf Giering offers a program for converting linear operator programs

into their adjoints. Actually, it does more than that. He says:[3]

> Given a Fortran routine (or collection of routines) for a function, TAMC produces Fortran routines for the computation of the derivatives of this function. The derivatives are computed in the reverse mode (adjoint model) or in the forward mode (tangent-linear model). In both modes Jacobian-Matrix products can be computed.

1.2.4 The word "adjoint"

In mathematics the word "**adjoint**" has two meanings. One of them, the so-called **Hilbert adjoint**, is the one generally found in physics and engineering and it is the one used in this book. In linear algebra is a different matrix, called the **adjugate** matrix. It is a matrix whose elements are signed cofactors (minor determinants). For invertible matrices, this matrix is the **determinant** times the **inverse matrix**. It can be computed without ever using division, so potentially the adjugate can be useful in applications where an inverse matrix does not exist. Unfortunately, the adjugate matrix is sometimes called the adjoint matrix, particularly in the older literature. Because of the confusion of multiple meanings of the word adjoint, in the first printing of PVI, I avoided the use of the word and substituted the definition, "**conjugate transpose**". Unfortunately, this was often abbreviated to "conjugate," which caused even more confusion. Thus I decided to use the word adjoint and have it always mean the Hilbert adjoint found in physics and engineering.

1.2.5 Inverse operator

A common practical task is to fit a vector of observed data $\mathbf{d}_{\text{obs}}$ to some modeled data $\mathbf{d}_{\text{model}}$ by the adjustment of components in a vector of model parameters $\mathbf{m}$.

$$\mathbf{d}_{\text{obs}} \approx \mathbf{d}_{\text{model}} = \mathbf{F}\mathbf{m} \tag{1.42}$$

A huge volume of literature establishes theory for two estimates of the model, $\hat{\mathbf{m}}_1$ and $\hat{\mathbf{m}}_2$, where

$$\hat{\mathbf{m}}_1 = (\mathbf{F}^*\mathbf{F})^{-1}\mathbf{F}^*\mathbf{d} \tag{1.43}$$
$$\hat{\mathbf{m}}_2 = \mathbf{F}^*(\mathbf{F}\mathbf{F}^*)^{-1}\mathbf{d} \tag{1.44}$$

Some reasons for the literature being huge are the many questions about the existence, quality, and cost of the inverse operators. Before summarizing that, let us quickly see why these two solutions are reasonable. Inserting equation (1.42) into equation (1.43), and inserting equation (1.44) into equation (1.42), we get the reasonable statements:

$$\hat{\mathbf{m}}_1 = (\mathbf{F}^*\mathbf{F})^{-1}(\mathbf{F}^*\mathbf{F})\mathbf{m} = \mathbf{m} \tag{1.45}$$
$$\hat{\mathbf{d}}_{\text{model}} = (\mathbf{F}\mathbf{F}^*)(\mathbf{F}\mathbf{F}^*)^{-1}\mathbf{d} = \mathbf{d} \tag{1.46}$$

Equation (1.45) says that the estimate $\hat{\mathbf{m}}_1$ gives the correct model $\mathbf{m}$ if you start from the modeled data. Equation (1.46) says that the model estimate $\hat{\mathbf{m}}_2$ gives the modeled data if

[3] http://www.autodiff.com/tamc/

we derive $\hat{\mathbf{m}}_2$ from the modeled data. Both of these statements are delightful. Now let us return to the problem of the inverse matrices.

Normally a rectangular matrix does not have an inverse. Surprising things often happen, but commonly, when $\mathbf{F}$ is a tall matrix (more data values than model values) then the matrix for finding $\hat{\mathbf{m}}_1$ is invertible while that for finding $\hat{\mathbf{m}}_2$ is not; and when the matrix is wide instead of tall (the number of data values is less than the number of model values) it is the other way around. In many applications neither $\mathbf{F}^*\mathbf{F}$ nor $\mathbf{F}\mathbf{F}^*$ is invertible. This difficulty is solved by "**damping**" as we will see in later chapters. If it happens that $\mathbf{F}\mathbf{F}^*$ or $\mathbf{F}^*\mathbf{F}$ equals $\mathbf{I}$ (unitary operator), then the adjoint operator $\mathbf{F}^*$ is the inverse $\mathbf{F}^{-1}$ by either equation (1.43) or (1.44).

Current computational power limits matrix inversion jobs to about 10^4 variables. This book specializes in big problems, those with more than about 10^4 variables. The iterative methods we learn here for giant problems are also excellent for smaller problems, so we rarely here speak of inverse matrices or worry much if neither $\mathbf{F}\mathbf{F}^*$ nor $\mathbf{F}^*\mathbf{F}$ is an identity.

circled wording has been previously addressed in my comments list

Chapter 2

Model fitting by least squares

The first level of computer use in science and engineering is **modeling**. Beginning from physical principles and design ideas, the computer mimics nature. After this, the worker looks at the result and thinks a while, then alters the modeling program and tries again. The next, deeper level of computer use is that the computer itself examines the results of modeling and reruns the modeling job. This deeper level is variously called "**fitting**" or "**estimation**" or "**inversion**." We inspect the **conjugate-direction method** of fitting and write a subroutine for it that will be used in most of the examples in this book.

2.1 UNIVARIATE LEAST SQUARES

A single parameter fitting problem arises in Fourier analysis, where we seek a "best answer" at each frequency, then combine all the frequencies to get a best signal. Thus emerges a wide family of interesting and useful applications. However, Fourier analysis first requires us to introduce complex numbers into statistical estimation.

Multiplication in the Fourier domain is **convolution** in the time domain. Fourier-domain division is time-domain **deconvolution**. This division is challenging when F has observational error. Failure erupts if zero division occurs. More insidious are the poor results we obtain when zero division is avoided by a near miss.

2.1.1 Dividing by zero smoothly

Think of any real numbers x, y, and f and any program containing $x = y/f$. How can we change the program so that it never divides by zero? A popular answer is to change $x = y/f$ to $x = yf/(f^2 + \epsilon^2)$, where ϵ is any tiny value. When $|f| >> |\epsilon|$, then x is approximately y/f as expected. But when the divisor f vanishes, the result is safely zero instead of infinity. The transition is smooth, but some criterion is needed to choose the value of ϵ. This method may not be the only way or the best way to cope with **zero division**, but it is a good way, and it permeates the subject of signal analysis.

To apply this method in the Fourier domain, suppose that X, Y, and F are complex numbers. What do we do then with $X = Y/F$? We multiply the top and bottom by the

complex conjugate $\overline{F}$, and again add ϵ^2 to the denominator. Thus,

$$X(\omega) \quad = \quad \frac{\overline{F(\omega)}\, Y(\omega)}{\overline{F(\omega)} F(\omega) \;+\; \epsilon^2} \tag{2.1}$$

Now the denominator must always be a positive number greater than zero, so division is always safe. Equation (2.1) ranges continuously from **inverse filtering**, with $X = Y/F$, to filtering with $X = \overline{F}Y$, which is called "**matched filtering**." Notice that for any complex number F, the phase of $1/F$ equals the phase of $\overline{F}$, so the filters have the same phase.

2.1.2 Damped solution

Another way to say $x = y/f$ is to say $fx - y$ is small, or $(fx-y)^2$ is small. This doesn't solve the problem of f going to zero, so we need the idea that x^2 does not get too big. To find x we minimize the quadratic function in x.

$$Q(x) \quad = \quad (fx-y)^2 + \epsilon^2 x^2 \tag{2.2}$$

The second term is called a "**damping** factor" because it prevents x from going to $\pm\infty$ when $f \to 0$. Set $dQ/dx = 0$, which gives

$$0 \quad = \quad f(fx-y) + \epsilon^2 x \tag{2.3}$$

This yields our earlier common-sense answer $x = fy/(f^2+\epsilon^2)$. It also leads is to wider areas of application where the elements are complex vectors and matrices.

With Fourier transforms, the signal X is a complex number at each frequency ω. So we generalize equation (2.2) to

$$Q(\bar{X}, X) \quad = \quad (\overline{FX-Y})(FX-Y) + \epsilon^2 \bar{X} X \quad = \quad (\bar{X}\bar{F} - \bar{Y})(FX-Y) + \epsilon^2 \bar{X} X \tag{2.4}$$

To minimize Q we could use a real-values approach, where we express $X = u + iv$ in terms of two real values u and v and then set $\partial Q/\partial u = 0$ and $\partial Q/\partial v = 0$. The approach we will take, however, is to use complex values, where we set $\partial Q/\partial X = 0$ and $\partial Q/\partial \bar{X} = 0$. Let us examine $\partial Q/\partial \bar{X}$:

$$\frac{\partial Q(\bar{X}, X)}{\partial \bar{X}} \quad = \quad \bar{F}(FX-Y) + \epsilon^2 X \quad = \quad 0 \tag{2.5}$$

The derivative $\partial Q/\partial X$ is the complex conjugate of $\partial Q/\partial \bar{X}$. So if either is zero, the other is too. Thus we do not need to specify both $\partial Q/\partial X = 0$ and $\partial Q/\partial \bar{X} = 0$. I usually set $\partial Q/\partial \bar{X}$ equal to zero. Solving equation (2.5) for X gives equation (2.1).

Equation (2.1) solves $Y = XF$ for X, giving the solution for what is called "the **deconvolution** problem with a known wavelet F." Analogously we can use $Y = XF$ when the filter F is unknown, but the input X and output Y are given. Simply interchange X and F in the derivation and result.

2.1.3 Formal path to the low-cut filter

This book defines many geophysical estimation applications. Many of them amount to statement of two goals. The first goal is a data fitting goal, the goal that the model should

imply some observed data. The second goal is that the model be not too big or too wiggly. We will state these goals as two residuals, each of which is ideally zero. A very simple data fitting goal would be that the model m equals the data d, thus the difference should vanish, say $0 \approx m - d$. A more interesting goal is that the model should match the data especially at high frequencies but not necessarily at low frequencies.

$$0 \quad \approx \quad -i\omega(m-d) \tag{2.6}$$

A danger of this goal is that the model could have a zero-frequency component of infinite magnitude as well as large amplitudes for low frequencies. To suppress this, we need the second goal, a model residual which is to be minimized. We need a small number ϵ. The model goal is

$$0 \quad \approx \quad \epsilon\, m \tag{2.7}$$

To see the consequence of these two goals, we add the squares of the residuals

$$Q(m) \quad = \quad \omega^2(m-d)^2 + \epsilon^2 m^2 \tag{2.8}$$

and then we minimize $Q(m)$ by setting its derivative to zero

$$0 \quad = \quad \frac{dQ}{dm} \quad = \quad 2\omega^2(m-d) + 2\epsilon^2 m \tag{2.9}$$

or

$$m \quad = \quad \frac{\omega^2}{\omega^2+\epsilon^2}\, d \tag{2.10}$$

Let us rename ϵ to give it physical units of frequency $\omega_0 = \epsilon$. Our expression says says m will match d except for low frequencies $|m| < |\omega_0|$ where it will tend to zero. This defines a low-cut filter with "cut-off frequency" ω_0.

2.1.4 The plane-wave destructor

We address the question of shifting signals into best alignment. The most natural approach might seem to be via cross correlations. That is indeed a good approach when signals are shifted by large amounts. Here we assume signals are shifted by small amounts, often less than a single pixel. We'll take an approach closely related to differential equations. Consider this definition of a residual.

$$0 \quad \approx \quad \text{residual}(t,x) \quad = \quad \left(\frac{\partial}{\partial x} + p\frac{\partial}{\partial t}\right) u(t,x) \tag{2.11}$$

By taking derivatives we see the residual vanishes when the two-dimensional observation $u(t,x)$ matches the equation of moving waves $u(t-px)$. The parameter p has units inverse to velocity, the velocity of propagation.

In practice, $u(t,x)$ might not be a perfect wave but an observed field of many waves that we might wish to fit to the idea of a single wave of a single p. We seek the parameter p. First we need a method of discretization that allows the mesh for $\partial du/\partial dt$ to overlay exactly $\partial u/\partial x$. To this end I chose to represent the t-derivative by averaging a finite difference at x with one at $x + \Delta x$.

$$\frac{\partial u}{\partial t} \approx \frac{1}{2}\left(\frac{u(t+\Delta t,x)-u(t,x)}{\Delta t}\right)+\frac{1}{2}\left(\frac{u(t+\Delta t,x+\Delta x)-u(t,x+\Delta x)}{\Delta t}\right) \tag{2.12}$$

Likewise there is an analogous expression for the x-derivative with t and x interchanged. The function $u(t,x)$ lies on a grid, and the differencing operator $\delta_x+p\delta_t$ lies atop it and convolves across it. The operator is a 2×2 convolution filter. We may represent equation (2.11) as a matrix operation,

$$\mathbf{0} \approx \mathbf{r}=\mathbf{A}\mathbf{u} \tag{2.13}$$

where the two-dimensional convolution with the difference operator is denoted $\mathbf{A}$.

The module `wavekill()` applies the operator $a\delta_x+b\delta_t$. Suitable choices of a and b give us the operators we need, namely $\delta_x, \delta_t, \delta_x+p_i\delta_t$.

wavekill().r90

```
module wavekill_mod{
  contains
  subroutine wavekill(aa,bb,nt,nx,uu,vv){
    real    :: aa,bb(:,:),uu(:,:),vv(:,:)
    integer :: it,ix,nt,nx
    real    :: s11(nt,nx),s12(nt,nx),s21(nt,nx),s22(nt,nx)
    s11 = -aa-bb;    s12 = aa-bb
    s21 = -aa+bb;    s22 = aa+bb
    vv=0.
    do ix=1,nx-1{
      do it=1,nt-1{
        vv(it,ix)=uu(it  ,ix  )*s11(it,ix)+&
                  uu(it  ,ix+1)*s12(it,ix)+&
                  uu(it+1,ix  )*s21(it,ix)+&
                  uu(it+1,ix+1)*s22(it,ix)
      }
    }
    vv(nt,:)=vv(nt-1,:)
    vv(:,nx)=vv(:,nx-1)
  }
}
```

Now let us find the numerical value of p that fits a plane wave $u(t-px)$ to observations $u(t,x)$. Let $\mathbf{x}$ be an abstract vector whose components are values of $\partial u/\partial x$ taken everywhere on a 2-D mesh in (t,x). Likewise, let $\mathbf{t}$ contain $\partial u/\partial t$. Since we want $\mathbf{x}+p\mathbf{t}\approx\mathbf{0}$, we minimize the quadratic function of p,

$$Q(p)=(\mathbf{x}+p\mathbf{t})\cdot(\mathbf{x}+p\mathbf{t}) \tag{2.14}$$

by setting to zero the derivative. We get

$$p = -\frac{\mathbf{x}\cdot\mathbf{t}}{\mathbf{t}\cdot\mathbf{t}} \tag{2.15}$$

Since data will not always fit the model very well, it may be helpful to have some way to measure how good the fit is. I suggest

$$C^2 = 1-\frac{(\mathbf{x}+p\mathbf{t})\cdot(\mathbf{x}+p\mathbf{t})}{\mathbf{x}\cdot\mathbf{x}} \tag{2.16}$$

which, on inserting $p = -(\mathbf{x} \cdot \mathbf{t})/(\mathbf{t} \cdot \mathbf{t})$, leads to C, where

$$C = \frac{\mathbf{x} \cdot \mathbf{t}}{\sqrt{(\mathbf{x} \cdot \mathbf{x})(\mathbf{t} \cdot \mathbf{t})}} \tag{2.17}$$

is known as the "**normalized correlation**." The program for this calculation is straightforward. The name `puck2d()` denotes *picking* on a continuum.

puck2d().r90

```
module puck2d_mod{
  use triangle_smooth
  use wavekill_mod
  contains
  subroutine puck2d(dat,coh,pp,res,boxsz,nt,nx){
    integer                 :: it,ix,nt,nx
    integer, intent( in) :: boxsz
    real,    intent( in) :: dat(:,:)
    real,    intent(out) :: coh(:,:),pp(:,:),res(:,:)
    real :: dt(nt,nx),dx(nt,nx),dtdt(nt,nx),dtdx(nt,nx),dxdx(nt,nx)
    pp=0.; call wavekill(1.,pp,nt,nx,dat,dx) # space derivative
    pp=1.; call wavekill(0.,pp,nt,nx,dat,dt) #  time derivative
    dtdx = dt*dx     # (x.t)
    dxdx = dx*dx     # (x.x)
    dtdt = dt*dt     # (t.t)
    do ix=1,nx{      # smooth along time axis
      call triangle(boxsz,nt,dtdt(:,ix),dtdt(:,ix))
      call triangle(boxsz,nt,dxdx(:,ix),dxdx(:,ix))
      call triangle(boxsz,nt,dtdx(:,ix),dtdx(:,ix))
    }
    coh = sqrt( (dtdx*dtdx) / (dtdt*dxdx) )
    pp  = -dtdx / dtdt
    call wavekill(1.,pp,nt,nx,dat,res)
  }
}
```

To suppress noise, the quadratic functions $\mathbf{x} \cdot \mathbf{x}$, $\mathbf{t} \cdot \mathbf{t}$, and $\mathbf{x} \cdot \mathbf{t}$ were smoothed over time with a triangle filter.

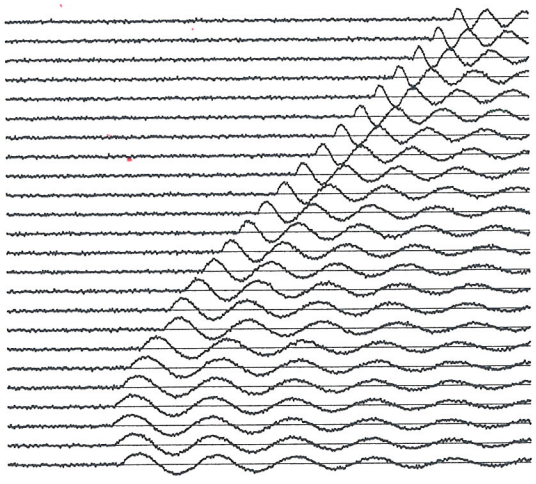

Figure 2.1: Input synthetic seismic data includes a low level of noise.
VIEW lsq/. puckin

Subroutine `puck2d` shows the code that generated Figure 2.1 through 2.3. An example based on synthetic data is shown in Figures 2.1-2.3. The synthetic data in Figure 2.1 mimics

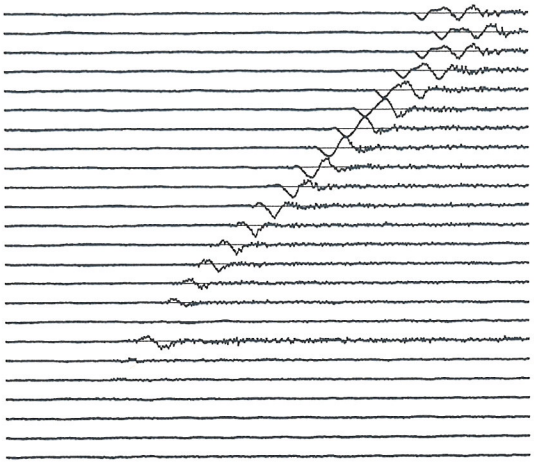

Figure 2.2: Residuals, i.e., an evaluation of $U_x + pU_t$. VIEW lsq/. residual

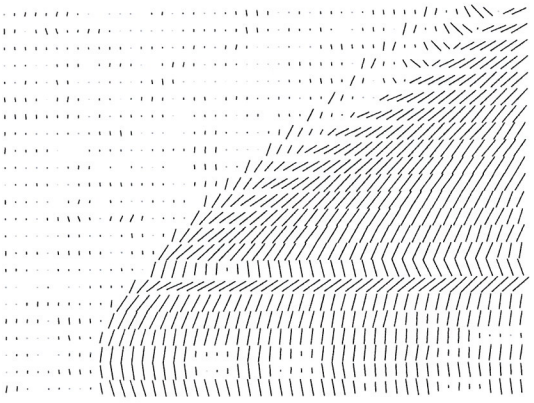

Figure 2.3: Output values of p are shown by the slope of short line segments. VIEW lsq/. puckout

a reflection seismic field profile, including one trace that is slightly delayed as if recorded on a patch of unconsolidated **soil**.

Figure 2.2 shows the **residual**. The residual is small in the central region of the data; it is large where the signal is not sampled densely enough and it is large at the transient onset of the signal. The residual is rough because of the noise in the signal, because it is made from derivatives, and because the synthetic data was made by nearest-neighbor interpolation. Notice that the residual is not particularly large for the delayed trace.

Figure 2.3 shows the dips. The most significant feature of this figure is the sharp localization of the dips surrounding the delayed trace. Other methods based on "beam stacks" or Fourier concepts might lead us to conclude that the aperture must be large to resolve a wide range of angles. Here we have a narrow aperture (two traces), but the dip can change rapidly and widely.

Once the stepout $p = dt/dx$ is known between each of the signals, it is a simple matter to integrate to get the total time shift. A real-life example is shown in Figure 2.4. In this

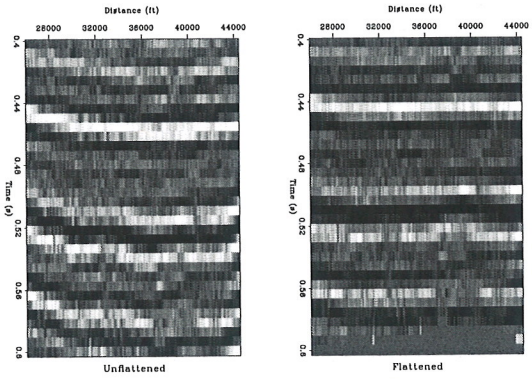

Figure 2.4: A seismic line before and after flattening. VIEW lsq/. TwoD

case the **flattening** was a function of x only. More interesting (and more complicated) cases arise when the stepout $p = dt/dx$ is a function of both x and t. The code shown here should work well in such cases.

A disadvantage, well known to people who routinely work with finite-difference solutions to partial differential equations, is that for short wavelengths a finite difference operator is not the same as a differential operator; therefore the numerical value of p is biased. This problem can be overcome in the following way. First estimate the slope $p = dt/dx$ between each trace. Then shift the traces to flatten them. Now there may be a residual p because of the bias in the initial estimate of p. This process can be iterated until the data is flattened. Everywhere in a plane we have solved a least squares problem for a single value p.

2.2 MULTIVARIATE LEAST SQUARES

2.2.1 Inside an abstract vector

In engineering uses, a vector has three scalar components that correspond to the three dimensions of the space in which we live. In least-squares data analysis, a vector is a one-dimensional array that can contain many different things. Such an array is an "**abstract**

vector." For example, in **earthquake** studies, the vector might contain the time an earthquake began, as well as its latitude, longitude, and depth. Alternatively, the abstract vector might contain as many components as there are seismometers, and each component might be the arrival time of an earthquake wave. Used in signal analysis, the vector might contain the values of a signal at successive instants in time or, alternatively, a collection of signals. These signals might be "**multiplexed**" (interlaced) or "demultiplexed" (all of each signal preceding the next). When used in image analysis, the one-dimensional array might contain an image, which could itself be thought of as an array of signals. Vectors, including abstract vectors, are usually denoted by **boldface letters** such as $\mathbf{p}$ and $\mathbf{s}$. Like physical vectors, abstract vectors are **orthogonal** when their dot product vanishes: $\mathbf{p} \cdot \mathbf{s} = 0$. Orthogonal vectors are well known in physical space; we will also encounter them in abstract vector space.

We consider first a hypothetical application with one data vector $\mathbf{d}$ and two fitting vectors $\mathbf{f}_1$ and $\mathbf{f}_2$. Each fitting vector is also known as a "**regressor**." Our first task is to approximate the data vector $\mathbf{d}$ by a scaled combination of the two regressor vectors. The scale factors m_1 and m_2 should be chosen so that the model matches the data; i.e.,

$$\mathbf{d} \quad \approx \quad \mathbf{f}_1 m_1 + \mathbf{f}_2 m_2 \tag{2.18}$$

Notice that we could take the partial derivative of the data in (2.18) with respect to an unknown, say m_1, and the result is the regressor $\mathbf{f}_1$. The **partial derivative** of all modeled data d_i with respect to any particular model parameter m_j gives a **regressor**.

> A **regressor** is a column in the matrix of partial-derivatives, $\partial d_i / \partial m_j$.

The fitting goal (2.18) is often expressed in the more compact mathematical matrix notation $\mathbf{d} \approx \mathbf{F}\mathbf{m}$, but in our derivation here we will keep track of each component explicitly and use mathematical matrix notation to summarize the final result. Fitting the observed data $\mathbf{d} = \mathbf{d}^{\text{obs}}$ to its two theoretical parts $\mathbf{f}_1 m_1$ and $\mathbf{f}_2 m_2$ can be expressed as minimizing the length of the residual vector $\mathbf{r}$, where

$$\mathbf{0} \quad \approx \quad \mathbf{r} \quad = \quad \mathbf{d}^{\text{theor}} - \mathbf{d}^{\text{obs}} \tag{2.19}$$

$$\mathbf{0} \quad \approx \quad \mathbf{r} \quad = \quad \mathbf{f}_1 m_1 + \mathbf{f}_2 m_2 \; - \; \mathbf{d} \tag{2.20}$$

We use a dot product to construct a sum of squares (also called a "**quadratic form**") of the components of the residual vector:

$$Q(m_1, m_2) \quad = \quad \mathbf{r} \cdot \mathbf{r} \tag{2.21}$$

$$Q(m_1, m_2) \quad = \quad (\mathbf{f}_1 m_1 + \mathbf{f}_2 m_2 - \mathbf{d}) \cdot (\mathbf{f}_1 m_1 + \mathbf{f}_2 m_2 - \mathbf{d}) \tag{2.22}$$

To find the gradient of the quadratic form $Q(m_1, m_2)$, you might be tempted to expand out the dot product into all nine terms and then differentiate. It is less cluttered, however, to remember the product rule, that

$$\frac{d}{dx} \mathbf{r} \cdot \mathbf{r} \quad = \quad \frac{d\mathbf{r}}{dx} \cdot \mathbf{r} + \mathbf{r} \cdot \frac{d\mathbf{r}}{dx} \tag{2.23}$$

Thus, the gradient of $Q(m_1, m_2)$ is defined by its two components:

$$\frac{\partial Q}{\partial m_1} = \mathbf{f}_1 \cdot (\mathbf{f}_1 m_1 + \mathbf{f}_2 m_2 - \mathbf{d}) + (\mathbf{f}_1 m_1 + \mathbf{f}_2 m_2 - \mathbf{d}) \cdot \mathbf{f}_1 \tag{2.24}$$

$$\frac{\partial Q}{\partial m_2} = \mathbf{f}_2 \cdot (\mathbf{f}_1 m_1 + \mathbf{f}_2 m_2 - \mathbf{d}) + (\mathbf{f}_1 m_1 + \mathbf{f}_2 m_2 - \mathbf{d}) \cdot \mathbf{f}_2 \tag{2.25}$$

Setting these derivatives to zero and using $(\mathbf{f}_1 \cdot \mathbf{f}_2) = (\mathbf{f}_2 \cdot \mathbf{f}_1)$ etc., we get

$$(\mathbf{f}_1 \cdot \mathbf{d}) = (\mathbf{f}_1 \cdot \mathbf{f}_1) m_1 + (\mathbf{f}_1 \cdot \mathbf{f}_2) m_2 \tag{2.26}$$

$$(\mathbf{f}_2 \cdot \mathbf{d}) = (\mathbf{f}_2 \cdot \mathbf{f}_1) m_1 + (\mathbf{f}_2 \cdot \mathbf{f}_2) m_2 \tag{2.27}$$

We can use these two equations to solve for the two unknowns m_1 and m_2. Writing this expression in matrix notation, we have

$$\begin{bmatrix} (\mathbf{f}_1 \cdot \mathbf{d}) \\ (\mathbf{f}_2 \cdot \mathbf{d}) \end{bmatrix} = \begin{bmatrix} (\mathbf{f}_1 \cdot \mathbf{f}_1) & (\mathbf{f}_1 \cdot \mathbf{f}_2) \\ (\mathbf{f}_2 \cdot \mathbf{f}_1) & (\mathbf{f}_2 \cdot \mathbf{f}_2) \end{bmatrix} \begin{bmatrix} m_1 \\ m_2 \end{bmatrix} \tag{2.28}$$

It is customary to use matrix notation without dot products. To do this, we need some additional definitions. To clarify these definitions, we inspect vectors $\mathbf{f}_1$, $\mathbf{f}_2$, and $\mathbf{d}$ of three components. Thus

$$\mathbf{F} = [\mathbf{f}_1 \quad \mathbf{f}_2] = \begin{bmatrix} f_{11} & f_{12} \\ f_{21} & f_{22} \\ f_{31} & f_{32} \end{bmatrix} \tag{2.29}$$

Likewise, the *transposed* matrix $\mathbf{F}^*$ is defined by

$$\mathbf{F}^* = \begin{bmatrix} f_{11} & f_{21} & f_{31} \\ f_{12} & f_{22} & f_{32} \end{bmatrix} \tag{2.30}$$

Using this matrix $\mathbf{F}^*$ there is a simple expression for the gradient calculated in equation (2.24). It is used in nearly every example in this book.

$$\mathbf{g} = \begin{bmatrix} \frac{\partial Q}{\partial m_1} \\ \frac{\partial Q}{\partial m_2} \end{bmatrix} = \begin{bmatrix} \mathbf{f}_1 \cdot \mathbf{r} \\ \mathbf{f}_2 \cdot \mathbf{r} \end{bmatrix} = \begin{bmatrix} f_{11} & f_{21} & f_{31} \\ f_{12} & f_{22} & f_{32} \end{bmatrix} \begin{bmatrix} r_1 \\ r_2 \\ r_3 \end{bmatrix} = \mathbf{F}^* \mathbf{r} \tag{2.31}$$

In words this expression says, the gradient is found by putting the residual into the adjoint operator $\mathbf{g} = \mathbf{F}^* \mathbf{r}$. Notice the gradient $\mathbf{g}$ has the same number of components as the unknown solution $\mathbf{m}$, so we can think of the gradient as a $\Delta\mathbf{m}$, something we could add to $\mathbf{m}$ getting $\mathbf{m} + \Delta\mathbf{m}$. Later we'll see how much of $\Delta\mathbf{m}$ we'll want to add to $\mathbf{m}$. We will have reached the best solution when we find the gradient $\mathbf{g} = \mathbf{0}$ vanishes, which happens, as equation (2.31) says, when the residual is orthogonal to all the fitting functions (all the rows in the matrix $\mathbf{F}^*$, the columns in $\mathbf{F}$, are perpendicular to $\mathbf{r}$).

The matrix in equation (2.28) contains dot products. Matrix multiplication is an abstract way of representing the dot products:

$$\begin{bmatrix} (\mathbf{f}_1 \cdot \mathbf{f}_1) & (\mathbf{f}_1 \cdot \mathbf{f}_2) \\ (\mathbf{f}_2 \cdot \mathbf{f}_1) & (\mathbf{f}_2 \cdot \mathbf{f}_2) \end{bmatrix} = \begin{bmatrix} f_{11} & f_{21} & f_{31} \\ f_{12} & f_{22} & f_{32} \end{bmatrix} \begin{bmatrix} f_{11} & f_{12} \\ f_{21} & f_{22} \\ f_{31} & f_{32} \end{bmatrix} \tag{2.32}$$

Thus, equation (2.28) without dot products is

$$\begin{bmatrix} f_{11} & f_{21} & f_{31} \\ f_{12} & f_{22} & f_{32} \end{bmatrix} \begin{bmatrix} d_1 \\ d_2 \\ d_3 \end{bmatrix} = \begin{bmatrix} f_{11} & f_{21} & f_{31} \\ f_{12} & f_{22} & f_{32} \end{bmatrix} \begin{bmatrix} f_{11} & f_{12} \\ f_{21} & f_{22} \\ f_{31} & f_{32} \end{bmatrix} \begin{bmatrix} m_1 \\ m_2 \end{bmatrix} \tag{2.33}$$

which has the matrix abbreviation

$$\mathbf{F}^* \mathbf{d} = (\mathbf{F}^* \mathbf{F})\mathbf{m} \tag{2.34}$$

Equation (2.34) is the classic result of least-squares fitting of data to a collection of regressors. Obviously, the same matrix form applies when there are more than two regressors and each vector has more than three components. Equation (2.34) leads to an **analytic solution** for $\mathbf{m}$ using an inverse matrix. To solve formally for the unknown $\mathbf{m}$, we premultiply by the inverse matrix $(\mathbf{F}^* \mathbf{F})^{-1}$:

$$\mathbf{m} = (\mathbf{F}^* \mathbf{F})^{-1} \mathbf{F}^* \mathbf{d} \tag{2.35}$$

> The central result of **least-squares** theory is $\mathbf{m} = (\mathbf{F}^* \mathbf{F})^{-1} \mathbf{F}^* \mathbf{d}$. We see it everywhere.

Let us examine all the second derivatives of $Q(m_1, m_2)$ defined by equation (2.22). Any multiplying $\mathbf{d}$ will not survive the second derivative, so the terms we are left with are

$$Q(m_1, m_2) = (\mathbf{f}_1 \cdot \mathbf{f}_1)m_1^2 + 2(\mathbf{f}_1 \cdot \mathbf{f}_2)m_1 m_2 + (\mathbf{f}_2 \cdot \mathbf{f}_2)m_2^2 \tag{2.36}$$

After taking the second derivative, we can organize all these terms in a matrix

$$\frac{\partial^2 Q}{\partial m_i \partial m_j} = \begin{bmatrix} (\mathbf{f}_1 \cdot \mathbf{f}_1) & (\mathbf{f}_1 \cdot \mathbf{f}_2) \\ (\mathbf{f}_2 \cdot \mathbf{f}_1) & (\mathbf{f}_2 \cdot \mathbf{f}_2) \end{bmatrix} \tag{2.37}$$

Comparing this to equation (2.32), we conclude that $\mathbf{F}^* \mathbf{F}$ is a matrix of second derivatives. This matrix is also known as the **Hessian**. This matrix often plays an important role in small problems.

Larger problems tend to have insufficient computer memory for the Hessian matrix because it is the size of model space squared. Where model space is a multidimensional earth image, that's a large number of values even before squaring. Therefore, this book rarely works with the Hessian, working instead with gradients.

Rearrange parentheses representing (2.33).

$$\mathbf{F}^* \mathbf{d} = \mathbf{F}^* (\mathbf{F}\mathbf{m}) \tag{2.38}$$

Equation (2.34) led to the "analytic" solution (2.35). In a later section on conjugate directions, we will see that equation (2.38) expresses better than (2.35) the philosophy of iterative methods.

Notice how equation (2.38) invites us to cancel the matrix $\mathbf{F}^*$ from each side. We cannot do that of course, because $\mathbf{F}^*$ is not a number, nor is it a square matrix with an inverse.

If you really want to cancel the matrix $\mathbf{F}^*$, you may, but the equation is then only an approximation that restates our original goal (2.18):

$$\mathbf{d} \approx \mathbf{F}\mathbf{m} \tag{2.39}$$

A speedy problem solver might ignore the mathematics covering the previous page, study his or her application until he or she is able to write the **statement of goals** (2.39) = (2.18), premultiply by $\mathbf{F}^*$, replace $\approx$ by $=$, getting (2.34), and take (2.34) to a simultaneous equation-solving program to get $\mathbf{m}$.

What I call "**fitting goals**" are called "**regressions**" by statisticians. In common language the word regression means to "trend toward a more primitive perfect state" which vaguely resembles reducing the size of (energy in) the residual $\mathbf{r} = \mathbf{F}\mathbf{m} - \mathbf{d}$. Formally this is often written as:

$$\min_{\mathbf{m}} \|\mathbf{F}\mathbf{m} - \mathbf{d}\| \tag{2.40}$$

The notation above with two pairs of vertical lines looks like double absolute value, but we can understand it as a reminder to square and sum all the components. This formal notation is more explicit about what is constant and what is variable during the fitting.

2.2.2 Normal equations

An important concept is that when energy is minimum, the residual is orthogonal to the fitting functions. The fitting functions are the column vectors $\mathbf{f}_1$, $\mathbf{f}_2$, and $\mathbf{f}_3$. Let us verify only that the dot product $\mathbf{r} \cdot \mathbf{f}_2$ vanishes; to do this, we'll show that those two vectors are orthogonal. Energy minimum is found by:

$$0 = \frac{\partial}{\partial m_2} \mathbf{r} \cdot \mathbf{r} = 2\,\mathbf{r} \cdot \frac{\partial \mathbf{r}}{\partial m_2} = 2\,\mathbf{r} \cdot \mathbf{f}_2 \tag{2.41}$$

(To compute the derivative refer to equation (2.20).) Equation (2.41) shows that the residual is orthogonal to a fitting function. The fitting functions are the column vectors in the fitting matrix.

The basic least-squares equations are often called the "normal" equations. The word "normal" means perpendicular. We can rewrite equation (2.38) to emphasize the perpendicularity. Bring both terms to the right, and recall the definition of the residual $\mathbf{r}$ from equation (2.20):

$$\mathbf{0} = \mathbf{F}^*(\mathbf{F}\mathbf{m} - \mathbf{d}) \tag{2.42}$$

$$\mathbf{0} = \mathbf{F}^*\mathbf{r} \tag{2.43}$$

Equation (2.43) says that the **residual** vector $\mathbf{r}$ is perpendicular to each row in the $\mathbf{F}^*$ matrix. These rows are the **fitting functions**. Therefore, the residual, after it has been minimized, is perpendicular to *all* the fitting functions.

2.2.3 Differentiation by a complex vector

Complex numbers frequently arise in physical applications, particularly those with Fourier series. Let us extend the multivariable least-squares theory to the use of complex-valued

unknowns $\mathbf{m}$. First recall how complex numbers were handled with single-variable least squares; i.e., as in the discussion leading up to equation (2.5). Use an asterisk, such as $\mathbf{m}^*$, to denote the complex conjugate of the transposed vector $\mathbf{m}$. Now write the positive **quadratic form** as

$$Q(\mathbf{m}^*, \mathbf{m}) \quad = \quad (\mathbf{F}\mathbf{m} - \mathbf{d})^* \, (\mathbf{F}\mathbf{m} - \mathbf{d}) \quad = \quad (\mathbf{m}^* \, \mathbf{F}^* - \mathbf{d}^*)(\mathbf{F}\mathbf{m} - \mathbf{d}) \tag{2.44}$$

Recall from equation (2.4) where we minimized a quadratic form $Q(\bar{X}, X)$ by setting to zero both $\partial Q/\partial \bar{X}$ and $\partial Q/\partial X$. We noted that only one of $\partial Q/\partial \bar{X}$ and $\partial Q/\partial X$ is necessarily zero because they are conjugates of each other. Now take the derivative of Q with respect to the (possibly complex, row) vector $\mathbf{m}^*$. Notice that $\partial Q/\partial \mathbf{m}^*$ is the complex conjugate transpose of $\partial Q/\partial \mathbf{m}$. Thus, setting one to zero sets the other to zero also. Setting $\partial Q/\partial \mathbf{m}^* = \mathbf{0}$ gives the normal equations:

$$\mathbf{0} \quad = \quad \frac{\partial Q}{\partial \mathbf{m}^*} \quad = \quad \mathbf{F}^* \, (\mathbf{F}\mathbf{m} - \mathbf{d}) \tag{2.45}$$

The result is merely the complex form of our earlier result (2.42). Therefore, differentiating by a complex vector is an abstract concept, but it gives the same set of equations as differentiating by each scalar component, and it saves much clutter.

2.2.4 From the frequency domain to the time domain

Where data fitting uses the notation $\mathbf{m} \rightarrow \mathbf{d}$, linear algebra and signal analysis often use the notation $\mathbf{x} \rightarrow \mathbf{y}$. Equation (2.4) is a frequency-domain quadratic form that we minimized by varying a single parameter, a Fourier coefficient. Now we will look at the same problem in the time domain. We will see that the time domain offers flexibility with boundary conditions, constraints, and weighting functions. The notation will be that a filter f_t has input x_t and output y_t. In Fourier space this is $Y = XF$. There are two applications to look at, unknown filter F and unknown input X.

Unknown filter

When inputs and outputs are given, the problem of finding an unknown filter appears to be overdetermined, so we write $\mathbf{y} \approx \mathbf{X}\mathbf{f}$ where the matrix $\mathbf{X}$ is a matrix of downshifted columns like (1.5). Thus the quadratic form to be minimized is a restatement of equation (2.44) with filter definitions:

$$Q(\mathbf{f}^*, \mathbf{f}) \quad = \quad (\mathbf{X}\mathbf{f} - \mathbf{y})^* \, (\mathbf{X}\mathbf{f} - \mathbf{y}) \tag{2.46}$$

The solution $\mathbf{f}$ is found just as we found (2.45), and it is the set of simultaneous equations $\mathbf{0} = \mathbf{X}^* \, (\mathbf{X}\mathbf{f} - \mathbf{y})$.

Unknown input: deconvolution with a known filter

For solving the unknown-input problem, we put the known filter f_t in a matrix of downshifted columns $\mathbf{F}$. Our statement of wishes is now to find x_t so that $\mathbf{y} \approx \mathbf{F}\mathbf{x}$. We can

expect to have trouble finding unknown inputs x_t when we are dealing with certain kinds of filters, such as **bandpass filters**. If the output is zero in a frequency band, we will never be able to find the input in that band and will need to prevent x_t from diverging there. We do this by the statement that we wish $\mathbf{0} \approx \epsilon\,\mathbf{x}$, where ϵ is a parameter that is small and whose exact size will be chosen by experimentation. Putting both wishes into a single, partitioned matrix equation gives:

$$\begin{bmatrix} \mathbf{0} \\ \mathbf{0} \end{bmatrix} \approx \begin{bmatrix} \mathbf{r}_1 \\ \mathbf{r}_2 \end{bmatrix} = \begin{bmatrix} \mathbf{F} \\ \epsilon\,\mathbf{I} \end{bmatrix} \mathbf{x} - \begin{bmatrix} \mathbf{y} \\ \mathbf{0} \end{bmatrix} \tag{2.47}$$

To minimize the residuals $\mathbf{r}_1$ and $\mathbf{r}_2$, we can minimize the scalar $\mathbf{r}^*\,\mathbf{r} = \mathbf{r}_1^*\,\mathbf{r}_1 + \mathbf{r}_2^*\,\mathbf{r}_2$. This is

$$\begin{aligned} Q(\mathbf{x}^*, \mathbf{x}) &= (\mathbf{F}\mathbf{x} - \mathbf{y})^*\,(\mathbf{F}\mathbf{x} - \mathbf{y}) + \epsilon^2 \mathbf{x}^*\,\mathbf{x} \\ &= (\mathbf{x}^*\,\mathbf{F}^* - \mathbf{y}^*)(\mathbf{F}\mathbf{x} - \mathbf{y}) + \epsilon^2 \mathbf{x}^*\,\mathbf{x} \end{aligned} \tag{2.48}$$

We solved this minimization in the frequency domain (beginning from equation (2.4)).

Formally the solution is found just as with equation (2.45), but this solution looks unappealing in practice because there are so many unknowns and because the problem can be solved much more quickly in the Fourier domain. To motivate ourselves to solve this problem in the time domain, we need either to find an approximate solution method that is much faster, or to discover that constraints or time-variable weighting functions are required in some applications. This is an issue we must be continuously alert to, whether the cost of a method is justified by its need.

2.3 KRYLOV SUBSPACE ITERATIVE METHODS

The **solution time** for simultaneous **linear equations** grows cubically with the number of unknowns. There are three regimes for solution; which one is applicable depends on the number of unknowns m. For m three or less, we use analytical methods. We also sometimes use analytical methods on matrices of size 4×4 if the matrix contains many zeros. My 1988 desktop workstation solved a 100×100 system in a minute. Ten years later it would do a 600×600 system in about a minute. A nearby more powerful computer would do 1000×1000 in a minute. Since the computing effort increases with the third power of the size, and since $4^3 = 64 \approx 60$, an hour's work solves a four times larger matrix, namely 4000×4000 on the more powerful machine. For significantly larger values of m, exact numerical methods must be abandoned and **iterative methods** must be used.

The compute time for a rectangular matrix is slightly more pessimistic. It is the product of the number of data points n times the number of model points squared m^2. This happens to be the cost of computing the matrix $\mathbf{F}^*\,\mathbf{F}$ from $\mathbf{F}$. Since the number of data points generally exceeds the number of model points $n > m$ by a substantial factor (to allow averaging of noises), it leaves us with significantly fewer than 4000 points in model space.

A square image packed into a 4096 point vector is a 64×64 array. The computer power for linear algebra to give us solutions that fit in a $k \times k$ image is thus proportional to k^6, which means that even though computer power grows rapidly, imaging resolution using "exact numerical methods" hardly grows at all from our 64×64 current practical limit.

The retina in our eyes captures an image of size about 1000×1000 which is a lot bigger than 64×64. Life offers us many occasions where final images exceed the 4000 points of a 64×64 array. To make linear algebra (and inverse theory) relevant to such applications, we investigate special techniques. A numerical technique known as the "**conjugate-direction method**" works well for all values of m and is our subject here. As with most simultaneous equation solvers, an exact answer (assuming exact arithmetic) is attained in a finite number of steps. And if n and m are too large to allow enough iterations, the iterative methods can be interrupted at any stage, the partial result often proving useful. Whether or not a partial result actually is useful is the subject of much research; naturally, the results vary from one application to the next.

2.3.1 Sign convention

On the last day of the survey, a storm blew up, the sea got rough, and the receivers drifted further downwind. The data recorded that day had a larger than usual difference from that predicted by the final model. We could call $(\mathbf{d} - \mathbf{Fm})$ the ***experimental error***. (Here $\mathbf{d}$ is data, $\mathbf{m}$ is model parameters, and $\mathbf{F}$ is their linear relation).

The alternate view is that our theory was too simple. It lacked model parameters for the waves and the drifting cables. Because of this model oversimplification we had a ***modeling error*** of the opposite polarity $(\mathbf{Fm} - \mathbf{d})$.

A strong experimentalist prefers to think of the error as experimental error, something for him or her to work out. Likewise a strong analyst likes to think of the error as a theoretical problem. (Weaker investigators might be inclined to take the opposite view.)

Regardless of the above, and opposite to common practice, I define the **sign convention** for the error (or residual) as $(\mathbf{Fm} - \mathbf{d})$. Here is why. Minus signs are a source of confusion and errors. Putting the minus sign on the field data limits it to one location while putting it in model space would spread it into as many parts as model space has parts.

> Beginners often feel disappointment when the data does not fit the model very well. They see it as a defect in the data instead of an opportunity to discover what our data contains that our theory does not.

2.3.2 Method of random directions and steepest descent

Let us minimize the sum of the squares of the components of the **residual** vector given by

$$\text{residual} = \text{transform} \quad \text{model space} \quad - \quad \text{data space} \tag{2.49}$$

$$\begin{bmatrix} \mathbf{r} \end{bmatrix} = \begin{bmatrix} \mathbf{F} \end{bmatrix} \begin{bmatrix} \mathbf{x} \end{bmatrix} - \begin{bmatrix} \mathbf{d} \end{bmatrix} \tag{2.50}$$

A contour plot is based on an altitude function of space. The altitude is the **dot product** $\mathbf{r} \cdot \mathbf{r}$. By finding the lowest altitude, we are driving the residual vector $\mathbf{r}$ as close as we can to zero. If the residual vector $\mathbf{r}$ reaches zero, then we have solved the simultaneous equations $\mathbf{d} = \mathbf{F}\mathbf{x}$. In a two-dimensional world the vector $\mathbf{x}$ has two components, (x_1, x_2). A contour is a curve of constant $\mathbf{r} \cdot \mathbf{r}$ in (x_1, x_2)-space. These contours have a statistical interpretation as contours of uncertainty in (x_1, x_2), with measurement errors in $\mathbf{d}$.

Let us see how a random search-direction can be used to reduce the residual $\mathbf{0} \approx \mathbf{r} = \mathbf{F}\mathbf{x} - \mathbf{d}$. Let $\Delta\mathbf{x}$ be an abstract vector with the same number of components as the solution $\mathbf{x}$, and let $\Delta\mathbf{x}$ contain arbitrary or random numbers. We add an unknown quantity α of vector $\Delta\mathbf{x}$ to the vector $\mathbf{x}$, and thereby create $\mathbf{x}_{\text{new}}$:

$$\mathbf{x}_{\text{new}} \quad = \quad \mathbf{x} + \alpha\Delta\mathbf{x} \tag{2.51}$$

This gives a new residual:

$$\mathbf{r}_{\text{new}} \quad = \quad \mathbf{F}\,\mathbf{x}_{\text{new}} - \mathbf{d} \tag{2.52}$$

$$\mathbf{r}_{\text{new}} \quad = \quad \mathbf{F}(\mathbf{x} + \alpha\Delta\mathbf{x}) - \mathbf{d} \tag{2.53}$$

$$\mathbf{r}_{\text{new}} \quad = \quad \mathbf{r} + \alpha\Delta\mathbf{r} \quad = \quad (\mathbf{F}\mathbf{x} - \mathbf{d}) + \alpha\mathbf{F}\Delta\mathbf{x} \tag{2.54}$$

which defines $\Delta\mathbf{r} = \mathbf{F}\Delta\mathbf{x}$.

Next we adjust α to minimize the dot product: $\mathbf{r}_{\text{new}} \cdot \mathbf{r}_{\text{new}}$

$$(\mathbf{r} + \alpha\Delta\mathbf{r}) \cdot (\mathbf{r} + \alpha\Delta\mathbf{r}) \quad = \quad \mathbf{r} \cdot \mathbf{r} + 2\alpha(\mathbf{r} \cdot \Delta\mathbf{r}) \; + \; \alpha^2\Delta\mathbf{r} \cdot \Delta\mathbf{r} \tag{2.55}$$

Set to zero its derivative with respect to α

$$0 \quad = \quad 2\mathbf{r} \cdot \Delta\mathbf{r} + 2\alpha\Delta\mathbf{r} \cdot \Delta\mathbf{r} \tag{2.56}$$

which says that the new residual $\mathbf{r}_{\text{new}} = \mathbf{r} + \alpha\Delta\mathbf{r}$ is perpendicular to the "fitting function" $\Delta\mathbf{r}$. Solving gives the required value of α.

$$\alpha \quad = \quad -\frac{(\mathbf{r} \cdot \Delta\mathbf{r})}{(\Delta\mathbf{r} \cdot \Delta\mathbf{r})} \tag{2.57}$$

A "computation **template**" for the method of random directions is

$$\begin{array}{lll}
\mathbf{r} & \longleftarrow & \mathbf{F}\mathbf{x} - \mathbf{d} \\
\text{iterate } \{ & & \\
\qquad \Delta\mathbf{x} & \longleftarrow & \text{random numbers} \\
\qquad \Delta\mathbf{r} & \longleftarrow & \mathbf{F}\,\Delta\mathbf{x} \\
\qquad \alpha & \longleftarrow & -(\mathbf{r} \cdot \Delta\mathbf{r})/(\Delta\mathbf{r} \cdot \Delta\mathbf{r}) \\
\qquad \mathbf{x} & \longleftarrow & \mathbf{x} + \alpha\Delta\mathbf{x} \\
\qquad \mathbf{r} & \longleftarrow & \mathbf{r} + \alpha\Delta\mathbf{r} \\
\qquad \} & &
\end{array}$$

A nice thing about the method of random directions is that you do not need to know the adjoint operator $\mathbf{F}^*$.

In practice, random directions are rarely used. It is more common to use the **gradient** direction than a random direction. Notice that a vector of the size of $\Delta\mathbf{x}$ is

$$\mathbf{g} \quad = \quad \mathbf{F}^* \, \mathbf{r} \tag{2.58}$$

Recall this vector can be found by taking the gradient of the size of the residuals:

$$\frac{\partial}{\partial \mathbf{x}^*} \, \mathbf{r} \cdot \mathbf{r} \quad = \quad \frac{\partial}{\partial \mathbf{x}^*} \, (\mathbf{x}^* \, \mathbf{F}^* \; - \; \mathbf{d}^*) \, (\mathbf{F}\,\mathbf{x} \; - \; \mathbf{d}) \quad = \quad \mathbf{F}^* \, \mathbf{r} \tag{2.59}$$

Choosing $\Delta\mathbf{x}$ to be the gradient vector $\Delta\mathbf{x} = \mathbf{g} = \mathbf{F}^* \, \mathbf{r}$ is called "the method of **steepest descent**."

Starting from a model $\mathbf{x} = \mathbf{m}$ (which may be zero), below is a **template** of pseudocode for minimizing the residual $\mathbf{0} \approx \mathbf{r} = \mathbf{F}\mathbf{x} - \mathbf{d}$ by the steepest-descent method:

$$\begin{array}{lcl}
\mathbf{r} & \longleftarrow & \mathbf{F}\mathbf{x} - \mathbf{d} \\
\text{iterate } \{ & & \\
\qquad \Delta\mathbf{x} & \longleftarrow & \mathbf{F}^* \, \mathbf{r} \\
\qquad \Delta\mathbf{r} & \longleftarrow & \mathbf{F} \, \Delta\mathbf{x} \\
\qquad \alpha & \longleftarrow & -(\mathbf{r} \cdot \Delta\mathbf{r}) / (\Delta\mathbf{r} \cdot \Delta\mathbf{r}) \\
\qquad \mathbf{x} & \longleftarrow & \mathbf{x} + \alpha \Delta\mathbf{x} \\
\qquad \mathbf{r} & \longleftarrow & \mathbf{r} + \alpha \Delta\mathbf{r} \\
\qquad \} & &
\end{array}$$

Good science and engineering is finding something unexpected. For this you look both in data space and in model space. In data space you look at the residual $\mathbf{r}$. In model space, you look at the residual projected there $\mathbf{F}^* \, \mathbf{r}$. What does it mean? It is simply Δm, the changes you need to make to your model. It will mean more in later chapters where the operator $\mathbf{F}$ is a column vector of operators that are fighting with one another to grab the data.

2.3.3 Why steepest descent is so slow

Before we can understand why the **conjugate-direction method** is so fast, we need to see why the **steepest-descent method** is so slow. The process of selecting α is called "**line search**", but for a linear problem like the one we have chosen here, we hardly recognize choosing α as searching a line. A more graphic understanding of the whole process is possible from considering a two-dimensional space where the vector of unknowns $\mathbf{x}$ has just two components, x_1 and x_2. Then the size of the residual vector $\mathbf{r} \cdot \mathbf{r}$ can be displayed with a contour plot in the plane of (x_1, x_2). Figure 2.5 shows a contour plot of the penalty function of $(x_1, x_2) = (m_1, m_2)$. The gradient is perpendicular to the contours. Contours and gradients are *curved lines*. When we use the steepest-descent method we start at a point and compute the gradient direction at that point. Then we begin a *straight-line* descent in that direction. The gradient direction curves away from our direction of travel, but we continue on our straight line until we have stopped descending and are about to ascend. There we stop, compute another gradient vector, turn in that direction, and descend along a new straight line. The process repeats until we get to the bottom, or until we get tired.

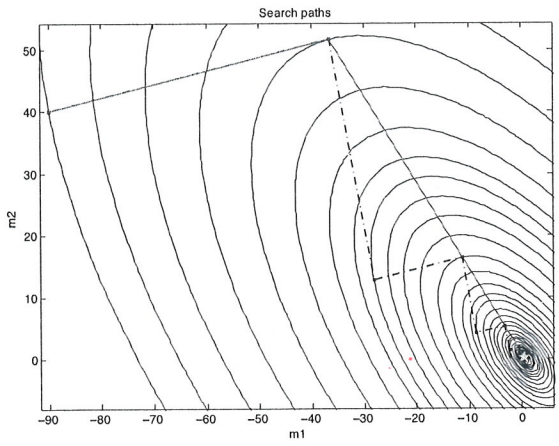

Figure 2.5: Route of steepest descent (black) and route of conjugate direction (light grey or red). lsq/. yunyue

What could be wrong with such a direct strategy? The difficulty is at the stopping locations. These occur where the descent direction becomes *parallel* to the contour lines. (There the path becomes level.) So after each stop, we turn 90° from parallel to perpendicular to the local contour line for the next descent. What if the final goal is at a 45° angle to our path? A 45° turn cannot be made. Instead of moving like a rain drop down the centerline of a rain gutter, we move along a fine-toothed zigzag path, crossing and recrossing the centerline. The gentler the slope of the rain gutter, the finer the teeth on the zigzag path.

2.3.4 Null space and iterative methods

In applications where we fit $\mathbf{d} \approx \mathbf{F}\mathbf{x}$, there might exist a vector (or a family of vectors) defined by the condition $\mathbf{0} = \mathbf{F}\mathbf{x}_{\text{null}}$. This family is called a **null space**. For example, if the operator $\mathbf{F}$ is a time derivative, then the null space is the constant function; if the operator is a second derivative, then the null space has two components, a constant function and a linear function, or combinations of them. The null space is a family of model components that have no effect on the data.

When we use the steepest-descent method, we iteratively find solutions by this updating:

$$\mathbf{x}_{i+1} = \mathbf{x}_i + \alpha \Delta \mathbf{x} \tag{2.60}$$

$$\mathbf{x}_{i+1} = \mathbf{x}_i + \alpha \mathbf{F}^* \mathbf{r} \tag{2.61}$$

$$\mathbf{x}_{i+1} = \mathbf{x}_i + \alpha \mathbf{F}^* (\mathbf{F}\mathbf{x} - \mathbf{d}) \tag{2.62}$$

After we have iterated to convergence, the gradient $\Delta \mathbf{x} = \mathbf{F}^* \mathbf{r}$ vanishes. Adding any $\mathbf{x}_{\text{null}}$ to $\mathbf{x}$ does not change the residual $\mathbf{r} = \mathbf{F}\mathbf{x} - \mathbf{d}$. Since $\mathbf{r}$ is unchanged, $\Delta \mathbf{x} = \mathbf{F}^* \mathbf{r}$ remains zero and $\mathbf{x}_{i+1} = \mathbf{x}_i$. Thus we conclude that any null space in the initial guess $\mathbf{x}_0$ will remain there unaffected by the gradient-descent process. So, in the presense of null space, the answer we get from an iterative method depends on the starting guess. Oops! The analytic solution does not do any better. It needs to deal with a singular matrix. Existence of a null space destroys the uniqueness of any resulting model.

Linear algebra theory enables us to dig up the entire null space should we so desire. On the other hand, the computer demands might be vast. Even the memory for holding the many $\mathbf{x}$ vectors could be prohibitive. A much simpler and more practical goal is to find out if the null space has any members, and if so, to view some of them. To try to see a member of the null space, we take two starting guesses and we run our iterative solver for each of them. If the two solutions, $\mathbf{x}_1$ and $\mathbf{x}_2$, are the same, there is no null space. If the solutions differ, the difference is a member of the null space. Let us see why: Suppose after iterating to minimum residual we find:

$$\mathbf{r}_1 = \mathbf{F}\mathbf{x}_1 - \mathbf{d} \tag{2.63}$$

$$\mathbf{r}_2 = \mathbf{F}\mathbf{x}_2 - \mathbf{d} \tag{2.64}$$

We know that the residual squared is a convex quadratic function of the unknown $\mathbf{x}$. Mathematically that means the minimum value is unique, so $\mathbf{r}_1 = \mathbf{r}_2$. Subtracting we find $0 = \mathbf{r}_1 - \mathbf{r}_2 = \mathbf{F}(\mathbf{x}_1 - \mathbf{x}_2)$ proving that $\mathbf{x}_1 - \mathbf{x}_2$ is a model in the null space. Adding $\mathbf{x}_1 - \mathbf{x}_2$ to any to any model $\mathbf{x}$ will not change the modeled data.

> A practical way to learn about the existence of null spaces and their general appearance is simply to try gradient-descent methods beginning from various different starting guesses.

"Did I fail to run my iterative solver long enough?" is a question you might have. If two residuals from two starting solutions are not equal, $\mathbf{r}_1 \neq \mathbf{r}_2$, then you should be running your solver through more iterations.

> If two different starting solutions produce two different residuals, then you didn't run your solver through enough iterations.

2.3.5 The magical property of the conjugate direction method

In the **conjugate-direction method**, not a line, but rather a plane, is searched. A plane is made from an arbitrary linear combination of two vectors. One vector will be chosen to be the gradient vector, say $\mathbf{g}$. The other vector will be chosen to be the previous descent step vector, say $\mathbf{s} = \mathbf{x}_j - \mathbf{x}_{j-1}$. Instead of $\alpha\,\mathbf{g}$ we need a linear combination, say $\alpha\mathbf{g} + \beta\mathbf{s}$. For minimizing quadratic functions the plane search requires only the solution of a two-by-two set of linear equations for α and β.

The conjugate-direction (CD) method described in this book has a magical property shared by the more famous conjugate-gradient method. This magical property is not proven in this book, but it may be found in many sources. Although these methods are iterative methods, they converge on the exact answer (assuming perfect numerical precision) in a fixed number of steps. That number is the number of components in model space $\mathbf{x}$.

Where we benefit from iterative methods is if they happen to require less than the theoretically required nunber of iterations. Whether that is so, depends on the problem at hand. Reflection seismology has many problems so massive they are said to be solved simply by one application of the adjoint operator. The idea that such solutions might be improved by a small number of iterations is very appealing.

2.3.6 Conjugate-direction theory for programmers

Fourier-transformed variables are often capitalized. This convention will be helpful here, so in this subsection only, we capitalize vectors transformed by the $\mathbf{F}$ matrix. As everywhere, a matrix such as $\mathbf{F}$ is printed in **boldface** type but in this subsection, vectors are *not* printed in boldface print. Thus we define the solution, the solution step (from one iteration to the next), and the gradient by

$$X = \mathbf{F}\, x \qquad \text{modeled data} = \mathbf{F}\ \text{model} \tag{2.65}$$
$$S_j = \mathbf{F}\, s_j \qquad \text{model solution step} \tag{2.66}$$
$$G_j = \mathbf{F}\, g_j \qquad \Delta\mathbf{r} = \mathbf{F}\Delta\mathbf{m} \tag{2.67}$$

A linear combination in solution space, say $s+g$, corresponds to $S+G$ in the conjugate space, the data space, because $S+G = \mathbf{F}s + \mathbf{F}g = \mathbf{F}(s+g)$. According to equation (2.50), the residual is the modeled data minus the observed data.

$$R = \mathbf{F}x - D = X - D \tag{2.68}$$

The solution x is obtained by a succession of steps s_j, say

$$x = s_1 + s_2 + s_3 + \cdots \tag{2.69}$$

The last stage of each iteration is to update the solution and the residual:

$$\text{solution update}: \qquad x \leftarrow x + s \tag{2.70}$$
$$\text{residual update}: \qquad R \leftarrow R + S \tag{2.71}$$

The *gradient* vector g is a vector with the same number of components as the solution vector x. A vector with this number of components is

$$g = \mathbf{F}^*\, R = \text{gradient} \tag{2.72}$$
$$G = \mathbf{F}\, g = \text{conjugate gradient} = \Delta r \tag{2.73}$$

The gradient g in the transformed space is G, also known as the **conjugate gradient**.

What will our solution update $\Delta\mathbf{x} = \mathbf{s}$ be? It will be some unknown amount α of the gradient $\mathbf{g}$ plus another unknown amount β of the previous step $\mathbf{s}$. Likewise in residual space.

$$\Delta\mathbf{x} = \alpha\mathbf{g} + \beta\mathbf{s} \qquad \text{model space} \tag{2.74}$$
$$\Delta\mathbf{r} = \alpha\mathbf{G} + \beta\mathbf{S} \qquad \text{data space} \tag{2.75}$$

The minimization (2.55) is now generalized to scan not only in a line with α, but simultaneously another line with β. The combination of the two lines is a plane. We now set out to find the location in this plane that minimizes the quadratic Q.

$$Q(\alpha,\beta) = (R+\alpha G+\beta S)\cdot(R+\alpha G+\beta S) \tag{2.76}$$

The minimum is found at $\partial Q/\partial\alpha = 0$ and $\partial Q/\partial\beta = 0$, namely,

$$0 = G\cdot(R+\alpha G+\beta S) \tag{2.77}$$
$$0 = S\cdot(R+\alpha G+\beta S) \tag{2.78}$$

$$-\begin{bmatrix} (G\cdot R) \\ (S\cdot R) \end{bmatrix} = \begin{bmatrix} (G\cdot G) & (S\cdot G) \\ (G\cdot S) & (S\cdot S) \end{bmatrix} \begin{bmatrix} \alpha \\ \beta \end{bmatrix} \tag{2.79}$$

This is a set of two equations for α and β. Recall the inverse of a 2×2 matrix, equation (2.100).

$$\begin{bmatrix} \alpha \\ \beta \end{bmatrix} = \frac{-1}{(G\cdot G)(S\cdot S) - (G\cdot S)^2} \begin{bmatrix} (S\cdot S) & -(S\cdot G) \\ -(G\cdot S) & (G\cdot G) \end{bmatrix} \begin{bmatrix} (G\cdot R) \\ (S\cdot R) \end{bmatrix} \tag{2.80}$$

The many applications in this book all need to find α and β with (2.80) and then update the solution with (2.70) and update the residual with (2.71). Thus we package these activities in a subroutine named `cgstep()`. To use that subroutine we will have a computation **template** with repetitive work done by subroutine `cgstep()`. This template (or pseudocode) for minimizing the residual $\mathbf{0} \approx \mathbf{r} = \mathbf{F}\mathbf{x} - \mathbf{d}$ by the conjugate-direction method is

$$\begin{aligned} &\mathbf{r} \longleftarrow \mathbf{F}\mathbf{x} - \mathbf{d} \\ &\text{iterate } \{ \\ &\qquad \Delta\mathbf{x} \longleftarrow \mathbf{F}^*\,\mathbf{r} \\ &\qquad \Delta\mathbf{r} \longleftarrow \mathbf{F}\,\Delta\mathbf{x} \\ &\qquad (\mathbf{x},\mathbf{r}) \longleftarrow \text{cgstep}(\mathbf{x},\mathbf{r},\Delta\mathbf{x},\Delta\mathbf{r}) \\ &\qquad \} \end{aligned}$$

where the subroutine `cgstep()` remembers the previous iteration and works out the step size and adds in the proper proportion of the $\Delta\mathbf{x}$ of the previous step.

2.3.7 Routine for one step of conjugate-direction descent

Because **Fortran** does not recognize the difference between upper- and lower-case letters, the conjugate vectors G and S in the program are denoted by `gg` and `ss`. The inner part of the conjugate-direction task is in function `cgstep()`.

one step of CD.r90

```
module cgstep_mod {
    real, dimension (:), allocatable, private    :: s, ss
contains
    integer function cgstep( first, x, g, rr, gg) {
        real, dimension (:)   :: x, g, rr, gg
        logical               :: first
        double precision      :: sds, gdg, gds, determ, gdr, sdr, alfa, beta
        if( .not. allocated (s)) {   first = .true.
                    allocate ( s (size ( x)))
                    allocate (ss (size (rr)))
                    }
        if( first){ s = 0.;   ss = 0.;   beta = 0.d0    # steepest descent
                    if( dot_product(gg, gg) == 0 )
                            call erexit('cgstep: grad vanishes identically')
                    alfa = - sum( dprod( gg, rr)) / sum( dprod( gg, gg))
                    }
        else{ gdg = sum( dprod( gg, gg))        # search plane by solving 2-by-2
```

```
                sds = sum( dprod( ss , ss ))          #  G . (R - G*alfa - S*beta) = 0
                gds = sum( dprod( gg , ss ))          #  S . (R - G*alfa - S*beta) = 0
                if( gdg==0. .or. sds==0.)  { cgstep = 1;  return }
                determ = gdg * sds * max (1.d0 - (gds/gdg)*(gds/sds), 1.d-12)
                gdr = - sum( dprod( gg , rr ))
                sdr = - sum( dprod( ss , rr ))
                alfa = ( sds * gdr - gds * sdr ) / determ
                beta = (-gds * gdr + gdg * sdr ) / determ
                }
            s  = alfa *  g + beta *  s                # update solution step
            ss = alfa * gg + beta * ss                # update residual step
            x  =  x +  s                              # update solution
            rr = rr + ss                              # update residual
            first = .false.;    cgstep = 0
        }
        subroutine cgstep_close ( ) {
             if( allocated( s))  deallocate( s , ss)
        }
}
```

Observe the `cgstep()` function has a logical parameter called `first`. This parameter does not need to be input. In the normal course of things, `first` will be true on the first iteration and false on subsequent iterations. This refers to the fact that on the first iteration, there is no previous step, so the conjugate direction method is reduced to the steepest descent method. At any iteration, however, you have the option to set `first=.true.` which amounts to restarting the calculation from the current location, something we rarely find reason to do.

2.3.8 A basic solver program

There are many different methods for iterative least-square estimation some of which will be discussed later in this book. The conjugate-gradient (CG) family (including the first order conjugate-direction method described above) share the property that theoretically they achieve the solution in n iterations, where n is the number of unknowns. The various CG methods differ in their numerical errors, memory required, adaptability to non-linear optimization, and their requirements on accuracy of the adjoint. What we do in this section is to show you the generic interface.

None of us is an expert in both geophysics and in optimization theory (OT), yet we need to handle both. We would like to have each group write its own code with a relatively easy interface. The problem is that the OT codes must invoke the physical operators yet the OT codes should not need to deal with all the data and parameters needed by the physical operators.

In other words, if a practitioner decides to swap one solver for another, the only thing needed is the name of the new solver.

The operator entrance is for the geophysicist, who formulates the estimation application. The solver entrance is for the specialist in numerical algebra, who designs a new optimization method.

The Fortran-90 programming language allows us to achieve this design goal by means of generic function interfaces.

A generic solver subroutine `solver()` is shown in module `smallsolver`. It is simplified substantially from the library version, which has a much longer list of optional arguments.

generic solver.r90

```
module smallsolver {
  logical, parameter, private :: AJ = .true., FW = .false.
  logical, parameter, private :: AD = .true., ZP = .false.
  logical           , private :: first
contains
  subroutine solver( oper, solv, x, dat, niter, x0, res) {
    optional                                  :: x0, res
    interface {
       integer function oper( adj, add, x, dat)     {
            logical, intent (in) :: adj, add
            real, dimension (:)  :: x, dat
            }
       integer function solv( first, x, dx, r, dr) {
            logical              :: first
            real, dimension (:) :: x, dx, r, dr
            }
       }
    real,    dimension (:),   intent (in)  :: dat, x0     # data, initial
    real,    dimension (:),   intent (out) :: x, res      # solution, residual
    integer,                  intent (in)  :: niter       # iterations
    real, dimension (size (x))             :: dx          # gradient
    real, dimension (size (dat))           :: r, dr       # residual, conj grad
    integer                                :: i, stat
    r = - dat
    if( present( x0)) {
        stat = oper( FW, AD, x0, r)                       # r <- F x0 - dat
        x = x0                                            # start with x0
        }
    else {
        x = 0.                                            # start with zero
        }
    first = .false.
    do i = 1, niter  {
       stat = oper( AJ, ZP, dx, r)                        # dx  <- F' r
       stat = oper( FW, ZP, dx, dr)                       # dr <- F  dx
       stat = solv( first, x, dx, r, dr)                  # step in x and r
       }
    if( present( res)) res = r
  }
}
```

(The `first` parameter is not needed by the solvers we discuss first.)

The two most important arguments in `solver()` are the operator function `oper`, which is defined by the interface from Chapter 1, and the solver function `solv`, which implements one step of an iterative estimation. For example, a practitioner who choses to use our new `cgstep()` for iterative solving the operator `matmult` would write the call

```
call solver ( matmult_lop, cgstep, ...
```

The other required parameters to `solver()` are `dat` (the data we want to fit), `x` (the model we want to estimate), and `niter` (the maximum number of iterations). There is also a couple of optional arguments. For example, `x0` is the starting guess for the model.

If this parameter is omitted, the model is initialized to zero. To output the final residual vector, we include a parameter called `res`, which is optional as well. We will watch how the list of optional parameters to the generic solver routine grows as we attack more and more complex applications in later chapters.

2.3.9 Fitting success and solver success

Every time we run a data modeling program we have access to two publishable numbers $1-|\mathbf{r}|/|\mathbf{d}|$ and $1-|\mathbf{F}^* \mathbf{r}|/|\mathbf{F}^* \mathbf{d}|$. The first says how well the model fits the data. The second says how well we did the job of finding out.

Define the residual $\mathbf{r} = \mathbf{F}\mathbf{m} - \mathbf{d}$ and the "size" of any vector, such as the data vector, as $|\mathbf{d}| = \sqrt{\mathbf{d} \cdot \mathbf{d}}$. The number $1 - |\mathbf{r}|/|\mathbf{d}|$ will be called the "success at fitting data." (Any data-space weighting function should have been incorporated in both $\mathbf{F}$ and $\mathbf{d}$.)

While the data fitting success is of interest to everyone, the second number $1-|\mathbf{F}^* \mathbf{r}|/|\mathbf{F}^* \mathbf{d}|$ is of interest in QA (quality analysis). In giant problems, especially those arising in seismology, running iterations to completion is impractical. A question always of interest is whether enough iterations have been run. This number gives us guidance to where more effort could be worthwhile.

0	$\leq$	Success	$\leq$ 1
Fitting success:		$1 - \|\mathbf{r}\|/\|\mathbf{d}\|$	
Numerical success:		$1 - \|\mathbf{F}^* \mathbf{r}\|/\|\mathbf{F}^* \mathbf{d}\|$	

2.3.10 Roundoff

Surprisingly, as a matter of practice, the simple conjugate-direction method defined in this book is more reliable than the conjugate-gradient method defined in the formal professional literature. I know this sounds unlikely, but I'll tell you why.

In large applications numerical roundoff can be a problem. Calculations need to be done in higher precision. The conjugate gradient method depends on you to supply an operator whose adjoint is correctly computed. Any roundoff in computing the operator should somehow be matched by the roundoff in the adjoint. This is unrealistic. Thus optimization may diverge while theoretically converging. The conjugate direction method doesn't mind the roundoff. It simply takes longer to converge.

Let us see an example of a situation where roundoff becomes a problem. Suppose we add 100 million ones. You expect the sum to be 100 million. I got a sum of 16.7 million. Why is this? After the sum gets to 16.7 million adding a one to it adds nothing. The extra 1.0 disappears in single precision roundoff.

```
real function one(sum);  one=1.;  return; end
integer i;   real sum
do i=1, 100000000
        sum = sum + one(sum)
```

```
        write (0,*) sum;     stop;  end
1.6777216E+07
```

The code above must be a little more complicated than I had hoped because modern compilers are so clever. When told to add all the values in a vector they know it is wise to add the numbers in groups, and then add the groups. Thus I had to hide the fact I was adding ones by getting them from a subroutine that seems to depend upon the sum (but really doesn't).

2.3.11 Test case: solving some simultaneous equations

Now we assemble a module `cgmeth` for solving simultaneous equations. Starting with the conjugate-direction module `cgstep_mod` we insert the module `matmult` as the linear operator.

demonstrate CD.r90

```
module cgmeth {
  use matmult
  use cgstep_mod
  use solver_tiny_mod
contains
  # setup of conjugate gradient descent, minimize  SUM rr(i)**2
  #                nx
  # rr(i)  =    sum fff(i,j) * x(j)  -  yy(i)
  #               j=1
  subroutine cgtest( x, yy, rr, fff, niter) {
    real, dimension (:), intent (out) :: x, rr
    real, dimension (:), intent (in)  :: yy
    real, dimension (:,:), pointer    :: fff
    integer,               intent (in)  :: niter
    call matmult_init( fff)
    call solver_tiny( m=x, d=yy, &
        Fop=matmult_lop, stepper=cgstep, &
        niter=niter, resd=rr)
    call cgstep_close ()
  }
}
```

Below shows the solution to 5×4 set of simultaneous equations. Observe that the "exact" solution is obtained in the last step. Because the data and answers are integers, it is quick to check the result manually.

```
d transpose
      3.00      3.00      5.00      7.00      9.00

F transpose
      1.00      1.00      1.00      1.00      1.00
      1.00      2.00      3.00      4.00      5.00
      1.00      0.00      1.00      0.00      1.00
      0.00      0.00      0.00      1.00      1.00

for iter = 0, 4
x    0.43457383  1.56124675  0.27362058  0.25752524
```

```
res -0.73055887  0.55706739  0.39193487 -0.06291389 -0.22804642
x    0.51313990  1.38677299  0.87905121  0.56870615
res -0.22103602  0.28668585  0.55251014 -0.37106210 -0.10523783
x    0.39144871  1.24044561  1.08974111  1.46199656
res -0.27836466 -0.12766013  0.20252672 -0.18477242  0.14541438
x    1.00001287  1.00004792  1.00000811  2.00000739
res  0.00006878  0.00010860  0.00016473  0.00021179  0.00026788
x    1.00000024  0.99999994  0.99999994  2.00000024
res -0.00000001 -0.00000001  0.00000001  0.00000002 -0.00000001
```

2.3.12 Why Fortran 90 is much better than Fortran 77

I'd like to digress from our geophysics-mathematics themes to explain why Fortran 90 has been a great step forward over Fortran 77. Many of the illustrations in this book were originally computed in F77. Then module `smallsolver()` was simply a subroutine. It was not one module for the whole book, as it is now, but it was many conceptually identical subroutines, dozens of them, one subroutine for each application. The reason for the proliferation was that F77 lacks the ability of F90 to represent operators as having two ways to enter, one for science and another for math. On the other hand, F77 did not require the half a page of definitions that we see here in F90. But the definitions are not difficult to understand, and they are a clutter that we must see once and never again. Another benefit is that the book in F77 had no easy way to switch from the `cgstep` solver to other solvers.

2.4 INVERSE NMO STACK

To illustrate an example of solving a huge set of simultaneous equations without ever writing down the matrix of coefficients, we consider how ***back projection*** can be upgraded towards ***inversion*** in the application called **moveout and stack**.

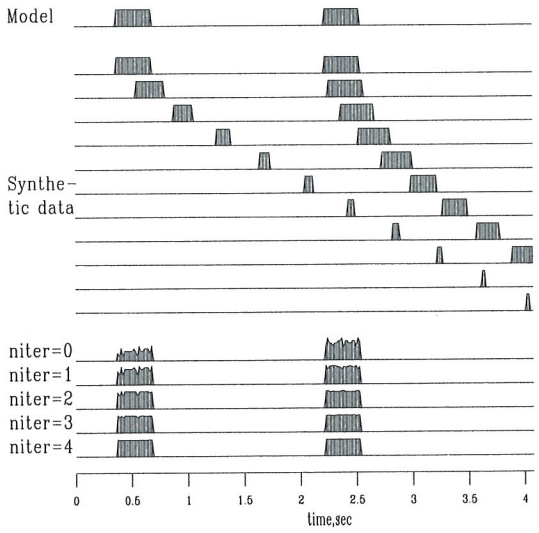

Figure 2.6: Top is a model trace **m**. Next are the synthetic data traces, $\mathbf{d} = \mathbf{Mm}$. Then, labeled `niter=0` is the **stack**, a result of processing by adjoint modeling. Increasing values of `niter` show **m** as a function of iteration count in the fitting goal $\mathbf{d} \approx \mathbf{Mm}$. (Carlos Cunha-Filho)
VIEW lsq/. invstack90

The seismograms at the bottom of Figure 2.6 show the first four iterations of conjugate-direction inversion. You see the original rectangle-shaped waveform returning as the it-

erations proceed. Notice also on the **stack** that the early and late events have unequal amplitudes, but after enough iterations they are equal, as they began. Mathematically, we can denote the top trace as the model $\mathbf{m}$, the synthetic data signals as $\mathbf{d} = \mathbf{Mm}$, and the stack as $\mathbf{M}^* \mathbf{d}$. The conjugate-gradient algorithm optimizes the fitting goal $\mathbf{d} \approx \mathbf{Mx}$ by variation of $\mathbf{x}$, and the figure shows $\mathbf{x}$ converging to $\mathbf{m}$. Because there are 256 unknowns in $\mathbf{m}$, it is gratifying to see good convergence occurring after the first four iterations. The fitting is done by module `invstack`, which is just like `cgmeth` except that the matrix-multiplication operator `matmult` has been replaced by `imospray`. Studying the program, you can deduce that, except for a scale factor, the output at `niter=0` is identical to the stack $\mathbf{M}^*\mathbf{d}$. All the signals in Figure 2.6 are intrinsically the same scale.

inversion stacking.r90

```
module invstack {
   use imospray
   use cgstep_mod
   use solver_tiny_mod
contains
   # NMO stack by inverse of forward modeling
   subroutine stack( nt, model, nx, gather,      t0,x0,dt,dx,slow, niter) {
   integer             nt,          nx,                             niter
   real                             model (:), gather (:), t0,x0,dt,dx,slow
   call imospray_init( slow, x0,dx, t0,dt, nt, nx)
   call solver_tiny( model, gather, imospray_lop, cgstep, niter)
   call cgstep_close (); call imospray_close ()   # garbage collection
   }
}
```

This simple inversion is inexpensive. Has anything been gained over conventional stack? First, though we used nearest-neighbor interpolation, we managed to preserve the spectrum of the input, apparently all the way to the Nyquist frequency. Second, we preserved the true amplitude scale without ever bothering to think about (1) dividing by the number of contributing traces, (2) the amplitude effect of NMO stretch, or (3) event truncation.

With depth-dependent velocity, wave fields become much more complex at wide offset. NMO soon fails, but wave-equation forward modeling offers interesting opportunities for inversion.

2.5 FLATTENING 3-D SEISMIC DATA

Here is an expression that on first sight seems to say nothing:

$$\nabla\tau \quad = \quad \begin{bmatrix} \frac{\partial \tau}{\partial x} \\ \\ \frac{\partial \tau}{\partial y} \end{bmatrix} \tag{2.81}$$

Equation (2.81) looks like a tautology, a restatement of basic mathematical notation. This is so, however, only if $\tau(x, y)$ is known and the derivatives come from it. When $\tau(x, y)$ is not known but the partial derivatives are observed, then we have two measurements at each (x, y) location for the one unknown τ at that location. In Figure 2.4 we have seen how to flatten 2-D seismic data. The 3-D process (x, y, τ) is much more interesting because of the possibility encountering a vector field that cannot be derived from a scalar field.

The easy case is when you can move around the (x, y) plane adding up τ by steps of $d\tau/dx$ and $d\tau/dy$ and find upon returning to your starting location that the total time change τ is zero. When $d\tau/dx$ and $d\tau/dy$ were derived from noisy data, that will not be so. Old time seismologists would say, "The survey lines don't tie." Mathematically it is like an electric field vector that may be derived from a potential field unless the loop encloses a changing magnetic field.

We would like a solution for τ that gives the best fit of all the data (the stepouts $d\tau/dx$ and $d\tau/dy$) in a volume. Given a volume of data $d(t, x, y)$ we seek the best $\tau(x, y)$ such that $w(t, x, y) = d(t - \tau(x, y), x, y)$ is flattened. Let's get it.

We write a regression, a residual $\mathbf{r}$ that we will work to get small to find a best fitting $\tau(x, y)$ or maybe $\tau(x, y, t)$. Let d be the measurements in the vector in equation (2.81), the measurements throughout the (t, x, y)-volume. Expressed as a regression equation (2.81) becomes

$$\mathbf{0} \approx \mathbf{r} = \nabla\tau - \mathbf{d} \tag{2.82}$$

Figure 2.7 shows slices through a cube of seismic data. A paper book is inadequate to display all the images required to compare before and after (one image of output is blended over multiple images of input), so we move on to a radar application of much the same idea, but in 2-D instead of 3-D.

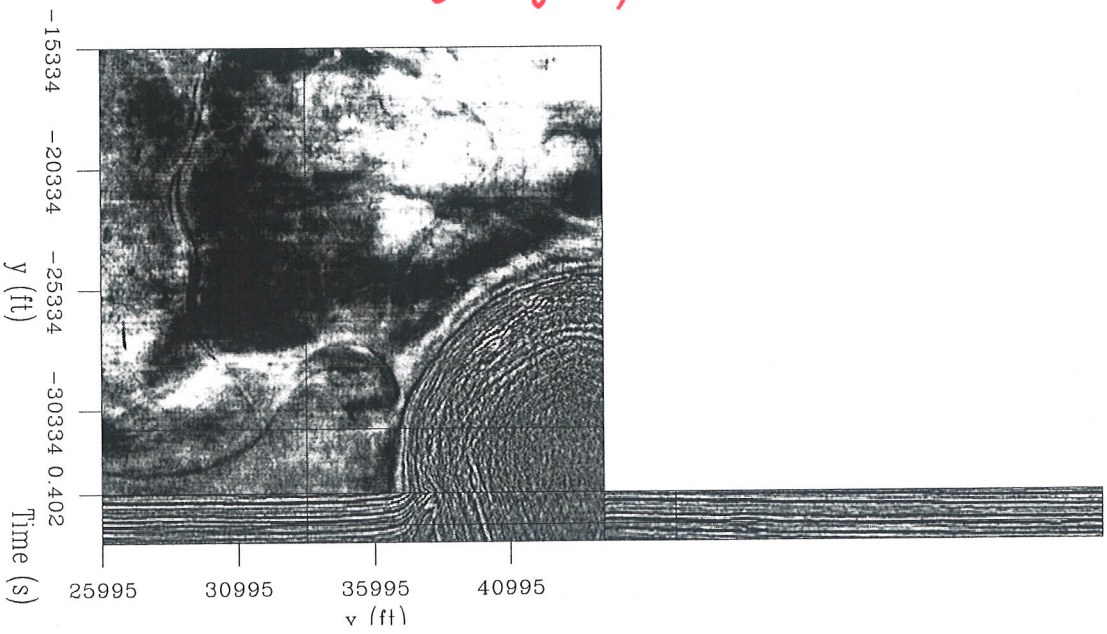

Figure 2.7: [Jesse Lomask] Chevron data cube from the Gulf of Mexico. A salt dome (lower left corner in the top plane) has pushed upwards, dragging bedding planes (seen in the bottom two orthogonal planes) along with it. VIEW lsq/. chev

2.6 VESUVIUS PHASE UNWRAPPING

Figure 2.8 shows radar images of Mt. Vesuvius[1] in Italy. These images are made from backscatter signals $s_1(t)$ and $s_2(t)$, recorded along two **satellite orbits** 800 km high and 54 m apart. The signals are very high frequency (the radar wavelength being 2.7 cm). They were Fourier transformed and one multiplied by the complex conjugate of the other, getting the product $Z = S_1(\omega)\bar{S}_2(\omega)$. The product's amplitude and phase are shown in Figure 2.8. Examining the data, you can notice that where the signals are strongest (darkest on the left), the phase (on the right) is the most spatially consistent.

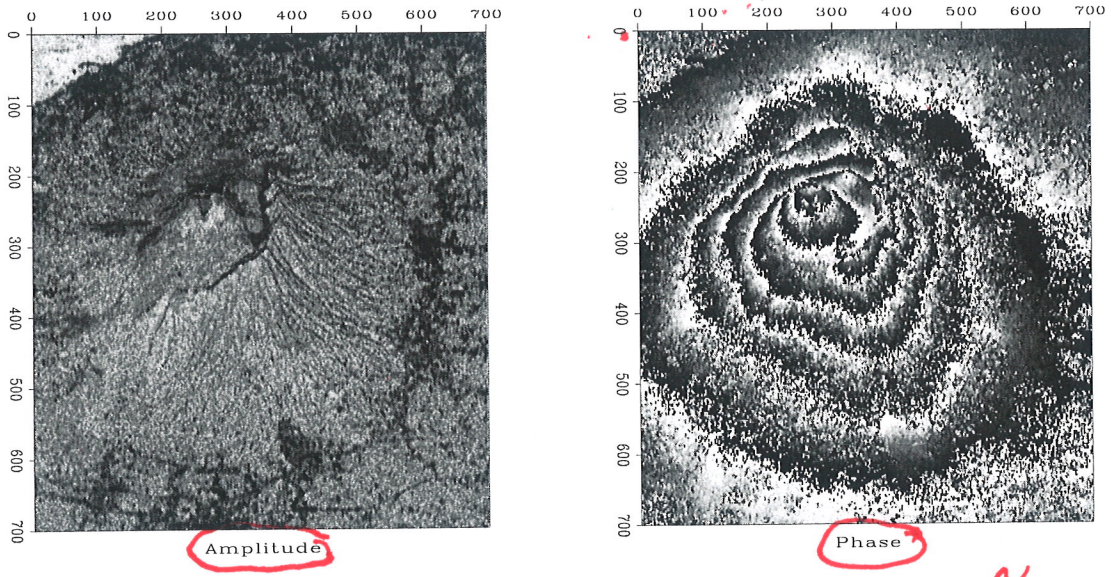

Figure 2.8: Radar image of Mt. Vesuvius. Left is the amplitude $|Z(x,y)|$. Non-reflecting ocean in upper left corner. Right is the phase $\arctan(\text{Re } Z(x,y), \text{Im } Z(x,y))$. (European Space Agency via Umberto Spagnolini) VIEW lsq/. vesuvio90

To reduce the time needed for analysis and printing, I reduced the data size two different ways, by decimation and by local averaging, as shown in Figure 2.9. The decimation was to about 1 part in 9 on each axis, and the local averaging was done in 9×9 windows giving the same spatial resolution in each case. The local averaging was done independently in the plane of the real part and the plane of the imaginary part. Putting them back together again showed that the phase angle of the averaged data behaves much more consistently.

From Figures 2.8 and 2.9 we see that contours of constant phase appear to be contours of constant altitude; this conclusion leads us to suppose that a study of radar theory would lead us to a relation like $Z(x,y) = e^{ih(x,y)}$ where $h(x,y)$ is altitude. We non-radar-specialists often think of phase in $e^{i\phi} = e^{i\omega t_0(x,y)}$ as being caused by some time delay, and being defined for some constant frequency ω. Knowledge of this ω (as well as some angle parameters) would define the physical units of $h(x,y)$.

Because the flat land away from the mountain is all at the same phase (as is the altitude), the distance as revealed by the phase does not represent the distance from the ground to

[1] A web search engine quickly finds you other views.

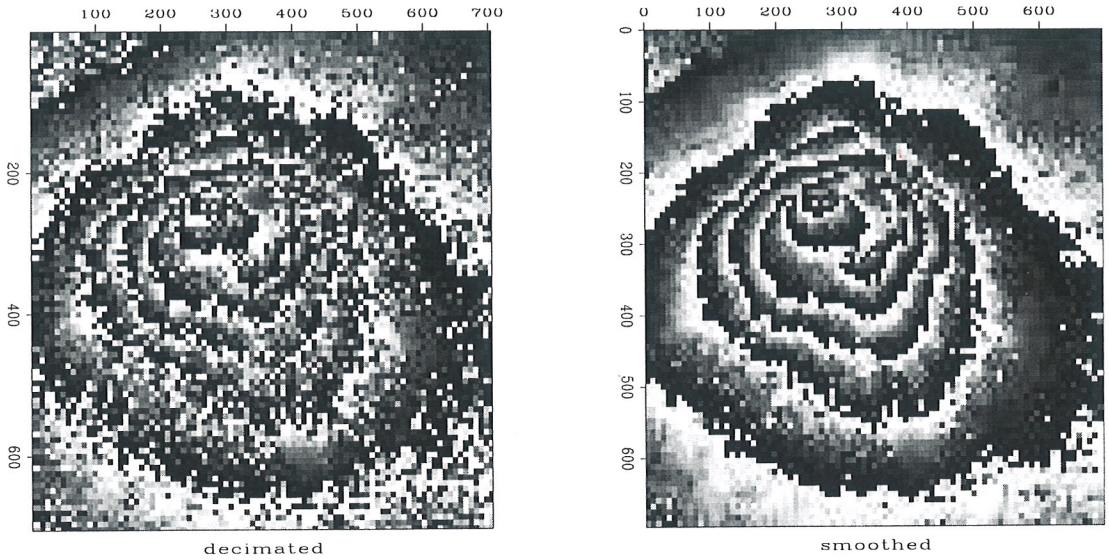

Figure 2.9: Phase based on decimated data (left) and smoothed data (right). VIEW lsq/. squeeze90

the satellite viewer. We are accustomed to measuring altitude along a vertical line to a datum, but here the distance seems to be measured from the ground along a 23° angle from the vertical to a datum at the satellite height.

Phase is a troublesome measurement because we generally see it modulo 2π. Marching up the mountain we see the phase getting lighter and lighter until it suddenly jumps to black which then continues to lighten as we continue up the mountain to the next jump. Let us undertake to compute the phase including all of its jumps of 2π. Begin with a complex number Z representing the complex-valued image at any location in the (x, y)-plane.

$$re^{i\phi} = Z \tag{2.83}$$

$$\ln|r| + i\phi = \ln Z \tag{2.84}$$

$$\phi(x,y) = \text{Im } \ln Z(x,y) + 2\pi N(x,y) \tag{2.85}$$

A computer will find the imaginary part of the logarithm with the arctan function of two arguments, `atan2(y,x)`, which will put the phase in the range $-\pi < \phi \leq \pi$ although any multiple of 2π could be added. We seem to escape the $2\pi N$ phase ambiguity by differentiating:

$$\frac{\partial \phi}{\partial x} = \text{Im } \frac{1}{Z}\frac{\partial Z}{\partial x} = \frac{\text{Im } \bar{Z}\frac{\partial Z}{\partial x}}{\bar{Z}Z} \tag{2.86}$$

For every point on the y-axis, equation (2.86) is a differential equation on the x-axis, and we could integrate them all to find $\phi(x, y)$. That sounds easy. On the other hand, the same equations are valid when x and y are interchanged, so we get twice as many equations as unknowns. For ideal data, either of these sets of equations should be equivalent to the other; but for real data we expect to be fitting the fitting goal

$$\nabla\phi \approx \frac{\text{Im } \bar{Z}\nabla Z}{\bar{Z}Z} \tag{2.87}$$

where $\nabla = (\frac{\partial}{\partial x}, \frac{\partial}{\partial y})$. This is essentially the same application we solved flattening seismic data with the regression $\nabla\tau \approx \mathbf{d}$. Taking measurements to be phase differences between neighboring mesh points, it is more correct to interpret equation (2.87) as a difference equation than a differential equation. Since we measure phase differences only over tiny distances (one pixel), we hope not to worry about phases greater than 2π. But if such jumps do occur, they will contribute to overall error.

Let us consider a typical location in the (x, y) plane where the complex numbers $Z_{i,j}$ are given. Define a shorthand a, b, c, and d as follows:

$$\begin{bmatrix} a & b \\ c & d \end{bmatrix} = \begin{bmatrix} Z_{i,j} & Z_{i,j+1} \\ Z_{i+1,j} & Z_{i+1,j+1} \end{bmatrix} \tag{2.88}$$

With this shorthand, the difference equation representation of the fitting goal (2.87) is:

$$\begin{aligned} \phi_{i+1,j} - \phi_{i,j} &\approx \Delta\phi_{ac} \\ \phi_{i,j+1} - \phi_{i,j} &\approx \Delta\phi_{ab} \end{aligned} \tag{2.89}$$

Now let us find the phase jumps between the various locations. Complex numbers a and b may be expressed in polar form, say $a = r_a e^{i\phi_a}$ and $b = r_b e^{i\phi_b}$. The complex number $\bar{a}b = r_a r_b e^{i(\phi_b - \phi_a)}$ has the desired phase $\Delta\phi_{ab}$. To obtain it we take the imaginary part of the complex logarithm $\ln|r_a r_b| + i\Delta\phi_{ab}$

$$\begin{aligned} \phi_b - \phi_a &= \Delta\phi_{ab} = \text{Im}\ \ln \bar{a}b \\ \phi_d - \phi_c &= \Delta\phi_{cd} = \text{Im}\ \ln \bar{c}d \\ \phi_c - \phi_a &= \Delta\phi_{ac} = \text{Im}\ \ln \bar{a}c \\ \phi_d - \phi_b &= \Delta\phi_{bd} = \text{Im}\ \ln \bar{b}d \end{aligned} \tag{2.90}$$

which gives the information needed to fill in the right-hand side of (2.89), as done by subroutine `makedata()` from module `unwrap`.

The operator needed is `igrad2`, gradient with its adjoint, the divergence.

gradient 2-D..lop

```
module igrad2 {                              # 2-D gradient with adjoint,  r= grad( p)
integer :: n1, n2
#%_init   (n1, n2)
#%_lop ( p(n1, n2),  r(n1,n2,2))
integer i,j
do i= 1, n1-1 {
do j= 1, n2-1 {
        if( adj) {
                p(i+1,j  ) +=  r(i,j,1)
                p(i  ,j  ) -=  r(i,j,1)
                p(i  ,j+1) +=  r(i,j,2)
                p(i  ,j  ) -=  r(i,j,2)
                }
        else {  r(i,j,1)  +=  ( p(i+1,j) - p(i,j))
                r(i,j,2)  +=  ( p(i,j+1) - p(i,j))
                }
        }}
}
```

2.6.1 Estimating the inverse gradient

To optimize the fitting goal (2.89), module unwrap() uses the conjugate-direction method like the modules cgmeth() and invstack().

Inverse 2-D gradient.r90

```
module unwrap {
        use cgstep_mod
        use igrad2
        use solver_smp_mod
contains
        subroutine makedata( z, n1,n2, rt ) {
        integer  i, j,           n1,n2
        real                  rt( n1,n2,2)
        complex                z( n1,n2  ),          a,b,c
        rt = 0.
        do i= 1, n1-1 {
        do j= 1, n2-1 {
                a =  z(i   ,j   )
                c =  z(i+1,j   );    rt(i,j,1) = aimag( clog( c * conjg(a)))
                b =  z(i,   j+1);    rt(i,j,2) = aimag( clog( b * conjg(a)))
                }}
        }
        # Phase unwraper.   Starting from phase hh, improve it.
        subroutine unwraper( zz, hh, niter) {
        integer  n1,n2,              niter
        complex               zz(:,:)
        real                  hh(:)
        real, allocatable ::   rt(:)
        n1 = size( zz, 1)
        n2 = size( zz, 2)
        allocate( rt( n1*n2*2))
        call makedata( zz,n1,n2, rt)
        call igrad2_init(  n1,n2)
        call solver_smp( hh, rt, igrad2_lop, cgstep, niter, m0=hh)
        call cgstep_close ()
        deallocate( rt)
        }
}
```

An open question is whether the required number of iterations is reasonable or whether we would need to uncover a preconditioner or more rapid solution method. I adjusted the frame size (by the amount of smoothing in Figure 2.9) so that I would get the solution in about ten seconds with 400 iterations. Results are shown in Figure 2.10.

2.6.2 Analytical solutions

We have found a numerical solution to fitting applications such as this

$$\mathbf{0} \quad \approx \quad \nabla\tau \; - \; \mathbf{d} \tag{2.91}$$

An analytical solution will be much faster. From any regression we get the least squares solution when we multiply by the transpose of the operator. Thus

$$\mathbf{0} \quad = \quad \nabla^* \, \nabla\tau \; - \; \nabla^* \, \mathbf{d} \tag{2.92}$$

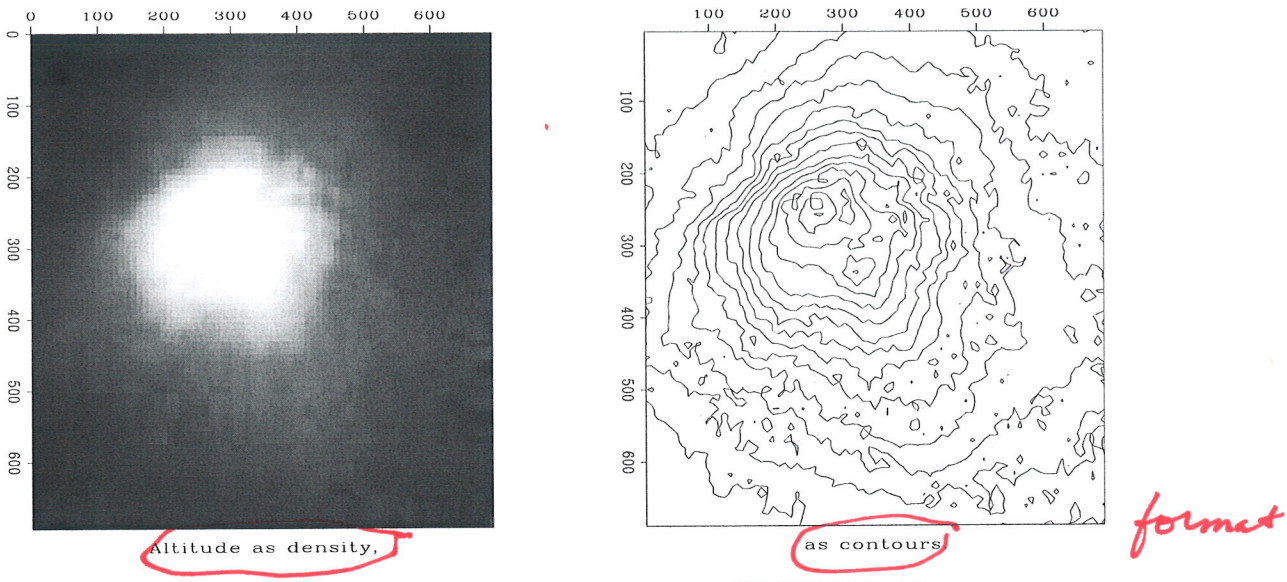

Figure 2.10: Estimated altitude. VIEW lsq/. veshigh90

We need to understand what is the transpose of the gradient operator. Recall the finite difference representation of a derivative in chapter 1. Ignoring end effects, the transpose of a derivative is the negative of a derivative. Since the transpose of a column vector is a row vector, the adjoint of a gradient ∇, namely, ∇^* is more commonly known as the vector divergence $(\nabla \cdot)$. Likewise $\nabla^* \nabla$ is a positive definite matrix, the negative of the Laplacian ∇^2. Thus, in more conventional mathematical notation, the solution τ is that of Poisson's equation.

$$\nabla^2 \tau \quad = \quad -\nabla \cdot \mathbf{d} \tag{2.93}$$

In the Fourier domain we can have an analytic solution. There $-\nabla^2 = k_x^2 + k_y^2$ where (k_x, k_y) are the Fourier frequencies on the (x, y) axes. Instead of thinking of equation (2.93) as a convolution in physical space, think of it as a product in Fourier space. Thus, the analytic solution is

$$\tau(x,y) \quad = \quad \mathbf{FT}^{-1} \frac{\mathbf{FT} \ \nabla \cdot \mathbf{d}}{k_x^2 + k_y^2} \tag{2.94}$$

where **FT** denotes two-dimensional Fourier transform over x and y . Here is a trick from numerical analysis that gives better results: Instead of representing the denominator $k_x^2 + k_y^2$ in the most obvious way, let us represent it in a manner consistent with the finite-difference way we expressed the numerator $\nabla \cdot \mathbf{d}$. Recall that $-i\omega\Delta t \approx i\hat{\omega}\Delta t = 1 - Z = 1 - \exp(-i\omega\Delta t)$ which is a Fourier domain way of saying that difference equations tend to differential equations at low frequencies. Likewise a symmetric second time derivative has a finite-difference representation proportional to $(-2 + Z + 1/Z)$ and in a two-dimensional space, a finite-difference representation of the Laplacian operator is proportional to $(-4 + X + 1/X + Y + 1/Y)$ where $X = \exp(ik_x\Delta x)$ and $Y = \exp(ik_y\Delta y)$. Fourier solutions have their own peculiarities (periodic boundary conditions) which are not always appropriate in practice, but having these solutions available is often a nice place to start from when solving an application that cannot be solved in Fourier space.

For example, suppose we feel some data values are bad and we would like to throw out the regression equations involving the bad data points. At Vesuvius we might consider the strength of the radar return (which we have previously ignored) and use it as a weighting function $\mathbf{W}$. Now our regression (2.91) becomes

$$\mathbf{0} \quad \approx \quad \mathbf{W}\,(\nabla\phi - \mathbf{d}) \quad = \quad (\mathbf{W}\nabla)\phi \;-\; \mathbf{W}\mathbf{d} \tag{2.95}$$

This is a problem we know how to solve, a regression with an operator $\mathbf{W}\nabla$ and data $\mathbf{W}\mathbf{d}$. The weighted problem is not solvable in the Fourier domain because the operator $(\mathbf{W}\nabla)^*\,\mathbf{W}\nabla$ has no simple expression in the Fourier domain. Thus we would use the analytic solution to the unweighted problem as a starting guess for the iterative solution to the real problem.

With the Vesuvius data we could construct a weight $\mathbf{W}$ from the signal strength. We also have available the curl, which should vanish. Vanishing is an indicator of questionable data which could be weighted down relative to other data.

2.7 THE WORLD OF CONJUGATE GRADIENTS

Nonlinearity arises in two ways: First, modeled data might be a nonlinear function of the model parameters. Second, observed data could contain imperfections that force us to use **nonlinear methods** of statistical estimation.

2.7.1 Physical nonlinearity

When standard methods of physics relate modeled data $\mathbf{d}_{\text{theor}}$ to model parameters $\mathbf{m}$, they often use a nonlinear relation, say $\mathbf{d}_{\text{theor}} = \mathbf{f}(\mathbf{m})$. The power-series approach then leads to representing modeled data as

$$\mathbf{d}_{\text{theor}} \quad = \quad \mathbf{f}(\mathbf{m}_0 + \Delta\mathbf{m}) \quad \approx \quad \mathbf{f}(\mathbf{m}_0) + \mathbf{F}\Delta\mathbf{m} \tag{2.96}$$

where $\mathbf{F}$ is the matrix of partial derivatives of data values by model parameters, say $\partial d_i/\partial m_j$, evaluated at $\mathbf{m}_0$. The modeled data $\mathbf{d}_{\text{theor}}$ minus the observed data $\mathbf{d}_{\text{obs}}$ is the residual we minimize.

$$\mathbf{0} \quad \approx \quad \mathbf{d}_{\text{theor}} - \mathbf{d}_{\text{obs}} \quad = \quad \mathbf{F}\Delta\mathbf{m} + [\mathbf{f}(\mathbf{m}_0) - \mathbf{d}_{\text{obs}}] \tag{2.97}$$

$$\mathbf{r}_{\text{new}} \quad = \quad \mathbf{F}\Delta\mathbf{m} + \mathbf{r}_{\text{old}} \tag{2.98}$$

It is worth noticing that the residual updating (2.98) in a nonlinear application is the same as that in a linear application (2.54). If you make a large step $\Delta\mathbf{m}$, however, the new residual will be different from that expected by (2.98). Thus you should always re-evaluate the residual vector at the new location, and if you are reasonably cautious, you should be sure the residual norm has actually decreased before you accept a large step.

The pathway of inversion with physical nonlinearity is well developed in the academic literature and Bill **Symes** at Rice University has a particularly active group.

There are occasions to change the weighting function during model fitting. Then one simply restarts the calculation from the current model. In the code you would flag a restart with the expression `first=.false.`

2.7.2 Coding nonlinear fitting problems

We can solve nonlinear least-squares problems in about the same way as we do iteratively reweighted ones. A simple adaptation of a linear method gives us a nonlinear solver if the residual is recomputed at each iteration. Omitting the weighting function (for simplicity) the **template** is:

```
iterate {
    r  <--  f(m) - d
    Define F = ∂d/∂m.
    Δm  <--  F* r
    Δr  <--  F Δm
    (m, r)  <--  step(m, r, Δm, Δr)
}
```

A formal theory for the optimization exists, but we are not using it here. The assumption we make is that the step size will be small, so that familiar line-search and plane-search approximations will succeed in reducing the residual. Unfortunately this assumption is not reliable. What we should do is test that the residual really does decrease, and if it does not we should revert to steepest descent with a smaller step size. Perhaps we should test an incremental variation on the status quo: where inside `solver`, we check to see if the residual diminished in the *previous* step, and if it did not, restart the iteration (choose the *current* step to be steepest descent instead of CD).

Experience shows that nonlinear applications have many pitfalls. Start with a linear problem, add a minor physical improvement or abnormal noise, and the problem becomes nonlinear and probably has another solution far from anything reasonable. When solving such a nonlinear problem, we cannot arbitrarily begin from zero as we do with linear problems. We must choose a reasonable starting guess. Chapter 3 on the topic of regularization offers an additional way to reduce the dangers of nonlinearity.

2.7.3 Inverse of a 2×2 matrix

$$\mathbf{A}^{-1} \quad \mathbf{A} \quad = \quad \mathbf{I} \tag{2.99}$$

$$\frac{1}{ad-bc}\begin{bmatrix} d & -b \\ -c & a \end{bmatrix}\begin{bmatrix} a & b \\ c & d \end{bmatrix} = \begin{bmatrix} 1 & 0 \\ 0 & 1 \end{bmatrix} \tag{2.100}$$

EXERCISES:

1. It is possible to reject two dips with the operator

$$(\partial_x + p_1\partial_t)(\partial_x + p_2\partial_t) \tag{2.101}$$

This is equivalent to

$$\left(\frac{\partial^2}{\partial x^2} + a\frac{\partial^2}{\partial x \partial t} + b\frac{\partial^2}{\partial t^2}\right) u(t,x) \quad = \quad v(t,x) \quad \approx \quad 0 \tag{2.102}$$

where u is the input signal and v is the output signal. Show how to solve for a and b by minimizing the energy in v.

2. Given a and b from the previous exercise, what are p_1 and p_2?

3. Reduce $\mathbf{d} = \mathbf{Fm}$ to the special case of one data point and two model points like this

$$d = \begin{bmatrix} 2 & 1 \end{bmatrix} \begin{bmatrix} m_1 \\ m_2 \end{bmatrix} \tag{2.103}$$

What is the null space?

4. In 1695, 150 years before Lord Kelvin's absolute temperature scale, 120 years before Sadi Carnot's PhD thesis, 40 years before Anders Celsius, and 20 years before Gabriel Fahrenheit, the French physicist Guillaume Amontons, deaf since birth, took a mercury manometer (pressure gauge) and sealed it inside a glass pipe (a constant volume of air). He heated it to the boiling point of water at 100°C. As he lowered the temperature to freezing at 0°C, he observed the pressure dropped by 25%. He could not drop the temperature any further but he supposed that if he could drop it further by a factor of three, the pressure would drop to zero (the lowest possible pressure) and the temperature would have been the lowest possible temperature. Had he lived after Anders Celsius he might have calculated this temperature to be -300°C (Celsius). Absolute zero is now known to be -273°C.

It is your job to be Amontons' lab assistant. Your ith measurement of temperature T_i you make with Issac Newton's thermometer and you measure pressure P_i and volume V_i in the metric system. Amontons needs you to fit his data with the regression $0 \approx \alpha(T_i - T_0) - P_i V_i$ and calculate the temperature shift T_0 that Newton should have made when he defined his temperature scale. Do not solve this problem! Instead, cast it in the form of equation (2.23), identifying the data d and the two column vectors f_1 and f_2 that are the fitting functions. Relate the model parameters x_1 and x_2 to the physical parameters α and T_0. Suppose you make ALL your measurements at room temperature, can you find T_0? Why or why not?

5. One way to remove a mean value m from signal $s(t) = \mathbf{s}$ is with the fitting goal $\mathbf{0} \approx \mathbf{s} - m$. What operator matrix is involved?

6. What linear operator subroutine from Chapter 1 can be used for finding the mean?

7. How many CD iterations should be required to get the exact mean value?

8. Write a mathematical expression for finding the mean by the CG method.

Chapter 3

Regularization is model styling

Regularization is a method used in mathematics and statistics to deal with insufficient information. The reader must supply additional information in the form of an operator. Where is this operator to come from, and what does it mean? It amounts to us practitioners specifying a "style" of model. Where the model is a signal or an image it amounts to specifying one weighting function in physical space and another in Fourier space.

3.1 EMPTY BINS AND INVERSE INTERPOLATION

A method for restoring **missing data** is to ensure that the restored data, after specified filtering, has minimum energy. Specifying the filter chooses the interpolation philosophy. Generally the filter is a **roughening** filter. When a roughening filter goes off the end of smooth data, it typically produces a big end transient. Minimizing energy implies a choice for unknown data values at the end to minimize the transient. We will examine five cases and then make some generalizations.

> A method for restoring missing data is to ensure that the restored data, after specified filtering, has **minimum energy**.

Let u denote an unknown (missing) value. The dataset on which the examples are based is $(\cdots, u, u,\ 1, u, 2, 1, 2, u, u, \cdots)$. Theoretically we could adjust the missing u values (each different) to minimize the energy in the unfiltered data. Those adjusted values would obviously turn out to be all zeros. The unfiltered data is data that has been filtered by an impulse function. To find the missing values that minimize energy out of other filters, we can use subroutine `mis1()`. Figure 3.1 shows interpolation of the dataset with $(1, -1)$ as a roughening filter. The interpolated data matches the given data where they overlap.

Figures 3.1–3.4 illustrate that the rougher the filter, the smoother the interpolated data and vice versa. Let us switch our attention from the residual spectrum to the residual itself. The residual for Figure 3.1 is the *slope* of the signal (because the filter $(1, -1)$ is a *first derivative*), and the slope is constant (uniformly distributed) along the straight lines where the least-squares procedure is choosing signal values. So these examples confirm the idea that the **least-squares method** abhors large values (because they are squared).

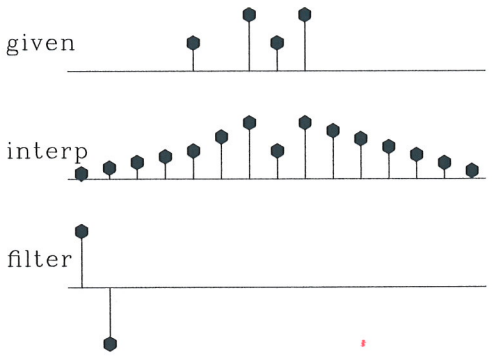

Figure 3.1: Top is given data. Middle is given data with interpolated values. Missing values seem to be interpolated by straight lines. Bottom shows the filter $(1, -1)$, whose output has minimum energy. VIEW iin/. mlines90

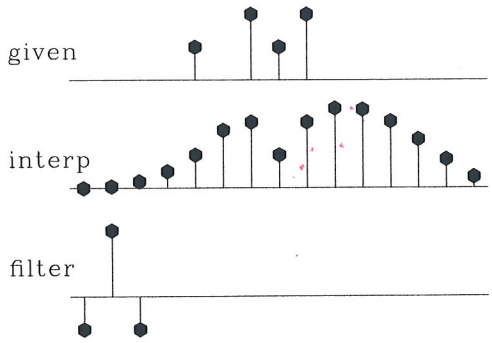

Figure 3.2: Top is the same input data as in Figure 3.1. Middle is interpolated. Bottom shows the filter $(-1, 2, -1)$. The missing data seems to be interpolated by parabolas. VIEW iin/. mparab90

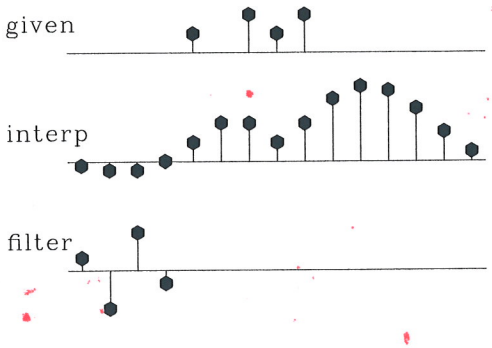

Figure 3.3: Top is the same input. Middle is interpolated. Bottom shows the filter $(1, -3, 3, -1)$. The missing data is very smooth. It shoots upward high off the right end of the observations, apparently to match the data slope there. VIEW iin/. mseis90

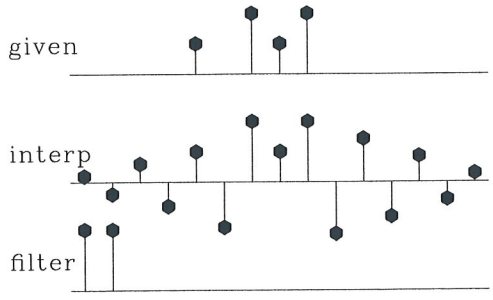

Figure 3.4: Bottom shows the filter $(1, 1)$. The interpolation is rough. Like the given data itself, the interpolation has much energy at the Nyquist frequency. But unlike the given data, it has little zero-frequency energy. VIEW iin/. moscil90

Thus, least squares tends to distribute residuals uniformly in both time and frequency to the extent allowed by the **constraints**.

This idea helps us answer the question, what is the best filter to use? It suggests choosing the filter to have an amplitude spectrum that is inverse to the spectrum we want for the interpolated data. A systematic approach is given in chapter 7, but I offer a simple subjective analysis here: Looking at the data, we see that all points are positive. It seems, therefore, that the data is rich in low frequencies; thus the filter should contain something like $(1, -1)$, which vanishes at zero frequency. Likewise, the data seems to contain Nyquist frequency; so the filter should contain $(1, 1)$. The result of using the filter $(1, -1) * (1, 1) = (1, 0, -1)$ is shown in Figure 3.5. This is my best subjective interpolation based on the idea that the missing data should look like the given data. The **interpolation** and **extrapolations** are so good that you can hardly guess which data values are given and which are interpolated.

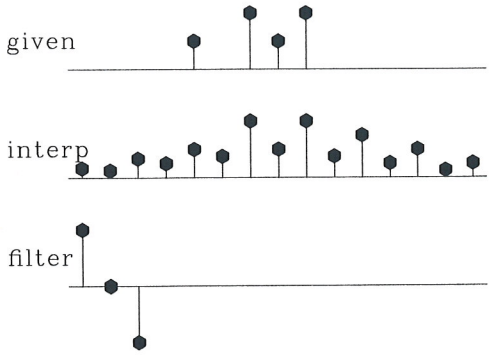

Figure 3.5: Top is the same as in Figures 3.1 to 3.4. Middle is interpolated. Bottom shows the filter $(1, 0, -1)$, which comes from the coefficients of $(1, -1) * (1, 1)$. Both the given data and the interpolated data have significant energy at both zero and Nyquist frequencies. VIEW iin/. mbest90

3.1.1 Missing-data program

Now let us see how Figures 3.1-3.5 could have been calculated and how they were calculated. They could have been calculated with matrices where the matrices were pulled apart according to subscripts of known and missing data. Instead I computed them with operators, and applied only operators and their adjoints. First we inspect the matrix approach because it is more conventional.

Matrix approach to missing data

Customarily, we have referred to data by the symbol $\mathbf{d}$. Now that we are dividing the data space into two parts, known and unknown (or missing), we will refer to this complete space as the model (or map) space $\mathbf{m}$.

There are 15 data points in Figures 3.1-3.5. Of the 15, 4 are known and 11 are missing. Denote the known by k and the missing by u. Then the sequence of missing and known is $(u, u, u, u, k, u, k, k, k, u, u, u, u, u, u)$. Because I cannot print 15×15 matrices, please allow me to describe instead a data space of 6 values $(m_1, m_2, m_3, m_4, m_5, m_6)$ with known values only m_2 and m_3, that is arranged like (u, k, k, u, u, u).

Our approach is to minimize the energy in the residual, which is the filtered map (model)

space. We state the fitting goals $\mathbf{0} \approx \mathbf{Fm}$ as

$$\begin{bmatrix} 0 \\ 0 \\ 0 \\ 0 \\ 0 \\ 0 \\ 0 \\ 0 \end{bmatrix} \approx \mathbf{r} = \begin{bmatrix} a_1 & 0 & 0 & 0 & 0 & 0 \\ a_2 & a_1 & 0 & 0 & 0 & 0 \\ a_3 & a_2 & a_1 & 0 & 0 & 0 \\ 0 & a_3 & a_2 & a_1 & 0 & 0 \\ 0 & 0 & a_3 & a_2 & a_1 & 0 \\ 0 & 0 & 0 & a_3 & a_2 & a_1 \\ 0 & 0 & 0 & 0 & a_3 & a_2 \\ 0 & 0 & 0 & 0 & 0 & a_3 \end{bmatrix} \begin{bmatrix} m_1 \\ m_2 \\ m_3 \\ m_4 \\ m_5 \\ m_6 \end{bmatrix} \tag{3.1}$$

We rearrange the above fitting goals, bringing the columns multiplying known data values (m_2 and m_3) to the left, getting $\mathbf{y} = -\mathbf{F}_k\mathbf{m}_k \approx \mathbf{F}_u\mathbf{m}_u$.

$$\begin{bmatrix} y_1 \\ y_2 \\ y_3 \\ y_4 \\ y_5 \\ y_6 \\ y_7 \\ y_8 \end{bmatrix} = - \begin{bmatrix} 0 & 0 \\ a_1 & 0 \\ a_2 & a_1 \\ a_3 & a_2 \\ 0 & a_3 \\ 0 & 0 \\ 0 & 0 \\ 0 & 0 \end{bmatrix} \begin{bmatrix} m_2 \\ m_3 \end{bmatrix} \approx \begin{bmatrix} a_1 & 0 & 0 & 0 \\ a_2 & 0 & 0 & 0 \\ a_3 & 0 & 0 & 0 \\ 0 & a_1 & 0 & 0 \\ 0 & a_2 & a_1 & 0 \\ 0 & a_3 & a_2 & a_1 \\ 0 & 0 & a_3 & a_2 \\ 0 & 0 & 0 & a_3 \end{bmatrix} \begin{bmatrix} m_1 \\ m_4 \\ m_5 \\ m_6 \end{bmatrix} \tag{3.2}$$

This is the familiar form of an overdetermined system of equations $\mathbf{y} \approx \mathbf{F}_u\mathbf{m}_u$ which we could solve for $\mathbf{m}_u$ as illustrated earlier by conjugate directions, or by a wide variety of well-known methods.

The trouble with this matrix approach is that it is awkward to program the partitioning of the operator into the known and missing parts, particularly if the application of the operator uses arcane techniques, such as those used by the fast–Fourier-transform operator or various numerical approximations to differential or partial differential operators that depend on regular data sampling. Even for the modest convolution operator, we already have a library of convolution programs that handle a variety of end effects, and it would be much nicer to use the library as it is rather than recode it for all possible geometrical arrangements of missing data values.

Note: Here I take the main goal to be the clarity of the code, not the efficiency or accuracy of the solution. So, if your application consumes too many resources, and if you have many more known points than missing ones, maybe you should fit $\mathbf{y} \approx \mathbf{F}_u\mathbf{m}_u$ and ignore the suggestions below.

Operator approach to missing data

For the operator approach to the fitting goal $-\mathbf{F}_k\mathbf{m}_k \approx \mathbf{F}_u\mathbf{m}_u$ we rewrite it as $-\mathbf{F}_k\mathbf{m}_k \approx \mathbf{FJm}$ where

$$-\mathbf{F}_k\mathbf{m}_k \approx \begin{bmatrix} a_1 & 0 & 0 & 0 & 0 & 0 \\ a_2 & a_1 & 0 & 0 & 0 & 0 \\ a_3 & a_2 & a_1 & 0 & 0 & 0 \\ 0 & a_3 & a_2 & a_1 & 0 & 0 \\ 0 & 0 & a_3 & a_2 & a_1 & 0 \\ 0 & 0 & 0 & a_3 & a_2 & a_1 \\ 0 & 0 & 0 & 0 & a_3 & a_2 \\ 0 & 0 & 0 & 0 & 0 & a_3 \end{bmatrix} \begin{bmatrix} 1 & . & . & . & . & . \\ . & 0 & . & . & . & . \\ . & . & 0 & . & . & . \\ . & . & . & 1 & . & . \\ . & . & . & . & 1 & . \\ . & . & . & . & . & 1 \end{bmatrix} \begin{bmatrix} m_1 \\ m_2 \\ m_3 \\ m_4 \\ m_5 \\ m_6 \end{bmatrix} = \mathbf{FJm} \quad (3.3)$$

Notice the introduction of the new diagonal matrix $\mathbf{J}$, called a **mask**ing matrix or a **constraint-mask** matrix because it multiplies constrained variables by zero leaving freely adjustable variables untouched. Experience shows that a better name than "mask matrix" is "**selector** matrix" because what comes out of it, that which is selected, is a less-confusing name for it than which is rejected. With a selector matrix the whole data space seems freely adjustable, both the missing data values and known values. We see that the CD method does not change the known (constrained) values. In general, we derive the fitting goal (3.3) by

$$\begin{aligned} \mathbf{0} &\approx \mathbf{Fm} && (3.4)\\ \mathbf{0} &\approx \mathbf{F}(\mathbf{J}+(\mathbf{I}-\mathbf{J}))\mathbf{m} && (3.5)\\ \mathbf{0} &\approx \mathbf{FJm}+\mathbf{F}(\mathbf{I}-\mathbf{J})\mathbf{m} && (3.6)\\ \mathbf{0} &\approx \mathbf{FJm}+\mathbf{Fm}_{\text{known}} && (3.7)\\ \mathbf{0} \approx \mathbf{r} &= \mathbf{FJm}+\mathbf{r}_0 && (3.8) \end{aligned}$$

As usual, we find a direction to go $\Delta\mathbf{m}$ by the gradient of the residual energy.

$$\Delta\mathbf{m} = \frac{\partial}{\partial \mathbf{m}^*}\,\mathbf{r}^*\mathbf{r} = \left(\frac{\partial}{\partial \mathbf{m}^*}\,\mathbf{r}^*\right)\mathbf{r} = \left(\frac{\partial}{\partial \mathbf{m}^*}\,(\mathbf{m}^*\mathbf{J}^*\mathbf{F}^*+\mathbf{r}_0^*)\right)\mathbf{r} = \mathbf{J}^*\mathbf{F}^*\mathbf{r} \quad (3.9)$$

We begin the calculation with the known data values where missing data values are replaced by zeros, namely $(\mathbf{I}-\mathbf{J})\mathbf{m}$. Filter this data, getting $\mathbf{F}(\mathbf{I}-\mathbf{J})\mathbf{m}$, and load it into the residual $\mathbf{r}_0$. With this initialization completed, we begin an iteration loop. First we compute $\Delta\mathbf{m}$ from equation (3.9).

$$\Delta\mathbf{m} \quad \longleftarrow \quad \mathbf{J}^*\mathbf{F}^*\mathbf{r} \quad (3.10)$$

$\mathbf{F}^*$ applies a *crosscorrelation* of the filter to the residual and then $\mathbf{J}^*$ sets to zero any changes proposed to known data values. Next, compute the change in residual $\Delta\mathbf{r}$ from the proposed change in the data $\Delta\mathbf{m}$.

$$\Delta\mathbf{r} \quad \longleftarrow \quad \mathbf{FJ}\Delta\mathbf{m} \quad (3.11)$$

This applies the filtering again. Then use the method of steepest descent (or conjugate direction) to choose the appropriate scaling (or inclusion of previous step) of $\Delta\mathbf{m}$ and $\Delta\mathbf{r}$, and update $\mathbf{m}$ and $\mathbf{r}$ accordingly and iterate.

I could have passed a new operator $\mathbf{FJ}$ into the old solver, but found it worthwhile to write a new, more powerful solver having built-in constraints. To introduce the masking operator $\mathbf{J}$ into the `solver_smp` subroutine I introduce an optional operator `Jop`, which is initialized with a logical array of the model size. Two lines in the `solver_tiny` module

```
stat = Fop( AJ, ZP, dm, rd)                          #  dm = F' Rd
stat = Fop( FW, ZP, dm, dr)                          #  dR = F  dm
```

become three lines in the standard library module `solver_smp`. (We use a temporary array `tm` of the size of model space.) $\Delta\mathbf{m}$ is `dm` and $\Delta\mathbf{r}$ is `dr`.

```
stat = Fop( AJ, ZP, dm, rd)                                    # dm = F' Rd
if ( present( Jop)) { tm=dm;  stat= Jop( FW, ZP, tm, dm)       # dm = J dm
stat = Fop( FW, ZP, dm, dr)                                    # dR = F dm
```

The full code includes all the definitions we had earlier in `solver-tiny` module. Merging it with the above bits of code we have the simple solver `solver-smp`.

simple solver.r90

```
module solver_smp_mod {                                  # 0 = W (F J m - d)
  use chain0_mod + solver_report_mod
  logical, parameter, private  :: AJ = .true., FW = .false.
  logical, parameter, private  :: AD = .true., ZP = .false.
contains
  subroutine solver_smp( m,d, Fop, stepper, niter &
  ,                      Wop,Jop,m0,err,resd,mmov,rmov,verb) {
    optional :: Wop,Jop,m0,err,resd,mmov,rmov,verb
    interface { #------------------------------ begin definitions ----------
      integer function Fop(adj,add,m,d){real::m(:),d(:);logical::adj,add}
      integer function Wop(adj,add,m,d){real::m(:),d(:);logical::adj,add}
      integer function Jop(adj,add,m,d){real::m(:),d(:);logical::adj,add}
      integer function stepper(first,m,dm,r,dr) {
        real, dimension(:)  ::        m,dm,r,dr
        logical             :: first             }
    }
    real, dimension(:),     intent(in)          :: d, m0
    integer,                intent(in)          :: niter
    logical,                intent(in)          :: verb
    real, dimension(:),     intent(out)         :: m,err, resd
    real, dimension(:,:),   intent(out)         ::        rmov, mmov
    real, dimension(size(m))                    :: dm
    real, dimension(size(d)),          target   :: r, dr
    real, dimension(size(d)+size(m)), target    :: tt
    real, dimension(:), pointer                 :: rd, drd, td
    real, dimension(:), pointer                 :: rm, drm, tm
    integer                                     :: iter, stat
    logical                                     :: first
    rd  => r(1:size(d));
    drd => dr(1:size(d));
    td  => tt(1:size(d));    tm => tt(1+size(d):)
    if(present( Wop)) stat=Wop(FW,ZP,-d,rd) # begin initialization ----------
    else rd = -d                                                  #Rd = -W  d
    if(present( m0)){ m=m0                                        #m  =     m0
       if(present( Wop)) call chain0(Wop,Fop,FW,AD,m,rd,td)
       else              stat =           Fop(FW,AD,m,rd    ) #Rd+= WF m0
    } else m=0
    first = .true.; #------------------------------ begin iterations ---------
    do iter = 1,niter {
       if(present(Wop)) call chain0(Wop,Fop,AJ,ZP,dm,rd,td)
       else             stat =         Fop(AJ,ZP,dm,rd    )   #dm  = (WF)'Rd
       if(present(Jop)){ tm=dm;  stat  = Jop(FW,ZP,tm, dm  )} #dm  =   J  dm
       if(present(Wop)) call chain0(Wop,Fop,FW,ZP,dm,drd,td)
```

```
        else                stat =           Fop(FW,ZP,dm,drd    )  #dRd = (WF) dm
        stat = stepper(first , m,dm, r,dr)                          #m+=dm; R+=dR
        if(stat ==1) exit # got stuck descending
        if(present( mmov)) mmov(:,iter) =  m(:size(mmov,1)) # report -----
        if(present( rmov)) rmov(:,iter) = rd(:size(rmov,1))
        if(present( err ))  err(  iter) = dot_product(rd,rd)
        if(present( verb)){ if(verb) call solver_report(iter,m,dm,rd)}
        first=.false.
      }
      if(present( resd)) resd = rd
    }
}
```

There are two methods of invoking the solver. Comment cards in the code indicate the slightly more verbose method of solution which matches the theory presented in the book.

The subroutine to find missing data is `mis1()`. It assumes that zero values in the input data correspond to missing data locations. It uses our convolution operator `tcai1()`. You can also check the Index for other **operators** and **modules**.

1-D missing data.r90

```
module mis_mod {
  use tcai1+mask1+cgstep_mod+solver_smp_mod
#  use mtcai1
contains
# fill in missing data on 1-axis by minimizing power out of a given filter.
  subroutine mis1 ( niter, mm, aa) {
    integer,                intent (in)       :: niter    # number of iterations
    real, dimension (:), pointer              :: aa       # roughening filter
    real, dimension (:), intent (in out)      :: mm       # in - data with zeroes
                                                          # out - interpolated
    real, dimension (:),allocatable           :: zero     # filter output
    logical, dimension(:), pointer            :: msk
    integer                                   :: stat
#   real, dimension (:),allocatable            :: dd
    allocate(zero(size(mm)+size(aa))); zero = 0.
    allocate( msk(size(mm)))
#   allocate(  dd(size(mm)+size(aa)))
    # solve     F     m = 0  w/ J
    msk=(mm==0.); call mask1_init(msk)
    call tcai1_init(aa)
    call solver_smp( mm, zero, tcai1_lop, cgstep, niter, m0=mm, Jop=mask1_lop)
    # solve  (F J) m = d
#   call mtcai1_init(aa,msk)                  #       F(I-J)
#   stat = mtcai1_lop(.false.,.false.,mm,dd) #       F(I-J) m
#   dd = - dd                                 # d = - F(I-J) m
#   msk=(mm==0.); call mask1_init(msk)        #            J
#   call solver_smp( mm, dd, mtcai1_lop, cgstep, niter, m0=mm)
    call cgstep_close ()
    deallocate(zero)
    }
}
```

I sought reference material on conjugate gradients with constraints and didn't find anything, leaving me to fear that this chapter was in error and that I had lost the magic property of convergence in a finite number of iterations. I tested the code and it did converge in a

finite number of iterations. The explanation is that these constraints are almost trivial. We pretended we had extra variables, and computed a $\Delta\mathbf{m} = \mathbf{g}$ for each of them. Using $\mathbf{J}$ we then set the gradient $\Delta\mathbf{m} = \mathbf{g}$ to zero, hence making no changes to anything, like as if we had never calculated the extra $\Delta\mathbf{m}$'s.

3.2 WELLS NOT MATCHING THE SEISMIC MAP

Accurate knowledge comes from a **wells**, but wells are expensive and far apart. Less accurate knowledge comes from surface seismology, but this knowledge is available densely in space and can indicate significant **trends** between the wells. For example, a prospective area may contain 15 wells but 600 or more seismic stations. To choose future well locations, it is helpful to match the known well data with the seismic data. Although the seismic data is delightfully dense in space, it often mismatches the wells because there are systematic differences in the nature of the measurements. These discrepancies are sometimes attributed to velocity **anisotropy**. To work with such measurements, we do not need to track down the physical model, we need only to merge the information somehow so we can appropriately **map** the trends between wells and make a proposal for the next drill site. Here we consider only a scalar value at each location. Take $\mathbf{w}$ to be a vector of 15 components, each component being the seismic travel time to some fixed depth in a well. Likewise let $\mathbf{s}$ be a 600-component vector each with the seismic travel time to that fixed depth as estimated wholly from surface seismology. Such empirical corrections are often called "**fudge factors**". An example is the Chevron oil field in Figure 3.6. The binning of the seismic data in

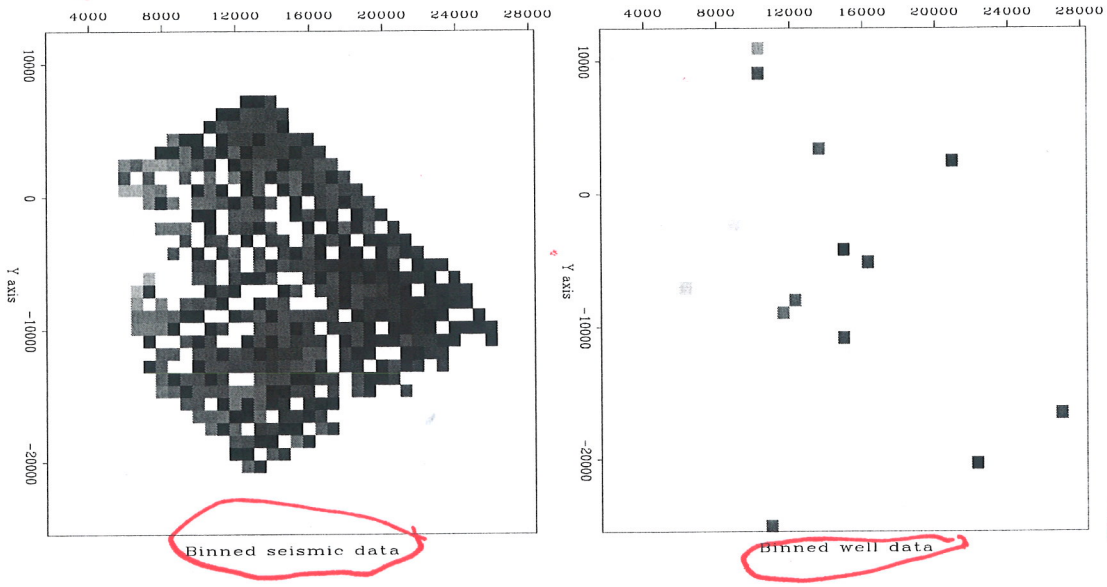

Figure 3.6: Binning by data push. Left is seismic data. Right is well locations. Values in bins are divided by numbers in bins. (Toldi) VIEW iin/. wellseis90

Figure 3.6 is not really satisfactory when we have available the techniques of missing data estimation to fill the empty bins. Using the ideas of subroutine `mis1()` we can extend the seismic data into the empty part of the plane. We use the same principle that we minimize the energy in the filtered map where the map must match the data where it is known. I

chose the filter $\mathbf{A} = \nabla^* \nabla = -\nabla^2$ to be the Laplacian operator (actually, its negative) to obtain the result in Figure 3.7.

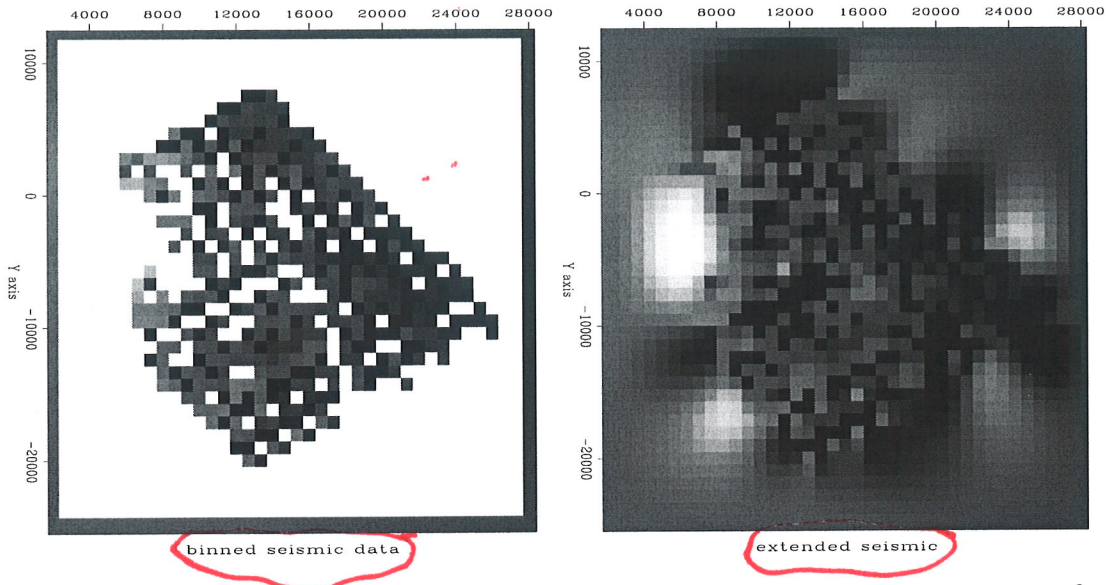

Figure 3.7: Seismic binned (left) and extended (right) by minimizing energy in ∇^2s.
VIEW iin/. misseis90

There are basically two ways to handle boundary conditions. First as we did in Figure 3.1, by using a transient filter operator which assumes zero outside to region of interest. Second is to use an internal filter operator. It's a bit trickier. Solutions could be growing at the boundaries. That's almost never desirable. In that case it is better to assign boundary values. That is what I did here in Figure 3.7. I didn't do it because it is better, but to minimize the area surrounding the data of interest.

The first job is to fill the gaps in the seismic data. We just finished doing a job like this in one dimension. I'll give you more computational details later. Let us call the extended seismic data **s**.

Think of a map of a model space **m** of infinitely many hypothetical wells that must match the real wells, where we have real wells. We must find a map that matches the wells exactly and somehow matches the seismic information elsewhere. Let us define the vector **w** as shown in Figure 3.6 so **w** is observed values at wells and zeros elsewhere.

Where the seismic data contains sharp bumps or streaks, we want our final earth model to have those features. The wells cannot provide the rough features because the wells are too far apart to provide high spatial frequencies. The well information generally conflicts with the seismic data at low spatial frequencies because of systematic discrepancies between the two types of measurements. Thus we must accept that **m** and **s** may differ at low spatial frequencies (where gradient and Laplacian are small).

Our final map **m** would be very unconvincing if it simply jumped from a well value at one point to a seismic value at a neighboring point. The map would contain discontinuities around each well. Our philosophy of finding an earth model **m** is that our earth map

should contain no obvious "footprint" of the data acquisition (well locations). We adopt the philosophy that the difference between the final map (extended wells) and the seismic information $\mathbf{x} = \mathbf{m} - \mathbf{s}$ should be smooth. Thus, we seek the minimum residual $\mathbf{r}$ which is the roughened difference between the seismic data $\mathbf{s}$ and the map $\mathbf{m}$ of hypothetical omnipresent wells. With roughening operator $\mathbf{A}$ we fit

$$\mathbf{0} \quad \approx \quad \mathbf{r} \quad = \quad \mathbf{A}(\mathbf{m} - \mathbf{s}) \quad = \quad \mathbf{A}\mathbf{x} \tag{3.12}$$

along with the constraint that the map should match the wells at the wells. We could write this as $\mathbf{0} = (\mathbf{I} - \mathbf{J})(\mathbf{m} - \mathbf{w})$. We honor this constraint by initializing the map $\mathbf{m} = \mathbf{w}$ to the wells (where we have wells, and zero elsewhere). After we find the gradient direction to suggest some changes to $\mathbf{m}$, we simply will not allow those changes at well locations. We do this with a mask. We apply a "missing data selector" to the gradient. It zeros out possible changes at well locations. Like with the goal (3.7), we have

$$\mathbf{0} \quad \approx \quad \mathbf{r} \quad = \quad \mathbf{A}\mathbf{J}\mathbf{x} + \mathbf{A}\mathbf{x}_{\text{known}} \tag{3.13}$$

After minimizing $\mathbf{r}$ by adjusting $\mathbf{x}$, we have our solution $\mathbf{m} = \mathbf{x} + \mathbf{s}$.

Now we prepare some roughening operators $\mathbf{A}$. We have already coded a 2-D gradient operator `igrad2`. Let us combine it with its adjoint to get the 2-D laplacian operator. (You might notice that the laplacian operator is "self-adjoint", meaning that the operator does the same calculation that its adjoint does. Any operator of the form $\mathbf{A}^*\mathbf{A}$ is self-adjoint because $(\mathbf{A}^*\mathbf{A})^* = \mathbf{A}^*(\mathbf{A}^*)^* = \mathbf{A}^*\mathbf{A}$.)

Laplacian in 2-D.lop

```
module laplac2 {                                        # Laplacian operator in 2-D
use igrad2
logical, parameter, private  :: AJ = .true., FW = .false.
logical, parameter, private  :: AD = .true., ZP = .false.
real, dimension (m1*m2*2), allocatable :: tmp
#%_init     (m1, m2)
    integer m1, m2
    call igrad2_init (m1, m2)
#%_lop (x, y)
    integer stat1, stat2
    if( adj) {
        stat1 = igrad2_lop ( FW,   ZP, y, tmp)   # tmp = grad y
        stat2 = igrad2_lop ( AJ,  add, x, tmp)   # x = x + grad' tmp
    } else   {
        stat1 = igrad2_lop ( FW,   ZP, x, tmp)   # tmp = grad x
        stat2 = igrad2_lop ( AJ,  add, y, tmp)   # y = y + grad' tmp
    }
}
```

Subroutine `lapfill2()` is the same idea as `mis1()` except that the filter $\mathbf{A}$ has been specialized to the laplacian implemented by module `laplac2`.

Find 2-D missing data.r90

```
module lapfill {  # fill empty 2-D bins by minimum output of Laplacian operator
  use laplac2
  use cgstep_mod
  use mask1
  use solver_smp_mod
```

```
contains
  subroutine lapfill2( niter , m1, m2, yy, mfixed) {
    integer ,                    intent (in)      :: niter , m1, m2
    logical , dimension (m1*m2), intent (in)      :: mfixed # mask for known
    real ,     dimension (m1*m2), intent (in out) :: yy     # model
    real ,     dimension (m1*m2)                  :: zero   # laplacian output
    logical , dimension (:) ,      pointer        :: msk
    allocate(msk(size(mfixed)))
    msk=.not.mfixed
    call mask1_init(msk)
    call laplac2_init ( m1,m2);                zero = 0.      # initialize
    call solver_smp(m=yy, d=zero , Fop=laplac2_lop , stepper=cgstep , &
                    niter=niter , m0=yy, Jop=mask1_lop)
    call laplac2_close ()                                     # garbage collection
    call cgstep_close ()                                      # garbage collection
  }
}
```

Subroutine `lapfill2()` can be used for each of our two applications: (1) extending the seismic data to fill space, and (2) fitting the map exactly to the wells and approximately to the seismic data. When extending the seismic data, the initially non-zero components $\mathbf{s} \neq \mathbf{0}$ are fixed and cannot be changed. That is done by calling `lapfill2()` with `mfixed=(s/=0.)`. When extending wells, the initially non-zero components $\mathbf{w} \neq \mathbf{0}$ are fixed and cannot be changed. That is done by calling `lapfill2()` with `mfixed=(w/=0.)`.

The final map is shown in Figure 3.8.

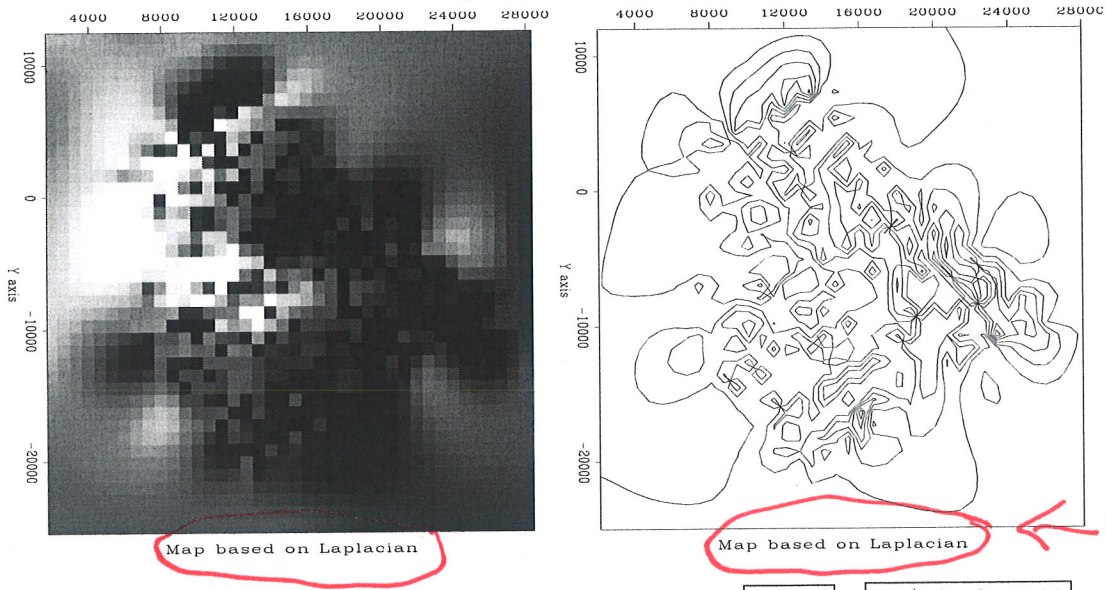

Figure 3.8: Final map based on Laplacian roughening. VIEW iin/. finalmap90

Results can be computed with various filters. I tried both ∇^2 and ∇. There are disadvantages of each, ∇ being too cautious and ∇^2 perhaps being too aggressive. Figure 3.8 shows the difference $\mathbf{x}$ between the extended seismic data and the extended wells. Notice that for ∇ the difference shows a localized "tent pole" disturbance about each well. For ∇^2 there could be large overshoot between wells, especially if two nearby wells have significantly

different values. I don't see that problem here.

My overall opinion is that the Laplacian does the better job in this case. I have that opinion because in viewing the extended gradient I can clearly see where the wells are. The wells are where we have acquired data. We'd like our map of the world to not show where we acquired data. Perhaps our estimated map of the world cannot help but show where we have and have not acquired data, but we'd like to minimize that aspect.

A good image of the earth hides our data **acquisition footprint**.

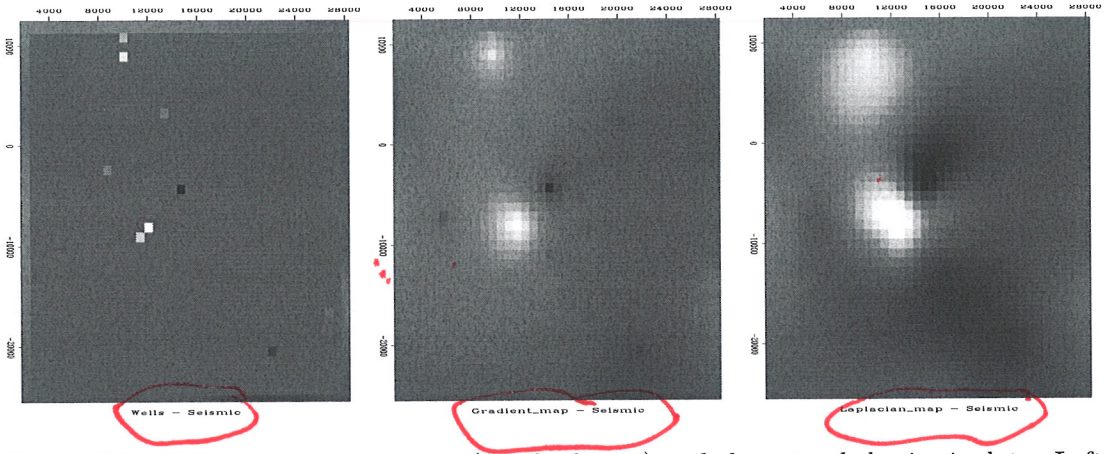

Figure 3.9: Difference between wells (the final map) and the extended seismic data. Left is plotted at the wells (with gray background for zero). Center is based on gradient roughening and shows tent-pole-like residuals at wells. Right is based on Laplacian roughening. VIEW iin/. diffdiff90

To understand the behavior theoretically, recall that in one dimension the filter ∇ interpolates with straight lines and ∇^2 interpolates with cubics. This is because the fitting goal $\mathbf{0} \approx \nabla \mathbf{m}$, leads to $\frac{\partial}{\partial \mathbf{m}^*} \mathbf{m}^* \nabla^* \nabla \mathbf{m} = \mathbf{0}$ or $\nabla^* \nabla \mathbf{m} = \mathbf{0}$, whereas the fitting goal $\mathbf{0} \approx \nabla^2 \mathbf{m}$ leads to $\nabla^4 \mathbf{m} = \mathbf{0}$ which is satisfied by cubics. In two dimensions, minimizing the output of ∇ gives us solutions of Laplace's equation with sources at the known data. It is as if ∇ stretches a rubber sheet over poles at each well, whereas ∇^2 bends a stiff plate.

Just because ∇^2 gives smoother maps than ∇ does not mean those maps are closer to reality. This is a deeper topic addressed in Chapter 7. It is the same issue we noticed when comparing figures 3.1-3.5.

3.3 SEARCHING THE SEA OF GALILEE

Figure 3.10 shows a bottom-sounding survey of the Sea of Galilee[1] at various stages of processing. The ultimate goal is not only a good map of the depth to bottom, but images useful for the purpose of identifying **archaeological**, geological, or geophysical details of the sea bottom. The Sea of Galilee is unique because it is a *fresh*-water lake *below* sea-level.

[1] Data collected by Zvi **ben Avraham**, TelAviv University. Please communicate with him `zvi@jupiter1.tau.ac.il` for more details or if you make something publishable with his data.

It seems to be connected to the great rift (pull-apart) valley crossing east Africa. We might delineate the Jordan River delta. We might find springs on the water bottom. We might find archaeological objects.

The raw data is 132,044 triples, (x_i, y_i, z_i), where x_i ranges over about 12 km and where y_i ranges over about 20 km. The lines you see in Figure 3.10 are sequences of data points, i.e., the track of the survey vessel. The depths z_i are recorded to an accuracy of about 10 cm.

The first frame in Figure 3.10 shows simple binning. A coarser mesh would avoid the empty bins but lose resolution. As we refine the mesh for more detail, the number of empty bins grows as does the care needed in devising a technique for filling them. This first frame uses the simple idea from Chapter 1 of spraying all the data values to the nearest bin with `bin2()` and dividing by the number in the bin. Bins with no data obviously need to be filled in some other way. I used a missing data program like that in the recent section on "wells not matching the seismic map." Instead of roughening with a Laplacian, however, I used the gradient operator `igrad2`. The solver is `grad2fill()`.

low cut missing data.r90

```
module grad2fill {    # min r(m) = L J m + L known   where L is a lowcut filter.
  use igrad2
  use cgstep_mod
  use mask1
  use solver_smp_mod
contains
  subroutine grad2fill2( niter , m1, m2, mm, mfixed) {
    integer ,                       intent (in)      :: niter , m1,m2
    logical , dimension (m1*m2),    intent (in)      :: mfixed       # mask for known
    real ,    dimension (m1*m2),    intent (in out)  :: mm           # model
    real ,    dimension (m1*m2*2)                    :: yy           # lowcut output
    logical , dimension (:),        pointer          :: msk
    allocate(msk(size(mfixed)))
    msk=.not.mfixed
    call mask1_init(msk)
    call igrad2_init(m1,m2);                           yy = 0.      # initialize
    call solver_smp(m=mm, d=yy, Fop=igrad2_lop , stepper=cgstep , niter=niter , &
                    m0=mm, Jop=mask1_lop)
    call cgstep_close ()
  }
}
```

The output of the roughening operator is an image, a filtered version of the depth, a filtered version of something real. Such filtering can enhance the appearance of interesting features. For example, scanning the shoreline of the roughened image (after missing data was filled), we see several ancient shorelines, now submerged. The roughened map is often more informative than the map itself.

The views expose several defects of the data acquisition and of our data processing. The impulsive glitches (St. Peter's fish?) need to be removed but we must be careful not to throw out the sunken ships along with the bad data points. Even our best image shows clear evidence of the recording vessel's tracks. Strangely, some tracks are deeper than others. Perhaps the survey is assembled from work done in different seasons and the water level varied by season. Perhaps some days the vessel was more heavily loaded and the depth

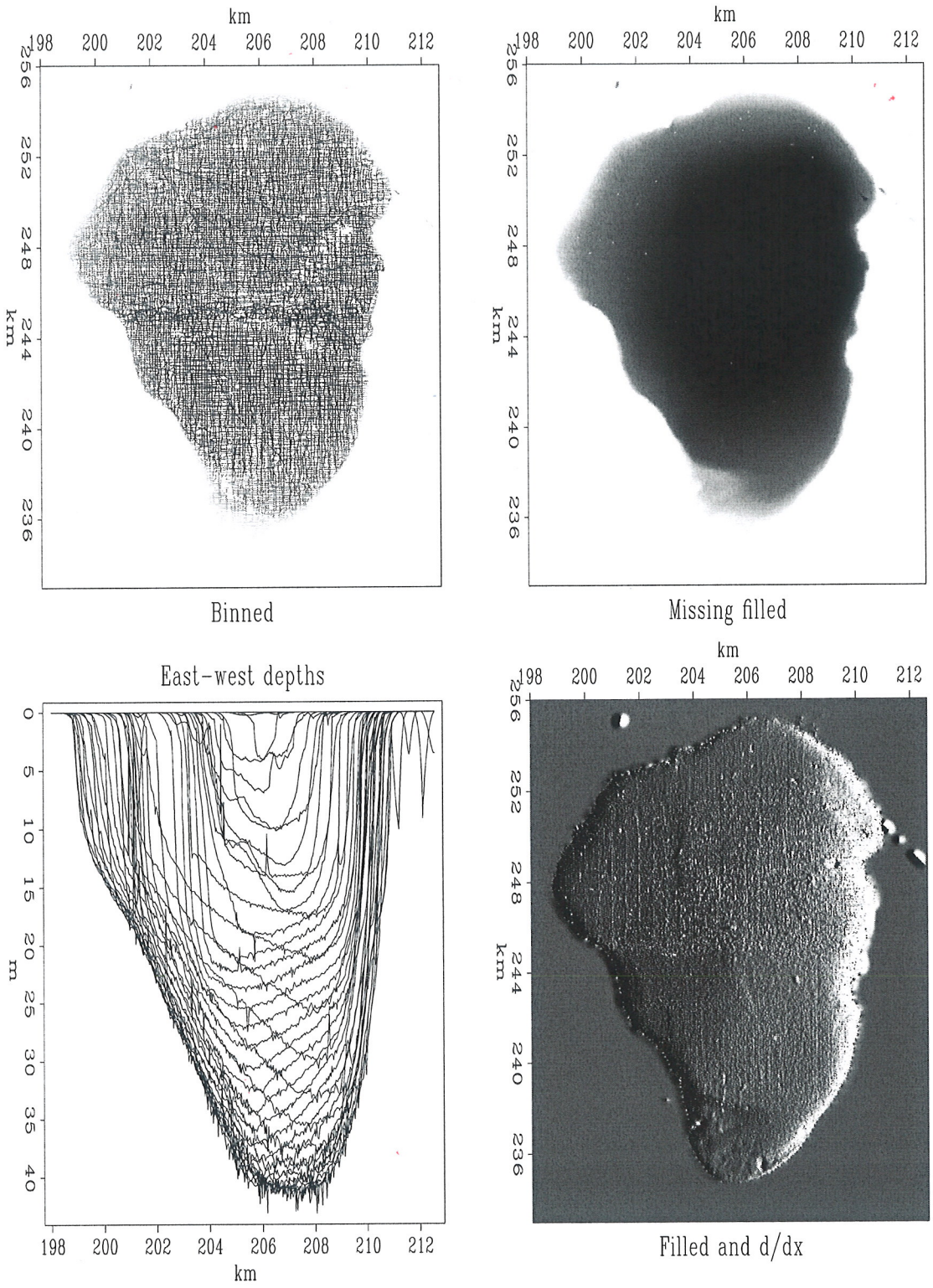

Figure 3.10: Views of the bottom of the Sea of Galilee. VIEW iin/. locfil90

sounder was on a deeper keel. As for the navigation equipment, we can see that some data values are reported outside the lake!

We want the sharpest possible view of this classical site. A treasure hunt is never easy and no one guarantees we will find anything of great value but at least the exercise is a good warm-up for submarine petroleum exploration.

3.4 CODE FOR THE REGULARIZED SOLVER

In Chapter 1 we defined **linear interpolation** as the extraction of values from between mesh points. In a typical setup (occasionally the role of data and model are swapped), a model is given on a uniform mesh and we solve the easy problem of extracting values between the mesh points with subroutine `lint1()`. The genuine problem is the inverse problem, which we attack here. Data values are sprinkled all around, and we wish to find a function on a uniform mesh from which we can extract that data by **linear interpolation**. The adjoint operator for subroutine `lint1()` simply piles data back into its proper location in model space without regard to how many data values land in each region. Thus some model values may have many data points added to them while other model values get none. We could interpolate by minimizing the energy in the model gradient, or that in the second derivative of the model, or that in the output of any other roughening filter applied to the model.

Formalizing now our wish that data $\mathbf{d}$ be extractable by **linear interpolation** $\mathbf{F}$, from a model $\mathbf{m}$, and our wish that application of a roughening filter with an operator $\mathbf{A}$ have minimum energy, we write the fitting goals:

$$\begin{aligned} \mathbf{0} &\approx \mathbf{Fm} - \mathbf{d} \\ \mathbf{0} &\approx \mathbf{Am} \end{aligned} \tag{3.14}$$

Suppose we take the roughening filter to be the second difference operator $(1, -2, 1)$ scaled by a constant ϵ, and suppose we have a data point near each end of the model and a third data point exactly in the middle. Then, for a model space 6 points long, the fitting goal could look like

$$\left[\begin{array}{cccccc} .8 & .2 & . & . & . & . \\ . & . & 1 & . & . & . \\ . & . & . & . & .5 & .5 \\ \hline \epsilon & . & . & . & . & . \\ -2\epsilon & \epsilon & . & . & . & . \\ \epsilon & -2\epsilon & \epsilon & . & . & . \\ . & \epsilon & -2\epsilon & \epsilon & . & . \\ . & . & \epsilon & -2\epsilon & \epsilon & . \\ . & . & . & \epsilon & -2\epsilon & \epsilon \\ . & . & . & . & \epsilon & -2\epsilon \\ . & . & . & . & . & \epsilon \end{array}\right] \left[\begin{array}{c} m_0 \\ m_1 \\ m_2 \\ m_3 \\ m_4 \\ m_5 \end{array}\right] - \left[\begin{array}{c} d_0 \\ d_1 \\ d_2 \\ \hline 0 \\ 0 \\ 0 \\ 0 \\ 0 \\ 0 \\ 0 \end{array}\right] = \left[\begin{array}{c} \mathbf{r}_d \\ \mathbf{r}_m \end{array}\right] \approx \mathbf{0} \tag{3.15}$$

The residual vector has two parts, a data part $\mathbf{r}_d$ on top and a model part $\mathbf{r}_m$ on the bottom. The data residual should vanish except where contradictory data values happen to lie in the same place. The model residual is the roughened model.

Finding something unexpected is good science and engineering. For this we look both in data space and in model space. In data space we look at the residual $\mathbf{r}$. In model space, we look at the residual projected there $\Delta\mathbf{m} = \mathbf{F}^*\mathbf{r}$. After iterating to completion we have $\Delta\mathbf{m} = \mathbf{0} = \mathbf{F}^*\mathbf{r}_d + \mathbf{A}^*\mathbf{r}_m$, a sum of two images identical but for polarity. They tell us what we have learned from the data; how the model differs from what we thought it would be.

Two fitting goals (3.14) are so common in practice that it is convenient to adopt our least-square fitting subroutine `solver-smp` accordingly. The modification is shown in module `solver-reg`. In addition to specifying the "data fitting" operator $\mathbf{F}$ (parameter `Fop`), we need to pass the "model regularization" operator $\mathbf{A}$ (parameter `Aop`) and the size of its output (parameter `nAop`) for proper memory allocation.

(When I first looked at module `solver-reg` I was appalled by the many lines of code, especially all the declarations. Then I realized how much much worse was Fortran 77 where I needed to write a new solver for every pair of operators. This one solver module works for all operator pairs and for many optimization descent strategies because these "objects" are arguments. These more powerful objects require declarations that are more complicated than the simple objects of Fortran 77. As an author I have a dilemma: To make algorithms compact (and seem simple) requires many careful definitions. When these definitions put in the code, they are careful, but the code becomes annoyingly verbose. Otherwise, the definitions must go in the surrounding natural language where they are not easily made precise.)

generic solver with regularization.r90

```
module solver_reg_mod {                                  # 0 = W (F J m - d)
  use chain0_mod + solver_report_mod                     # 0 =     A   m
  logical, parameter, private  :: AJ = .true., FW = .false.
  logical, parameter, private  :: AD = .true., ZP = .false.
contains
  subroutine solver_reg( m,d, Fop, Aop, stepper, nAop, niter,eps &
  ,             Wop,Jop,m0,rm0,err,resd,resm,mmov,rmov,verb) {
    optional :: Wop,Jop,m0,rm0,err,resd,resm,mmov,rmov,verb
    interface { #------------------------- begin definitions ----------
       integer function Fop(adj,add,m,d){real::m(:),d(:);logical::adj,add}
       integer function Aop(adj,add,m,d){real::m(:),d(:);logical::adj,add}
       integer function Wop(adj,add,m,d){real::m(:),d(:);logical::adj,add}
       integer function Jop(adj,add,m,d){real::m(:),d(:);logical::adj,add}
       integer function stepper(first,m,dm,r,dr) {
         real, dimension(:)  ::        m,dm,r,dr
         logical             :: first             }
    }
    real, dimension(:),     intent(in)          :: d, m0,rm0
    integer,                intent(in)          :: niter, nAop
    logical,                intent(in)          :: verb
    real,                   intent(in)          :: eps
    real, dimension(:),     intent(out)         :: m,err, resd,resm
    real, dimension(:,:),   intent(out)         ::          rmov,mmov
    real, dimension(size(m))                    :: dm
    real, dimension(size(d) + nAop), target     :: r, dr, tt
    real, dimension(:), pointer                 :: rd, drd, td
    real, dimension(:), pointer                 :: rm, drm, tm
    integer                                     :: iter, stat
    logical                                     :: first
    rd  => r(1:size(d));  rm  => r(1+size(d):)
    drd => dr(1:size(d)); drm => dr(1+size(d):)
```

```
    td  => tt(1:size(d)); tm  => tt(1+size(d):)
    if(present(Wop)) stat=Wop(FW,ZP,-d,rd) # begin initialization ----------
    else rd = -d                                                  #Rd  = -W  d
    rm = 0.; if(present(rm0)) rm=rm0                              #Rm  =     Rm0
    if(present( m0)){ m=m0                                        #m   =     m0
       if(present(Wop)) call chain0(Wop,Fop,FW,AD,m,rd,td)
       else             stat=       Fop(FW,AD,m,rd    )         #Rd += WF m0
       stat = Aop(FW,AD,eps*m0,rm)                                #Rm += e A m0
    } else m=0
    first = .true.; #------------------------------ begin iterations ---------
    do iter = 1,niter {
       if(present( Wop)) call chain0(Wop,Fop,AJ,ZP,dm,rd,td)
       else              stat =      Fop(AJ,ZP,dm,rd    )       #dm  = (WF)'Rd
       stat =  Aop(AJ,AD,dm,eps*rm)                               #dm += e A'Rm
       if(present( Jop)){ tm=dm;     stat=Jop(FW,ZP,tm,dm   )} #dm  =   J  dm
       if(present( Wop)) call chain0(Wop,Fop,FW,ZP,dm,drd,td)
       else              stat =      Fop(FW,ZP,dm,drd   )       #dRd = (WF) dm
       stat =  Aop(FW,ZP,eps*dm,drm)                              #dRm =  e A dm
       stat = stepper(first , m,dm, r,dr)                         #m+=dm; R+=dR
       if(stat ==1) exit # got stuck descending
       if(present( mmov)) mmov(:,iter) =  m(:size(mmov,1)) # report ------
       if(present( rmov)) rmov(:,iter) = r(:size(rmov,1))
       if(present( err )) err(  iter) = dot_product(rd,rd)
       if(present( verb)){ if(verb) call solver_report(iter,m,dm,rd,rm)}
       first=.false.
    }
    if(present( resd)) resd = rd
    if(present( resm)) resm = rm(:size(resm))
  }
}
```

After all the definitions, we load the negative of the data into the residual. If a starting model $\mathbf{m}_0$ is present, then we update the data part of the residual $\mathbf{r}_d = \mathbf{F}\mathbf{m}_0 - \mathbf{d}$ and we load the model part of the residual $\mathbf{r}_m = \mathbf{A}\mathbf{m}_0$. Otherwise we begin from a zero model $\mathbf{m}_0 = \mathbf{0}$ and thus the model part of the residual $\mathbf{r}_m$ is also zero. After this initialization, subroutine `solver_reg()` begins an iteration loop by first computing the proposed model perturbation $\Delta\mathbf{m}$ (called `g` in the program) with the adjoint operator:

$$\Delta\mathbf{m} \quad \longleftarrow \quad \begin{bmatrix} \mathbf{F}^* & \mathbf{A}^* \end{bmatrix} \begin{bmatrix} \mathbf{r}_d \\ \mathbf{r}_m \end{bmatrix} \tag{3.16}$$

Using this value of $\Delta\mathbf{m}$, we can find the implied change in residual $\Delta\mathbf{r}$ as

$$\Delta \begin{bmatrix} \mathbf{r}_d \\ \mathbf{r}_m \end{bmatrix} \quad \longleftarrow \quad \begin{bmatrix} \mathbf{F} \\ \mathbf{A} \end{bmatrix} \Delta\mathbf{m} \tag{3.17}$$

and the last thing in the loop is to use the optimization step function `stepper()` to choose the length of the step size and to choose how much of the previous step to include.

An example of using the new solver is subroutine `invint1`. I chose to implement the model roughening operator $\mathbf{A}$ with the convolution subroutine `tcai1()` which has transient end effects (and an output length equal to the input length plus the filter length). The adjoint of subroutine `tcai1()` suggests perturbations in the convolution input (not the filter).

invers linear interp..r90

```
module invint {                          # invint -- INVerse INTerpolation in 1-D.
  use lint1
  use tcai1
  use cgstep_mod
  use solver_reg_mod
contains
  subroutine invint1( niter, coord, dd, o1, d1, aa, mm, eps, mmov) {
    integer,                intent (in)    :: niter                  # iterations
    real,                   intent (in)    :: o1, d1, eps            # axis, scale
    real, dimension (:),    pointer        :: coord, aa              # aa is filter
    real, dimension (:),    intent (in)    :: dd                     # data
    real, dimension (:),    intent (out)   :: mm                     # model
    real, dimension (:,:),  intent (out)   :: mmov                   # movie
    integer                                :: nreg                   # size of A m
    nreg = size( aa) + size( mm)                                     # transient
    call lint1_init( o1, d1, coord )                                 # interpolation
    call tcai1_init( aa)                                             # filtering
    call solver_reg( m=mm, d=dd, Fop=lint1_lop, stepper=cgstep, niter=niter, &
        Aop=tcai1_lop, nAop = nreg, eps = eps,mmov = mmov, verb=.true.)
    call cgstep_close( )
    }
}
```

Figure 3.11 shows an example for a $(1, -2, 1)$ filter with $\epsilon = 1$. The continuous curve representing the model $\mathbf{m}$ passes through the data points. Because the models are computed with transient convolution end-effects, the models tend to damp linearly to zero outside the region where signal samples are given.

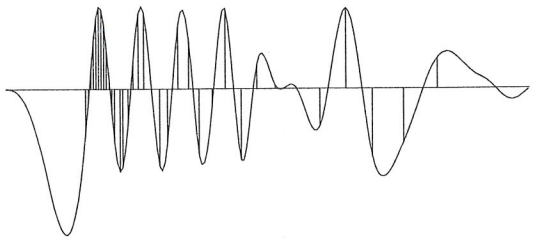

Figure 3.11: Sample points and estimation of a continuous function through them. VIEW iin/. im1-2+190

To show an example where the result is clearly a theoretical answer, I prepared another figure with the simpler filter $(1, -1)$. When we minimize energy in the first derivative of the waveform, the residual distributes itself uniformly between data points so the solution there is a straight line. Theoretically it should be a straight line because a straight line has a vanishing second derivative, and that condition arises by differentiating by $\mathbf{x}^*$, the minimized quadratic form $\mathbf{x}^*\mathbf{A}^*\mathbf{A}\mathbf{x}$, and getting $\mathbf{A}^*\mathbf{A}\mathbf{x} = \mathbf{0}$. (By this logic, the curves between data points in Figure 3.11 must be cubics.) The $(1, -1)$ result is shown in Figure 3.12.

The example of Figure 3.12 has been a useful test case for me. You'll see it again in later chapters. What I would like to show you here is a movie showing the convergence to Figure 3.12. Convergence occurs rapidly where data points are close together. The large gaps, however, fill at a rate of one point per iteration.

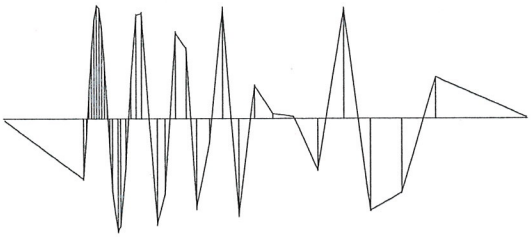

Figure 3.12: The same data samples and a function through them that minimizes the energy in the first derivative. VIEW iin/. im1-1a90

3.4.1 Abandoned theory for matching wells and seismograms

Let us consider theory to construct a map $\mathbf{m}$ that fits dense seismic data $\mathbf{s}$ and the well data $\mathbf{w}$. The first goal $\mathbf{0} \approx \mathbf{Lm} - \mathbf{w}$ says that when we linearly interpolate from the map, we should get the well data. The second goal $\mathbf{0} \approx \mathbf{A}(\mathbf{m} - \mathbf{s})$ (where $\mathbf{A}$ is a roughening operator like ∇ or ∇^2) says that the map $\mathbf{m}$ should match the seismic data $\mathbf{s}$ at high frequencies but need not do so at low frequencies.

$$\begin{aligned} \mathbf{0} &\approx \mathbf{Lm} - \mathbf{w} \\ \mathbf{0} &\approx \mathbf{A}(\mathbf{m} - \mathbf{s}) \end{aligned} \tag{3.18}$$

Although (3.18) is the way I originally formulated the well-fitting application, I abandoned it for several reasons: First, the map had ample pixel resolution compared to other sources of error, so I switched from linear interpolation to binning. Once I was using binning, I had available the simpler empty-bin approaches. These have the further advantage that it is not necessary to experiment with the relative weighting between the two goals in (3.18). A formulation like (3.18) is more likely to be helpful where we need to handle rapidly changing functions where binning is inferior to linear interpolation, perhaps in reflection seismology where high resolution is meaningful.

3.5 PRECONCEPTION AND CROSS VALIDATION

First we first look at data $\mathbf{d}$. Then we think about a model $\mathbf{m}$, and an operator $\mathbf{L}$ to link the model and the data. Sometimes the operator is merely the first term in a series expansion about $(\mathbf{m}_0, \mathbf{d}_0)$. Then we fit $\mathbf{d} - \mathbf{d}_0 \approx \mathbf{L}(\mathbf{m} - \mathbf{m}_0)$. To fit the model, we must reduce the fitting residuals. Realizing that the importance of a data residual is not always simply the size of the residual but is generally a function of it, we conjure up (topic for later chapters) a weighting function (which could be a filter) operator $\mathbf{W}$. This defines our data residual:

$$\mathbf{r}_d \quad = \quad \mathbf{W}[\mathbf{L}(\mathbf{m} - \mathbf{m}_0) \; - \; (\mathbf{d} - \mathbf{d}_0)] \tag{3.19}$$

Next we realize that the data might not be adequate to determine the model, perhaps because our comfortable dense sampling of the model ill fits our economical sparse sampling of data. Thus we adopt a fitting goal that mathematicians call "regularization" and we might call a "model style" goal or more simply, a quantification of our preconception of the best model. We express this by choosing an operator $\mathbf{A}$, often simply a roughener like a gradient (the choice again a topic in this and later chapters). It defines our model residual by $\mathbf{Am}$ or $\mathbf{A}(\mathbf{m} - \mathbf{m}_0)$, say we choose:

$$\mathbf{r}_m \quad = \quad \mathbf{Am} \tag{3.20}$$

In an ideal world, our model preconception (prejudice?) would not conflict with measured data, but real life is much more interesting than that. Since conflicts between data and preconceived notions invariably arise (they are why we pay for data acquisition) we need an adjustable parameter that measures our "**bullheadedness**", how much we intend to stick to our preconceived notions in spite of contradicting data. This parameter is generally called epsilon ϵ because we like to imagine that our bullheadedness (prejudice?) is small. (In mathematics, ϵ is often taken to be an infinitesimally small quantity.) Although any bullheadedness seems like a bad thing, it must be admitted that measurements are imperfect too. Thus as a practical matter we often find ourselves minimizing

$$\min \quad := \quad \mathbf{r}_d \cdot \mathbf{r}_d \; + \; \epsilon^2 \, \mathbf{r}_m \cdot \mathbf{r}_m \tag{3.21}$$

and wondering what to choose for ϵ. I have two suggestions: My simplest suggestion is to choose ϵ so that the residual of data fitting matches that of model styling. Thus

$$\epsilon \quad = \quad \sqrt{\frac{\mathbf{r}_d \cdot \mathbf{r}_d}{\mathbf{r}_m \cdot \mathbf{r}_m}} \tag{3.22}$$

My second suggestion is to think of the force on our final solution. In physics, force is associated with a gradient. We have a gradient for the data fitting and another for the model styling:

$$\mathbf{g}_d \quad = \quad \mathbf{L}^* \mathbf{W}^* \mathbf{r}_d \tag{3.23}$$

$$\mathbf{g}_m \quad = \quad \mathbf{A}^* \mathbf{r}_m \tag{3.24}$$

We could balance these forces by the choice

$$\epsilon \quad = \quad \sqrt{\frac{\mathbf{g}_d \cdot \mathbf{g}_d}{\mathbf{g}_m \cdot \mathbf{g}_m}} \tag{3.25}$$

Although we often ignore ϵ in discussing the formulation of an application, when time comes to solve the problem, reality intercedes. Generally, $\mathbf{r}_d$ has different physical units than $\mathbf{r}_m$ (likewise $\mathbf{g}_d$ and $\mathbf{g}_m$) and we cannot allow our solution to depend on the accidental choice of units in which we express the problem. I have had much experience choosing ϵ, but it is only recently that I boiled it down to the above two suggestions. Normally I also try other values, like double or half those of the above choices, and I examine the solutions for subjective appearance. If you find any insightful examples, please tell me about them.

Computationally, we could choose a new ϵ with each iteration, but it is more expeditious to freeze ϵ, solve the problem, recompute ϵ, and solve the problem again. I have never seen a case where more than one repetition was necessary.

People who work with small applications (less than about 10^3 vector components) have access to an attractive theoretical approach called cross-validation. Simply speaking, we could solve the problem many times, each time omitting a different data value. Each solution would provide a model that could be used to predict the omitted data value. The quality of these predictions is a function of ϵ and this provides a guide to finding it. My objections to cross validation are two-fold: First, I don't know how to apply it in the large applications like we solve in this book (I should think more about it); and second, people who worry much about ϵ, perhaps first should think more carefully about their choice of the filters $\mathbf{W}$ and $\mathbf{A}$, which is the focus of this book. Notice that both $\mathbf{W}$ and $\mathbf{A}$ can be defined with a scaling factor which is like scaling ϵ. Often more important in practice, with $\mathbf{W}$ and $\mathbf{A}$ we have a scaling factor that need not be constant but can be a function of space or spatial frequency within the data space and/or model space.

EXERCISES:

1 Figures 3.1–3.4 seem to extrapolate to vanishing signals at the side boundaries. Why is that so, and what could be done to leave the sides unconstrained in that way?

2 Show that the interpolation curve in Figure 3.2 is not parabolic as it appears, but cubic. (HINT: First show that $(\nabla^2)^* \nabla^2 u = \mathbf{0}$.)

3 Verify by a program example that the number of iterations required with simple constraints is the number of free parameters.

4 A signal on a uniform mesh has missing values. How should we estimate the mean?

5 It is desired to find a compromise between the Laplacian roughener and the gradient roughener. What is the size of the residual space?

6 Like the seismic prospecting industry, you have solved a huge problem using binning. You have computer power left over to do a few iterations with linear interpolation. How much does the cost per iteration increase? Should you refine your model mesh, or can you use the same model mesh that you used when binning?

7 Nuclear energy having finally reached its potential has dried up the prospecting industries so you find yourself doing **medical imaging** (or **earthquake seismology**). You probe the human body from all sides on a dense regular mesh in cylindrical coordinates. Unfortunately you need to represent your data in fourier space. There is no such thing as a fast fourier transform in cylindrical coordinates, and slow fourier transforms are pitifully slow. Your only hope to keep up with your competitors is to somehow do your FT's in cartesian coordinates. Write down the sequence of steps to achieve your goals using the methods of this chapter.

Chapter 4

The helical coordinate

For many years it has been true that our most powerful signal-analysis techniques are in *one*-dimensional space, while our most important applications are in *multi*-dimensional space. The helical coordinate system makes a giant step towards overcoming this difficulty.

Many geophysical map estimation applications appear to be multidimensional, but actually they are not. To see the tip of the iceberg, consider this example: On a two-dimensional cartesian mesh, the function

0	0	0	0
0	1	1	0
0	1	1	0
0	0	0	0

has the autocorrelation

1	2	1
2	4	2
1	2	1

.

Likewise, on a one-dimensional cartesian mesh,

the function

1	1	0	0	$\cdots$	0	1	1

has the autocorrelation

1	2	1	0	$\cdots$	0	2	4	2	0	$\cdots$	1	2	1

.

Observe the numbers in the one-dimensional world are identical with the numbers in the two-dimensional world. This correspondence is no accident.

4.1 FILTERING ON A HELIX

Figure 4.1 shows some two-dimensional shapes that are convolved together. The left panel shows an impulse response function, the center shows some impulses, and the right shows the superposition of responses.

A surprising, indeed amazing, fact is that Figure 4.1 was not computed with a two-dimensional convolution program. It was computed with a one-dimensional computer program. It could have been done with anybody's one-dimensional convolution program, either in the time domain or in the fourier domain. This magical trick is done with the helical coordinate system.

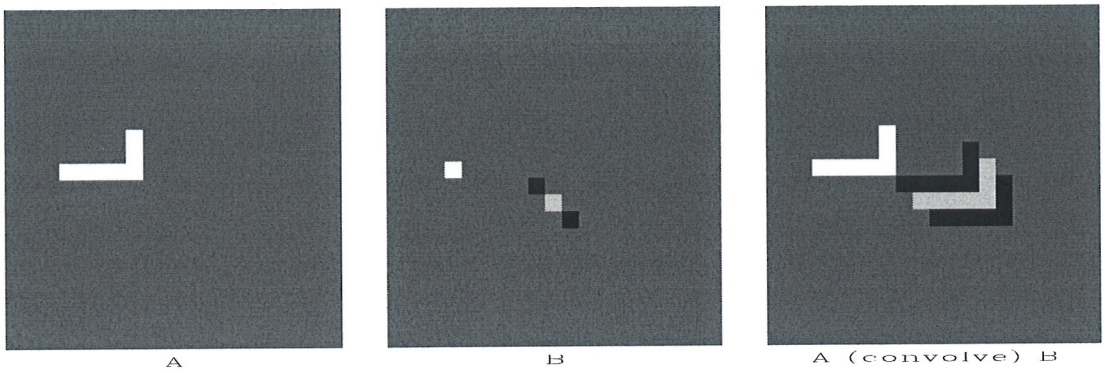

Figure 4.1: Two-dimensional convolution as performed in one dimension by module `helicon` VIEW hlx/. diamond90

A basic idea of filtering, be it in one dimension, two dimensions, or more, is that you have some filter coefficients and some sampled data; you pass the filter over the data; at each location you find an output by crossmultiplying the filter coefficients times the underlying data and summing the terms.

The helical coordinate system is much simpler than you might imagine. Ordinarily, a plane of data is thought of as a collection of columns, side by side. Instead, imagine the columns stored end-to-end, and then coiled around a cylinder. This is the helix. Fortran programmers will recognize that fortran's way of storing 2-D arrays in one-dimensional memory is exactly what we need for this helical mapping. Seismologists sometimes use the word "supertrace" to describe a collection of seismograms stored "end-to-end".

Figure 4.2 shows a helical mesh for 2-D data on a cylinder. Darkened squares depict a 2-D filter shaped like the Laplacian operator $\partial_{xx} + \partial_{yy}$. The input data, the filter, and the output data are all on helical meshes all of which could be unrolled into linear strips. A compact 2-D filter like a Laplacian on a helix is a sparse 1-D filter with long empty gaps.

Since the values output from filtering can be computed in any order, we can slide the filter coil over the data coil in any direction. The order that you produce the outputs is irrelevant. You could compute the results in parallel. We could, however, slide the filter over the data in the screwing order that a nut passes over a bolt. The screw order is the same order that would be used if we were to unwind the coils into one-dimensional strips and convolve them across one another. The same filter coefficients overlay the same data values if the 2-D coils are unwound into 1-D strips. The helix idea allows us to obtain the same convolution output in either of two ways, a one-dimensional way or a two-dimensional way. I used the one-dimensional way to compute the obviously two-dimensional result in Figure 4.1.

4.1.1 Review of 1-D recursive filters

Convolution is the operation we do on polynomial coefficients when we multiply polynomials. Deconvolution is likewise for polynomial division. Often these ideas are described

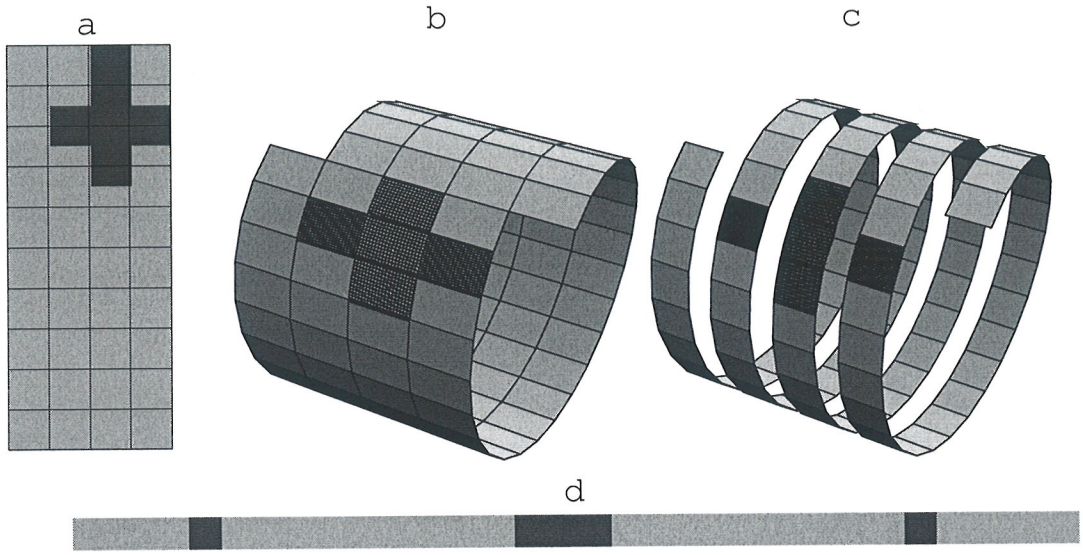

Figure 4.2: Filtering on a helix. The same filter coefficients overlay the same data values if the 2-D coils are unwound into 1-D strips. (*Mathematica* drawing by Sergey Fomel) VIEW hlx/. sergey-helix

as polynomials in the variable Z. Take $X(Z)$ to denote the polynomial whose coefficients are samples of input data, and let $A(Z)$ likewise denote the filter. The convention I adopt here is that the first coefficient of the filter has the value $+1$, so the filter's polynomial is $A(Z) = 1 + a_1 Z + a_2 Z^2 + \cdots$. To see how to convolve, we now identify the coefficient of Z^k in the product $Y(Z) = A(Z)X(Z)$. The usual case (k larger than the number N_a of filter coefficients) is

$$y_k = x_k + \sum_{i=1}^{N_a} a_i x_{k-i} \tag{4.1}$$

Convolution computes y_k from x_k, whereas deconvolution (also called back substitution) does the reverse. Rearranging (4.1) we get

$$x_k = y_k - \sum_{i=1}^{N_a} a_i x_{k-i} \tag{4.2}$$

where now we are finding the output x_k from its past outputs x_{k-i} and from the present input y_k. We see that the deconvolution process is essentially the same as the convolution process, except that the filter coefficients are used with opposite polarity; and they are applied to the past *outputs* instead of the past *inputs*. That is why deconvolution must be done sequentially while convolution can be done in parallel.

4.1.2 Multidimensional deconvolution breakthrough

Deconvolution (polynomial division) can undo convolution (polynomial multiplication). A magical property of the helix is that we can consider 1-D convolution to be the same as 2-D convolution. Hence is a second magical property: We can use 1-D *de*convolution to undo convolution, whether that convolution was 1-D or 2-D. Thus, we have discovered how to undo 2-D convolution. We have discovered that 2-D deconvolution on a helix is equivalent to 1-D deconvolution. The helix enables us to do multidimensional deconvolution.

Deconvolution is recursive filtering. Recursive filter outputs cannot be computed in parallel, but must be computed sequentially as in one dimension, namely, in the order that the nut screws on the bolt.

Recursive filtering sometimes solves big problems with astonishing speed. It can propagate energy rapidly for long distances. Unfortunately, recursive filtering can also be unstable. The most interesting case, near resonance, is also near instability. There is a large literature and extensive technology about recursive filtering in one dimension. The helix allows us to apply that technology to two (and more) dimensions. It is a huge technological breakthrough.

In 3-D we simply append one plane after another (like a 3-D fortran array). It is easier to code than to explain or visualize a spool or torus wrapped with string, etc.

4.1.3 Examples of simple 2-D recursive filters

Let us associate x- and y-derivatives with a finite-difference stencil or template. (For simplicity take $\Delta x = \Delta y = 1$.)

$$\frac{\partial}{\partial x} \quad = \quad \boxed{1 \mid -1} \tag{4.3}$$

$$\frac{\partial}{\partial y} \quad = \quad \begin{array}{|c|}\hline 1 \\ \hline -1 \\ \hline \end{array} \tag{4.4}$$

Convolving a data plane with the stencil (4.3) forms the x-derivative of the plane. Convolving a data plane with the stencil (4.4) forms the y-derivative of the plane. On the other hand, *deconvolving* with (4.3) integrates data along the x-axis for each y. Likewise, deconvolving with (4.4) integrates data along the y-axis for each x. Next we look at a fully two-dimensional operator (like the cross derivative ∂_{xy}).

A nontrivial two-dimensional convolution stencil is

$$\begin{array}{|r|l|}\hline 0 & -1/4 \\ \hline 1 & -1/4 \\ \hline -1/4 & -1/4 \\ \hline \end{array} \tag{4.5}$$

We will convolve and deconvolve a data plane with this operator. Although everything is shown on a plane, the actual computations are done in one dimension with equations (4.1) and (4.2). Let us manufacture the simple data plane shown on the left in Figure 4.3. Beginning with a zero-valued plane, we add in a copy of the filter (4.5) near the top of the frame. Nearby add another copy with opposite polarity. Finally add some impulses near

the bottom boundary. The second frame in Figure 4.3 is the result of deconvolution by the filter (4.5) using the one-dimensional equation (4.2). Notice that deconvolution turns the filter itself into an impulse, while it turns the impulses into comet-like images. The use of a helix is evident by the comet images wrapping around the vertical axis.

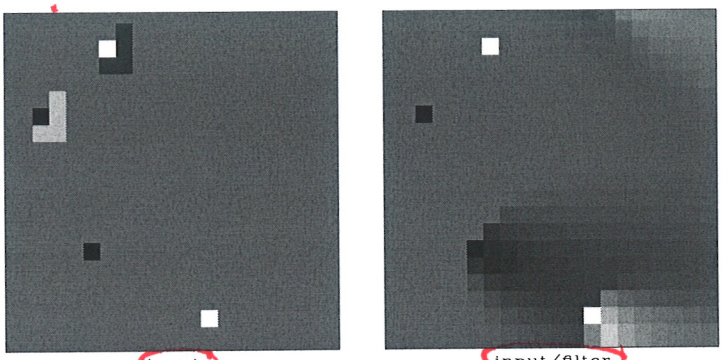

Figure 4.3: Illustration of 2-D deconvolution. Left is the input. Right is after deconvolution with the filter (4.5) as preformed by by module `polydiv`. VIEW hlx/. wrap90

The filtering in Figure 4.3 ran along a helix from left to right. Figure 4.4 shows a second filtering running from right to left. Filtering in the reverse direction is the adjoint. After deconvolving both ways, we have accomplished a symmetrical smoothing. The final frame undoes the smoothing to bring us exactly back to where we started. The smoothing was done with two passes of *deconvolution* and it is undone by two passes of *convolution*. No errors, no evidence remains of any of the boundaries where we have wrapped and truncated.

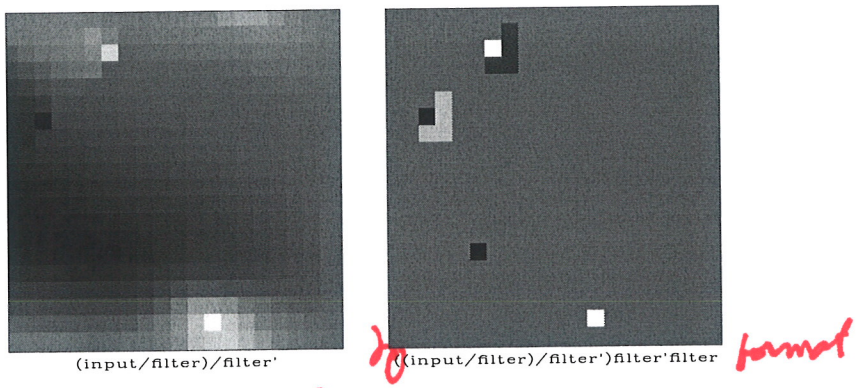

Figure 4.4: Recursive filtering backwards (leftward on the space axis) is done by the *adjoint* of 2-D deconvolution. Here we see that 2-D *deconvolution* compounded with its adjoint is exactly inverted by 2-D *convolution* and its adjoint. VIEW hlx/. hback90

Chapter 5 explains the important practical role to be played by a multidimensional operator for which we know the exact inverse. Other than multidimensional Fourier transformation, transforms based on polynomial multiplication and division on a helix are the only known easily invertible linear operators.

In seismology we often have occasion to steer summation along beams. Such an impulse response is shown in Figure 4.6.

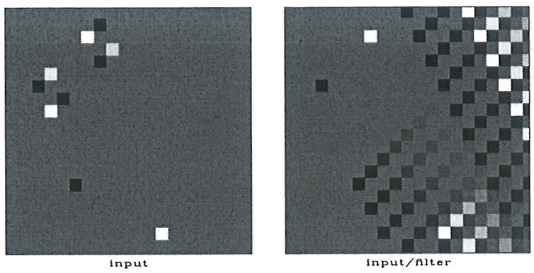

Figure 4.5: A simple low-order 2-D filter whose inverse contains plane waves of two different dips. One of them is spatially aliased. VIEW hlx/. waves90

Of special interest are filters that destroy plane waves. The inverse of such a filter creates plane waves. Such filters are like wave equations. A filter that creates two plane waves is illustrated in figure 4.5.

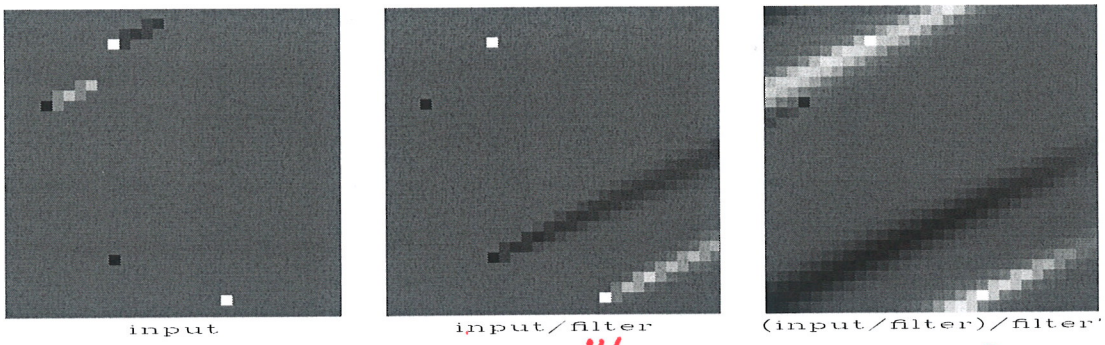

Figure 4.6: A simple low-order 2-D filter whose inverse times its inverse adjoint is approximately a dipping seismic arrival. VIEW hlx/. dip90

4.1.4 Coding multidimensional de/convolution

Let us unroll the filter helix seen in Figure 4.2 and see what we have. Start from the idea that a 2-D filter is generally made from a cluster of values near one another in two dimensions similar to the Laplacian operator in the figure. We see that in the helical approach, a 2-D filter is a 1-D filter containing some long intervals of zeros. The intervals are about the length of a 1-D seismogram.

Our program for 2-D convolution with a 1-D convolution program, could convolve with the somewhat long 1-D strip, but it is much more cost effective to ignore the many zeros, which is what we do. We do not multiply by the backside zeros, nor do we even store them in memory. Whereas an ordinary convolution program would do time shifting by a code line like `iy=ix+lag`, Module `helicon` ignores the many zero filter values on backside of the tube by using the code `iy=ix+lag(ia)` where a counter `ia` ranges over the nonzero filter coefficients. Before operator `helicon` is invoked, we need to prepare two lists, one list containing nonzero filter coefficients `flt(ia)`, and the other list containing the corresponding lags `lag(ia)` measured to include multiple wraps around the helix. For example, the 2-D

Laplace operator can be thought of as the 1-D filter

1	0	···	0	1	−4	1	0	···	0	1

→ helical boundaries

	1	
1	−4	1
	1	

(4.6)

The first filter coefficient in equation (4.6) is +1 as implicit to module `helicon`. To apply the Laplacian on a 1000 × 1000 mesh requires the filter inputs:

```
 i    lag(i)   flt(i)
---   ------   -----
 1      999      1.
 2     1000     -4.
 3     1001      1.
 4     2000      1.
```

Here we choose to use "declaration of a type", a modern computer language feature that is absent from Fortran 77. Fortran 77 has the built in complex arithmetic type. In module `helix` we define a type `filter`, actually, a helix filter. After making this definition, it will be used by many programs. The helix filter consists of three vectors, a real valued vector of filter coefficients, an integer valued vector of filter lags, and an optional vector that has logical values "`.TRUE.`" for output locations that will not be computed (either because of boundary conditions or because of missing inputs). The filter vectors are the size of the nonzero filter coefficients (excluding the leading 1.) while the logical vector is long and relates to the data size. The `helix` module allocates and frees memory for a helix filter. By default, the logical vector is not allocated but is set to `null` with the `nullify` operator and ignored. This directive is used by the compiler for optimization. When the logical array is unneeded it is neither allocated nor accessible.

definition for helix-type filters.r90

```
module helix {                                  # DEFINE helix filter type
  type filter {
    real,    dimension( :), pointer :: flt      # (nh) filter coefficients
    integer, dimension( :), pointer :: lag      # (nh) filter lags
    logical, dimension( :), pointer :: mis      # (nd) boundary conditions
  }
contains
  subroutine allocatehelix( aa, nh ) {          # allocate a filter
    type( filter) :: aa
    integer       :: nh                         # count of filter coefs (excl 1)
    allocate( aa%flt( nh), aa%lag( nh))         # allocate filter and lags.
    nullify( aa%mis)                            # set null pointer for "mis".
    aa%flt = 0.                                 # zero filter coef values
  }
  subroutine deallocatehelix( aa) {             # destroy a filter
    type( filter) :: aa
    deallocate( aa%flt, aa%lag)                 # free memory
    if( associated( aa%mis))                    # if logicals were allocated
        deallocate( aa%mis)                     # free them
  }
}
```

For those of you with no Fortran 90 experience, the "%" appearing in the helix module denotes a pointer. Fortran 77 has no pointers (or everything is a pointer). The C, C++,

and Java languages use "." to denote pointers. C and C++ also have a second type of pointer denoted by "->". The behavior of pointers is somewhat different in each language. Never-the-less, the idea is simple. In module `helicon` you see the expression `aa%flt(ia)`. It refers to the filter named `aa`. Any filter defined by the `helix` module contains three vectors, one of which is named `flt`. The second component of the `flt` vector in the `aa` filter is referred to as `aa%flt(2)` which in the example above refers to the value 4.0 in the center of the laplacian operator. For data sets like above with 1000 points on the 1-axis, this value 4.0 occurs after 1000 lags, thus `aa%lag(2)=1000`.

Our first convolution operator `tcai1` was limited to one dimension and a particular choice of end conditions. With the helix and Fortran 90 pointers, the operator `helicon` is a *multidimensional* filter with considerable flexibility (because of the `mis` vector) to work around boundaries and missing data.

helical convolution.lop

```
module helicon {                          # Convolution, inverse to deconvolution.
#               Requires the filter be causal with an implicit "1." at the onset.
use helix
type( filter) :: aa
#%  _init( aa)
#%  _lop ( xx,  yy)
integer iy, ix, ia
if( adj)                  # zero lag
        xx += yy
else
        yy += xx
do ia = 1, size( aa%lag) {
      do iy = 1  + aa%lag( ia), size( yy) {
            if( associated( aa%mis)) { if( aa%mis( iy)) cycle}
            ix = iy - aa%lag( ia)
            if( adj)
                        xx(ix) += yy(iy) * aa%flt(ia)
            else
                        yy(iy) += xx(ix) * aa%flt(ia)
            }
      }
}
```

The code fragment `aa%lag(ia)` corresponds to `b-1` in `tcai1`.

Operator `helicon` did the convolution job for Figure 4.1. As with `tcai1` the adjoint of filtering is filtering backwards which means unscrewing the helix.

The companion to convolution is deconvolution. The module `polydiv` is essentially the same as `polydiv1` but here it was coded using our new `filter` type in module `helix` which will simplify our many future uses of convolution and deconvolution. Although convolution allows us to work around missing input values, deconvolution does not (any input affects all subsequent outputs), so `polydiv` never references `aa%mis(ia)`.

helical deconvolution.lop

```
module polydiv {                                # Helix polynomial division
use helix
integer                                 :: nd
type( filter)                           :: aa
real, dimension (nd), allocatable       :: tt
```

```
#%  _init ( nd, aa)
#%  _lop  ( xx, yy)
integer  ia, ix, iy
tt = 0.
if( adj) {
        do ix= nd, 1, -1 {
                tt( ix) = yy( ix)
                do ia = 1, size( aa%lag) {
                        iy = ix + aa%lag( ia);      if( iy > nd)  next
                        tt( ix) -=  aa%flt( ia) * tt( iy)
                        }
                }
        xx += tt
 } else {
        do iy= 1, nd {
                tt( iy) = xx( iy)
                do ia = 1, size( aa%lag) {
                        ix = iy - aa%lag( ia);      if( ix < 1)  next
                        tt( iy) -=  aa%flt( ia) * tt( ix)
                        }
                }
        yy += tt
        }
}
```

4.2 KOLMOGOROFF SPECTRAL FACTORIZATION

Spectral factorization addresses a deep mathematical problem not solved by mathematicians until 1939. Given any spectrum $|F(\omega)|$, find a causal time function $f(t)$ with this spectrum. A causal time function is one that vanishes at negative time $t < 0$. We will mix spectral factorization with the helix idea to find many applications in geophysical image estimation.

The most abstract method of spectral factorization is that of the Russian mathematician A.N.Kolmogoroff. I include it here because it is by far the fastest, so much so that giant problems become practical such as the solar physics example coming up.

Given that $C(\omega)$ fourier transforms to a causal function of time, it is next proven that e^C fourier transforms to a causal function of time. Its filter inverse is e^{-C}. Grab yourself a cup of coffee and hide yourself away in a quiet place while you focus on the proof in the next paragraph.

A causal function c_τ vanishes at negative τ. Its Z transform $C(Z) = c_0 + c_1 Z + c_2 Z^2 + c_3 Z^3 + \cdots$, with $Z = e^{i\omega \Delta t}$ is really a Fourier sum. Its square $C(Z)^2$ convolves a causal with itself so it is causal. Each power of $C(Z)$ is causal, hence $e^C = 1 + C + C^2/2 + \cdots$, a sum of causals, is causal. The time-domain coefficients for e^C could be computed putting polynomials into power series or faster by Fourier transforms. The wavelet e^C has inverse e^{-C} also causal. A causal with a causal inverse is said to be "minimum phase". The filter $1 - Z/2$ with inverse $1 + Z/2 + Z^2/4 + \cdots$ is so. The delay filter Z^5 has the noncausal inverse Z^{-5} is not (output before input).

The next paragraph defines "Kolmogoroff spectral factorization". This arises in applications where one begins with an energy spectrum $|r|^2$ and factors it into an $re^{i\phi}$ times its conjugate. The inverse fourier transform of that $re^{i\phi}$ is causal.

Relate amplitude $r = r(\omega)$ and phase $\phi = \phi(\omega)$ to a causal time function c_τ.

$$|r|e^{i\phi} \quad = \quad e^{\ln|r|}e^{i\phi} \quad = \quad e^{\ln|r|+i\phi} \quad = \quad e^{c_0+c_1Z+c_2Z^2+c_3Z^3+\cdots} \quad = \quad e^{\sum_{\tau=0} c_\tau Z^\tau} \tag{4.7}$$

Given a spectrum $r(\omega)$, we will find a filter with that spectrum. Since $r(\omega)$ is a real even function of ω, so is its logarithm. Let the inverse Fourier transform of $\ln|r(\omega)|$ be u_τ, where u_τ is a real even function of time. Imagine a real odd function of time v_τ.

$$|r|e^{i\phi} \quad = \quad e^{\ln|r|+i\phi} \quad = \quad e^{\sum_\tau (u_\tau+v_\tau)Z^\tau} \tag{4.8}$$

The phase $\phi(\omega)$ transforms to v_τ. We can assert causality by choosing v_τ so that $u_\tau + v_\tau = 0$ $(= c_\tau)$ for all negative τ. This defines v_τ at negative τ. Since v_τ is odd, it is known at positive lags too. More simply, v_τ is created when u_τ is multiplied by a step function of size 2. This causal exponent $(c_0, c_1, \cdots)$ creates a causal filter $|r|e^{i\phi}$ with the specified spectrum $r(\omega)$.

We easily manufacture an inverse filter by changing the polarity of the c_τ. This filter is also causal by the same reasoning. Thus these filters are causal with a causal inverse. Such filters are commonly called "minimum phase".

Spectral factorization arises in a variety of contexts. Here's one: Rain drops showering on a tin roof create for you a signal whose spectrum you can compute, but what would be the wavelet of a single drop? Spectral factorization gives it. Divide this wavelet out from the data to get a record of impulses, one for each rain drop (theoretically!). The boiling surface of the sun is coming soon.

4.2.1 Kolmogoroff code

```
subroutine kolmogoroff( n, cx)  # Spectral factorization.
integer                 i, n      # input:  cx = amplitude spectrum
complex                 cx(n)     # output: cx = FT of min phase wavelet
do i= 1, n
        cx(i) = clog( cx(i) )
call ftu( -1., n, cx)
do i= 2, n/2 {                  # Make it causal changing only the odd part.
        cx(i)     = cx(i) * 2.
        cx(n-i+2) = 0.
        }
call ftu( +1., n, cx)
do i= 1, n
        cx(i) = cexp( cx(i))
return; end
```

Everyone has their own favorite fourier transform code, so why am I offering mine? Because you MUST get the scale factors correct. Few worries if you accidentally replace e^C by $2e^C$, because your humble plotting program might do that. But if you accidentally replace e^C by e^{2C}, you have squared it!

```
subroutine ftu( signi, nx, cx )          # Fourier transform
```

```
#   complex fourier transform with traditional scaling (FGDP)
#
#              1          nx           signi*2*pi*i*(j-1)*(k-1)/nx
#   cx(k)  =  -------- * sum cx(j) * e
#              scale      j=1              for k=1,2,...,nx=2**integer
#
#  scale=1 for forward transform signi=1, otherwise scale=1/nx
integer nx, i, j, k, m, istep
real    signi, arg
complex cx(nx), cmplx, cw, cdel, ct
i=1;  while( i<nx) i=2*i
if( i != nx )    call erexit('ftu: nx not a power of 2')
do i= 1, nx
        if( signi<0.)
                cx(i) = cx(i) / nx
j = 1;  k = 1
do i= 1, nx {
        if (i<=j) { ct = cx(j); cx(j) = cx(i); cx(i) = ct }
        m = nx/2
        while (j>m && m>1) { j = j-m; m = m/2 }         # "&&" means .AND.
        j = j+m
        }
repeat {
        istep = 2*k;    cw = 1.;    arg = signi*3.14159265/k
        cdel = cmplx( cos(arg), sin(arg))
        do m= 1, k {
                do i= m, nx, istep
                        { ct=cw*cx(i+k);  cx(i+k)=cx(i)-ct;  cx(i)=cx(i)+ct }
                cw = cw * cdel
                }
        k = istep
        if(k>=nx) break
        }
return; end
```

The ftu fast Fourier transform code above has a restriction that the data length must be a power of 2. Zero time and frequency are the first point in the vector, then positive times, then negative times.

It is a exercise for the student to show that a complex-valued time function has a positive spectrum that is non-symmetrical in frequency but it may be factored with the same code.

4.2.2 Constant Q medium

From the absorption law of a material, spectral factorization yields its impulse response. The most basic absorption law is the *constant* Q model. According to it, for a downgoing wave the absorption is proportional to the frequency ω, proportional to time in the medium z/v, and inversely proportional to the "quality" Q of the medium. Altogether the spectrum of a wave passing through a thickness z will be changed by the factor $e^{-|\omega|\tau} = e^{-|\omega|(z/v)/Q}$. This frequency function is plotted in the top line of Figure 4.7.

The middle function in Figure 4.7 is the autocorrelation giving on top the spectrum $e^{-|\omega|\tau}$. The third function is the factorization. An impulse entering the medium comes out with this shape. There is no physics in this analysis, only mathematics which assumes the

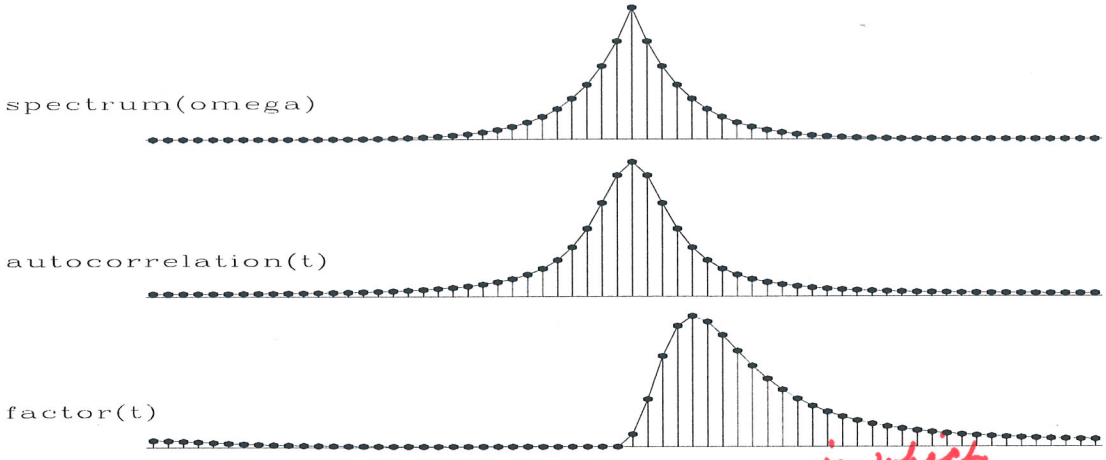

Figure 4.7: Autocorrelate the bottom signal to get the middle whose FT is the top. Spectral factorization works the other way, from top to bottom. hlx/. futterman

broadened pulse is causal with an abrupt arrival. The short wavelengths are concentrated near the sharp corner, while the long wavelengths are spread throughout. A physical system could cause the pulse to spread further (effectively by an additional all-pass filter), but physics cannot make it more compact.

All distances from the source see the same shape, but stretched in proportion to distance. The apparent Q is the traveltime to the source divided by the width of the pulse.

4.2.3 Causality in two dimensions

Our foundations, the basic convolution-deconvolution pair (4.1) and (4.2) are applicable only to filters with all coefficients *after* zero lag. Filters of physical interest generally concentrate their coefficients near zero lag. Requiring causality in 1-D and concentration in 2-D leads to shapes such as these:

$$\begin{array}{ccc} h & c & 0 \\ p & d & 0 \\ q & e & \mathbf{1} \\ s & f & a \\ u & g & b \end{array} \quad = \quad \begin{array}{ccc} h & c & \cdot \\ p & d & \cdot \\ q & e & \cdot \\ s & f & a \\ u & g & b \end{array} \quad + \quad \begin{array}{ccc} \cdot & \cdot & 0 \\ \cdot & \cdot & 0 \\ \cdot & \cdot & \mathbf{1} \\ \cdot & \cdot & \cdot \\ \cdot & \cdot & \cdot \end{array} \tag{4.9}$$

$$2-\text{D filter} \quad = \quad \text{variable} \quad + \quad \text{constrained}$$

where $a, b, c, ..., u$ are coefficients we will find by least squares.

The complete story is rich in mathematics and in concepts, but to sum up, filters fall into two categories according to the numerical values of their coefficients. There are filters for which equations (4.1) and (4.2) work as desired and expected. These filters are called "minimum phase". There are also filters for which (4.2) is a disaster numerically, the feedback process diverging to infinity.

Divergent cases correspond to physical processes that are not simply described by initial conditions but require also reflective boundary conditions so information flows backwards, i.e. anticausally. Equation (4.2) only allows for initial conditions.

I oversimplify by trying to collapse an entire book (FGDP) into a few sentences by saying here that for any fixed 1-D spectrum there exist many filters. Of these, only one has stable polynomial division. That filter has its energy compacted as soon as possible after the "1.0" at zero lag.

Which side of the little rectangular patch of coefficients we choose to place the 1.0 is rather arbitrary. The important matter is that as a matter of principle, the 1.0 is expected to lie along one side of the little patch. We never put the "1" at the corner of a patch because that would be excluding locations near the "1" that could be correlated with it. It is important that beyond the 1.0 (in whatever direction that may be) the filter coefficients must be zero because in one dimension, these coefficients lie before zero lag.

4.2.4 Causality in three dimensions

The top plane in Figure 4.8 is the 2-D filter seen in equation (4.9). Geometrically, the three-dimensional generalization of a helix, Figure 4.8 shows a causal filter in three dimensions. Think of the little cubes as packed with the string of the causal 1-D function. Under the "1" is packed with string, but none above it. Behind the "1" is packed with string, but none in front of it. The top plane can be visualized as the area around the end of the 1-D string. Above the top plane are zero-valued anticausal filter coefficients. This 3-D cube is

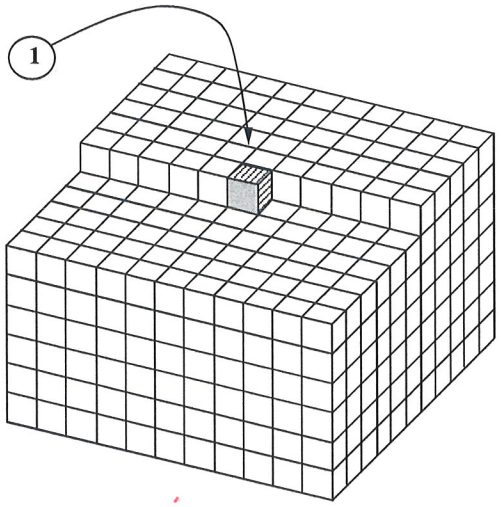

Figure 4.8: A 3-D causal filter at the starting end of a 3-D helix. VIEW hlx/. 3dpef

like the usual Fortran packing of a 3-D array with one confusing difference. The starting location where the "1" is located is not at the Fortran (1,1,1) location. Details of indexing are essential, but complicated, and found near the end of this chapter.

4.2.5 Blind deconvolution and the solar cube

An area of applications that leads directly to spectral factorization is "blind deconvolution." Here we begin with a signal. We form its spectrum and factor it. We could simply inspect the filter and interpret it, or we might deconvolve it out from the original data. This topic deserves a fuller exposition, say for example as defined in some of my earlier books. Here we inspect a novel example that incorporates the helix.

Solar physicists have learned how to measure the seismic field of the sun surface. It's chaotic. If you created an impulsive explosion on the surface of the sun, what would the response be? James Rickett and I applied the helix idea along with Kolmogoroff spectral factorization to find the impulse response of the sun. Figure 4.9 shows a raw data cube and the derived impulse response. The sun is huge so the distance scale is in megameters (Mm). The United States is 5 Mm wide. Vertical motion of the sun is measured with a video-camera like device that measures vertical motion by an optical doppler shift. From an acoustic/seismic point of view, the surface of the sun is a very noisy place. The figure shows time in kiloseconds (Ks). We see about 15 cycles in 5 Ks which is 1 cycle in about 333 sec. Thus the sun seems to oscillate vertically with about a 5 minute period. The top plane of the raw data in Figure 4.9 (left panel) happens to have a sun spot in the center. The data analysis here is not affected by the sun spot so please ignore it.

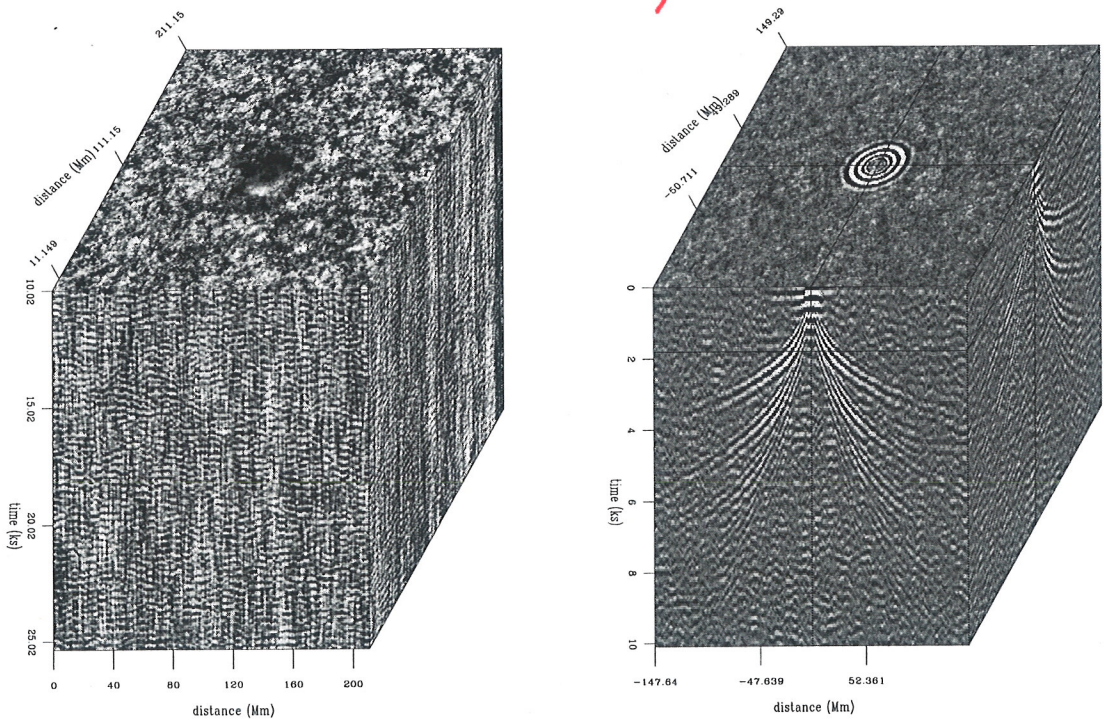

Figure 4.9: Raw seismic data on the sun (left). Impulse response of the sun (right) derived by Helix-Kolmogoroff spectral factorization. VIEW hlx/. solar

The first step of the data processing is to transform the raw data to its spectrum. With the helix assumption, computing the spectrum is virtually the same thing in 1-D space as in

3-D space. The resulting spectrum was passed to Kolmogoroff spectral factorization code, a 1-D code. The resulting impulse response is on the right side of Figure 4.9. The plane we see on the right top is not lag time $\tau = 0$; it is lag time $\tau = 2$ Ks. It shows circular rings, as ripples on a pond. Later lag times (not shown) would be the larger circles of expanding waves. The front and side planes show tent-like shapes.

The slope of the tent gives the (inverse) velocity of the wave (as seen on the surface of the sun). The horizontal velocity we see on the sun surface turns out (by Snell's law) to be the same as that at the bottom of the ray. On the front face at early times we see the low velocity (steep) wavefronts and at later times we see the faster waves. This is because the later arrivals reach more deeply into the sun.

Look carefully, and you can see two (or even three!) tents inside one another. These "inside tents" are the waves that have bounced once (or more!) from the surface of the sun. When a ray goes down and back up to the sun surface, it reflects and takes off again with the same ray shape. The result is that a given slope on the traveltime curve can be found again at twice the distance at twice the time. Very close to $t = 0$ see horizontal waveforms extending only a short distance from the origin. These are electromagnetic waves of essentially infinite velocity.

4.3 FACTORED LAPLACIAN == HELIX DERIVATIVE

I had learned spectral factorization as a method for single seismograms. After I learned it, every time I saw a positive function I'd wonder if it made sense to factor it. When total field magnetometers were invented, I found it as a way to deduce vertical and horizontal **magnetic** components. A few pages back you saw how to use factorization to deduce the waveform passing through an absorptive medium. Then we saw how the notion of "impulse response" applies not only to signals, but allows use of random noise on the sun to deduce the 3-D impulse response there. But the most useful application of spectral factorization so far is what comes next, factoring the Laplace operator, $-\nabla^2$. Its fourier transform $-((ik_x)^2 + (ik_y)^2) \geq 0$ is positive, so it is a spectrum. The useful tool we'll uncover I dub the "helix derivative".

The signal

$$\mathbf{r} \quad = \quad -\nabla^2 \quad = \quad \boxed{-1 \mid 0 \mid \cdots \mid 0 \mid -1 \mid 4 \mid -1 \mid 0 \mid \cdots \mid 0 \mid -1} \tag{4.10}$$

is an autocorrelation function because it is symmetrical about the "4," and the Fourier transform of $-\nabla^2$ is $-((ik_x)^2 + (ik_y)^2) \geq 0$ which is positive for all frequencies (k_x, k_y). Kolmogoroff spectral-factorization gives this wavelet $\mathbf{h}$:

$$\mathbf{h} \quad = \quad \boxed{1.791 \mid -.651 \mid -.044 \mid -.024 \mid \cdots \mid \cdots \mid -.044 \mid -.087 \mid -.200 \mid -.558} \tag{4.11}$$

In other words, the autocorrelation of (4.11) is (4.10). This is not obvious from the numbers themselves because the computation requires a little work, but dropping all the smaller numbers allows you a rough check.

In this book section only I use abnormal notation for bold letters. Here $\mathbf{h}$, $\mathbf{r}$ are signals, while $\mathbf{H}$ and $\mathbf{R}$ are images, neither being matrices or vectors. Recall from chapter 1 that a filter is a signal packed into a matrix to make a filter operator.

Let the time reversed version of $\mathbf{h}$ be denoted $\mathbf{h}^*$. This notation is consistent with an idea from Chapter 1 that the adjoint of a filter matrix is another filter matrix with a reversed filter. In engineering it is conventional to use the asterisk symbol "$*$" to denote convolution. Thus, the idea that the autocorrelation of a signal $\mathbf{h}$ is a convolution of the signal $\mathbf{h}$ with its time reverse (adjoint) can be written as $\mathbf{h}^* * \mathbf{h} = \mathbf{h} * \mathbf{h}^* = \mathbf{r}$.

Wind the signal $\mathbf{r}$ around a vertical-axis helix to see its two-dimensional shape $\mathbf{R}$:

$$\mathbf{r} \quad \rightarrow \text{helical boundaries} \quad \begin{array}{|c|c|c|}\hline & -1 & \\ \hline -1 & 4 & -1 \\ \hline & -1 & \\ \hline \end{array} \quad = \quad \mathbf{R} \tag{4.12}$$

This 2-D image (which can be packed into a filter operator) is the negative of the finite-difference representation of the Laplacian operator, generally denoted $\nabla^2 = \frac{\partial^2}{\partial x^2} + \frac{\partial^2}{\partial y^2}$. Now for the magic: Wind the signal $\mathbf{h}$ around the same helix to see its two-dimensional shape $\mathbf{H}$:

$$\mathbf{H} \quad = \quad \begin{array}{|c|c|c|c|c|c|c|c|c|}\hline & & & & 1.791 & -.651 & -.044 & -.024 & \cdots \\ \hline \cdots & -.044 & -.087 & -.200 & -.558 & & & & \\ \hline \end{array} \tag{4.13}$$

In the representation (4.13) we see the coefficients diminishing rapidly away from maximum value 1.791. My claim is that the two-dimensional autocorrelation of (4.13) is (4.12). You verified this idea earlier when the numbers were all ones. You can check it again in a few moments if you drop the small values, say 0.2 and smaller.

Physics on a helix can be viewed thru the eyes of matrices and numerical analysis. This is not easy because the matrices are so huge. Discretize the (x, y)-plane to an $N \times M$ array and pack the array into a vector of $N \times M$ components. Likewise pack the Laplacian operator $\partial_{xx} + \partial_{yy}$ into a matrix. For a 4×3 plane, that matrix is shown in equation (4.14).

$$-\nabla^2 \quad = \quad \left[\begin{array}{cccc|cccc|cccc} 4 & -1 & \cdot & \cdot & -1 & \cdot & \cdot & \cdot & \cdot & \cdot & \cdot & \cdot \\ -1 & 4 & -1 & \cdot & \cdot & -1 & \cdot & \cdot & \cdot & \cdot & \cdot & \cdot \\ \cdot & -1 & 4 & -1 & \cdot & \cdot & -1 & \cdot & \cdot & \cdot & \cdot & \cdot \\ \cdot & \cdot & -1 & 4 & h & \cdot & \cdot & -1 & \cdot & \cdot & \cdot & \cdot \\ \hline -1 & \cdot & \cdot & h & 4 & -1 & \cdot & \cdot & -1 & \cdot & \cdot & \cdot \\ \cdot & -1 & \cdot & \cdot & -1 & 4 & -1 & \cdot & \cdot & -1 & \cdot & \cdot \\ \cdot & \cdot & -1 & \cdot & \cdot & -1 & 4 & -1 & \cdot & \cdot & -1 & \cdot \\ \cdot & \cdot & \cdot & -1 & \cdot & \cdot & -1 & 4 & h & \cdot & \cdot & -1 \\ \hline \cdot & \cdot & \cdot & \cdot & -1 & \cdot & \cdot & h & 4 & -1 & \cdot & \cdot \\ \cdot & \cdot & \cdot & \cdot & \cdot & -1 & \cdot & \cdot & -1 & 4 & -1 & \cdot \\ \cdot & \cdot & \cdot & \cdot & \cdot & \cdot & -1 & \cdot & \cdot & -1 & 4 & -1 \\ \cdot & \cdot & \cdot & \cdot & \cdot & \cdot & \cdot & -1 & \cdot & \cdot & -1 & 4 \end{array}\right] \tag{4.14}$$

The two-dimensional matrix of coefficients for the Laplacian operator is shown in (4.14), where on a cartesian space, $h = 0$, and in the helix geometry, $h = -1$. (A similar partitioned matrix arises from packing a cylindrical surface into a 4×3 array.) Notice that the partitioning becomes transparent for the helix, $h = -1$. With the partitioning thus invisible, the matrix simply represents one-dimensional convolution and we have an alternative analytical approach, one-dimensional Fourier Transform. We often need to solve sets of simultaneous equations with a matrix similar to (4.14). The method we use is triangular factorization.

Although the autocorrelation $\mathbf{r}$ has mostly zero values, the factored autocorrelation $\mathbf{a}$ has a great number of nonzero terms. Fortunately they seem to be converging rapidly (in the middle) so truncation (of the middle coefficients) seems reasonable. I wish I could show you a larger matrix, but all I can do is to pack the signal $\mathbf{a}$ into shifted columns of a lower triangular matrix $\mathbf{A}$ like this:

$$\mathbf{A} = \begin{bmatrix}
1.8 & . & . & . & . & . & . & . & . & . & . & . \\
-.6 & 1.8 & . & . & . & . & . & . & . & . & . & . \\
\ddots & -.6 & 1.8 & . & . & . & . & . & . & . & . & . \\
-.2 & \ddots & -.6 & 1.8 & . & . & . & . & . & . & . & . \\
-.6 & -.2 & \ddots & -.6 & 1.8 & . & . & . & . & . & . & . \\
. & -.6 & -.2 & \ddots & -.6 & 1.8 & . & . & . & . & . & . \\
. & . & -.6 & -.2 & \ddots & -.6 & 1.8 & . & . & . & . & . \\
. & . & . & -.6 & -.2 & \ddots & -.6 & 1.8 & . & . & . & . \\
. & . & . & . & -.6 & -.2 & \ddots & -.6 & 1.8 & . & . & . \\
. & . & . & . & . & -.6 & -.2 & \ddots & -.6 & 1.8 & . & . \\
. & . & . & . & . & . & -.6 & -.2 & \ddots & -.6 & 1.8 & . \\
. & . & . & . & . & . & . & -.6 & -.2 & \ddots & -.6 & 1.8
\end{bmatrix} \tag{4.15}$$

If you will allow me some truncation approximations, I now claim that the laplacian represented by the matrix in equation (4.14) is factored into two parts $-\nabla^2 = \mathbf{A}^*\mathbf{A}$ which are upper and lower triangular matrices whose product forms the autocorrelation seen in (4.14). Recall that triangular matrices allow quick solutions of simultaneous equations by backsubstitution. That is what we do with our deconvolution program.

Spectral factorization produces not merely a causal wavelet with the required autocorrelation. It produces one that is stable in deconvolution. Using $\mathbf{H}$ in one-dimensional polynomial division, we can solve many formerly difficult problems very rapidly. Consider the Laplace equation with sources (Poisson's equation). Polynomial division and its reverse (adjoint) gives us $\mathbf{p} = (\mathbf{q}/\mathbf{H})/\mathbf{H}^*$ which means that we have solved $\nabla^2\mathbf{p} = -\mathbf{q}$ by using polynomial division on a helix. Using the seven coefficients shown, the cost is fourteen multiplications (because we need to run both ways) per mesh point. An example is shown in Figure 4.10.

Figure 4.10 contains both the helix derivative and its inverse. Contrast them to the x- or y-derivatives (doublets) and their inverses (axis-parallel lines in the (x, y)-plane). Simple derivatives are highly directional whereas the helix derivative is only slightly directional achieving its meagre directionality entirely from its phase spectrum.

4.4 HELIX LOW-CUT FILTER

Since the autocorrelation of $\mathbf{H}$ is $\mathbf{H}^* * \mathbf{H} = \mathbf{R} = -\nabla^2$ is a second derivative, the operator $\mathbf{H}$ must be something like a first derivative. As a geophysicist, I found it natural to compare the operator $\frac{\partial}{\partial y}$ with $\mathbf{H}$ by applying them to a local topographic map. The result shown in Figure 4.11 is that $\mathbf{H}$ enhances drainage patterns whereas $\frac{\partial}{\partial y}$ enhances mountain ridges.

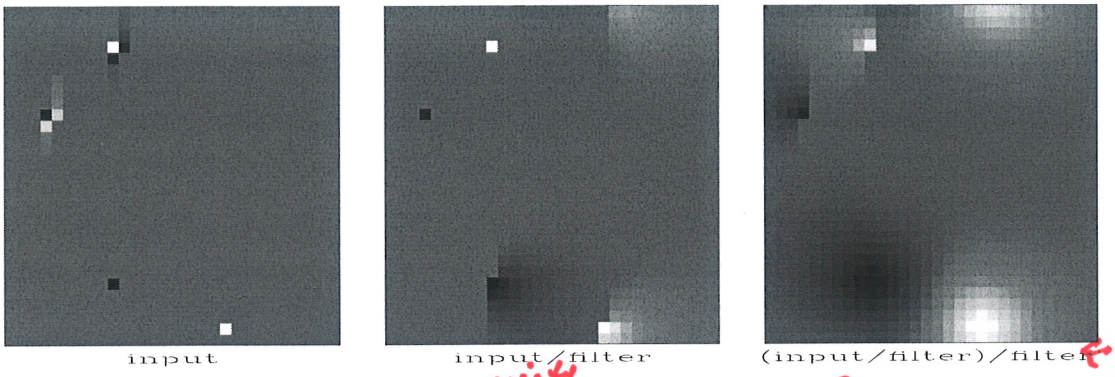

Figure 4.10: Deconvolution by a filter whose autocorrelation is the two-dimensional Laplacian operator. Amounts to solving the Poisson equation. Left is $\mathbf{q}$; Middle is $\mathbf{q}/\mathbf{H}$; Right is $(\mathbf{q}/\mathbf{H})/\mathbf{H}^*$. VIEW hlx/. lapfac90

The operator $\mathbf{H}$ has curious similarities and differences with the familiar gradient and divergence operators. In two-dimensional physical space, the gradient maps one field to *two* fields (north slope and east slope). The factorization of $-\nabla^2$ with the helix gives us the operator $\mathbf{H}$ that maps one field to *one* field. Being a one-to-one transformation (unlike gradient and divergence) the operator $\mathbf{H}$ is potentially invertible by deconvolution (recursive filtering).

I have chosen the name "helix derivative" or "helical derivative" for the operator $\mathbf{H}$. A flag pole has a narrow shadow behind it. The helix integral (middle frame of Figure 4.10) and the helix derivative (left frame) show shadows with an angular bandwidth approaching 180°.

Our construction makes $\mathbf{H}$ have the energy spectrum $k_x^2 + k_y^2$, so the magnitude of the Fourier transform is $\sqrt{k_x^2 + k_y^2}$. It is a cone centered and with value zero at the origin. By contrast, the components of the ordinary gradient have amplitude responses $|k_x|$ and $|k_y|$ that are lines of zero across the (k_x, k_y)-plane.

The rotationally invariant cone in the Fourier domain contrasts sharply with the nonrotationally invariant function shape in (x, y)-space. The difference must arise from the phase spectrum. The factorization (4.13) is nonunique in that causality associated with the helix mapping can be defined along either x- or y-axes; thus the operator (4.13) can be rotated or reflected.

In practice we often require an isotropic filter. Such a filter is a function of $k_r = \sqrt{k_x^2 + k_y^2}$. It could be represented as a sum of helix derivatives to integer powers.

If you want to see some tracks on the side of a hill, you want to subtract the hill and see only the tracks. Usually, however, you don't have a very good model for the hill. As an expedient you could apply a low-cut filter to remove all slowly variable functions of altitude. In chapter 1 we found the Sea of Galilee in Figure 1.3 to be too smooth for viewing pleasure so we made the roughened versions in Figure 1.6, a one-dimensional filter that we could apply over the x-axis or the y-axis. In Fourier space such a filter has a response function of

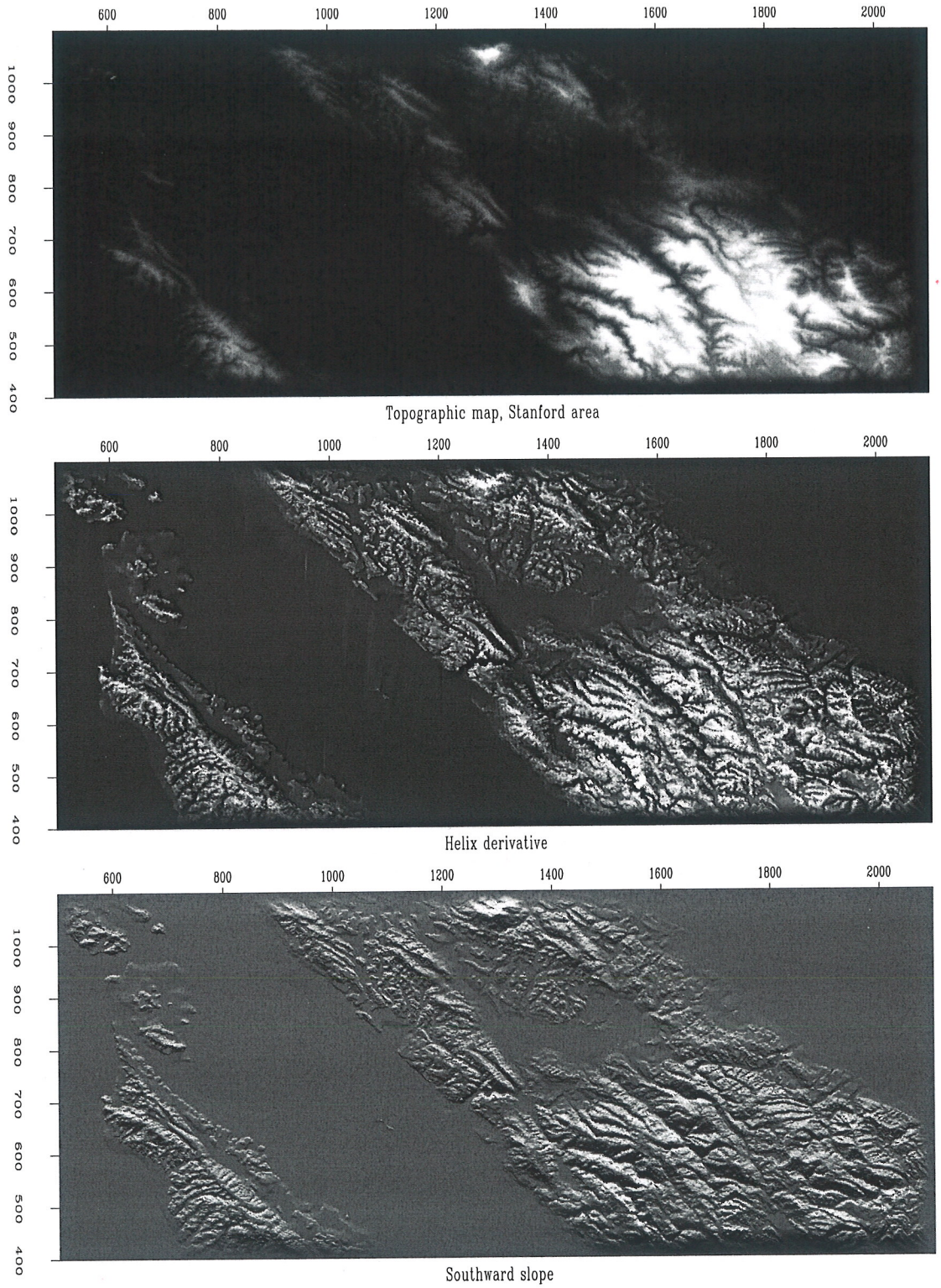

Figure 4.11: Topography, helical derivative, slope south. VIEW hlx/. helocut90

k_x or a function of k_y. The isotropy of physical space tells us it would be more logical to design a filter that is a function of $k_x^2 + k_y^2$. In Figure 4.11 we saw that the helix derivative $\mathbf{H}$ does a nice job. The Fourier magnitude of its impulse response is $k_r = \sqrt{k_x^2 + k_y^2}$. There is a little anisotropy connected with phase (which way should we wind the helix, on x or y?) but it is not nearly so severe as that of either component of the gradient, the two components having wholly different spectra, amplitude $|k_x|$ or $|k_y|$.

4.4.1 Improving low-frequency behavior

It is nice having the 2-D helix derivative, but we can imagine even nicer 2-D low-cut filters. In one dimension we designed a filter with an adjustable parameter, a cutoff frequency. In 1-D we compounded a first derivative (which destroys low frequencies) with a leaky integration (which undoes the derivative at all other frequencies). The analogous filter in 2-D would be $-\nabla^2/(-\nabla^2 + k_0^2)$, which would first be expressed as a finite difference $(-Z^{-1} + 2.00 - Z)/(-Z^{-1} + 2.01 - Z)$ and then factored as we did the helix derivative.

We can visualize a plot of the magnitude of the 2-D Fourier transform of the filter equation (4.13). It is a 2-D function of k_x and k_y and it should resemble $k_r = \sqrt{k_x^2 + k_y^2}$. The point of the cone $k_r = \sqrt{k_x^2 + k_y^2}$ becomes rounded by the filter truncation so k_r does not reach zero at the origin of the (k_x, k_y)-plane. We can force it to vanish at zero frequency by subtracting .183 from the lead coefficient 1.791. I did not do that subtraction in Figure 4.12 which explains the whiteness in the middle of the lake. I gave up on playing with both k_0 and filter length; and now merely play with the sum of the filter coefficients.

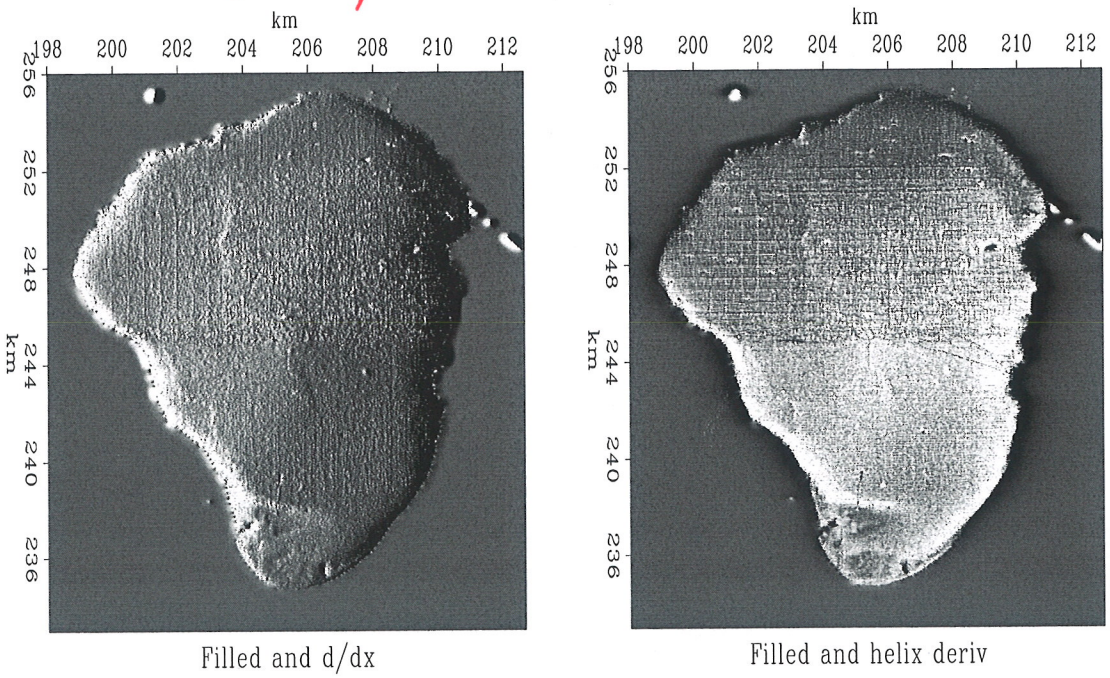

Figure 4.12: Galilee roughened by gradient and by helical derivative. hlx/. helgal

4.4.2 Filtering mammograms

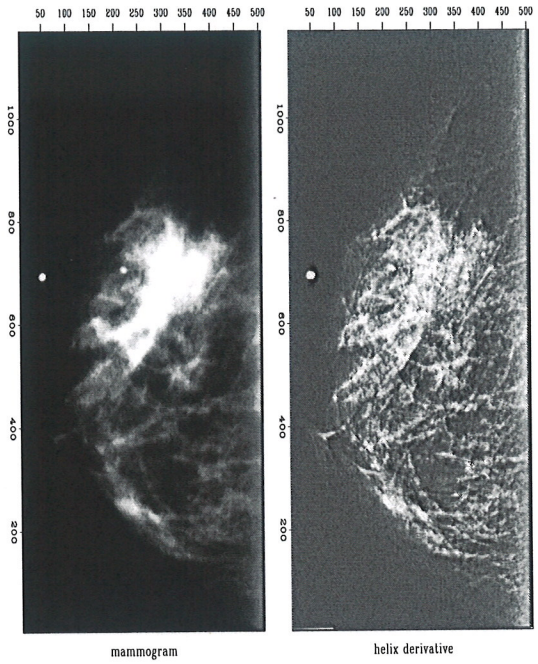

Figure 4.13: Mammogram (medical X-ray). The cancer is the "spoked wheel." (I apologize for the inability of paper publishing technology to exhibit a clear grey image.) The tiny white circles are metal foil used for navigation. The little halo around a circle exhibits the impulse response of the helix derivative. VIEW hlx/. mam

I prepared a half dozen medical X-rays like Figure 4.13. The doctor brought her young son to my office one evening to evaluate the results. In a dark room I would show the original X-ray on a big screen and then suddenly switch to the helix derivative. Every time I did this, her son would exclaim "Wow!" The doctor was not so easily impressed, however. She was not accustomed to the unfamiliar image. Fundamentally, the helix derivative applied to her data does compress the dynamic range making weaker features more readily discernible. We were sure of this from theory and from various geophysical examples. The subjective problem was her unfamiliarity with our display. I found that I could always spot anomalies more quickly on the filtered display, but then I would feel more comfortable when I would discover those same anomalies also present (though less evident) in the original data. Thinking this through, I decided the doctor would likely have been more impressed had I used a spatial low-cut filter instead of the helix derivative. That would have left the details of her image (above the cutoff frequency) unchanged altering only the low frequencies, thereby allowing me to increase the gain.

First I had a problem preparing Figure 4.13. It shows shows the application of the helix derivative to a medical X-ray. The problem was that the original X-ray was all positive values of brightness so there was a massive amount of spatial low frequency present. Obviously an x-derivative or a y-derivative would eliminate the low frequency, but the helix derivative did not. This unpleasant surprise arises because the filter in equation (4.13) was truncated after a finite number of terms. Adding up the terms actually displayed in equation (4.13), they sum to .183 whereas theoretically the sum of all the terms should be zero. From the ratio of .183/1.791 we can say that the filter pushes zero frequency amplitude 90% of the way to zero value. When the image contains very much zero frequency amplitude, this is not good enough. Better results could be obtained with more coefficients, and I did use more coefficients, but simply removing the mean saved me from needing a costly number of

filter coefficients.

A final word about the doctor. As she was about to leave my office she suddenly asked whether I had scratched one of her X-rays. We were looking at the helix derivative and it did seem to show a big scratch. What should have been a line was broken into a string of dots. I apologized in advance and handed her the original film negatives which she proceeded to inspect. "Oh," she said, "Bad news. There are calcification nodules along the ducts." So the scratch was not a scratch, but an important detail that had not been noticed on the original X-ray. Times have changed since then. Nowadays mammography has become digital and appropriate filtering is defaulted into their presentation.

In preparing an illustration for here, I learned one more lesson. The scratch was small, so I enlarged a small portion of the mammogram for display. The very process of selecting a small portion followed by scaling the amplitude between maximum and minimum darkness of printer ink had the effect enhancing the visibility of the scratch on the mammogram itself. Now Figure 4.14 shows it to be perhaps even clearer than on the helix derivative.

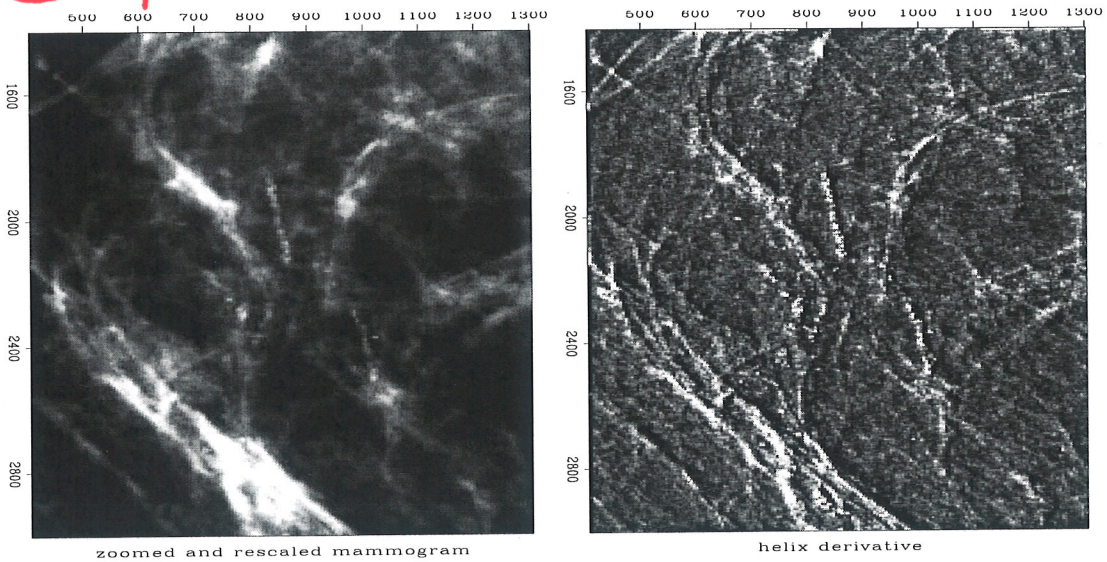

Figure 4.14: Not a scratch. Reducing the (x, y)-space range of the illustration allowed boosting the gain, thus making the non-scratch more prominent. VIEW hlx/. scratch

4.5 SUBSCRIPTING A MULTIDIMENSIONAL HELIX

Basic utilities transform back and forth between multidimensional matrix coordinates and helix coordinates. The essential module used repeatedly in applications later in this book is `createhelixmod`. We begin here from its intricate underpinnings.

Fortran77 has a concept of a multidimensional array being equivalent to a one-dimensional array. Given that the hypercube specification `nd=(n1,n2,n3,...)` defines the storage `dimension` of a data array, we can refer to a data element as either `dd(i1,i2,i3,...)` or `dd( i1 +n1*(i2-1) +n1*n2*(i3-1) +...)`. The helix says to refer to the multidimen-

sional data by its equivalent one-dimensional index (sometimes called its vector subscript or linear subscript).

The filter, however, is a much more complicated story than the data: First, we require all filters to be causal. In other words, the Laplacian doesn't fit very well, since it is intrinsically noncausal. If you really want noncausal filters, you will need to provide your own time shifts outside the tools supplied here. Second, a filter is usually a small hypercube, say `aa(a1,a2,a3,...)` and would often be stored as such. For the helix we must store it in a special one-dimensional form. Either way, the numbers `na= (a1,a2,a3,...)` specify the dimension of the hypercube. In cube form, the entire cube could be indexed multidimensionally as `aa(i1,i2,...)` or it could be indexed one-dimensionally as `aa(ia,1,1,...)` or sometimes[1] `aa(ia)` by letting `ia` cover a large range. When a filter cube is stored in its normal "tightly packed" form the formula for computing its one-dimensional index `ia` is

```
ia = i1 +a1*(i2-1) +a1*a2*(i3-1) + ...
```

When the filter cube is stored in an array with the same dimensions as the data, `data(n1,n2,n3,...)`, the formula for `ia` is

```
ia = i1 +n1*(i2-1) +n1*n2*(i3-1) + ...
```

The fortran compiler knows how to convert from the multidimensional cartesian indices to the linear index. We will need to do that, as well as the converse. Module `cartesian` below contains two subroutines that explicitly provide us the transformations between the linear index `i` and the multidimensional indices `ii= (i1,i2,...)`. The two subroutines have the logical names `cart2line` and `line2cart`.

helical-cartesian coordinate conversion.r90

```
module cartesian {       # index transform (vector to matrix) and its inverse
contains
  subroutine line2cart( nn, i, ii) {
    integer, dimension( :), intent( in) :: nn    # cartesian axes (n1,n2,n3,...)
    integer, dimension( :), intent(out) :: ii    # cartesn coords (i1,i2,i3,...)
    integer               , intent( in) :: i     # equivalent 1-D linear index
    integer                             :: axis, n123
    n123 = 1
    do axis = 1, size( nn) {
        ii( axis) = mod( ( i-1)/n123, nn( axis)) + 1
        n123 = n123 * nn( axis)
        }
    }
  subroutine cart2line( nn, ii, i) {
    integer, dimension( :), intent( in) :: nn, ii
    integer                             :: i, axis, n123
    n123 = 1;     i = 1
    do axis = 1, size( nn) {
        i = i + ( ii( axis)-1)*n123
```

[1] Some programming minutia: Fortran77 does not allow you to refer to an array by both its cartesian coordinates and by its linear subscript in the same subroutine. To access it both ways, you need a subroutine call, or you dimension it as `data(n1,n2,...)` and then you refer to it as `data(id,1,1,...)`. Fortran90 follows the same rule outside modules. Where modules use other modules, the compiler does not allow you to refer to data both ways, unless the array is declared as `allocatable`.

```
            n123 = n123 * nn( axis)
            }
        }
}
```

The fortran linear index is closely related to the helix. There is one major difference, however, and that is the origin of the coordinates. To convert from the linear index to the helix lag coordinate, we need to subtract the fortran linear index of the "1.0" which is usually taken at `center= (1+a1/2, 1+a2/2, ..., 1)`. (On the last dimension, there is no shift because nobody stores the volume of zero values that would occur before the 1.0.) The `cartesian` module fails for negative subscripts. Thus we need to be careful to avoid thinking of the filter's 1.0 (shown in Figure 4.8) as the origin of the multidimensional coordinate system although the 1.0 is the origin in the one-dimensional coordinate system.

Even in one dimension (see the matrix in equation (1.4)), to define a filter *operator* we need to know not only filter coefficients and a filter length, but we also need to know the data length. To define a multidimensional filter using the helix idea, besides the properties intrinsic to the filter, we also need to know the circumference of the helix, i.e., the length on the 1-axis of the data's hypercube as well as the other dimensions `nd=(n1,n2,...)` of the data's hypercube.

Thinking about convolution on the helix, it is natural to think about the filter and data being stored in the same way, that is, by reference to the data size. This would waste so much space, however, that our helix filter module `helix` instead stores the filter coefficients in one vector and their lags in another. The `i`-th coefficient value of the filter goes in `aa%flt(i)` and the `i`-th lag `ia(i)` goes in `aa%lag(i)`. The lags are the same as the fortran linear index except for the overall shift of the 1.0 of a cube of data dimension `nd`. Our module for convolution on a helix, `helicon` has already an implicit "1.0" at the filter's zero lag so we do not store it. (It is an error to do so.)

Module `createhelixmod` allocates memory for a helix filter and builds filter lags along the helix from the hypercube description. The hypercube description is not the literal cube seen in Figure 4.8 but some integers specifying that cube: the data cube dimensions `nd`, likewise the filter cube dimensions `na`, the parameter `center` identifying the location of the filter's "1.0", and a `gap` parameter used in a later chapter. To find the lag table, module `createhelixmod` first finds the fortran linear index of the `center` point on the filter hypercube. Everything before that has negative lag on the helix and can be ignored. (Likewise, in a later chapter we see a gap parameter that effectively sets even more filter coefficients to zero so their lags can be ignored too.) Then it sweeps from the center point over the rest of the filter hypercube calculating for a data-sized cube `nd`, the fortran linear index of each filter element.

constructing helix filter in N-D.r90

```
module createhelixmod {                          # Create helix filter lags and mis
use helix
use cartesian
contains
  function createhelix( nd, center, gap, na)  result( aa) {
    type( filter)                        :: aa       # needed by helicon.
    integer, dimension(:), intent(in) :: nd, na   # data and filter axes
    integer, dimension(:), intent(in) :: center   # normally (na1/2,na2/2,...,1)
    integer, dimension(:), intent(in) :: gap      # normally ( 0,   0,  0,...,0)
```

```
    integer, dimension( size( nd))     :: ii       # cartesian indexes
    integer                            :: na123, ia, ndim, nh, lag0a,lag0d
    integer, dimension(:), allocatable :: lag
          nh= 0;   na123 = product( na);   ndim = size( nd)
    allocate(  lag( na123 ) )            # filter cube size
    call cart2line ( na, center, lag0a)  # lag0a = index pointing to the "1.0"
    do ia = 1+lag0a, na123 {             #    ia  is fortran linear index.
       call line2cart( na, ia, ii)       # ii(ia) is fortran array  indices.
       if( any( ii <= gap))    next      # ignore some locations
       nh = nh + 1                       # got another live one.
       call cart2line( nd, ii, lag(nh))  # get its fortran linear index
       }
    call cart2line(  nd, center, lag0d)  # lag0d is center shift for nd_cube
    call allocatehelix( aa, nh)          # nh becomes size of filter on helix.
    aa%lag = lag(1:nh) - lag0d;          # lag = fortran_linear_index - center
    aa%flt = 0.0;              deallocate( lag)
    }
}
```

Near the end of the code you see the calculation of a parameter `lag0d`. This is the count of the number of zeros that a data-sized fortran array would store in a filter cube before the filter's 1.0. We need to subtract this shift from the filter's fortran linear index to get the lag on the helix.

A filter can be represented literally as a multidimensional cube like equation (4.9) shows us in two dimensions or like Figure 4.8 shows us in three dimensions. Unlike the helical form, in literal cube form, the zeros preceding the "1.0" are explicitly present so `lag0` needs to be added back in to get the fortran subscript. To convert a helix filter `aa` to fortran's multidimensional hypercube `cube(n1,n2,...)` is module `box`:

Convert helix filter.r90

```
module box {          # Convert helix filter to hypercube: cube(na(1),na(2),...)
use helix
use cartesian
contains
  subroutine boxn( nd, center, na, aa, cube) {
    integer, dimension (:), intent( in)  :: nd, center, na    # (ndim)
    type( filter),          intent( in)  :: aa
    real,    dimension( :), intent( out) :: cube
    integer, dimension( size( nd))       :: ii
    integer                              :: j, lag0a, lag0d, id, ia
    cube = 0.;                          # cube=0
    call cart2line( na, center, lag0a)  # locate the 1.0 in the na_cube.
    cube( lag0a) = 1.                   # place it.
    call cart2line( nd, center, lag0d)  # locate the 1.0 in the nd_cube.
    do j = 1, size( aa%lag) {           # inspect the entire helix
       id = aa%lag( j) + lag0d          # index = helix_lag + center_d
       call line2cart( nd, id, ii)      # ii(id) = cartesian indices
       call cart2line( na,     ii, ia)  # ia(ii) = linear index in aa
       cube( ia) = aa%flt( j)           # copy the filter coefficient
       }
    }
}
```

The `box` module is normally used to display or manipulate a filter that was estimated in helical form (usually estimated by the least-squares method).

The inverse process to box is to convert a fortran hypercube to a helix filter. For this we have module unbox. It abandons all zero-valued coefficients such as those that should be zero before the box's 1.0. It abandons the "1.0" as well, because it is implicitly present in the helix convolution module helicon.

Convert hypercube filter to helix.r90

```
module unbox {                                  # helixfilter aa = cube(a1,a2,...)
use helix
use cartesian
contains
  function unboxn( nd, center, na, cube)  result( aa) {
    type( filter)                              :: aa
    integer, dimension( :), intent( in) :: nd, center, na      # (ndim)
    real,    dimension( :), intent( in) :: cube                # cube(a1,a2,...)
    logical, dimension( size( cube))    :: keep                # keep(a1*a2*...)
    integer, dimension( size( nd))      :: ii                  # (ndim)
    integer                             :: ic, lag0a, lag0d, i, h
    call cart2line(  na, center, lag0a)
    call cart2line(  nd, center, lag0d)
    keep = ( abs( cube) > epsilon( cube))     # epsilon is a Fortran intrinsic
    keep( lag0a) = .false.                    # throw away the 1.0.
    call allocatehelix( aa, count( keep));  h = 0
    do ic = 1, size( cube) {                                  # sweep cube
          if( keep( ic) ) {                             h = h + 1  # only the keepers
               call line2cart(  na, ic, ii)                       # ii(ic)= indices on na
               call cart2line(  nd,     ii, i)           # i     = index   on nd
               aa%lag( h) = i - lag0d                     # lag = index - center
               aa%flt( h) = cube( ic)                     # copy coefs.
               }
          }
    }
}
```

An example of using unbox would be copying some numbers such as the factored laplacian in equation (4.13) into a cube and then converting it to a helix.

A reasonable arrangement for a small 3-D filter is na=(5,3,2) and center=(3,2,1). Using these arguments, I used createhelixmod to create a filter. I set all the helix filter coefficients to 2. Then I used module box to put it in a convenient form for display. After this conversion, the coefficient aa(3,2,1) is 1, not 2. Finally, I printed it:

```
0.000  0.000  0.000  0.000  0.000
0.000  0.000  1.000  2.000  2.000
2.000  2.000  2.000  2.000  2.000
-------------------------------
2.000  2.000  2.000  2.000  2.000
2.000  2.000  2.000  2.000  2.000
2.000  2.000  2.000  2.000  2.000
```

Different data sets have different sizes. To convert a helix filter from one data size to another, we could drop the filter into a cube with module cube. Then we could extract it with module unbox specifying any data set size we wish. Instead we use module regrid prepared by Sergey Fomel which does the job without reference to an underlying filter cube. He explains his regrid module thus:

Imagine a filter being cut out of a piece of paper and glued on another paper, which is then rolled to form a helix.

We start by picking a random point (let's call it `rand`) in the cartesian grid and placing the filter so that its center (the leading 1.0) is on top of that point. `rand` should be larger than (or equal to) `center` and smaller than `min (nold, nnew)`, otherwise the filter might stick outside the grid (our piece of paper.) `rand=nold/2` will do (assuming the filter is small), although nothing should change if you replace `nold/2` with a random integer array between `center` and `nold - na`.

The linear coordinate of `rand` is `h0` on the old helix and `h1` on the new helix. Recall that the helix lags `aa%lag` are relative to the center. Therefore, we need to add `h0` to get the absolute helix coordinate (`h`). Likewise, we need to subtract `h1` to return to a relative coordinate system.

Convert filter to different data size.r90

```
module regrid {          # convert a helix filter from one size data to another
use helix
use cartesian
contains
  subroutine regridn( nold, nnew, aa) {
    integer, dimension (:), intent (in) :: nold, nnew  # old and new helix grid
    type( filter)                       :: aa
    integer, dimension( size( nold))    :: ii
    integer                             :: i, h0, h1, h
    call cart2line( nold, nold/2, h0)   # lag of any near middle point on nold
    call cart2line( nnew, nold/2, h1)   # lag                           on nnew
    do i = 1, size( aa%lag) {           # forall given filter coefficients
       h = aa%lag( i) + h0              # what is this?
       call line2cart( nold, h, ii)     #
       call cart2line( nnew,    ii, h)  #
       aa%lag( i) = h - h1              # what is this
    }
  }
}
```

4.6 INVERSE FILTERS AND OTHER FACTORIZATIONS

Mathematics sometimes seems a mundane subject, like when it does the "accounting" for an engineer. Other times it brings unexpected amazing new concepts into our lives. This is the case with the study of causality and spectral factorization. There are many little-known, amazing, fundamental ideas here, some merely named, one worked through to results.

Start with an example. Consider a mechanical object. We can strain it and watch it stress or we can stress it and watch it strain. We feel knowledge of the present and past stress history is all we need to determine the present value of strain. Likewise, the converse, history of strain should tell us the stress. We could say there is a filter that takes us from stress to strain; likewise another filter takes us from strain to stress. What we have here is a pair of filters that are mutually inverse under convolution. In the Fourier domain, one is literally the inverse of the other. What is remarkable is that in the time domain, both are causal. They both vanish before zero lag $\tau = 0$.

Not all causal filters have a causal inverse. The best known name for one that does is "minimum-phase filter." Unfortunately, this name is not suggestive of the fundamental property of interest, "causal with a causal (convolutional) inverse." I could call it CCI. An example of a causal filter without a causal inverse is the unit delay operator —with Z-transforms, the operator Z itself. If you delay something, you can't get it back without seeing into the future, which you are not allowed to do. Mathematically, $1/Z$ cannot be expressed as a polynomial (actually, a convergent infinite series) in positive powers of Z.

Physics books don't tell us where to expect to find transfer functions that are CCI. I think I know why they don't. Any causal filter has a "sharp edge" at zero time lag where it switches from non responsiveness to responsiveness. The sharp edge might cause the spectrum to be large at infinite frequency. If so, the inverse filter is small at infinite frequency. Either way, one of the two filters is unmanageable with Fourier transform theory which (you might have noticed in the mathematical fine print) requires signals (and spectra) to have finite energy which means the function must get real small in that immense space on the t-axis and the ω axis. It is impossible for a function to be small and its inverse be small. These imponderables become manageable in the world of Time Series Analysis (discretized time axis).

4.6.1 Uniqueness and invertability

Interesting questions arise when we are given a spectrum and find ourselves asking how to find a filter that has that spectrum. Is the answer unique? We'll see not. Is there always an answer that is causal? Almost always, yes. Is there always an answer that is causal with a causal inverse (CCI)? Almost always, yes.

Let us have an example. Consider a filter like the familiar time derivative $(1, -1)$ except let us down weight the -1 a tiny bit, say $(1, -\rho)$ where $0 << \rho < 1$. Now the filter $(1, -\rho)$ has a spectrum $(1 - \rho Z)(1 - \rho/Z)$ with autocorrelation coefficients $(-\rho, 1 + \rho^2, -\rho)$ that look a lot like a second derivative, but it is a tiny bit bigger in the middle. Two different waveforms, $(1, -\rho)$ and its time reverse both have the same autocorrelation. In principle, spectral factorization could give us both $(1, -\rho)$ and $(\rho, -1)$ but we always want only the one that is CCI which is the one we get from Kolmogoroff. The bad one is weaker on its first pulse. Its inverse is not causal. Below are two expressions for the filter inverse to $(\rho, -1)$, the first divergent (filter coefficients at infinite lag are infinitely strong), the second convergent but non causal.

$$\frac{1}{\rho - Z} = \frac{1}{\rho}\left(1 + Z/\rho + Z^2/\rho^2 + \cdots\right) \tag{4.16}$$

$$\frac{1}{\rho - Z} = \frac{-1}{Z}\left(1 + \rho/Z + \rho^2/Z^2 + \cdots\right) \tag{4.17}$$

(Please multiply each equation by $\rho - Z$ and see it reduce to $1 = 1$).

We begin with a power spectrum and our goal is to find a CCI filter with that spectrum. If we input to the filter an infinite sequence of random numbers (white noise) we should output something with the original power spectrum.

We easily inverse Fourier transform the square root of the power spectrum getting a symmetrical time function, but we need a function that vanishes before $\tau = 0$. On the

other hand, if we already had a causal filter with the correct spectrum we could manufacture many others. To do so all we need is a family of delay operators to convolve with. A pure delay filter does not change the spectrum of anything. Same for frequency-dependent delay operators. Here is an example of a frequency-dependent delay operator: First convolve with (1,2) and then deconvolve with (2,1). Both these have the same amplitude spectrum so their ratio has a unit amplitude (and nontrivial phase). If you multiply $(1+2Z)/(2+Z)$ by its Fourier conjugate (replace Z by $1/Z$) the resulting spectrum is 1 for all ω.

Anything whose nature is delay is death to CCI. The CCI has its energy as close as possible to $\tau = 0$. More formally, my first book, FGDP, proves that the CCI filter has for all time τ more energy between $t = 0$ and $t = \tau$ than any other filter with the same spectrum.

Spectra can be factorized by an amazingly wide variety of techniques, each of which gives you a different insight into this strange beast. They can be factorized by factoring polynomials, by inserting power series into other power series, by solving least squares problems, by taking logarithms and exponentials in the Fourier domain. I've coded most of them and still find them all somewhat mysterious.

Theorems in Fourier analysis can be interpreted physically in two different ways, one as given, the other with time and frequency reversed. For example, convolution in one domain amounts to multiplication in the other. If we were to express the CCI concept with reversed domains, instead of saying the "energy comes as quick as possible after $\tau = 0$" we would say "the frequency function is as close to $\omega = 0$ as possible." In other words, it is minimally wiggly with time. Most applications of spectral factorization begin with a spectrum, a real, positive function of frequency. I once recognized the opposite case and achieved minor fame by starting with a real, positive function of space, a total **magnetic** field $\sqrt{H_x^2 + H_z^2}$ measured along the x-axis and I reconstructed the magnetic field components H_x and H_z that were minimally wiggly in space (FGDP p.61).

4.6.2 Cholesky decomposition

Conceptually the simplest computational method of spectral factorization might be "Cholesky decomposition." For example, the matrix of (4.15) could have been found by Cholesky factorization of (4.14). The Cholesky algorithm takes a positive-definite matrix $\mathbf{Q}$ and factors it into a triangular matrix times its transpose, say $\mathbf{Q} = \mathbf{T}^* \mathbf{T}$.

It is easy to reinvent the Cholesky factorization algorithm. To do so, simply write all the components of a 3×3 triangular matrix $\mathbf{T}$ and then explicitly multiply these elements times the transpose matrix $\mathbf{T}^*$. You will find that you have everything you need to recursively build the elements of $\mathbf{T}$ from the elements of $\mathbf{Q}$. Likewise for a 4×4 matrix, etc.

The 1×1 case shows that the Cholesky algorithm requires square roots. Matrix elements are not always numbers. Sometimes they are polynomials such as Z-transforms. To avoid square roots there is a variation of the Cholesky method. In this variation, we factor $\mathbf{Q}$ into $\mathbf{Q} = \mathbf{T}^* \mathbf{D} \mathbf{T}$ where $\mathbf{D}$ is a diagonal matrix.

Once a matrix has been factored into upper and lower triangles, solving simultaneous equations is simply a matter of two back substitutions: (We looked at a special case of back substitution with equation (1.22).) For example, we often encounter simultaneous equations

of the form $\mathbf{B}^*\mathbf{B}\mathbf{m} = \mathbf{B}^*\mathbf{d}$. Suppose the positive-definite matrix $\mathbf{B}^*\mathbf{B}$ has been factored into triangle form $\mathbf{T}^*\mathbf{T}\mathbf{m} = \mathbf{B}^*\mathbf{d}$. To find $\mathbf{m}$ we first backsolve $\mathbf{T}^*\mathbf{x} = \mathbf{B}^*\mathbf{d}$ for the vector $\mathbf{x}$. Then we back solve $\mathbf{T}\mathbf{m} = \mathbf{x}$. When $\mathbf{T}$ happens to be a band matrix, then the first back substitution is filtering down a helix and the second is filtering back up it. Polynomial division is a special case of back substitution.

Poisson's equation $\nabla^2\mathbf{p} = -\mathbf{q}$ requires boundary conditions which we can honor when we filter starting from both ends. We cannot simply solve Poisson's equation as an initial-value problem. We could insert the laplace operator into the polynomial division program, but the solution would diverge.

Being a matrix method, the Cholesky method of factorization has a cost proportional to the cube of the size of the matrix. Because our applications are very large and because the Cholesky method does not produce a useful result if we stop part way to completion, we look further. The Cholesky method is a powerful method but it does more than we require. The Cholesky method does not require band matrices, yet these matrices are what we very often find in applications, so we seek methods that take advantage of the special properties of band matrices.

4.6.3 Toeplitz methods

Band matrices are often called Toeplitz matrices. In the subject of Time Series Analysis are found spectral factorization methods that require computations proportional to the dimension of the matrix squared. They can often be terminated early with a reasonable partial result. Two Toeplitz methods, the Levinson method and the Burg method are described in my first textbook, FGDP. Our interest is multidimensional data sets so the matrices of interest are truely huge and the cost of Toeplitz methods is proportional to the square of the matrix size. Thus, before we find Toeplitz methods especially useful, we may need to find ways to take advantage of the sparsity of our filters.

EXERCISES:

1 Observe the matrix (1.4) which corresponds to subroutine `tcai1`. What is the matrix corresponding to `helicon` ?

Chapter 5

Preconditioning

In Chapter 1 we developed adjoints and in Chapter 2 we developed inverse operators. Logically, correct solutions come only through inversion. Real life, however, seems nearly the opposite. This is puzzling but intriguing. It seems an easy path to fame and profit would be to go beyond adjoints by introducing some steps of inversion. It is not that easy. Images contain so many unknowns. Mostly we cannot iterate to completion and need concern ourselves with the rate of convergence. Often necessity will limit us to a handful of iterations where in principle millions or billions are required.

When you fill your car with gasoline, it derives more from an adjoint than an inverse. Industrial seismic data processing relates more to adjoints than to inverses though there is a place for both, of course. It cannot be much different with medical imaging.

First consider cost. For simplicity, consider a data space with N values and a model (or image) space of the same size. The computational cost of applying a dense adjoint operator increases in direct proportion to the number of elements in the matrix, in this case N^2. To achieve the minimum discrepancy between modeled data and observed data (inversion) theoretically requires N iterations raising the cost to N^3.

Consider an image of size $m \times m = N$. Continuing, for simplicity, to assume a dense matrix of relations between model and data, the cost for the adjoint is m^4 whereas the cost for inversion is m^6. We'll consider computational costs for the year 2000, but noticing that costs go as the sixth power of the mesh size, the overall situation will not change much in the foreseeable future. Suppose you give a stiff workout to a powerful machine; you take an hour to invert a 4096×4096 matrix. The solution, a vector of 4096 components could be laid into an image of size $64 \times 64 = 2^6 \times 2^6 = 4096$. Here is what we are looking at for costs:

adjoint cost	$(m \times m)^2$	$(512 \times 512)^2$	$(2^9 2^9)^2$	2^{36}
inverse cost	$(m \times m)^3$	$(64 \times 64)^3$	$(2^6 2^6)^3$	2^{36}

These numbers tell us that for applications with dense operators, the biggest images that we are likely to see coming from inversion methods are 64×64 whereas those from adjoint methods are 512×512. For comparison, your vision is comparable to your computer screen at 1000×1000.

Figure 5.1: Jos greets Andrew, "Welcome back Andrew" from the Peace Corps. At a resolution of 512 × 512, this picture is about the same as the resolution as the paper it is printed on, or the same as your viewing screen, if you have scaled it up to 50% of screen size. VIEW prc/. 512x512

Web http://sep.stanford.edu/sep/jon/family/jos/gifmovie.html holds a movie blinking between Figures 5.1 and 5.2.

This cost analysis is oversimplified in that most applications do not require dense operators. With sparse operators, the cost advantage of adjoints is even more pronounced since for adjoints, the cost savings of operator sparseness translate directly to real cost savings. The situation is less favorable and more muddy for inversion. The reason that Chapter 2 covers iterative methods and neglects exact methods is that in practice iterative methods are not run to their theoretical completion, but they run until we run out of patience. But that leaves hanging the question of what percent of theoretically dictated work is actually necessary. If we struggle to accomplish merely one percent of the theoretically required work, can we hope to achieve anything of value?

Cost is a big part of the story, but the story has many other parts. Inversion, while being the only logical path to the best answer, is a path littered with pitfalls. The first pitfall is that the data is rarely able to determine a complete solution reliably. Generally there are aspects of the image that are not learnable from the data.

When I first realized that practical imaging methods in with wide industrial use amounted merely to the adjoint of forward modeling, I (and others) thought an easy way to achieve fame and fortune would be to introduce the first steps towards inversion along the lines of Chapter 2. Although inversion generally requires a prohibitive number of steps, I felt that moving in the gradient direction, the direction of steepest descent, would move us rapidly in the direction of practical improvements. This turned out to be optimistic. It was too slow. But then I learned about the conjugate gradient method that spectacularly overcomes a well-known speed problem with the method of steepest descent. I came to realize that it was still too slow. I learned this by watching the convergence in Figure 5.8. This led me to the helix method in Chapter 4. Here we'll see how it speeds many applications.

We'll also come to understand why the gradient is such a poor direction both for steepest descent and for conjugate gradients. An indication of our path is found in the contrast

Figure 5.2: Jos greets Andrew, "Welcome back Andrew" again. At a resolution of 64×64 the pixels are clearly visible. From far the pictures are the same. From near, examine their glasses. VIEW prc/. 64x64

between an exact solution and the gradient.

$$\mathbf{m} = (\mathbf{A}^*\mathbf{A})^{-1}\mathbf{A}^*\mathbf{d} \tag{5.1}$$

$$\Delta\mathbf{m} = \mathbf{A}^*\mathbf{d} \tag{5.2}$$

They differ by the factor $(\mathbf{A}^*\mathbf{A})^{-1}$. This factor is sometimes called a spectrum and in some situations it literally is a frequency spectrum. Our updates do not have the spectrum of the thing we are trying to build. No wonder it's slow! Here we'll find for many applications that "preconditioning" with the helix is a better way.

5.1 PRECONDITIONED DATA FITTING

Iterative methods (like conjugate-directions) can sometimes be accelerated by a **change of variables**. The simplest change of variable is called a "trial solution". Formally, we write the solution as

$$\mathbf{m} = \mathbf{S}\mathbf{p} \tag{5.3}$$

where $\mathbf{m}$ is the map we seek, columns of the matrix $\mathbf{S}$ are "shapes" that we like, and coefficients in $\mathbf{p}$ are unknown coefficients to select amounts of the favored shapes. The variables $\mathbf{p}$ are often called the "preconditioned variables". It is not necessary that $\mathbf{S}$ be an invertible matrix, but we'll see later that invert-ability is helpful. Inserting the trial solution $\mathbf{m} = \mathbf{S}\mathbf{p}$ into $\mathbf{0} \approx \mathbf{F}\mathbf{m} - \mathbf{d}$ gives

$$\mathbf{0} \approx \mathbf{F}\mathbf{m} - \mathbf{d} \tag{5.4}$$

$$\mathbf{0} \approx \mathbf{F}\mathbf{S}\mathbf{p} - \mathbf{d} \tag{5.5}$$

We pass the operator $\mathbf{F}\mathbf{S}$ to our iterative solver. After finding the best fitting $\mathbf{p}$, we merely evaluate $\mathbf{m} = \mathbf{S}\mathbf{p}$ to get the solution to the original problem.

We hope this change of variables has saved effort. For each iteration, there is a little more work: Instead of the iterative application of $\mathbf{F}$ and $\mathbf{F}^*$ we have iterative application of $\mathbf{F}\mathbf{S}$ and $\mathbf{S}^*\mathbf{F}^*$.

Our hope is that the number of iterations decreases because we are clever, or because we have been lucky in our choice of $\mathbf{S}$. Hopefully, the extra work of the preconditioner operator $\mathbf{S}$ is not large compared to $\mathbf{F}$. If we should be so lucky that $\mathbf{S} = \mathbf{F}^{-1}$, then we get the solution immediately. Obviously we would try any guess with $\mathbf{S} \approx \mathbf{F}^{-1}$. Where I have known such $\mathbf{S}$ matrices, I have often found that convergence is accelerated, but not by much. Sometimes it is worth using $\mathbf{FS}$ for a while in the beginning, but later it is cheaper and faster to use only $\mathbf{F}$. A practitioner might regard the guess of $\mathbf{S}$ as prior information, like the guess of the initial model $\mathbf{m}_0$.

For a square matrix $\mathbf{S}$, the use of a preconditioner should not change the ultimate solution. Taking $\mathbf{S}$ to be a tall rectangular matrix reduces the number of adjustable parameters, changes the solution, gets it quicker, but lower resolution.

5.1.1 Preconditioner with a starting guess

We often have a starting solution $\mathbf{m}_0$. You might worry that you could not find the starting preconditioned variable $\mathbf{p}_0 = \mathbf{S}^{-1}\mathbf{m}_0$ because you did not know the inverse of $\mathbf{S}$. We solve this problem using a shifted unknown $\tilde{\mathbf{m}}$.

$$
\begin{array}{rcll}
\mathbf{0} & \approx & \mathbf{F}\mathbf{m} - \mathbf{d} & \text{typical regression} \\
\mathbf{0} & \approx & \mathbf{F}(\tilde{\mathbf{m}} + \mathbf{m}_0) - \mathbf{d} & \text{Define } \mathbf{m} = \tilde{\mathbf{m}} + \mathbf{m}_0 \\
\mathbf{0} & \approx & \mathbf{F}\tilde{\mathbf{m}} + \mathbf{F}\mathbf{m}_0 - \mathbf{d} & \\
\mathbf{0} & \approx & \mathbf{F}\tilde{\mathbf{m}} - \tilde{\mathbf{d}} & \text{Defines } \tilde{\mathbf{d}} \\
 & & & \text{Implicitly define } \mathbf{p} \text{ by } \tilde{\mathbf{m}} = \mathbf{S}\mathbf{p}. \\
\mathbf{0} & \approx & \mathbf{F}\mathbf{S}\mathbf{p} - \tilde{\mathbf{d}} & \text{You iterate for } \mathbf{p}. \\
\tilde{\mathbf{m}} & = & \mathbf{S}\mathbf{p} & \text{from your definition} \\
\mathbf{m} & = & \tilde{\mathbf{m}} + \mathbf{m}_0 & \text{Got the answer.}
\end{array}
$$

which solves the problem never needing $\mathbf{S}^{-1}$. Unfortunately, as we will see later, this conclusion is only valid while there is no regularization.

5.1.2 Guessing the preconditioner

We are tasked with coming up with "trial solutions". That's a pretty vague assignment. Some kind of a scaling, smoothing, or shaping transformation $\mathbf{S}$ of some mysterious "preconditioned space" $\mathbf{p}$ should represent the model $\mathbf{m}$ we seek. We begin by investigating how the shaper $\mathbf{S}$ alters the gradient.

$$
\begin{array}{rcll}
\mathbf{m} & = & \mathbf{S}\mathbf{p} & \text{introduces } \mathbf{S}\text{, implicitly defines } \mathbf{p} \\
\Delta\mathbf{m} & = & \mathbf{S}\Delta\mathbf{p} & \text{consequence of the above} \\
\Delta\mathbf{m} & = & \mathbf{F}^*\mathbf{r} & \text{gradient is adjoint upon residual} \\
\mathbf{0} \approx \mathbf{r} & = & \mathbf{F}\mathbf{m} - \mathbf{d} & \text{residual in terms of } \mathbf{m} \\
\mathbf{r} & = & \mathbf{F}(\mathbf{S}\mathbf{p}) - \mathbf{d} & \text{residual in terms of } \mathbf{p} \\
\mathbf{0} \approx \mathbf{r} & = & (\mathbf{F}\mathbf{S})\mathbf{p} - \mathbf{d} & \text{reordering calculation} \\
\Delta\mathbf{p} & = & (\mathbf{F}\mathbf{S})^*\mathbf{r} & \text{gradient is adjoint upon residual} \\
\Delta\mathbf{p} & = & \mathbf{S}^*\mathbf{F}^*\mathbf{r} & \text{reordering} \\
\Delta\mathbf{m} & = & (\mathbf{S}\mathbf{S}^*)\mathbf{F}^*\mathbf{r} & \text{recalling } \Delta\mathbf{m} = \mathbf{S}\Delta\mathbf{p}
\end{array}
$$

We may compare the gradient $\Delta\mathbf{m}$ with and without preconditioning.

$$\begin{aligned} \Delta\mathbf{m} &= \mathbf{F}^*\mathbf{r} && \text{original} \\ \Delta\mathbf{m} &= (\mathbf{S}\mathbf{S}^*)\mathbf{F}^*\mathbf{r} && \text{with preconditioning transformation} \end{aligned}$$

When the first vanishes, the second will. When the second vanishes, the first will provided $(\mathbf{S}\mathbf{S}^*)$ is a nonsingular matrix. As our choice of $\mathbf{S}$ is quite arbitrary, it is marvelous the freedom we have to monkey with the gradient.

Remember that $\mathbf{r}$ starts off being $-\mathbf{d}$. Compare the $(\mathbf{S}\mathbf{S}^*)$ scaled gradient to the analytic solution.

$$\begin{aligned} \Delta\mathbf{m} &= (\mathbf{S}\mathbf{S}^*)\ \mathbf{F}^*\mathbf{r} && \text{modified gradient} \\ \mathbf{m} &= (\mathbf{F}^*\mathbf{F})^{-1}\mathbf{F}^*\mathbf{d} && \text{analytic solution} \end{aligned}$$

Mathematically we see it would be delightful if $(\mathbf{S}\mathbf{S}^*)$ were something like $(\mathbf{F}^*\mathbf{F})^{-1}$ but we rarely have ideas how to accomplish that. We do however, have some understanding of the world of images, and understand where on the image we would like iterations to concentrate first, and what spatial frequencies are more relevant than others. If we cannot go all the way, as we cannot in giant imaging problems, it is important to make the important steps early.

5.2 PRECONDITIONING THE REGULARIZATION

The basic formulation of a geophysical estimation problem consists of setting up *two* goals, one for data fitting, and the other for model shaping. With two goals, preconditioning is somewhat different. The two goals may be written as:

$$\mathbf{0} \approx \mathbf{F}\mathbf{m} - \mathbf{d} \tag{5.6}$$

$$\mathbf{0} \approx \mathbf{A}\mathbf{m} \tag{5.7}$$

which defines two residuals, a so-called "data residual" and a "model residual" that are usually minimized by conjugate-direction, least-squares methods.

To fix ideas, let us examine a toy example. The data and the first three rows of the matrix below are random numbers truncated to integers. The model roughening operator $\mathbf{A}$ is a first differencing operator times 100.

d(m)	F(m,n)										iter	Sum(|grad|)
-100.	62.	18.	2.	75.	99.	45.	93.	-41.	-15.	80.	1	69262.0000
-83.	31.	80.	92.	-67.	72.	81.	-41.	87.	-17.	-38.	2	19012.8203
20.	3.	-21.	58.	38.	9.	18.	-81.	22.	-14.	20.	3	10639.0791
0.	100.	-100.	0.	0.	0.	0.	0.	0.	0.	0.	4	4578.7988
0.	0.	100.	-100.	0.	0.	0.	0.	0.	0.	0.	5	2332.3352
0.	0.	0.	100.	-100.	0.	0.	0.	0.	0.	0.	6	1676.6978
0.	0.	0.	0.	100.	-100.	0.	0.	0.	0.	0.	7	622.7415
0.	0.	0.	0.	0.	100.	-100.	0.	0.	0.	0.	8	454.1242
0.	0.	0.	0.	0.	0.	100.	-100.	0.	0.	0.	9	290.6053
0.	0.	0.	0.	0.	0.	0.	100.	-100.	0.	0.	10	216.0749
0.	0.	0.	0.	0.	0.	0.	0.	100.	-100.	0.	11	1.0488
0.	0.	0.	0.	0.	0.	0.	0.	0.	100.	-100.	12	0.0061
0.	0.	0.	0.	0.	0.	0.	0.	0.	0.	100.	13	0.0000

The rightmost column shows the sum of the absolute values of the gradient. Notice at the tenth iteration, the gradient suddenly plunges. Since there are ten unknowns and the matrix is obviously full-rank, conjugate-gradient theory tells us to expect the exact solution at the tenth iteration. This is the first miracle of conjugate gradients. Failure to achieve a precisely zero gradient at the 11th step is a precision issue that could be addressed with double precision arithmetic. The residual itself (not shown) does not approach zero. Thirteen linear equations defeat the ten adjustable coefficients.

5.2.1 The second miracle of conjugate gradients

The second miracle of conjugate gradients is exhibited below. The data and data fitting matrix are the same, but the model damping is simplified.

d(m)	F(m,n)										iter	Sum(|grad|)
-100.	62.	18.	2.	75.	99.	45.	93.	-41.	-15.	80.	1	69262.0000
-83.	31.	80.	92.	-67.	72.	81.	-41.	87.	-17.	-38.	2	5486.2095
20.	3.	-21.	58.	38.	9.	18.	-81.	22.	-14.	20.	3	2755.6702
0.	100.	0.	0.	0.	0.	0.	0.	0.	0.	0.	4	0.0012
0.	0.	100.	0.	0.	0.	0.	0.	0.	0.	0.	5	0.0011
0.	0.	0.	100.	0.	0.	0.	0.	0.	0.	0.	6	0.0006
0.	0.	0.	0.	100.	0.	0.	0.	0.	0.	0.	7	0.0006
0.	0.	0.	0.	0.	100.	0.	0.	0.	0.	0.	8	0.0005
0.	0.	0.	0.	0.	0.	100.	0.	0.	0.	0.	9	0.0005
0.	0.	0.	0.	0.	0.	0.	100.	0.	0.	0.	10	0.0012
0.	0.	0.	0.	0.	0.	0.	0.	100.	0.	0.	11	0.0033
0.	0.	0.	0.	0.	0.	0.	0.	0.	100.	0.	12	0.0033
0.	0.	0.	0.	0.	0.	0.	0.	0.	0.	100.	13	0.0000

Even though the matrix is full-rank, we see the residual drop about 6 decimal places after the third iteration! This convergence behavior is well known in the computational mathematics literature. Despite its practical importance, it doesn't seem to have a name or identified discoverer. So I call it the "second miracle."

Practitioners usually don't like the identity operator for model-shaping. Generally they prefer to penalize wiggliness. For practitioners, the lesson of the second miracle of conjugate gradients is that we have a choice of many iterations for learning to transform independent

variables so that the regularization operator becomes an identity matrix. Basically, such a transformation reduces the iteration count from something about the size of the model space to something about the size of the data space. Such a transformation is called preconditioning.

More generally, the model goal $\mathbf{0} \approx \mathbf{Am}$ introduces a roughening operator like a gradient, a Laplacian, or in chapter 7 a Prediction-Error Filter (PEF). Thus the model goal is usually a filter, unlike the data-fitting goal which involves all manner of geometry and physics. When the model goal is a filter its inverse is also a filter. Of course this includes multidimensional filters with a helix.

The preconditioning transformation $\mathbf{m} = \mathbf{Sp}$ gives us

$$\begin{aligned} \mathbf{0} &\approx \mathbf{FSp} - \mathbf{d} \\ \mathbf{0} &\approx \mathbf{ASp} \end{aligned} \tag{5.8}$$

The operator $\mathbf{A}$ is a roughener while $\mathbf{S}$ is a smoother. The choices of both $\mathbf{A}$ and $\mathbf{S}$ are somewhat subjective. This suggests that we eliminate $\mathbf{A}$ altogether by *defining* it to be proportional to the inverse of $\mathbf{S}$, thus $\mathbf{AS} = \mathbf{I}$. The fitting goals become

$$\begin{aligned} \mathbf{0} &\approx \mathbf{FSp} - \mathbf{d} \\ \mathbf{0} &\approx \epsilon\, \mathbf{p} \end{aligned} \tag{5.9}$$

which enables us to benefit from the "second miracle". After finding $\mathbf{p}$, we obtain the final model with $\mathbf{m} = \mathbf{Sp}$.

The solution $\mathbf{m}$ is likely to come out smooth because we typically over-sample axes of physical quantities. We typically penalize roughness in it by our choice of a regularizaton operator. That means the precondioning variable $\mathbf{p}$ typically has a wider frequency bandwidth than $\mathbf{p}$. In chapter 7 we will see how to make the spectrum of $\mathbf{p}$ come out white (tending to flat spectrum).

5.2.2 Importance of scaling

Another simple toy example shows us the importance of scaling. We use the same example as above except but we make the diagonal penalty function vary slowly with location.

```
 d(m)      F(m,n)                                                    iter   Sum(|grad|)

-100.      62.  16.   2.  53.  59.  22.  37. -12.  -3.   8.      1  42484.1016
 -83.      31.  72.  74. -47.  43.  40. -16.  26.  -3.  -4.      2   8388.0635
  20.       3. -19.  46.  27.   5.   9. -32.   7.  -3.   2.      3   4379.3032
   0.     100.   0.   0.   0.   0.   0.   0.   0.   0.   0.      4   1764.9844
   0.       0.  90.   0.   0.   0.   0.   0.   0.   0.   0.      5    868.9418
   0.       0.   0.  80.   0.   0.   0.   0.   0.   0.   0.      6    502.5179
   0.       0.   0.   0.  70.   0.   0.   0.   0.   0.   0.      7    450.0512
   0.       0.   0.   0.   0.  60.   0.   0.   0.   0.   0.      8    185.2923
   0.       0.   0.   0.   0.   0.  50.   0.   0.   0.   0.      9    247.1021
   0.       0.   0.   0.   0.   0.   0.  40.   0.   0.   0.     10    338.7060
   0.       0.   0.   0.   0.   0.   0.   0.  30.   0.   0.     11    119.5686
   0.       0.   0.   0.   0.   0.   0.   0.   0.  20.   0.     12     34.3372
   0.       0.   0.   0.   0.   0.   0.   0.   0.   0.  10.     13      0.0000
```

We observe that solving the same problem for the scaled variables has required a severe increase in the number of iterations required to get the solution. We lost the benefit of the second CG miracle. Even the rapid convergence predicted for the 10-th iteration is delayed until the 12-th.

Another curious fact may be noted here. The gradient does not decrease monotonically. It is known theoretically that the residual does decrease monotonically, but the gradient need not. I did not show the norm of the residual, because I wanted to display a function that vanishes at convergence, and the residual does not.

5.3 YOU BETTER MAKE YOUR RESIDUALS IID!

In the statistical literature is a concept that repeatedly arises, the idea that some statistical variables are IID, namely Independent, Identically Distributed. In practice we'll see many random looking variables, some much closer than others to IID. Theoretically, the ID part of IID means the random variables come from Identical probability Density functions. In practice, the ID part mostly means the variables have the same variance. The "I" before the ID means that the variables are statistically Independent of one another. Neighboring values should not be positively correlated, meaning low frequencies are present. In the subject area of this book, signals, images, and earth volumes, the "I" before the ID means that our residual spaces are white – have all frequencies present in roughly equal amounts. In other words the "I" means the statistical variables have no significant correlation in time or space. Chapter 7 gives a method of finding a filter as a model styler (regularizer) that accomplishes this goal. IID random variables have fairly uniform variance in both physical space and in Fourier space.

> IID random variables have uniform variance in both physical space and Fourier space.

In a geophysical project it is important the residual between observed data and modeled data is not far from IID. To raw residuals we should apply weights and filters to get IID residuals. We minimize sums of squares of residuals. If any residuals are small, their squares are tiny, so such regression equations are effectively ignored. We would hardly ever want that. Consider echo seismograms. They get weak at late time. So even with a bad fit the difference between real and theoretical seismograms is necessarily weak at late times. We don't want the data at late times to be ignored. So we boost up the residual there. We choose $\mathbf{W}$ to be a diagonal matrix that boosts late times in the regression $\mathbf{0} \approx \mathbf{r} = \mathbf{W}(\mathbf{Fm} - \mathbf{d})$.

An example with too much low (spatial) frequency in a residual might arise in a topographic study. It is not unusual for the topographic wavelength to exceed the survey size. Here we should choose $\mathbf{W}$ to be a filter to boost up the higher frequencies. Perhaps $\mathbf{W}$ should contain a derivative or a Laplacian. If you set up and solve a data modeling problem and then find $\mathbf{r}$ is not IID, you should consider changing your $\mathbf{W}$. Chapter 7 coming up provides a systematic approach to whitening residuals.

Now let us include regularization $\mathbf{0} \approx \mathbf{Am}$ and a preconditioning variable $\mathbf{p}$. We have our data fitting goal and our model styling goal, the first with a residual $\mathbf{r}_d$ in data space, the second with a residual $\mathbf{r}_m$ in model space. We have had to choose a regularization

operator $\mathbf{A} = \mathbf{S}^{-1}$ and a scaling factor ϵ.

$$0 \approx \mathbf{r}_d = \mathbf{W}(\mathbf{FSp} - \mathbf{d}) = \tilde{\mathbf{F}}\mathbf{Sp} - \tilde{\mathbf{d}} \quad (5.10)$$

$$0 \approx \mathbf{r}_m = \epsilon\, \mathbf{p} \quad (5.11)$$

This system of two regressions could be packed into one; the two residual vectors stacked on top of each other, likewise the operators $\mathbf{F}$ and $\epsilon\mathbf{I}$. The IID notion seems to apply to this unified system. That gives us a clue how we should have chosen the regularization operator $\mathbf{A}$. Not only should $\mathbf{r}_d$ be IID, but also should $\mathbf{r}_m$. But within a scale ϵ, $\mathbf{r}_m = \mathbf{p}$. Thus the preconditioning variable is not simply something to speed computational convergence. It is a variable that should be IID. If it is not coming out that way, we should consider changing $\mathbf{A}$. Chapter 7 addresses the task of choosing an $\mathbf{A}$ so that $\mathbf{r}_m$ comes out IID.

> We should choose a weighting function (and/or operator) $\mathbf{W}$ so data residuals are IID. We should also choose our regularization operator $\mathbf{A} = \mathbf{S}^{-1}$ so the preconditioning variable $\mathbf{p}$ comes out IID.

5.3.1 Choice of a unitless epsilon

The parameter epsilon ϵ strikes the balance between our data-fitting goal and our model-styling goal. These two regression systems typically have differing physical units, hence the numerical value of ϵ is accidental, for example comparing milliseconds to meters.

$$\mathbf{0} \approx \mathbf{r}_d = \mathbf{W}(\mathbf{FSp} - \mathbf{d}) \quad (5.12)$$

$$\mathbf{0} \approx \mathbf{r}_m = \epsilon\, \mathbf{p} \quad (5.13)$$

The numerical value of ϵ is meaningless before we learn to express the idea in a unitless (dimensionless) manner. Without pretending we are doing physics, let us use some of the language of thermodynamics, a physical field that does deal with equilibria and random fluctuations. Define an energy ratio u and a volume ratio v that can be used to bring ϵ to unitless form. Naturally, the square roots arise because we will be minimizing quadratic functions of residuals.

$$u = \text{energy ratio} = \sqrt{\frac{\mathbf{r}_d \cdot \mathbf{r}_d}{\mathbf{p} \cdot \mathbf{p}}}$$

$$v = \text{volume ratio} = \sqrt{\frac{n_{r_d}}{n_p}}$$

Can we really think of "volume" as related to the number n_p of components in the model space? Perhaps. Likewise the data space? Less likely. And is the energy measure really an appropriate one? Maybe. What is the goal of these speculative thoughts? The goal is to give you a starting numerical value for ϵ, say $\epsilon = 1$. Your final guide is your own experimental experience. Try either one of these:

$$\mathbf{0} \approx \mathbf{r}_m = \epsilon_{\text{extrinsic}}\, u\, \mathbf{p} \quad (5.14)$$

$$\mathbf{0} \approx \mathbf{r}_m = \epsilon_{\text{intrinsic}}\, (u/v)\, \mathbf{p} \quad (5.15)$$

5.4 THE PRECONDITIONED SOLVER

Summing up the ideas above, we start from fitting goals

$$\begin{aligned} \mathbf{0} &\approx \mathbf{Fm} - \mathbf{d} \\ \mathbf{0} &\approx \mathbf{Am} \end{aligned} \tag{5.16}$$

and we change variables from $\mathbf{m}$ to $\mathbf{p}$ using $\mathbf{m} = \mathbf{A}^{-1}\mathbf{p}$

$$\begin{aligned} \mathbf{0} &\approx \mathbf{Fm} - \mathbf{d} = \mathbf{FA}^{-1}\ \mathbf{p} - \mathbf{d} \\ \mathbf{0} &\approx \mathbf{Am} = \mathbf{I}\ \mathbf{p} \end{aligned} \tag{5.17}$$

Preconditioning means iteratively fitting by adjusting the $\mathbf{p}$ variables and then finding the model by using $\mathbf{m} = \mathbf{A}^{-1}\mathbf{p}$. You'll notice the code below allows for common additional features, a weighting function on the data residuals, allows for a starting $\mathbf{p}_0$, allows for masking constraints $\mathbf{J}$ on $\mathbf{p}$, and allows for scaling the regularization by an ϵ.

A new reusable preconditioned solver is the module `solver-prc`. Likewise the modeling operator $\mathbf{F}$ is called `Fop` and the smoothing operator $\mathbf{A}^{-1}$ is called `Sop`. Details of the code are only slightly different from the regularized solver `solver-reg`.

Preconditioned solver.r90

```
module solver_prc_mod{                                  # 0 = W (F S J p - d)
  use chain0_mod + solver_report_mod                    # 0 =       I   p
  logical, parameter, private  :: AJ = .true., FW = .false.
  logical, parameter, private  :: AD = .true., ZP = .false.
contains
  subroutine solver_prc( m,d, Fop, Sop, stepper, nSop, niter,eps &
  ,            Wop,Jop,p0,rm0,err,resd,resm,mmov,rmov,verb) {
    optional :: Wop,Jop,p0,rm0,err,resd,resm,mmov,rmov,verb
    interface { #------------------------------ begin definitions ----------
       integer function Fop(adj,add,m,d){real::m(:),d(:);logical::adj,add}
       integer function Sop(adj,add,m,d){real::m(:),d(:);logical::adj,add}
       integer function Wop(adj,add,m,d){real::m(:),d(:);logical::adj,add}
       integer function Jop(adj,add,m,d){real::m(:),d(:);logical::adj,add}
       integer function stepper(first,m,dm,r,dr) {
         real, dimension(:)  ::        m,dm,r,dr
         logical             :: first             }
    }
    real, dimension(:),     intent(in)          :: d, p0,rm0
    integer,                intent(in)          :: niter, nSop
    logical,                intent(in)          :: verb
    real,                   intent(in)          :: eps
    real, dimension(:),     intent(out)         :: m,err, resd,resm
    real, dimension(:,:),   intent(out)         ::          rmov,mmov
    real, dimension(size(m))                    :: p , dm
    real, dimension(size(d)+nSop), target       :: r, dr, tt
    real, dimension(:), pointer                 :: rd, drd, td
    real, dimension(:), pointer                 :: rm, drm, tm
    integer                                     :: iter, stat
    logical                                     :: first
    rd  => r (1:size(d));  rm => r(1+size(d):)
    drd => dr(1:size(d));  drm => dr(1+size(d):)
    td  => tt(1:size(d));  tm => tt(1+size(d):)
    if(present(Wop)) stat=Wop(FW,ZP,-d,rd) # begin initialization ----------
    else rd = -d                                                  #Rd  = -W    d
```

```
    rm = 0.; if(present(rm0)) rm=rm0                                    #Rm  =      Rm0
    if(present( p0)){ p=p0                                              # p  =       p0
      if(present( Wop)) call chain0(Wop,Fop,Sop,FW,AD,p,rd,tm,td)
      else              call chain0(    Fop,Sop,FW,AD,p,rd,tm )#Rd += WFS  p0
      rm = rm + eps*p                                                   #Rm +=  e I  p0
    } else p=0
    first = .true.; #------------------------------ begin iterations ----------------
    do iter = 1,niter {
       if(present(Wop)) call chain0(Wop,Fop,Sop,AJ,ZP,dm,rd,tm,td)
       else             call chain0(    Fop,Sop,AJ,ZP,dm,rd,tm ) #dm  = (WFS)'Rd
       dm = dm + eps*rm                                                 #dm +=   e I 'Rm
       if(present(Jop)){ tm=dm;          stat=Jop(FW,ZP,tm,dm    )}#dm  =      J dm
       if(present(Wop)) call chain0(Wop,Fop,Sop,FW,ZP,dm,drd,tm,td)
       else             call chain0(    Fop,Sop,FW,ZP,dm,drd,tm) #dRd = (WFS) dm
       drm   = eps*dm                                                   #dRm =   e I dm
       stat = stepper(first, p,dm, r,dr)                                #m+=dm; R+=dR
       if(stat ==1) exit # got stuck descending
       stat = Sop(FW,ZP,p,m)                                             #m  = S p
       if(present( mmov)) mmov(:,iter) =  m(:size(mmov,1)) # report ------
       if(present( rmov)) rmov(:,iter) = r(:size(rmov,1))
       if(present( err )) err(  iter) = dot_product(rd,rd)
       if(present( verb)){ if(verb) call solver_report(iter,m,dm,rd,rm)}
       first=.false.
    }
    if(present( resd)) resd = rd
    if(present( resm)) resm = rm(:size(resm))
  }
}
```

5.5 OPPORTUNITIES FOR SMART DIRECTIONS

Recall the fitting goals (5.10) with weights $\mathbf{W}$ being absorbed into the operator $\mathbf{F}$ and the data $\mathbf{d}$.

$$\begin{array}{rcccccccc} \mathbf{0} & \approx & \mathbf{r}_d & = & \mathbf{Fm} & - & \mathbf{d} & = & \mathbf{FA}^{-1}\ \mathbf{p} - \mathbf{d} \\ \mathbf{0} & \approx & \mathbf{r}_m & = & \mathbf{Am} & & & = & \mathbf{I}\ \ \mathbf{p} \end{array} \tag{5.18}$$

Without preconditioning we have the search direction

$$\Delta\mathbf{m}_{\text{bad}} \quad = \quad \begin{bmatrix} \mathbf{F}^* & \mathbf{A}^* \end{bmatrix} \begin{bmatrix} \mathbf{r}_d \\ \mathbf{r}_m \end{bmatrix} \tag{5.19}$$

and with preconditioning we have the search direction

$$\Delta\mathbf{p}_{\text{good}} \quad = \quad \begin{bmatrix} (\mathbf{FA}^{-1})^* & \mathbf{I} \end{bmatrix} \begin{bmatrix} \mathbf{r}_d \\ \mathbf{r}_m \end{bmatrix} \tag{5.20}$$

The essential feature of preconditioning is not that we perform the iterative optimization in terms of the variable $\mathbf{p}$. The essential feature is that we use a search direction that is a gradient with respect to $\mathbf{p}^*$ not $\mathbf{m}^*$. Using $\mathbf{Am} = \mathbf{p}$ we have $\mathbf{A}\Delta\mathbf{m} = \Delta\mathbf{p}$. This enables us to define a good search direction in $\mathbf{m}$ space.

$$\Delta\mathbf{m}_{\text{good}} \quad = \quad \mathbf{A}^{-1}\Delta\mathbf{p}_{\text{good}} \quad = \quad \mathbf{A}^{-1}(\mathbf{A}^{-1})^*\mathbf{F}^*\mathbf{r}_d + \mathbf{A}^{-1}\mathbf{r}_m \tag{5.21}$$

Define the gradient by $\mathbf{g} = \mathbf{F}^* \mathbf{r}_d$ and notice that $\mathbf{r}_m = \mathbf{p}$.

$$\Delta \mathbf{m}_{\text{good}} \quad = \quad \mathbf{A}^{-1}(\mathbf{A}^{-1})^* \, \mathbf{g} + \mathbf{m} \tag{5.22}$$

The search direction (5.22) shows a positive-definite operator scaling the gradient. Each component of any gradient vector is independent of each other. All independently point (negatively) to a direction for descent. Obviously, each can be scaled by any positive number. Now we have found that we can also scale a gradient vector by a positive definite matrix and we can still expect the conjugate-direction algorithm to descend, as always, to the "exact" answer in a finite number of steps. This is because modifying the search direction with $\mathbf{A}^{-1}(\mathbf{A}^{-1})^*$ is equivalent to solving a conjugate-gradient problem in $\mathbf{p}$. We'll see in Chapter 7, that our specifying $\mathbf{A}^{-1}(\mathbf{A}^{-1})^*$ amounts to us specifying a prior expectation of the spectrum of the model $\mathbf{m}$.

5.5.1 The meaning of the preconditioning variable p

To accelerate convergence of iterative methods we often change variables. The model-styling regression $\mathbf{0} \approx \epsilon \mathbf{A}\mathbf{m}$ is changed to $\mathbf{0} \approx \epsilon \mathbf{p}$. Experience shows, however, that the variable $\mathbf{p}$ is often more interesting to look at than the model $\mathbf{m}$. Why should a new variable introduced for computational convenience turn out to have more interpretive value? There is a little theory underlying this. Begin from

$$\mathbf{0} \quad \approx \quad \mathbf{W}(\mathbf{F}\mathbf{m} - \mathbf{d}) \tag{5.23}$$

$$\mathbf{0} \quad \approx \quad \epsilon \, \mathbf{A}\mathbf{m} \tag{5.24}$$

Introduce the preconditioning variable $\mathbf{p}$.

$$\mathbf{0} \quad \approx \quad \mathbf{W}(\mathbf{F}\mathbf{A}^{-1}\mathbf{p} - \mathbf{d}) \tag{5.25}$$

$$\mathbf{0} \quad \approx \quad \epsilon \, \mathbf{p} \tag{5.26}$$

Rewrite this as a single regression

$$\mathbf{0} \quad \approx \quad \begin{bmatrix} \mathbf{r}_d \\ \mathbf{r}_m \end{bmatrix} \quad = \quad \begin{bmatrix} \mathbf{W}\mathbf{F}\mathbf{A}^{-1} \\ \epsilon \, \mathbf{I} \end{bmatrix} \mathbf{p} \quad - \quad \begin{bmatrix} \mathbf{W}\mathbf{d} \\ \mathbf{0} \end{bmatrix} \tag{5.27}$$

The gradient vanishes at the best solution. To get the gradient we put the residual into the adjoint operator. Thus we put the residuals (column vector) in (5.27) into the transpose of the operator in (5.27), the row $((\mathbf{W}\mathbf{F}\mathbf{A}^{-1})^*, \epsilon \mathbf{I})$. Finally replace the $\approx$ by $=$. Thus

$$\begin{aligned} \mathbf{0} \quad &= \quad (\mathbf{W}\mathbf{F}\mathbf{A}^{-1})^* \, \mathbf{r}_d + \epsilon \, \mathbf{r}_m \\ \mathbf{0} \quad &= \quad (\mathbf{W}\mathbf{F}\mathbf{A}^{-1})^* \, \mathbf{r}_d + \epsilon^2 \, \mathbf{p} \end{aligned} \tag{5.28}$$

The two terms in Equation (5.28) are identical but oppositely signed. These terms represent images in model space. This image represents the fight between the data space residual and the model space residual. You really do want to plot this image. It shows the battle of (1) the model wanted by the data against (2) our preconceived statistical model expressed by our model styling goal. That's why the preconditioned variable $\mathbf{p}$ is interesting to inspect and interpret. It is not simply a computational convenience. It is telling you what you have learned from data (that someone has recorded at great expense!).

The preconditioning variable $\mathbf{p}$ is not simply a computational convenience. This model-space image $\mathbf{p}$ tells us where our data contradicts our prior model. Admire it! Make a movie of it evolving with iteration.

If I were young and energetic like you I would write a new basic tool for optimization. Instead of scanning only the space of the gradient and previous step, it would scan also over the "smart" direction. This should offer the benefit of preconditioning the regularization at early iterations while offering more assured fitting data at late iterations. The improved module for `cgstep` would need to solve a 3×3 matrix. I'd also be looking for ways to make assure all $\Delta\mathbf{m}$ directions were scaled to have the prior model spectrum and prior energy function of space.

5.5.2 Need for an invertible preconditioner

It is important to use regularization to solve many examples. It is important to precondition because in practice computer power is often a limiting factor. It is important to be able to begin from a nonzero starting solution because in nonlinear problems then we must restart from the result of an earlier solution. Putting all three requirements together leads to a little problem. It turns out the three together lead us to needing a preconditioning transformation that is invertible. Let us see why this is so.

$$\begin{aligned} \mathbf{0} &\approx \mathbf{Fm} - \mathbf{d} \\ \mathbf{0} &\approx \mathbf{Am} \end{aligned} \tag{5.29}$$

First we change variables from $\mathbf{m}$ to $\mathbf{u} = \mathbf{m} - \mathbf{m}_0$. Clearly $\mathbf{u}$ starts from $\mathbf{u}_0 = 0$, and $\mathbf{m} = \mathbf{u} + \mathbf{m}_0$. Then our regression pair becomes

$$\begin{aligned} \mathbf{0} &\approx \mathbf{Fu} + (\mathbf{Fm}_0 - \mathbf{d}) \\ \mathbf{0} &\approx \mathbf{Au} + \mathbf{Am}_0 \end{aligned} \tag{5.30}$$

This result differs from the original regression in only two minor ways, (1) revised data, and (2) a little more general form of the regularization, the extra term $\mathbf{Am}_0$.

Now let us introduce preconditioning. From the regularization we see this introduces the preconditioning variable $\mathbf{p} = \mathbf{Au}$. Our regression pair becomes:

$$\begin{aligned} \mathbf{0} &\approx \mathbf{FA}^{-1}\mathbf{p} + (\mathbf{Fm}_0 - \mathbf{d}) \\ \mathbf{0} &\approx \mathbf{p} + \mathbf{Am}_0 \end{aligned} \tag{5.31}$$

Here is the problem: Now we require both $\mathbf{A}$ and $\mathbf{A}^{-1}$ operators. In 2- and 3-dimensional spaces we don't know very many operators with an easy inverse. Indeed, that is why I found myself pushed to come up with the helix methodology of Chapter 4 – because it provides invertible operators for smoothing and roughening.

5.6 INTERVAL VELOCITY

A bread-and-butter problem in seismology is building the velocity as a function of depth (or vertical travel time) starting from certain measurements. The measurements are described

elsewhere (BEI for example). They amount to measuring the integral of the velocity squared from the surface down to the reflector. It is known as the RMS (root-mean-square) velocity. Although good quality echoes may arrive often, they rarely arrive continuously for all depths. Good information is interspersed unpredictably with poor information. Luckily we can also estimate the data quality by the "coherency" or the "stack energy". In summary, what we get from observations and preprocessing are two functions of travel-time depth: (1) the integrated (from the surface) squared velocity, and (2) a measure of the quality of the integrated velocity measurement. Some definitions:

d is a data vector whose components range over the vertical traveltime depth τ and whose component values contain the scaled RMS velocity squared $\tau v_{\text{RMS}}^2/\Delta\tau$ where $\tau/\Delta\tau$ is the index on the time axis.

W is a diagonal matrix along which we lay the given measure of data quality. We will use it as a weighting function.

C is the matrix of causal integration, a lower triangular matrix of ones.

D is the matrix of causal differentiation, namely, $\mathbf{D} = \mathbf{C}^{-1}$.

u is a vector whose components range over the vertical traveltime depth τ and whose component values contain the interval velocity squared v_{interval}^2.

From these definitions, under the assumption of a stratified earth with horizontal reflectors (and no multiple reflections), the theoretical (squared) interval velocities enable us to define the theoretical (squared) RMS velocities by

$$\mathbf{Cu} \quad = \quad \mathbf{d} \tag{5.32}$$

In other words, any component of $\mathbf{d}_i$ measures the integral of a material property from the earth surface to the depth of i. We wish to find the material property everywhere. That will be **u**. If we integrate it from the surface downward with causal integration **C** we should get the measurements **d**.

With imperfect data, our data fitting goal is to minimize the residual

$$\mathbf{0} \quad \approx \quad \mathbf{W}\,[\mathbf{Cu} - \mathbf{d}] \tag{5.33}$$

where **W** is some weighting function we will need to choose. To find the interval velocity where there is no data (where the stack power theoretically vanishes) we have the "model damping" goal to minimize the wiggliness **p** of the squared interval velocity **u**.

$$\mathbf{0} \quad \approx \quad \mathbf{Du} \quad = \quad \mathbf{p} \tag{5.34}$$

We precondition these two goals by changing the optimization variable from interval velocity squared **u** to its wiggliness **p**. Substituting $\mathbf{u} = \mathbf{Cp}$ gives the two goals expressed as a function of wiggliness **p**.

$$\mathbf{0} \quad \approx \quad \mathbf{W}\left[\mathbf{C}^2\mathbf{p} - \mathbf{d}\right] \tag{5.35}$$

$$\mathbf{0} \quad \approx \quad \epsilon\,\mathbf{p} \tag{5.36}$$

5.6.1 Balancing good data with bad

Choosing the size of ϵ chooses the stiffness of the curve that connects regions of good data. Our first test cases gave solutions we interpreted to be too stiff at early times and too flexible at later times. This suggested we weaken ϵ at early times and strengthen it later. Since we wanted to keep ϵ constant with time, so we strengthened $\mathbf{W}$ at early times and weakened it at later times as you see in the program below.

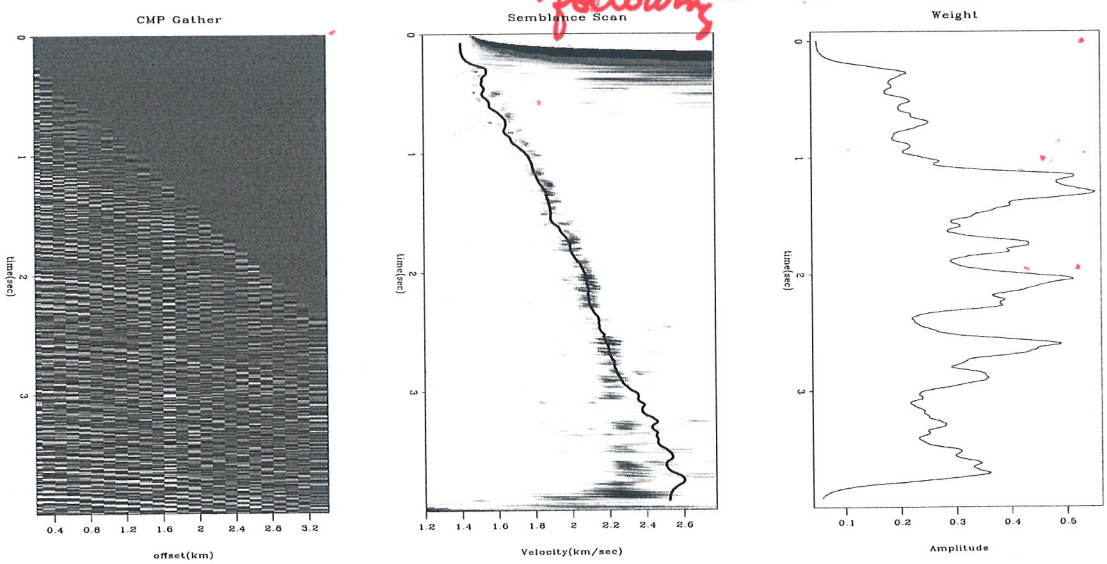

Figure 5.3: Raw CMP gather (left), Semblance scan (middle), and semblance value used for weighting function (right). VIEW prc/. clapp

Converting RMS to interval velocity.r90

```
module vrms2int_mod {                  # Transform from RMS to interval velocity
  use causint
  use weight
  use mask1
  use cgstep_mod
  use solver_prc_mod
contains
  subroutine vrms2int( niter, eps, weight, vrms, vint) {
    integer,                intent( in)      :: niter     # iterations
    real,                   intent( in)      :: eps       # scaling parameter
    real, dimension(:),     intent( in out)  :: vrms      # RMS velocity
    real, dimension(:),     intent( out)     :: vint      # interval velocity
    real, dimension(:),     pointer          :: weight    # data weighting
    integer                                  :: st,it,nt
    logical, dimension( size( vint))         :: mask
    logical, dimension(:),  pointer          :: msk
    real,    dimension( size( vrms))         :: dat ,wt
    real, dimension(:),     pointer          :: wght
    nt = size( vrms)
    do it= 1, nt {
       dat( it) = vrms( it) * vrms( it) * it
       wt( it) = weight( it)*(1./it)              # decrease weight with time
       }
```

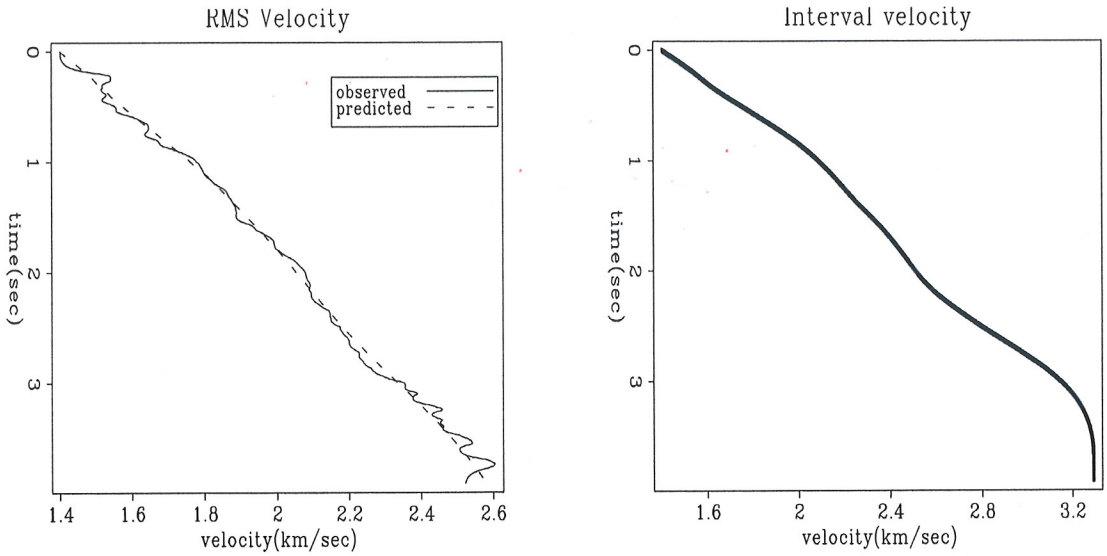

Figure 5.4: Observed RMS velocity and that predicted by a stiff model with $\epsilon = 4$. (Clapp) VIEW prc/. stiff

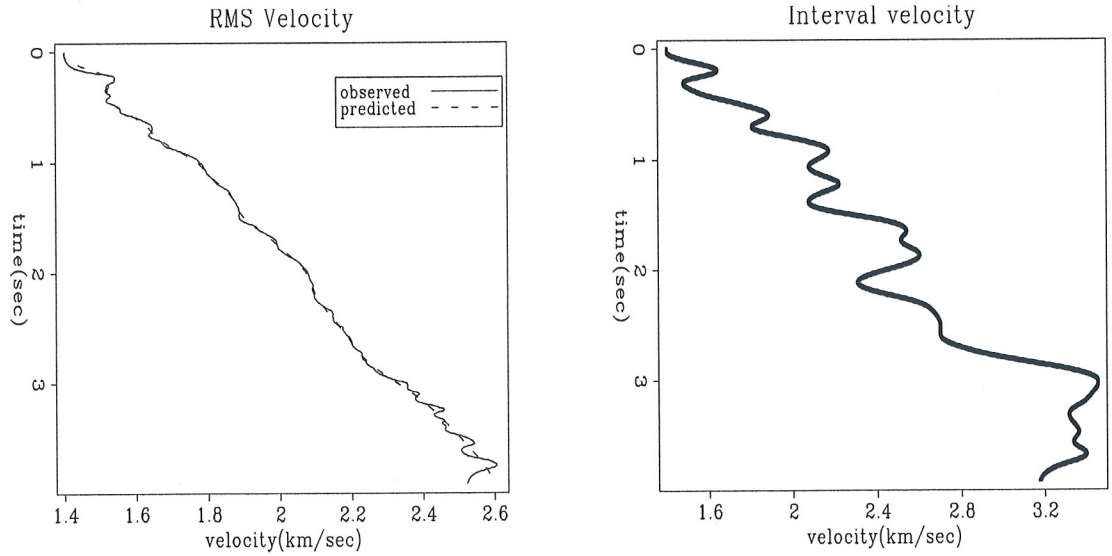

Figure 5.5: Observed RMS velocity and that predicted by a flexible model with $\epsilon = .25$ (Clapp) VIEW prc/. flex

```
    mask = .false.;    mask( 1) = .true.          # constrain first point
    vint = 0.      ;    vint( 1) = dat( 1)
    allocate(wght(size(wt)))
    wght=wt
    call weight_init(wght)
    allocate(msk(size(mask)))
    msk=.not.mask
    call mask1_init(msk)
    call solver_prc( m=vint, d=dat,Fop=causint_lop, stepper=cgstep, niter=niter, &
        Sop= causint_lop, nSop=nt, eps = eps,verb=.true.,Jop=mask1_lop, &
        p0=vint, Wop=weight_lop)
    call cgstep_close()
    st = causint_lop( .false., .false., vint, dat)
    do it= 1, nt
       vrms( it) = sqrt( dat( it)/it)
    vint = sqrt( vint)
    }
}
```

5.6.2 Lateral variations

The analysis above appears one dimensional in depth. Conventional interval velocity estimation builds a velocity-depth model independently at each lateral location. Here we have a logical path for combining measurements from various lateral locations. We can change the regularization to something like $\mathbf{0} \approx \nabla \mathbf{u}$. Instead of merely minimizing the vertical gradient of velocity we minimize its spatial gradient. Luckily we have preconditioning and the helix to speed the solution.

5.6.3 Blocky models

Sometimes we seek a velocity model that increases smoothly with depth through our scattered measurements of good-quality RMS velocities. Other times, we seek a blocky model. (Where seismic data is poor, a well log could tell us whether to choose smooth or blocky.) Here we see an estimation method that can choose the blocky alternative, or some combination of smooth and blocky.

Consider the five layer model in Figure 5.6. Each layer has unit traveltime thickness (so integration is simply summation). Let the squared interval velocities be (a, b, c, d, e) with strong reliable reflections at the base of layer c and layer e, and weak, incoherent, "bad" reflections at bases of (a, b, d). Thus we measure V_c^2 the RMS velocity squared of the top three layers and V_e^2 that for all five layers. Since we have no reflection from at the base of the fourth layer, the velocity in the fourth layer is not measured but a matter for choice. In a smooth linear fit we would want $d = (c + e)/2$. In a blocky fit we would want $d = e$.

Our screen for good reflections looks like $(0, 0, 1, 0, 1)$ and our screen for bad ones looks like the complement $(1, 1, 0, 1, 0)$. We put these screens on the diagonals of diagonal matrices $\mathbf{G}$ and $\mathbf{B}$. Our fitting goals are:

$$3V_c^2 \approx a + b + c \tag{5.37}$$

$$5V_e^2 \approx a + b + c + d + e \tag{5.38}$$

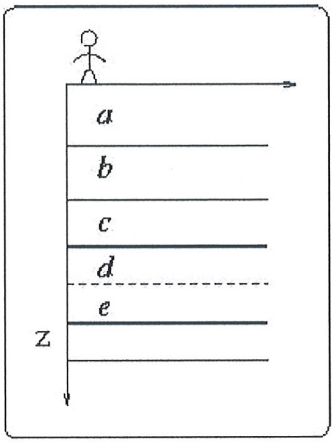

Figure 5.6: A layered earth model. The layer interfaces cause reflections. Each layer has a constant velocity in its interior. VIEW prc/. rosales

$$
\begin{aligned}
u_0 &\approx a && (5.39)\\
0 &\approx -a + b && (5.40)\\
0 &\approx -b + c && (5.41)\\
0 &\approx -c + d && (5.42)\\
0 &\approx -d + e && (5.43)
\end{aligned}
$$

For the blocky solution, we do not want the fitting goal (5.42). Further explanations await completion of examples.

5.7 INVERSE LINEAR INTERPOLATION

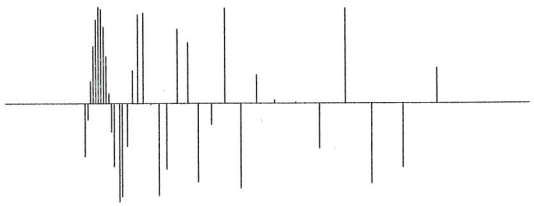

Figure 5.7: The input data are irregularly sampled. VIEW prc/. data

The first example is a simple synthetic test for 1-D inverse interpolation. The input data were randomly subsampled (with decreasing density) from a sinusoid (Figure 5.7). The forward operator $\mathbf{L}$ in this case is linear interpolation. We seek a regularly sampled model that could predict the data with a forward linear interpolation. Sparse irregular distribution of the input data makes the regularization enforcement a necessity. I applied convolution with the simple $(1, -1)$ difference filter as the operator $\mathbf{D}$ that forces model continuity (the first-order spline). An appropriate preconditioner $\mathbf{S}$ in this case is recursive causal integration.

As expected, preconditioning provides a much faster rate of convergence. Since iteration to the exact solution is never achieved in large-scale problems, the results of iterative optimization may turn out quite differently. Bill Harlan points out that the two goals in (5.16) conflict with each other: the first one enforces "details" in the model, while the second one tries to smooth them out. Typically, regularized optimization creates a complicated

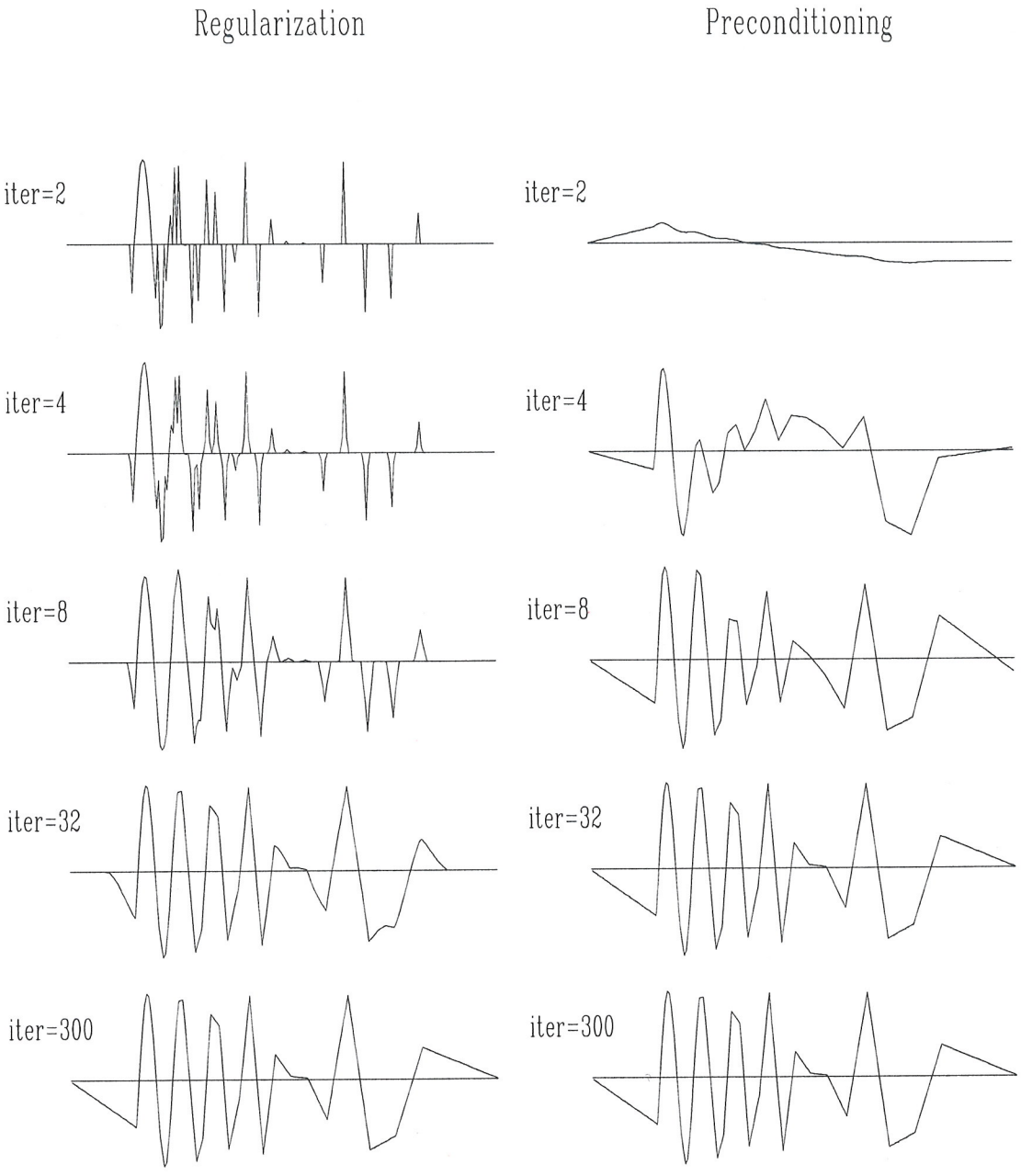

Figure 5.8: Convergence history of inverse linear interpolation. Left: regularization, right: preconditioning. The regularization operator $\mathbf{A}$ is the derivative operator (convolution with $(1, -1)$. The preconditioning operator $\mathbf{S}$ is causal integration. VIEW prc/. conv1

model at early iterations. At first, the data fitting goal (5.16) plays a more important role. Later, the regularization goal (5.16) comes into play and simplifies (smooths) the model as much as needed. Preconditioning acts differently. The very first iterations create a simplified (smooth) model. Later, the data fitting goal adds more details into the model. If we stop the iterative process early, we end up with an insufficiently complex model, not an insufficiently simplified one. Figure 5.8 provides a clear illustration of Harlan's observation.

Figure 5.9 measures the rate of convergence by the model residual, which is a distance from the current model to the final solution. It shows that preconditioning saves many iterations. Since the cost of each iteration for each method is roughly equal, the efficiency of preconditioning is evident.

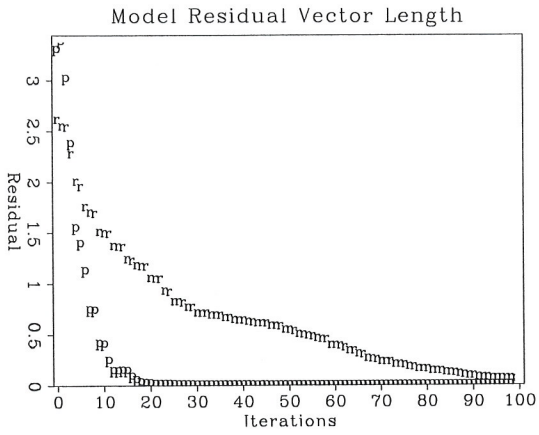

Figure 5.9: Convergence of the iterative optimization, measured in terms of the model residual. The "p" points stand for preconditioning; the "r" points, regularization. VIEW prc/. schwab1

The module `invint2` invokes the solvers to make Figures 5.8 and 5.9. We use convolution with `helicon` for the regularization and we use inverse convolution (recursion) with `polydiv` for the preconditioning. The code looks fairly straightforward except for the oxymoron `known=aa%mis`.

Inverse linear interpolation.r90

```
module invint2 {   # Inverse linear interpolation
  use lint1
  use helicon                                  # regularized    by helix    filtering
  use polydiv                                  # preconditioned by inverse filtering
  use cgstep_mod
  use solver_reg_mod
  use solver_prc_mod
contains
  subroutine invint( niter, coord,ord, o1,d1, mm,mmov, eps, aa, method) {
    logical,                    intent( in)  :: method
    integer,                    intent( in)  :: niter
    real,                       intent( in)  :: o1, d1, eps
    real,    dimension( :),     intent( in)  :: ord
    type( filter),              intent( in)  :: aa
    real,    dimension( :),     intent( out) :: mm
    real,    dimension( :,:),   intent( out) :: mmov          # model movie
    real,    dimension( :),     pointer      :: coord         # coordinate
    call lint1_init( o1, d1, coord)
    if( method) {                                            # preconditioning
       call polydiv_init( size(mm), aa)
       call solver_prc( Fop=lint1_lop, stepper=cgstep, niter=niter, m=mm, d=ord,
```

```
                Sop=polydiv_lop , nSop=size(mm), eps=eps , mmov=mmov, verb=.true.)
        call polydiv_close()
    } else {                                              # regularization
        call helicon_init( aa)
        call solver_reg( Fop=lint1_lop , stepper=cgstep , niter=niter , m=mm, d=ord ,
                Aop=helicon_lop , nAop=size(mm), eps=eps , mmov=mmov, verb=.true.)
    }
    call cgstep_close()
  }
}
```

5.8 EMPTY BINS AND PRECONDITIONING

There are at least three ways to fill empty bins. Two require a roughening operator $\mathbf{A}$ while the third requires a smoothing operator which (for comparison purposes) we denote $\mathbf{A}^{-1}$. The three methods are generally equivalent though they differ in significant details.

The original way in Chapter 3 is to restore missing data by ensuring that the restored data, after specified filtering, has minimum energy, say $\mathbf{Am} \approx \mathbf{0}$. Introduce the selection mask operator $\mathbf{K}$, a diagonal matrix with ones on the known data and zeros elsewhere (on the missing data). Thus $\mathbf{0} \approx \mathbf{A}(\mathbf{I} - \mathbf{K} + \mathbf{K})\mathbf{m}$ or

$$\mathbf{0} \quad \approx \quad \mathbf{A}(\mathbf{I} - \mathbf{K})\mathbf{m} \; + \; \mathbf{A}\mathbf{m}_k \;, \tag{5.44}$$

where we define $\mathbf{m}_k$ to be the data with missing values set to zero by $\mathbf{m}_k = \mathbf{Km}$.

A second way to find missing data is with the set of goals

$$\begin{aligned} \mathbf{0} &\approx \mathbf{Km} - \mathbf{m}_k \\ \mathbf{0} &\approx \epsilon\mathbf{Am} \end{aligned} \tag{5.45}$$

and take the limit as the scalar $\epsilon \to 0$. At that limit, we should have the same result as equation (5.44).

There is an important philosophical difference between the first method and the second. The first method strictly honors the known data. The second method acknowledges that when data misfits the regularization theory, it might be the fault of the data so the data need not be strictly honored. Just what balance is proper falls to the numerical choice of ϵ, a nontrivial topic.

A third way to find missing data is to precondition equation (5.45), namely, try the substitution $\mathbf{m} = \mathbf{A}^{-1}\mathbf{p}$.

$$\begin{aligned} \mathbf{0} &\approx \mathbf{KA}^{-1}\mathbf{p} - \mathbf{m}_k \\ \mathbf{0} &\approx \epsilon\mathbf{p} \end{aligned} \tag{5.46}$$

There is no simple way of knowing beforehand what is the best value of ϵ. Practitioners like to see solutions for various values of ϵ. Of course that can cost a lot of computational effort. Practical exploratory data analysis is more pragmatic. Without a simple clear theoretical basis, analysts generally begin from $\mathbf{p} = 0$ and abandon the fitting goal $\epsilon\mathbf{Ip} \approx 0$. Implicitly, they take $\epsilon = 0$. Then they examine the solution as a function of iteration, imagining that the solution at larger iterations corresponds to smaller ϵ. There is an eigenvector analysis indicating some kind of basis for this approach, but I believe there is no firm guidance.

5.8.1 SeaBeam

Figure 5.10 shows an image of deep sea water bottom in the Pacific of a sea-floor spreading center produced acoustically by a device called SeaBeam. Students here tried all three methods of filling empty bins on the this data using the laplacian as a regularizer. From an interpretive point of view, differences among the three methods were minor and as expected so only one is shown in Figure 5.10.

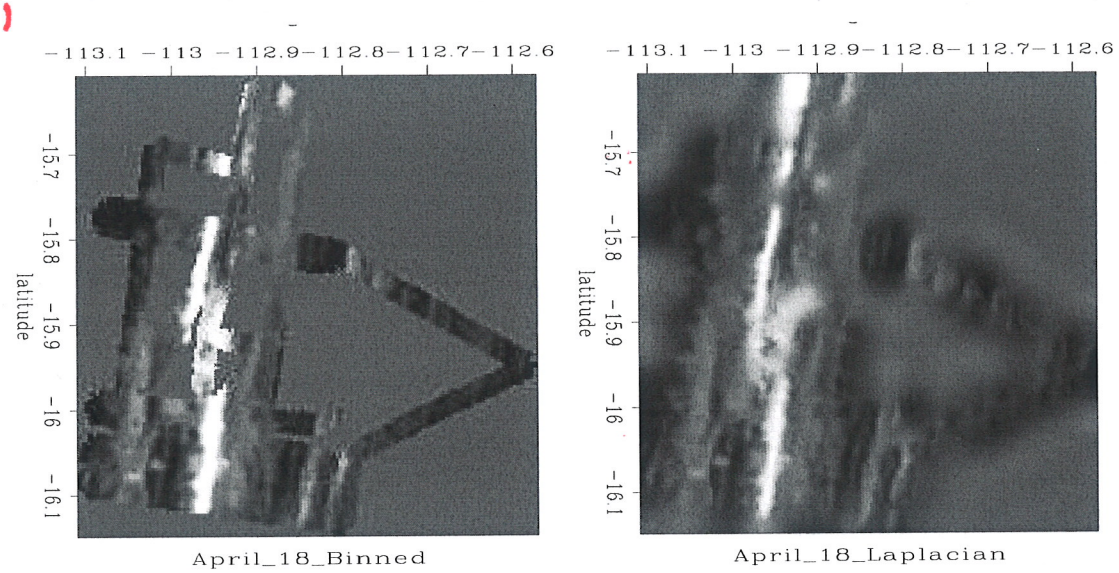

Figure 5.10: Seabeam data before and after empty bin filling with a laplacian. prc/. seaprc

5.9 GIANT PROBLEMS

This book does not solve giant problems, but it does solve personal-computer sized problems in the manner of giant problems. There is big money in solving giant problems. Big money brings specialist solutions beyond the scope of this book. But let us take a look. Closest to me is the seismic survey industry. Model space is three dimensional, a cube, roughly a thousand 2-D screen fulls, a screen full being a thousand by a thousand, a gigbyte in total. That's model space. Data space is *five* dimensional. A seismogram is a thousand time points. Our energy source lies in two dimensions on the earth surface plane, as do our receivers. All this compounds roughly to 1000 to the 5^{th} power, a thousand terrabytes, a petabyte. Fully convergent solutions needing 10^{15} iterations of operators is ridiculous, while more than a handful are nearly so. We think mainly of using only the adjoint. Theory and experimentation offer some guidance. Remember that adjoints are great when they are unitary (already an inverse). Adjoints can be improved by making them more unitary. They can be made more unitary by finding one good diagonal weighting function before and another after. Recalling "IID," adjoints are also made more unitary by band matrices that have the effect of whitening their output. Simple band matrices are the gradient and the Laplacian. More generally, a compact way to whiten spectra is multidimensional

autoregression, a method expounded in Chapter 7.

5.9.1 A hundred iterations

Lurking in every giant problem are many problems of smaller size. In the large scale seismic imaging problem lie problems of velocity estimation, multiple reflection elimination, and many more.

Envision a large problem feasible in a hundred iterations. Many of my colleagues work on such problems. Maybe half would also use exotic parallel computer architectures. Those with ample energy and intellectual capacity to tackle such machines are rewarded by speedup factors of ten to a hundred, rewarded also by a diverse population of industries hiring. This skill stays in demand because new architectures rapidly obsolete earlier generations. The other half, people like me, have the luxury of software (like in this book) decaying at a slower pace. That leaves us needed time to tune our imaginations to extracting the structure of more complex problems.

It is a giant leap of faith that we can accomplish something of value with a mere hundred iterations in a task that theoretically demands quadrillions. Experience shows that we often do, and we do so by experimenting with "intuitive" methods. The first I shall call "faking the epsilon".

5.9.2 Faking the epsilon

Burdened by a problem of oppressive size, any trick, honest or sly, is nice to know. I'll tell you a trick that is widely used. Many studies are done ignoring (abandoning) the model styling regression (second fitting regression below):

$$\begin{aligned} \mathbf{0} &\approx \mathbf{F}\mathbf{A}^{-1}\mathbf{p} - \mathbf{d} \\ \mathbf{0} &\approx \epsilon\, \mathbf{p} \end{aligned} \tag{5.47}$$

Since we have a numerically poor idea of what epsilon should be, it is nice to be rid of it. The pragmatic person iterates the data fitting regression only, watches the solution as a function of iteration, and stops when tired, or (more hopefully) stops at the iteration that is subjectively most pleasing. The epsilon-faking trick does not really speed things. But it eliminates the need for scan over epsilon. It also simplifies the coding :-)

Why does this crude approximation seem to work? The preconditioner is based on an analytic solution ($\mathbf{A}^{-1}$ is an inverse) to the regularization, so naturally, early iterations tend to already fit the regularization. That means early iterations are struggling instead to fit the data. The longer you run though, the better the data fit, and the more the actual regularization should be coming into play. But ongoing research often fails to run that far.

Figure 5.8 shows the idea that early iterations fit the straight lines. They are honoring the preconditioner. At later iterations the data fits better. Why do straight-line solutions honor the regularization? Refer to the discussion near Figure 3.12.

5.9.3 When preconditioning becomes a liability

Theoretically, preconditioning does not reduce the number of iterations required for an exact solution, but it gets us closer quicker, so we may hope to omit all the work of the later iterations. Surprisingly and unfortunately several of my colleagues have observed later iterations where preconditioning actually slows convergence. Then we are better off reverting to the non-preconditioned initial form. Sorry, but I am unable to offer guidance or any method to cope with this issue other than your own application-dependent experimentation.

5.9.4 Earthquake depth illustrates a null space

In the dawn of the era of computerized earthquake seismology someone decided to add earthquake depth to their catalog. Traditionally, they had solved for only three unknowns, latitude, longitude, and time of source at the source, i.e. origin time. Now they would add a fourth, the depth. They wrote down the 4×4 system of equations and solved it. Erratic results. So then they froze the depth at zero, solved for the old three variables, only then introducing the depth. Problem solved. (Compared to seismograph separation, zero depth is an excellent approximation.)

I first understood the earthquake experience as an issue with non-linear problems. True that earthquake travel time is not a linear function of distance, so the nonlinearity could lead to difficulty. But something more is going on. When any seismometer is far from the earthquake, the waves arrive propagating nearly vertically (earth curvature and $v(z)$ ray bending). Source depth affects such data in much the same way as time origin shift. Thus they are near a null-space. Whenever near a null space, especially with a non-linear problem, a good starting solution is needed.

5.9.5 The starting solution matters!

In principle, regularization solves the null-space problem, but that's only for those people lucky enough to have applications so small they can afford to iterate to completion. Think of this trivial 2-D null-space situation: A parabolic penalty on one spatial axis with no penalty on the other axis. Imagine a house facing north-east with a parabolic rain gutter mounted perfectly horizontally on one edge of the house roof. The null space is anywhere on the center line along the bottom of the gutter. Anywhere you begin, steepest descent brings you immediately to the gutter bottom in a location that depends on where you began. Now tilt the gutter a little bit so the water drips off one end of the rain drain. Steepest descent now overshoots a little so, as we saw in Chapter 2, a tortuous path of right angle turning ensues. (Recall Figure 2.5.) The conjugate direction method quickly solves this trivial 2-D problem, but in a 150,000 dimensional lake bottom problem, conjugate directions taken only a few dozen iterations will not do as well. When the data modeling operator contains a null space, only the regularization can pull us away from it, and a small number of iterations may be unable to do the job. So we need a good starting location.

> Textbook theory may tell us final solutions are independent of starting location, but we learn otherwise from non-linear problems, and we learn otherwise from linear but large problems.

5.9.6 Null space versus starting solution

The simplest null-space problem has one data point d emerging from two model points.

$$d \approx \begin{bmatrix} a & b \end{bmatrix} \begin{bmatrix} x \\ y \end{bmatrix} \tag{5.48}$$

The null space is any solution that produces no data. You can add an arbitrary amount β of the null space getting another solution as good as the first. Here is the full solution.

$$\begin{bmatrix} x \\ y \end{bmatrix} \approx \frac{d}{2ab} \begin{bmatrix} b \\ a \end{bmatrix} + \beta \begin{bmatrix} -b \\ a \end{bmatrix} \tag{5.49}$$

Iterative methods can neither subtract nor add any null space to your initial solution. It is obvious in this simple case because the gradient (here the matrix adjoint) dotted into the null-space vector vanishes. Suppose a and b are matrices while d, x, and y are vectors. Although more complicated, something similar happens. You can test whether an application involves a null space by comparing the results of various starting solutions.

Other traps arise in the world of images. Rarely are we able to iterate to full completion so we might say, "practically speaking this application has null spaces." For example, if we know that zero frequency is theoretically a null space, we would say, "The null space contains low frequencies." We cannot avoid such issues.

The textbook way of dealing with null spaces is to require the researcher to set up model styling goals (regularizations). This demands assumptions from the researcher, assumptions which are often hard to specify. Luckily there is another path to consider. We could choose the initial solution more carefully.

In regression (5.48) extended to images we might hope not to have a null-space problem when we begin iterating from $(\mathbf{x}, \mathbf{y}) = (\mathbf{0}, \mathbf{0})$ but this is not true. This is a pitfall which in an application context took me some years to recognize. Notice what happens the first step you move away from $(\mathbf{x}, \mathbf{y}) = (\mathbf{0}, \mathbf{0})$. Your solution becomes a constant β times the gradient. The image extension of (5.48) being

$$\begin{bmatrix} \mathbf{x} \\ \mathbf{y} \end{bmatrix} = \beta \begin{bmatrix} \mathbf{A}^* \mathbf{d} \\ \mathbf{B}^* \mathbf{d} \end{bmatrix} \tag{5.50}$$

If the operators $\mathbf{A}$ and $\mathbf{B}$ resemble filters, it is pretty clear that $\mathbf{x}$ and $\mathbf{y}$ will be correlated. Physically, this could be nonsense. We might be trying to discover if and how $\mathbf{x}$ and $\mathbf{y}$ are correlated. Or we might wish to demand they be uncorrelated.

I have no general method for you, but offer a suggestion that works for one family of applications and may be suggestive for others. Traditionally it might happen that $\mathbf{y}$ is

ignored, effectively taking $\mathbf{y} = \mathbf{0}$. That happens when the data is better explained by $\mathbf{A}$ alone than by $\mathbf{B}$ alone. Solve first for $\mathbf{x}$ alone. Call it $\mathbf{x}_0$. Now define a new variable $\tilde{\mathbf{x}}$ such that $\mathbf{x} = \mathbf{x}_0 + \tilde{\mathbf{x}}$. Introducing your innovative concept (estimating $\mathbf{y}$) your regression becomes:

$$\mathbf{0} \approx \mathbf{r} = \mathbf{A}(\mathbf{x}_0 + \tilde{\mathbf{x}}) + \mathbf{B}\mathbf{y} - \mathbf{d} \tag{5.51}$$

$$\mathbf{0} \approx \mathbf{r} = \mathbf{A}\tilde{\mathbf{x}} + \mathbf{B}\mathbf{y} - (\mathbf{d} - \mathbf{A}\mathbf{x}_0) \tag{5.52}$$

Start off from $(\tilde{\mathbf{x}}, \mathbf{y}) = (\mathbf{0}, \mathbf{0})$. Like equation (5.50) the first step leads to

$$\begin{bmatrix} \tilde{\mathbf{x}} \\ \mathbf{y} \end{bmatrix} = \beta \begin{bmatrix} \mathbf{A}^*\mathbf{r} \\ \mathbf{B}^*\mathbf{r} \end{bmatrix} \tag{5.53}$$

which is very different from equation (5.50) because $\mathbf{r}$ is very different from $\mathbf{d}$. Although we may still have an annoying or inappropriate correlation between $\tilde{\mathbf{x}}$ and $\mathbf{y}$, it is a lot less annoying than a correlation between $\mathbf{x}$ and $\mathbf{y}$.

> Solve an oversimplified physical problem first. Use its easy solution as the starting point for your glorious innovation.

Chapter 6

Noisy images, non-Gaussian

We have characterized images and signals by amplitude in space and time. We have also characterized them by frequencies. In Chapter 7 we characterize them by their multidimensional spectrum. Most often signal amplitudes and spectra have a consistent behavior. The classic well-behaved signal has a **Gaussian** statistical density, meaning that signal may have been built from many independent causes (central limit theorem). When these characteristics are unchanging, the signal is said to be stationary.

But sometimes signals just burst out in unpredictable ways and we are hard pressed to characterize. This can happen in model space as well as data space. As this is real life, we must have a chapter to deal with it, a usable theory to deal with it, and a fascinating data set loaded with it. This is the chapter.

Here we introduce erratic bursty noise which is difficult to fit in any statistical model. To handle it we need the robust estimation procedures introduced here. Here we will handle both bursty noise and stationary noise at the same time. As has been our theme, we'll take a path suited to large spaces.

6.1 MEANS, MEDIANS, MODES, AND MEASURES

Norms and penalty functions are positive measures of the size of a vector. For example, the square root of the sum of the squares of components of a data vector $\mathbf{d}$ is called its ℓ_2 norm denoted $\|\mathbf{d}\|^2$. We often have a model parameter, here m_2, make a residual $m_2 - \mathbf{d}$ from it, and then minimize the squared ℓ_2 **norm** of the residual

$$0 \quad = \quad \frac{d}{dm_2} \sum_{i=1}^{N} (m_2 - d_i)^2 \tag{6.1}$$

It is quick to find the numeric value for the model parameter m_2 which turns out to be the arithmetic **mean** of the data values, $m_2 = \frac{1}{N} \sum d_i$.

Inspiring this chapter is the ℓ_1 norm. Minimizing the ℓ_1 norm of the same residual we have

$$0 \quad = \quad \frac{d}{dm_1} \sum_{i=1}^{N} |m_1 - d_i| \tag{6.2}$$

Let us work it out. We need the derivative of the absolute value function. This derivative is called the signum function, denoted sgn(). It is +1 for positive residuals, −1 for negative residuals, and undefined for zero valued residuals. So equation (6.2) becomes

$$0 \quad = \quad \sum_{i=1}^{N} \text{sgn}(m_1 - d_i) \tag{6.3}$$

Equation (6.3) says m_1 must be chosen so that half the residuals are +1 and the other half are −1. In other words, m_1 is the **median** of the data. The median of the three values $(8, 7, 921)$ is 8. The median has shrugged off the huge outlier, the humongous value that had no business being there. The ℓ_1 norm also enables multivariate model building in the presence of erratic, bursty noise. A powerful tool!

Yet another average is the "**mode**." It is the most commonly occurring value. For example, in the number sequence $(1, 1, 2, 3, 5)$ the mode is 1 because it occurs the most times. Mathematically, the mode minimizes the zero norm of the residual. Recall that except for the number zero, any positive number raised to the zero power is +1. But zero raised to any power is zero, so every time m_0 matches a data value you get a zero. The minimum penalty goes to the value that matches the most data values. This book finds little use for the mode. If this book contained a probability density function we would note that the mode is at its maximum value.

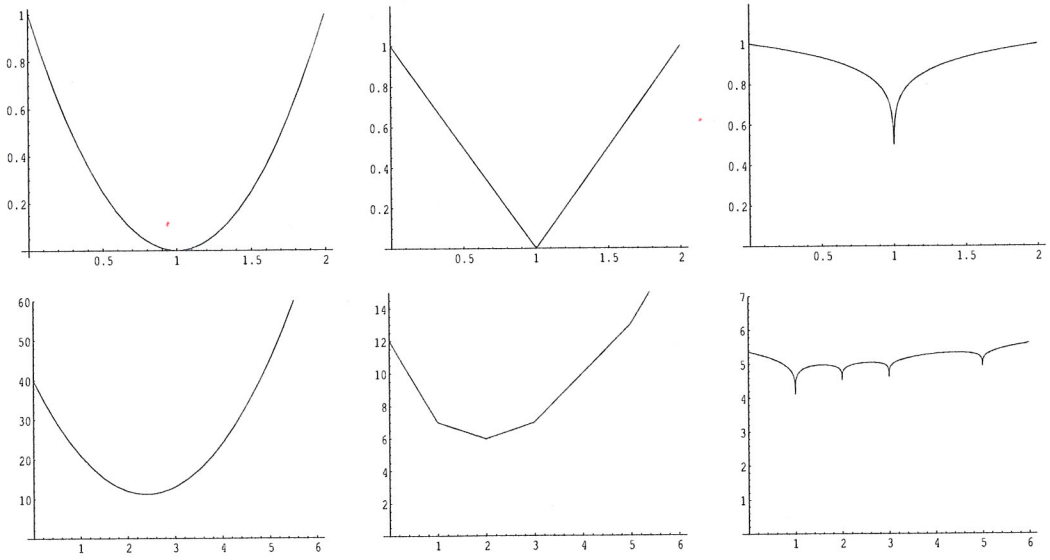

Figure 6.1: Mean, median, and mode. The coordinate is m. Top is the ℓ_2, ℓ_1, and $\ell_{1/10} \approx \ell_0$ measures of the scalar $m - 1$. Bottom is the same measures of the data set $m - (1, 1, 2, 3, 5)$. (Made with Mathematica.) VIEW noiz/. norms

$\ell_2(\mathbf{r})$ and $\ell_1(\mathbf{r})$ are convex functions (positive second derivative for any component of $\mathbf{r}$). This fact leads to the triangle inequalities $\ell_p(\mathbf{a}) + \ell_p(\mathbf{b}) \geq \ell_p(\mathbf{a} + \mathbf{b})$ for $p \geq 1$ and assures that gradients lead to a unique bottom. Because there is no triangle inequality for ℓ_0, mathematicians would not call it a "norm." They call it a "measure." Soon this chapter introduces another measure (penalty function) $h(\mathbf{r})$ that is not a norm because

$\alpha h(\mathbf{r}) \neq h(\alpha \mathbf{r})$ for $\alpha > 0$, but it is convex because its second derivative $h''(\mathbf{r}) \geq 0$ is everywhere positive. As with least squares, that means we can safely use gradients to find a unique minimum. Using $h(\mathbf{r})$, the final answer is independent of the initial guess.

6.1.1 Percentiles and Hoare's algorithm

The median is the 50-th **percentile**. After residuals are ordered from smallest to largest, the 90-th percentile is the value with 10% of the values above and 90% below. At our lab the default value for clipping plots of field data is at the 99th percentile. In other words, magnitudes above the 99-th percentile are plotted at the 99-th percentile. Any percentile is most easily defined if the population of values a_i, for $i = 1, 2, ..., n$ has been sorted into order so that $a_i \leq a_{i+1}$ for all i. Then the 90-th percentile is a_k where $k = (90n)/100$.

We can save much work by using **Hoare's algorithm**. It does not fully order the whole list, only enough of it to find the desired quantile. Hoare's algorithm is an outstanding example of the power of a recursive function, a function that calls itself. The main idea is this: We start by selecting a random value taken from the list of numbers. Then we split the list into two piles, one pile all values greater than the selected, the other pile all less. The quantile is in one of these piles, and by looking at their sizes, we know which one. So we repeat the process on that pile and ignore the other other one. Eventually the pile size reduces to one, and we have the answer.

In Fortran 77 or C it would be natural to split the list into two piles as follows:

> We divide the list of numbers into two groups, a group below a_k and another group above a_k. This reordering can be done "in place." Start one pointer at the top of the list and another at the bottom. Grab an arbitrary value from the list (such as the current value of a_k). March the two pointers towards each other until you have an upper value out of order with a_k and a lower value out of order with a_k. Swap the upper and lower value. Continue until the pointers merge somewhere midlist. Now you have divided the list into two sublists, one above your (random) value a_k and the other below.

Fortran 90 has some higher level intrinsic vector functions that simplify matters. When `a` is a vector and `ak` is a value, `a>ak` is a vector of logical values that are true for each component that is larger than `ak`. The integer count of how many components of `a` are larger than `ak` is given by the Fortran intrinsic function `count(a>ak)`. A vector containing only values less than `ak` is given by the Fortran intrinsic function `pack(a,a<ak)`.

Theoretically about $2n$ comparisons are expected to find the median of a list of n values. The code below (from Sergey Fomel) for this task is `quantile`.

percentile.r90

```
module quantile_mod {    # quantile finder.    median = quantile( size(a)/2, a)
contains
  recursive function quantile( k, a) result( value) {
    integer,              intent (in)  :: k          # position in array
    real, dimension (:), intent (in)  :: a
    real                               :: value      # output value of quantile
```

```
    integer                                 :: j
    real                                    :: ak
    ak = a( k)
    j = count( a < ak)                                  # how many a(:) < ak
    if( j >= k)
                value = quantile( k, pack( a, a < ak))
    else {
        j = count( a > ak) + k - size( a)
        if( j > 0)
                value = quantile( j, pack( a, a > ak))
        else
                value = ak
        }
    }
}
```

6.1.2 The weighted mean

The **weighted mean** m is

$$m = \frac{\sum_{i=1}^{N} w_i^2 d_i}{\sum_{i=1}^{N} w_i^2} \tag{6.4}$$

where $w_i^2 > 0$ is the squared weighting function. This is the solution to the ℓ_2 fitting problem $0 \approx w_i(m - d_i)$; in other words,

$$0 = \frac{d}{dm} \sum_{i=1}^{N} [w_i(m - d_i)]^2 \tag{6.5}$$

There is a weighed median too. It's needed in ℓ_1 line search. But we'll be taking another path more suited to image estimation.

6.2 HYPERBOLIC OR HYBRID (ℓ_1, ℓ_2) MODEL FITTING

I've seen many multi-variable applications improved when least-squares (ℓ_2) model fitting was changed to least absolute values (ℓ_1). I've never seen the reverse. Mathematicians love ℓ_1. Why not adopt it? Three reasons: (1) They haven't come up with a large scale solver as fast and convenient as ℓ_2. (2) Tiny residuals vote oppositely at the faintest perturbation. (3) We have something more suitable here, the hyperbolic penalty function (HPF). Convexity gives the HPF method a welcome stability and convergence not shared by its more primative forerunner, IRLS (Iterated Reweighted Least Squares).

Here our conjugate-direction method is merged with Newton iteration to give some of the useful ℓ_1 characteristics to familiar ℓ_2 formulations. The merged method we call the HYCD method. A hybrid penalty function for residuals r_i has a new parameter, a threshold at which ℓ_2 behavior transits to ℓ_1. Applications suggest two different thresholds, one for the data fitting, the other for the model styling (prior knowledge or regularization). Each fitting goal requires a threshold of residual, let us call it R_d for the data fitting, and R_m for the model styling. It is always annoying to need to specify parameters, but these two parameters, I claim, are a basic part of the application setting, not a requirement of numerical analysis.

The meaning of the thresholds R_d and R_m is quite clear. For a shot gather with about 30% of the area saturated with ground roll noise, choose R_d around the 70th percentile of the fitting residual. As for the model styling, we often seek earth models that are blocky. In other words, earth models whose derivatives are spiky. For blocks about 20 points long the spikes should average about 20 points apart. Thus about 95% of the residuals should be in the ℓ_2 area while only about 5% in the ℓ_1 area allowing 5% of the spikes to be of unlimited size. This is an R_m at about the 95^{th} percentile of $|\mathbf{r}_m| = |\epsilon m_i|$. (On early iterations you might omit the model styling by setting $\epsilon = 0$ leaving time to establish an initial $\mathbf{m}$.) Thus I conclude that in a wide variety of practical examples fitting goals for both data and model need not go far from the usual ℓ_2 norm, but they do need to incorporate some residual values out in the ℓ_1 zone, possibly far out in it.

A convex penalty function that smoothly transits from ℓ_2 to ℓ_1 behavior is the hyperbola. It is parabolic (ℓ_2 like) in the middle, but asymptotes to ℓ_1-like straight lines. A circle $t^2 = z^2 + x^2$ seen in (t, x) space is a hyperbola with a parameter z. This suggests the penalty function $h^2 = R^2 + r^2$ where r is the residual, R is the threshold parameter, and where $h(r)$ is the penalty. Customarily there is no penalty when the residual vanishes, so to accommodate that custom (making no fundamental change) we subtract the constant R from h. Thus the hybrid penalty function promoted here is the origin-shifted hyperbola $h(r) = \sqrt{R^2 + r^2} - R$. We could call this approach the Hyperbolic method or the Hybrid method. The word "hybrid" is suggestive of being between ℓ_1 and ℓ_2 norms, but it is not so precise a word as "hyperbolic". It may be tempting to call the hyperbolic penalty function (HPF) the hybrid norm, but actually it is not a norm. Mathematically, norms satisfy $\alpha\|\mathbf{r}\| = \|\alpha\mathbf{r}\|$ for $\alpha > 0$. HPF does not have this property.

In practice the thresholds R_d and R_m are superseded by their inverses, gains. Upon application of the properly chosen gain to the raw data (or model) we have new variables in the neighborhood of unity, and so the penalty function reduces to $h(r) = \sqrt{1 + g^2 r^2} - 1$. The simpler penalty function is nice, but the real reason to switch from thresholds to gains is that gains may be time and space variable, and even frequency variable. Many applications express gain by an operator $\mathbf{G}$ or an operator $\mathbf{W}$. More on that later.

6.2.1 Some convex functions and their derivatives

Consider now some choices for convex functions and their derivatives.

ℓ_2 norm = Least Squares:

$$C = r^2/2 \tag{6.6}$$
$$C' = r \tag{6.7}$$
$$C'' = 1 \quad > 0 \tag{6.8}$$

ℓ_1 norm:

$$C = |r| \tag{6.9}$$
$$C' = \text{sgn}(r) \tag{6.10}$$
$$C'' = 0 \text{ or } +\infty \quad \geq 0 \tag{6.11}$$

Hyperbolic (or Hybrid) Penalty Function (HPF):

$$h = (1+q^2)^{1/2} - 1 \tag{6.12}$$
$$h' = q \,/\, (1+q^2)^{1/2} \tag{6.13}$$
$$h'' = 1 \,/\, (1+q^2)^{3/2} \geq 0 \tag{6.14}$$

The hyperbolic (or hybrid) penalty function (HPF) is not expressed here as a function of residual r, but of scaled residual $q = gr$. By adjusting the scale g, equations (6.12-6.14) can look like either ℓ_2 or ℓ_1 depending on the numerical value of gr. In practice, the factor g is often taken to the inverse of the value of some percentile of residual magnitudes. Hence q is unit-free or dimensionless.

Because of the erratic behavior of C'' for ℓ_1 and our coming use of second order Taylor series, the conjugate direction solver we examine next is not intended for use near the ℓ_1 limit. It will turn out we can have many residuals at that limit, but not too many (whatever that means!). Luckily most applications do not require us to have most residuals near that limit.

Equation (6.13) plays such a large role in results to come that I give it the name "soft clip." The clip function itself arises in graphic display devices where a certain brightness of image is desired. When a physical limit (called "the clip") is reached, larger values are replaced by the maximum value. Likewise for minimum values.

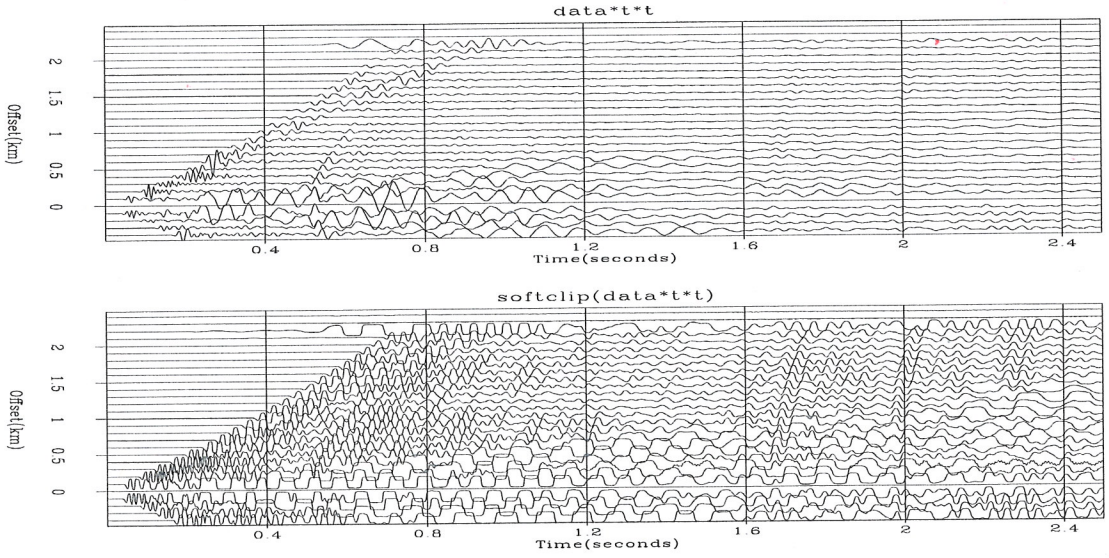

Figure 6.2: Reflection data $\mathbf{d}$ before (top) and after (bottom) soft clip $\mathbf{h}' = h'(\mathbf{d})$. Clipping large amplitudes enables small ones to be seen. VIEW noiz/. softclip

Equation (6.13) at small $|gr|$ behaves as $g\ell_2$, namely $h'(r) = gr$. At large $|gr|$ it behaves as ℓ_1, namely $h'(r) = \text{sgn}(r)$. Over its whole range $h'(r)$ behaves as a clip function, though with a soft transition near $|gr| = 1$. As a demonstration of the soft clip function, a family of not untypical seismic reflection signals $\mathbf{d}$ shown in Figure 6.2 is passed through $\mathbf{h}' = h'(\mathbf{d}) = \mathbf{h}'(\mathbf{d})$. The intended pleasing result is that large portions of signal of little practical

interest have become clipped (turned into "soft" rectangle functions) allowing a gain increase bringing smaller up into view (and up to where data fitting codes will notice them).

At convergence we find the vanishing of the gradient $\Delta\mathbf{m} = \mathbf{0}$. We will soon see the familiar gradient $\Delta\mathbf{m} = \mathbf{F}^*\mathbf{r}$ becomes $\Delta\mathbf{m} = \mathbf{F}^*\mathbf{h}'(\mathbf{q})$, the new aspect being that the scaled residual is now softclipped.

6.2.2 Filtered and gained residuals

The innovation here is that the residual becomes soft-clipped, but most applications additionally require residuals being transformed to IID by means of gains in physical space and fourier space embedded in an operator, say $\mathbf{G}$. We could embed the soft-clipping constant g with the operator $\mathbf{G}$, but the application analyst will be dealing with them separately. (This is like the regularization $\mathbf{0} \approx \epsilon\mathbf{Am}$ having the ϵ embedded into the $\mathbf{A}$.) For the moment, we'll take the g part to be embedded in filter/gain part $\mathbf{G}$ but we may pull it out later.

The gained residual $q_k = \sum_i g_{k,i} r_i$ occurs so often it has several names besides the "gained residual". It may be called the "statistical residual" or the "sparse residual". (We haven't used it long enough to know which name will stick.) In summary:

$$\mathbf{q} = \mathbf{G}(\mathbf{Fm} - \mathbf{d}) = \mathbf{Gr} \tag{6.15}$$

$$q_k = \sum_i g_{k,i} \left(\sum_j F_{i,j} m_j - d_i \right) \tag{6.16}$$

> Sorry to introduce a new variable name for an old idea, but to avoid coding bugs, you will be seeing much less of the residual $\mathbf{r}$ and more of the gained and filtered residual $\mathbf{q} = \mathbf{Gr}$.

The following derivation applies to any convex function C. Having little experience in choice of convex functions we specialize to the notation of the hyperbolic function $h(q)$. The average penalty measure for mismatch between theory and data is

$$\bar{h}(\mathbf{m}) = \frac{1}{N} \sum_{i=1}^{N} h(q_i) \tag{6.17}$$

Let $h'(q_i)$ denote dh/dq evaluated at q_i. Define the softclip vector $\mathbf{h}'(\mathbf{q})$ by applying $h'()$ to each component of $\mathbf{q}$. This is the slope of the penalty function. If the penalty function were that of least squares, we would have $\mathbf{h}' = \mathbf{q}$.

$$h'(\mathbf{q}) = \frac{dh(q_i)}{dq_i} = h'_i = \mathbf{h}' \tag{6.18}$$

We plan to minimize the average penalty $\bar{\mathbf{h}}(\mathbf{q}(\mathbf{m}))$. To change the statistical residual component q_k by changing the model component m_j we need from equation (6.16) the matrix of derivatives.

$$\frac{dq_k}{dm_j} = \sum_i g_{k,i} F_{i,j} \tag{6.19}$$

Viewed as a matrix dq_k/dm_j is rectangular with one dimension the size of model space $\mathbf{m}$, the other dimension the size of residual space $\mathbf{q}$. To multiply this matrix by a column vector the size of $\mathbf{m}$ we write it as $\mathbf{GF}$. To multiply it by a column vector the size of $\mathbf{q}$ we write it as $\mathbf{F}^*\mathbf{G}^*$. The search direction becomes

$$\Delta\mathbf{m} \;=\; N\,\frac{d\bar{h}}{dm_j} \;=\; \sum_k \frac{dh}{dq_k}\frac{dq_k}{dm_j} \;=\; \sum_k \frac{dq_k}{dm_j}\frac{dh}{dq_k} \;=\; \mathbf{F}^*\mathbf{G}^*\,\mathbf{h}'(\mathbf{q}) \tag{6.20}$$

This is simply the old **normal equations** result of chapter 2 that $\mathbf{0} = \Delta\mathbf{m} = \mathbf{F}^*\mathbf{r}$ complicated in appearance by the filter-gain $\mathbf{G}$ and the hyperbolic penalty $\mathbf{r} \to \mathbf{h}'(\mathbf{r})$.

> You've got the answer when the soft-clipped residual is orthogonal to all the fitting functions.

6.2.3 Gaining versus weighting

In the ℓ_2 world there is no distinction between gaining and weighting because $\sum_i (w_i r_i)^2$ is the same as $\sum_i w_i^2 r_i^2$. With HPF we might choose to distinguish gaining and weighting. We could minimize this expression that contains both:

$$\bar{h} \;=\; \sum_i w_i\; h(g_i r_i) \tag{6.21}$$

Both w and g enable us to suppress residuals. Why bother with w? In data fitting the ℓ_1/ℓ_2 threshold suppresses the giant residuals. In model styling the threshold may encourage chunkier models. Although weights seem largely supplanted by gains within a regression, when we include regularization or we have a row of models, scales like epsilon ϵ come into play again. Epsilon ϵ is a simple weight. An example of a "row of models" is water depth data as a sum of (1) tide and (2) location.

It seems wonderful that we may choose spatial patterns of weights and gaining functions quite arbitrarily, and it is well that we no longer need rely on the primitive expedient of tapering data near boundaries (falsifying data); but I have found this opportunity easily abused. One day upon minimizing energy in the weighted (down gained) residual of an image, I discovered all the energy had gone outside the boundaries! I had wished the residual instead spread throughout the image.

> The moral of the story is to view always both weighted and unweighted residuals.

Including model styling (regularization) we minimize the scalar:

$$\min_{\mathbf{m}} \quad \bar{h}(\mathbf{G}_d(\mathbf{F}\mathbf{m} - \mathbf{d})) \;+\; \epsilon\,\bar{h}(\mathbf{G}_m\mathbf{m}) \tag{6.22}$$

which we often express as two regression sets

$$\mathbf{0} \;\approx_h\; \mathbf{q}_d \;=\; \mathbf{G}_d(\mathbf{F}\mathbf{m} - \mathbf{d}) \tag{6.23}$$

$$\mathbf{0} \;\approx_h\; \mathbf{q}_m \;=\; \epsilon\,\mathbf{G}_m\mathbf{m} \tag{6.24}$$

Here we have introduced the notation that regression equations, normally denoted by $\approx$, when using the hyperbolic penalty function (HPF) are denoted by $\approx_h$.

Occasionally we might add something to the regularization like $\mathbf{G}_m\mathbf{m}_0$ or noise for geostat. These add to the line search, but do not change the gradient. Key to doing our job is the gradient:

$$\mathbf{0} \;=\; \Delta\mathbf{m} \;=\; \mathbf{F}^*\mathbf{G}_d^*\,\mathbf{h}'(\mathbf{G}_d\mathbf{r}) \;+\; \epsilon\,\mathbf{G}_m^*\,\mathbf{h}'(\mathbf{G}_m\mathbf{m}) \tag{6.25}$$

It's curious to notice the gradient now twice contains the gain, though once "softened".

6.3 THEORY FOR HYPERBOLIC FITTER CODE

The hyperbolic penalty function (HPF) is convex, so we know that convergence should be assured even though we are solving this non-linear problem. So let us begin with a simple solver. To avoid clutter, let the gain $\mathbf{G}$ be embedded in the operator $\mathbf{F}$ and data $\mathbf{d}$. Define a model update direction by the gradient $\Delta\mathbf{m} = \mathbf{F}^*\mathbf{G}^*\mathbf{h}'(\mathbf{G}\mathbf{r}) = \mathbf{F}^*\mathbf{G}^*\mathbf{h}'(\mathbf{q})$. Since $\mathbf{q} = \mathbf{G}(\mathbf{F}\mathbf{m} - \mathbf{d})$ the gained residual update direction is $\Delta\mathbf{q} = \mathbf{G}\mathbf{F}\Delta\mathbf{m}$. To find the distance α to move in those directions

$$\mathbf{m} \;\leftarrow\; \mathbf{m} + \alpha\Delta\mathbf{m} \tag{6.26}$$

$$\mathbf{q} \;\leftarrow\; \mathbf{q} + \alpha\Delta\mathbf{q} \tag{6.27}$$

choose the scalar α to minimize the average penalty

$$\bar{h}(\alpha) \;=\; \frac{1}{N}\sum_i h(q_i + \alpha\Delta q_i) \tag{6.28}$$

It is a one-dimensional function of α. Finding the minimum should not be difficult. We make a million Taylor series, one for each residual q_i. Inspect one of them. The first three terms of the Taylor series make a parabola tangent to the hyperbola at that residual. Even if this particular residual lies far out on the asymptote of the hyperbola the residual may move some distance before its Taylor series becomes a poor fit. Adding together the many second order polynomials in α, the sum is also a second order polynomial in α so we easily find the minimum. Let h_i' and h_i'' be first and second derivatives of $h(q_i)$ at q_i. Then equation (6.28) becomes a familiar least squares problem.

$$\bar{h}(\alpha) \;=\; \frac{1}{N}\sum_i h_i + (\alpha\Delta q_i)h_i' + (\alpha\Delta q_i)^2 h_i''/2 \tag{6.29}$$

To find α, set $d\bar{h}/d\alpha = 0$. Then solve for α.

$$0 \;=\; \frac{d\bar{h}}{d\alpha} \;=\; \sum_i \Delta q_i h_i' \;+\; \alpha(\Delta q_i)^2 h_i'' \tag{6.30}$$

The Newton method applied to the method of steepest descents is to first find α and then use it to update the residual $\mathbf{q}$ and the model $\mathbf{m}$.

$$\alpha \;=\; -\,\frac{\sum_i \Delta q_i h_i'}{\sum_i (\Delta q_i)^2 h_i''} \tag{6.31}$$

$$\mathbf{q} \;=\; \mathbf{q} + \alpha\,\Delta\mathbf{q} \tag{6.32}$$

$$\mathbf{m} \;=\; \mathbf{m} + \alpha\,\Delta\mathbf{m} \tag{6.33}$$

After this we are not finished because moving $\mathbf{q}$ changes the convex function values and all its derivatives (h_i, h_i', h_i''). The Newton algorithm is simply to iterate the sequence (6.31) to (6.33). This is Newton line search. It is cheap. Eventually we get to the bottom along the line we are scanning and are ready for a new line. That's when we pay the money to compute a new $\Delta\mathbf{m} = \mathbf{F}^*\mathbf{G}^*\mathbf{h}'(\mathbf{q})$ and a new $\Delta\mathbf{q} = \mathbf{GF}\Delta\mathbf{m}$. This is non-linear steepest descent. The reliability of the method is assured by the convexity of the hyperbolic function.

The new result (6.31) for α is closely related to our early result in chapter 2, equation (2.57). Take our current result to the ungained least squares case $h = r^2/2$, $h_i' = r_i$, and $h'' = 1$ so in equation (6.31), α reduces to the familiar $-\sum_i \Delta q_i\, q_i \;/\; \sum_i (\Delta q_i)^2 = \alpha = -(\Delta\mathbf{r}\cdot\mathbf{r})/(\Delta\mathbf{r}\cdot\Delta\mathbf{r})$. Recognizing that $\mathbf{r}$ has become $\mathbf{h}'(\mathbf{q})$, the new numerator is the same as the old but for gain and soft clipping, while the new denominator scales each term by h_i''. Equation (6.14) says the new denominator scales the larger residuals smaller. A single infinite residual would merely omit a single term from the denominator reducing it slightly and increasing α slightly, leaving us concerned only that there not be too many such bad residuals. With a crazy initial solution there might well be too many bad residuals. Then the residual might grow instead of shrinking. Seeing that we would simply reduce step size, $\alpha \leftarrow \alpha/2$, etc.

When there is model styling as well as data fitting, the gradient has a contribution from each. Either one or both may have a hyperbolic penalty function (HPF). The distance α in equation (6.31) is a ratio of sums over data space. Now we need to add sums over model space. With the extra terms the result is:

$$\alpha \;=\; -\;\frac{\sum_i \Delta q_i \;\; h'(q_i) \;+\; \epsilon \;\sum_i \;\Delta m_i \;\; h'(m_i)}{\sum_i (\Delta q_i)^2\, h''(q_i) \;+\; \epsilon \;\sum_i (\Delta m_i)^2\, h''(m_i)} \tag{6.34}$$

We are hoping the presence of some residuals out in the ℓ_1 region does not greatly increase the number of iterations compared to the usual ℓ_2 parabolic penalty function. Should anyone choose a gain $\mathbf{G}$ so large it drives many of the residuals into the ℓ_1 region, convergence may be slow. Experience suggests blindly starting with a model $\mathbf{m}_0$ might force very many iterations, so giving some thought to the starting $\mathbf{m}_0$ might well be worth while. This was steepest descent. Now for conjugate directions.

6.3.1 Newton plane search

Here we advance from steepest descent to conjugate directions as a method for using the hyperbolic penalty function (HPF). With the original ℓ_2 steepest-descent method we found a distance α to move in the direction $\Delta\mathbf{m} = \mathbf{g} = \mathbf{F}^*\mathbf{r}$. With the gained hyperbolic penalty function (HPF) this direction becomes $\Delta\mathbf{m} = \mathbf{g} = \mathbf{F}^*\mathbf{G}^*\,\mathbf{h}'(\mathbf{q})$.

Extending to the conjugate direction method there are two parameters, α and β, and two vectors. One vector is the gradient vector $\mathbf{g}$. The other vector is the previous step $\mathbf{s}$. These vectors may be viewed in data space or viewed in model space. We will take linear combinations of $\mathbf{g}$ and $\mathbf{s}$ in both spaces and need notation for recognizing and distinguishing them.

We are following the path we followed in Chapter 2, but now we have the added complication of hyperbolic penalty. In Chapter 2 the code followed directly from equation (2.80). Similar steps here will lead us here to equation (6.43).

As before we adopt unconventional notation. Conventionally in matrix analysis lower case letters are vectors while upper case letters are matrices. But in Fourier analysis lower case letters become upper case upon fourier transformation. Let us handle $\mathbf{g}$ and $\mathbf{s}$ this way: Keep using bold capitals for operators but now use ordinary italic for vectors with model space being lower case italic and data space being upper case italic so the familiar $\mathbf{d} = \mathbf{F}\mathbf{m}$ becomes $D = \mathbf{F}m$.

At the k^{th} iteration we will update the model m with gradient g and previous step s where

$$s_{k+1} = \alpha_k g_k + \beta_k s_k \tag{6.35}$$

and the scalars α and β are yet to be found. The corresponding change of the residual in data space is found by multiplying through with $\mathbf{GF}$. Please do not confuse the gain operator $\mathbf{G}$ with vector g going to vector G in data space.

$$\begin{aligned} \Delta q \quad = \quad S_{k+1} = \mathbf{GF}s_{k+1} \quad &= \quad \mathbf{GF}(\alpha_k g_k + \beta_k s_k) && (6.36)\\ &= \quad \alpha_k \mathbf{GF} g_k + \beta_k \mathbf{GF} s_k && (6.37)\\ \Delta\mathbf{q}(\alpha,\beta) \quad &= \quad \alpha_k G_k + \beta_k S_k && (6.38) \end{aligned}$$

In standard ℓ_2 optimization we had a 2×2 matrix to solve for (α, β). We proceed here in the same way with the hyperbolic penalty function (HPF).

So here we are, embedded in a giant multivariate regression where we have a bivariate regression (two unknowns). From the multivarate regression we are given three vectors in data space, G_i, S_i, and the gained (statistical) residual $\bar{q}_i$. Our next residual will be this perturbation of the old one.

$$q_i \quad = \quad \bar{q}_i \; + \; \alpha G_i \; + \; \beta S_i \tag{6.39}$$

Minimize the average penalty by variation of (α, β)

$$\bar{h}(\alpha,\beta) \quad = \quad \frac{1}{N} \sum_i h(\bar{q}_i + \alpha G_i + \beta S_i) \tag{6.40}$$

Let the coefficients (h_i, h_i', h_i'') refer to a Taylor expansion of $h(r)$ in small values of (α, β) about $\bar{q}_i$. Each residual of each data point has its own Taylor series fitting the hyperbola at its own location. So all residuals that do not move far have a good approximation.

$$\bar{h}(\alpha,\beta) \quad = \quad \frac{1}{N} \sum_i h(\bar{q}_i) \; + \; (\alpha G_i + \beta S_i) h_i' \; + \; (\alpha G_i + \beta S_i)^2 h_i''/2 \tag{6.41}$$

To find both α and β set $d\bar{h}/d\alpha = 0$ and $d\bar{h}/d\beta = 0$:

$$\begin{bmatrix} 0 \\ 0 \end{bmatrix} = \begin{bmatrix} \frac{d\bar{h}}{d\alpha} \\ \frac{d\bar{h}}{d\beta} \end{bmatrix} = \sum_i h_i' \begin{bmatrix} G_i \\ S_i \end{bmatrix} + h_i'' \left\{ \begin{bmatrix} \frac{\partial}{\partial\alpha} \\ \frac{\partial}{\partial\beta} \end{bmatrix} (\alpha G_i + \beta S_i) \right\} (\alpha G_i + \beta S_i) \tag{6.42}$$

This is a set of two equations for α and β. We are now at the stage we were back in Chapter 2 with equation (2.80) but now the sums include weights h_i' and h_i'' to manage the HPF.

$$\left\{ \sum_i h_i'' \left[\begin{pmatrix} G_i \\ S_i \end{pmatrix} (G_i \quad S_i) \right] \right\} \begin{bmatrix} \alpha \\ \beta \end{bmatrix} \quad = \quad - \sum_i h_i' \begin{bmatrix} G_i \\ S_i \end{bmatrix} \tag{6.43}$$

New here is the presence of h' and h''. On the right h'_i is the residual soft clipped. On the left is a familiar sum, formerly unweighted (because $C''_i = 1$), containing factors h''_i weakening the effect of large residuals. As with equation (6.34), the summations in equation (6.43) should include both data space terms and model space terms.

If you have forgotten the inverse of a 2×2 matrix, please refer to equation (2.100). The only difficulties arise when the determinant vanishes, which here is easy (luckily) to understand. Generally the gradient cannot point in the same direction of the previous step if the previous move went the proper distance. Hence the determinant does not vanish because of ill-conditioning. It does vanish when the gradient and previous step are both tending to zero, i.e. when the solution has been already attained. You did more iterations than required, or data and initial model both vanish.

As with steepest descent, after updating $\mathbf{m} \leftarrow \mathbf{m} + \alpha\mathbf{g} + \beta\mathbf{s}$ and updating the residuals, at the new residual location the values of (h_i, h'_i, h''_i) have changed. Thus we repeat to update α and β a second time or more. Don't mess with $\mathbf{s}$ yet! After some iterations we have finished the plane search. It's usually cheap. Now it's time to pay the money (run the operator $\mathbf{F}^*\mathbf{G}^*$) to compute a new $\mathbf{g} = \mathbf{F}^*\mathbf{G}^*\mathbf{h}'(\mathbf{q})$. Now is the time define a new $\mathbf{s}$, how far we moved since the old place. This is the non-linear conjugate direction method. With $h(r)$ being the hyperbola, I call it the HYCD method.

6.3.2 Code for the hyperbolic fitter

The code for the hyperbolic fitter should closely follow that for `cgstep` from Chapter 2. It is easy enough to include the extra weights h' and h'' in the sums. You will need to find a way to input or compute the gain $\mathbf{G}$. What should we call the new solver? A good name might be `hycdstep()` for Hyperbolic Conjugate Direction Stepper.

6.3.3 Measuring success with the hyperbolic measure

I propose the measure of data fitting success be defined by

$$\text{Fitting success} = 1 - \bar{\mathbf{q}} \,/\, \bar{\mathbf{d}} \tag{6.44}$$

The measure of success at solving the normal equations must be measured in model space where our curious expression $\bar{\mathbf{q}}$ is not appropriate. The normal equations say that the fitting functions are orthogonal to the "hyperbolic residual", namely, $\mathbf{0} = \mathbf{F}^*\mathbf{h}'(\mathbf{q})$. Taking the computational success to be measured by the degree of satisfying the normal equations suggests we measure success by

$$\text{Computational success} = 1 - \text{avg}(\mathbf{F}^*\mathbf{G}\mathbf{h}'(\mathbf{q})) \,/\, \text{avg}(\mathbf{F}^*\mathbf{G}\mathbf{h}'(\mathbf{d})) \tag{6.45}$$

but a good question is, "What averaging method should be used in equation (6.45)?" The ℓ_2 norm? Unfortunately, it can be shown it does not lead to monotonic improvement with iteration (even though the fitting residual diminishes monotonically with iteration). Thus it is not an ideal measure of success, never-the-less, for the time being, we will be using it as a measure of success.

6.4 MIGRATION INVERSION

Seismometers cost money so we often fail to have enough of them. This is especially true when theory calls for the 2-dimensional earth surface to be covered with them. In reality there might be tens of thousands on the 2-D surface, but even that is not enough. The simpler example shown here has merely a line of 16 receivers. A scattering point in the earth at (x_0, z_0) creates a spherical wave moving upward to the seismometers. The wave bouncing from the scatterer is an impulse on the surface $t^2 v^2 = (z - z_0)^2 + (x - x_0)^2$. Here the data plane is (t, x) at $z = 0$ and the model plane is (z_0, x_0). An impulse in the model creates a hyperbola in the data plane. Figure 6.3 shows about 8 such hyperbolas observed at about 16 locations. Our goal is to manufacture the artificial data seen on the right side of Figure 6.3. Notice on the sparsely sampled data the implied hyperbola tops are usually missing.

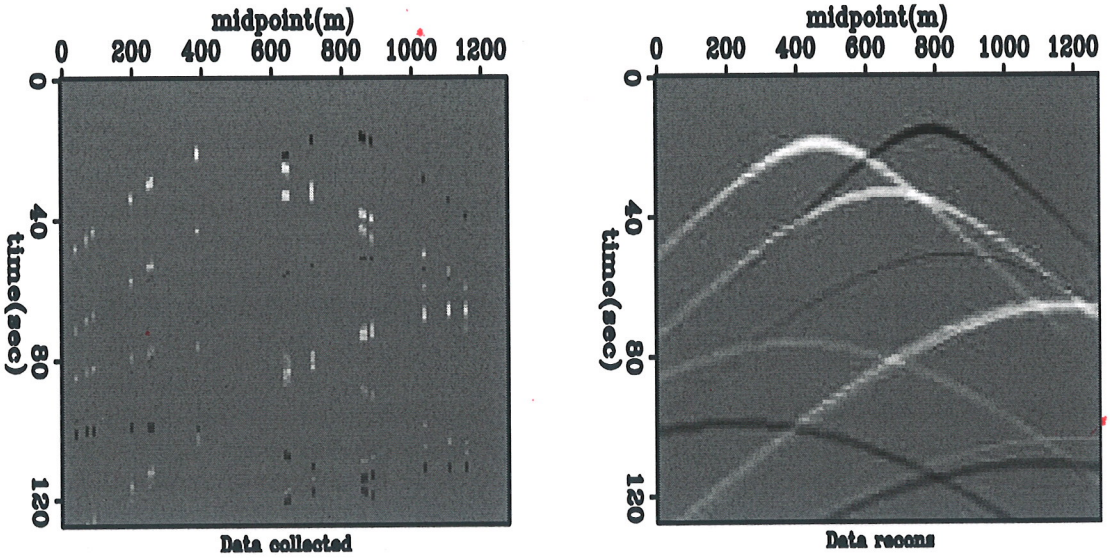

Figure 6.3: Left: Sparse hyperbola data. Right: Reconstructed. noiz/. yangzos

There is some magic here in that a small data space generates a large sharply resolved model space. The method depends critically on the model space containing many zeros. More precisely, model space is mostly small inconsequential values. This is not the place to examine where this assumption would be true in practice. What is important to realize is this: Model space might really be large but sparsely populated (mostly inconsequential values) but in reality we generally do not know where the small values are and where the big values should be. This is where robust fitting can be useful. With least-squares fitting we do not get sparse models in large model spaces without having large data spaces.

Seeing the good results motivates us to examine the theory. Let $\mathbf{H}$ be an operator that copies model impulses into data hyperbolas. (Please do not confuse it with the hyperbolic penalty function (HPF) $H(\mathbf{q})$.) Depending on various details of the definition of $\mathbf{H}$, its adjoint is known in industry as downward continuation or demigration. The example here

is called migration/demigration. The fitting goals are

$$\mathbf{0} \approx_2 \mathbf{q}_d = \mathbf{H}\mathbf{m} - \mathbf{d} \tag{6.46}$$

$$\mathbf{0} \approx_h \mathbf{q}_m = \epsilon\,\mathbf{m} \tag{6.47}$$

where $\approx_2$ denotes parabolic fitting, and where $\approx_h$ denotes hyperbolic fitting. For coding $\approx_2$ is really the same as $\approx_h$ with a large threshold.

When the solution is found, the fitting functions are orthogonal to the soft clipped the residuals. But those residuals have the model space parts. Recall the fitting functions are the rows in the $[\mathbf{H}^*, \epsilon\,\mathbf{I}]$ matrix.

$$\mathbf{0} = \Delta\mathbf{m} = \mathbf{H}^*\mathbf{q}_d + \epsilon\,\mathbf{h}'(\epsilon\mathbf{m}) \tag{6.48}$$

The vanishing gradient $\Delta\mathbf{m}$ is made from two parts which must be identical (but for sign). Ordinarily we might say the final model $\mathbf{m}$ battles the data misfit $\mathbf{H}^*\mathbf{q}_d$, but here we say the soft clip $\mathbf{h}'(\mathbf{m})$ has thrown more of the smaller soldiers into the struggle, more accurately, less of the burden is now borne by the greatest soldiers. In some physical situations it may be said that "the side lobes cannot shirk the task as ℓ_2 had allowed them."

> Ordinarily the model struggles to reduce the data misfit. Soft clipping the model brings more of the population (parts of model space) into the task.

6.5 ESTIMATING BLOCKY INTERVAL VELOCITIES

In seismology measurements are made of the integral through depth of the squared material velocity. This observation is called the RMS velocity V_{RMS}. The goal is to find the velocity as a function of depth which is called the interval velocity $v = v_{\text{int}}$. We begin by presuming that the RMS velocity is measured at a dense uniform sampling of depths. They may be known well at some depths but are measurably poor at most depths. In practice, one would have and would include a weighting function to allow for the variable quality of RMS velocity with depth. By contrast, the interval velocity squared v_{int}^2 is a model space, so we may freely take it to be regularly sampled in depth (actually vertical travel-time depth) that for numerical purposes we have in a vector $\mathbf{u}$. We take the data vector $\mathbf{d}$ to contain depth times V_{RMS}^2. The relation of model to data is simply causal integration $\mathbf{C}$.

The physical expression and the algebraic expression are:

$$\sum_{i=1}^{k} v_i^2 = kV_k^2 \tag{6.49}$$

$$\mathbf{C}\mathbf{u} = \mathbf{d} \tag{6.50}$$

Because the RMS velocities are noisy we must add a regularization. Here we choose that to be the depth derivative $\mathbf{D}_z$. In algebraic form we have what is called the Dix problem:

$$\mathbf{0} \approx_h \mathbf{q}_d = \mathbf{G}_d(\mathbf{C}\mathbf{u} - \mathbf{d}) \tag{6.51}$$

$$\mathbf{0} \approx_h \mathbf{q}_m = \epsilon\,\mathbf{G}_m\mathbf{D}_z\mathbf{u} \tag{6.52}$$

A barrel of issues are hidden in the two gains, $\mathbf{G}_d$ and $\mathbf{G}_m$. Required filtering is done by $\mathbf{D}_z$ so $\mathbf{G}_m$ is simply a gain, not a filter. The gain would be such as to first bring components $\mathbf{q}_m$ up to a level about unity. This is the ℓ_1/ℓ_2 threshold. This might be done by dividing the data by the value of some chosen quantile. In other words if you wanted half the gained residuals in the ℓ_1 zone you would divide the residuals by their median. Then, in a manner remniscent of ϵ, the gain was adjusted for a suitable number of blocks in the solution. $\mathbf{G}_d$ is also a gain, not a filter. When the analyst has reliable external information about data quality $\mathbf{G}_d$ would function like the usual weighing function. Where the data quality has large unexpected errors the hyperbolic penalty can catch them. The analyst has three scales to monkey with, that of $\mathbf{G}_d$, $\mathbf{G}_m$, and ϵ. What rationale for ϵ? I don't know.

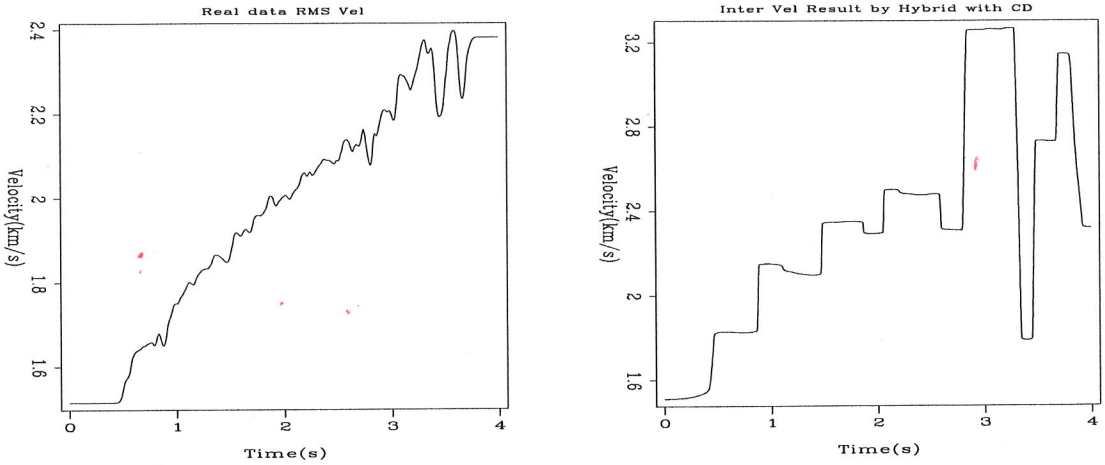

Figure 6.4: Left: Input RMS velocity. Right: Output interval velocity, blocky as desired. (thanks to Elita) noiz/. blockyvel

The input RMS velocity is in the left panel of Figure 6.4. Irregularities on this function result from noises in the measurement process. The oscillations at late time are violent. They may not look large, but the negative swings imply a negative v^2_{interval} which means an imaginary velocity! This violent behavior results from the impossibility of making measurements this precise. Hyperbolic penalty aids overcoming this large error.

Rock velocity may vary continuously with depth, or rocks may come in fairly homogeneous layers. In the layered case, we say the desired model is "blocky" so its derivative $\mathbf{D}_z\mathbf{u}$ has spikes. The hyperbolic penalty function (HPF) allows those spikes while the usual parabolic penalty function suppresses them. What we are demonstrating on the right side of Figure 6.4 is that using the HPF enables us to obtain blocky velocity models.

6.6 DEFEATING NOISE AND SHIP TRACKS IN GALILEE

The Sea of Galilee data set exhibits a great number of the problems encountered in real life. It's a blessing to learn from. Only 132,044 pings give rise to its 132,044 depth measurements. If this were reflection seismology we would have that many 1000 point seismograms at 1000 receivers, a million times more data! Students have asked, "Why don't we just hand edit out the bad data points?" The answer is we need an easy warm up for real life when there is

far too much data to hand edit. In other words, we wish to think about theories and codes that work when transported to other environments. The Galilee data set is a marvelous practice case. There is much to learn here.

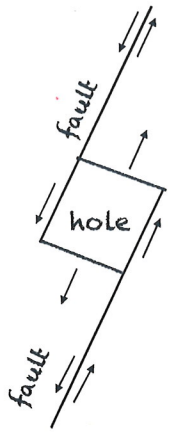

Figure 6.5: Geologist view of the Sea of Galilee. This lake is below sea level. Here is the reason. Regional **faults** continuing southward into Africa are "left lateral" (standing on either side you see the other side moving left). Perhaps in Figure 6.13 you see lines such as these.
noiz/. gfault

Although the Sea of Galilee is a fresh-water lake, it is below sea-level. It seems to be connected to the Great Rift (pull-apart) valley crossing East Africa. The ultimate goal is to produce a good map of the depth to bottom, and images useful for identifying archeological, geological, and geophysical details of the water bottom. In particular, we hope to identify some ancient shorelines around the lake and meaningful geological features inside the lake. The ancient shorelines might reveal early settlements of archeological interest or old fishing ports. The pertinence of this data set to our daily geophysical applications is four fold: (1) We often need to interpolate irregular data. (2) The data has noise bursts of various types. (3) The data has systematic error (drift) which tends to leave data-acquisition tracks in the resulting image. (4) Results invite an extended model, but that introduces a difficult null-space problem.

The Galilee data set was introduced in Chapter 3 and recently plotted in Figure 3.10. Actually, that figure is a view of 2-D model space. One of the first things I learned (the hard way) is the importance of viewing all four of the model space, the data space, and the residuals in both spaces. Data space is often larger and more difficult to view than model space, but in this study it was the key to understanding basic physical phenomena.

> Be sure to plot data and residuals in both model space and data space. You might learn from movies of each as iteration progresses.

The raw data (Figure 6.6), is distributed irregularly across the lake surface. It is 132,044 triples (x_i, y_i, z_i), where x_i ranges over about 12 km, where y_i ranges over about 20 km, and z_i is depth in multiples of 10 cm up to about 43 meters. The 10 cm suggests a sense of the measurement accuracy. The ship surveyed a different amount of distance every day of the survey. Figure 6.6 displays the whole survey as one long track. On one traverse across the lake, the depth record is U shaped. A few V shaped tracks result from deep-water vessel turn arounds. All depth values (data points) used for building the final map are shown here. Each point corresponds to one depth measurement inside the lake. In Figure 6.6 the

long signal is broken into 23 strips of 5718 depth measurements ($23 \times 5718 = 131,514$). We have no way to know that sometimes the ship stops a little while with the data recorder running; sometimes it shuts down overnight or longer; but mostly it progresses at some unknown convenient speed. So the horizontal axis in data space is a measurement number that scales in some undocumented way to distance along some unknown track.

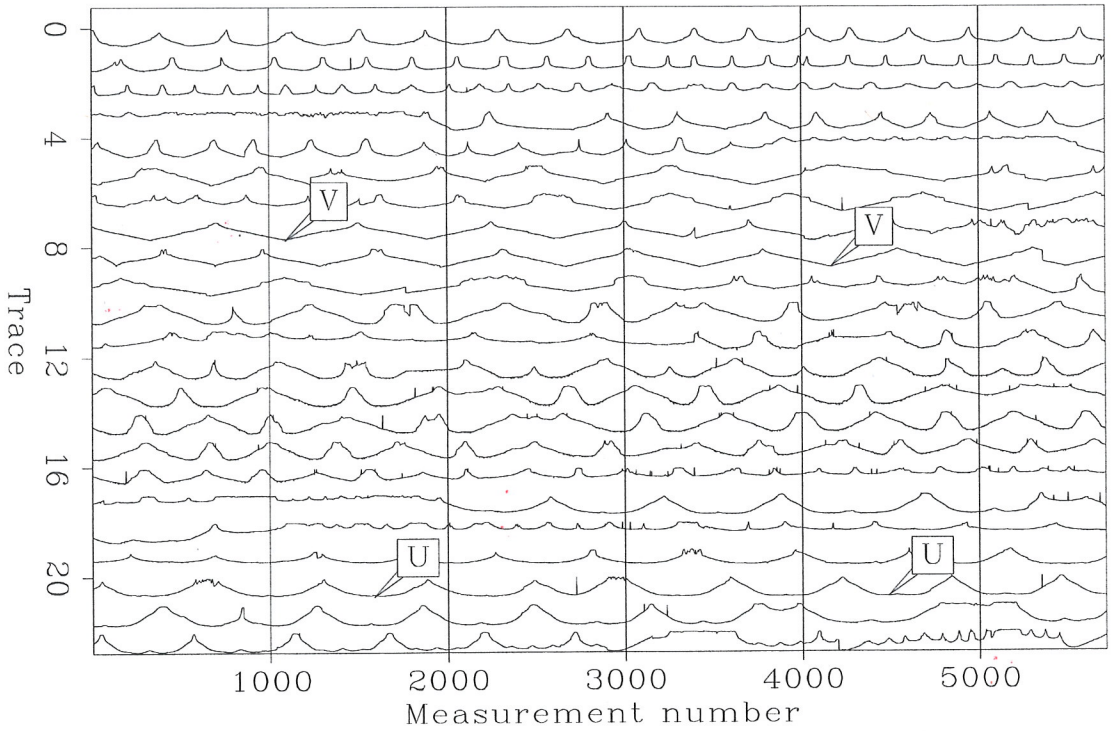

Figure 6.6: The complete Galilee data space. VIEW noiz/. antoine1

6.6.1 Attenuation of noise bursts and glitches

Let $\mathbf{m}$ be an abstract vector containing as components the water depth over a 2-D spatial mesh. Let $\mathbf{d}$ be an abstract vector whose successive components are depths along the vessel tracks shown in Figure 6.6. One way to grid irregular data is to minimize the length of the residual vector $\mathbf{r}_d(\mathbf{m})$:

$$\mathbf{0} \quad \approx \quad \mathbf{r}_d \quad = \quad \mathbf{G}\mathbf{m} \; - \; \mathbf{d} \tag{6.53}$$

where $\mathbf{G}$ is a geography operator, the adjoint of binning or linear interpolation, the operator that copies data from a 2-D map to a 1-D data survey track. Here $\mathbf{r}_d$ is the data residual, the modeled data less the observed data. Because we are defining $\mathbf{G}$ and not its inverse we need not concern ourselves that bins may be empty or tracks may cross inconsistently.

Some model-space bins will be empty. For them we need an additional "model styling" goal, i.e. regularization. For simplicity we might minimize the gradient.

$$\begin{array}{lllll} \mathbf{0} & \approx & \mathbf{r}_d & = & \mathbf{G}\mathbf{m} \; - \; \mathbf{d} \\ \mathbf{0} & \approx & \mathbf{r}_m & = & \epsilon \, \nabla \mathbf{m} \end{array} \tag{6.54}$$

where $\nabla = \left(\frac{\partial}{\partial x}, \frac{\partial}{\partial y}\right)$ and $\mathbf{r}_m$ is the model space residual. Choosing a large scaling factor ϵ will tend to smooth our entire image, not just the areas of empty bins. We would like ϵ to be any number small enough that its main effect is to smooth areas of empty bins. When we get into this further we'll see that because of noise some smoothing across the nonempty bins is desirable too.

6.6.2 Preconditioning for accelerated convergence

As usual we precondition by changing variables so that the regularization operator becomes an identity matrix. The gradient ∇ in equation (6.54) has no inverse, but its spectrum $-\nabla^* \nabla$, can be factored ($-\nabla^* \nabla = \mathbf{A}^* \mathbf{A}$) into triangular parts $\mathbf{A}$ and $\mathbf{A}^*$ where $\mathbf{A}$ here is typically the helix derivative of Chapter 4. This $\mathbf{A}$ is invertible by deconvolution. The quadratic form $\mathbf{m}^* \nabla^* \nabla \mathbf{m} = \mathbf{m}^* \mathbf{A}^* \mathbf{A} \mathbf{m}$ suggests the new preconditioning variable $\mathbf{p} = \mathbf{A}\mathbf{m}$. The fitting goals in equation (6.54) thus become

$$\begin{aligned} \mathbf{0} &\approx \mathbf{r}_d = \mathbf{G}\mathbf{A}^{-1}\mathbf{p} - \mathbf{d} \\ \mathbf{0} &\approx \mathbf{r}_p = \epsilon \mathbf{p} \end{aligned} \tag{6.55}$$

with $\mathbf{r}_p$ the residual for the new variable $\mathbf{p}$. Experience shows that an iterative solution for $\mathbf{p}$ converges much more rapidly than an iterative solution for $\mathbf{m}$, thus showing that $\mathbf{A}$ is a good choice for preconditioning. We could view the estimated final map $\mathbf{m} = \mathbf{A}^{-1}\mathbf{p}$, however in practice because the depth function is so smooth, we usually prefer to view the roughened depth $\mathbf{p}$ which we call "the image."

There is no simple way of knowing beforehand the best value of ϵ. What we have done here is described at equation (5.47) in Chapter 5 as "faking the epsilon," namely, we set $\epsilon = 0$ doing about 50 iterations without it.

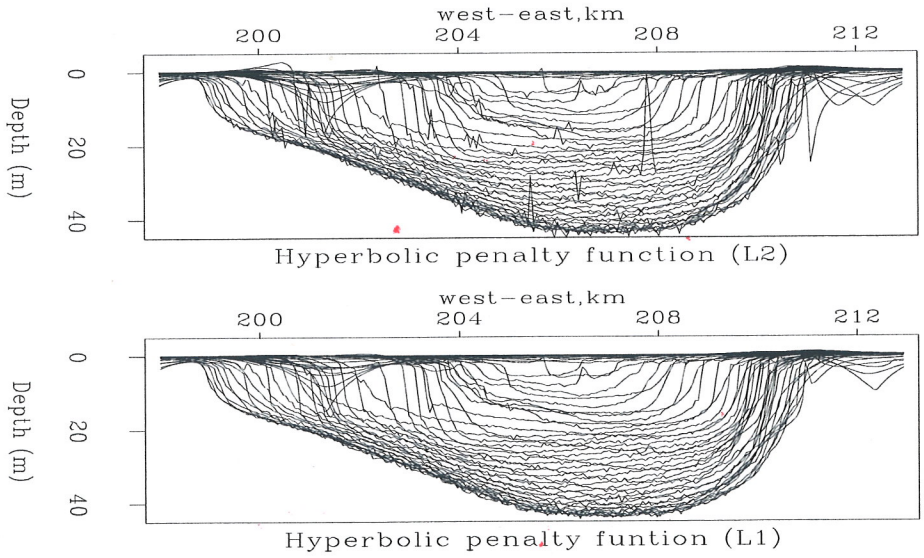

Figure 6.7: Several east-west cross sections of the lake bottom ($\mathbf{m} = \mathbf{A}^{-1}\mathbf{p}$). Top with the ℓ_2 solution. Bottom with the hyperbolic penalty. VIEW noiz/. antoine3

Figure 6.7 shows the bottom of the Sea of Galilee ($\mathbf{m} = \mathbf{A}^{-1}\mathbf{p}$) with ℓ_2 fitting (top) and hyperbolic fitting (bottom). Each line represents one east-west transect, transects at half-kilometer intervals on the north-south axis. Our new robust fitting with the hyperbolic penalty is a nice improvement over the ℓ_2 maps. The glitches inside and outside the lake have mostly disappeared.

Although not visible everywhere in all the figures, topography is produced outside the lake. Indeed, the effect of regularization is to produce synthetic topography, a natural continuation of the lake floor surface.

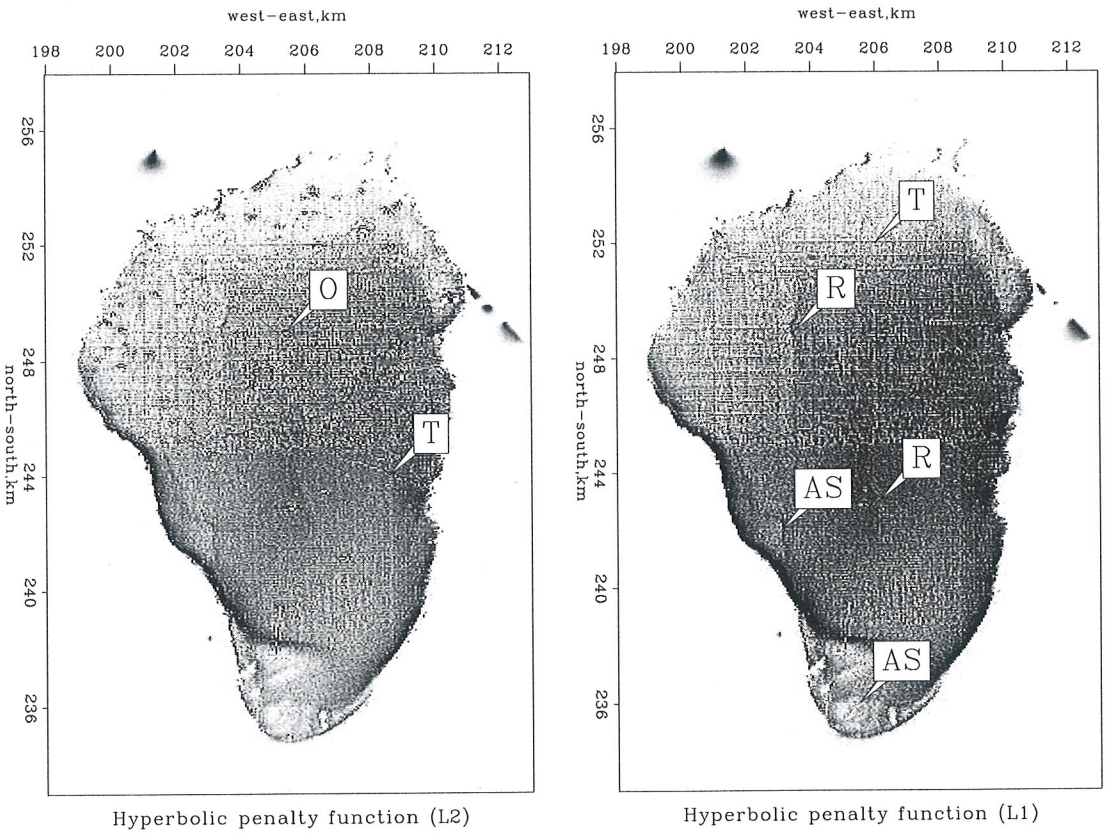

Figure 6.8: Estimated $\mathbf{p}$ with ℓ_2 norm (left) and with hyperbolic penalty (right). Pleasingly, isolated spikes are attenuated. Some interesting features are shown by the arrows: AS points to few ancient shores, O points to some outliers, T points boat tracks, and R points to a curious feature. Data outside the lake asserts sporadic track location errors suggesting there may be a few such tracks inside the lake that are not readily apparent. A stray data point outside the lake has sprayed into the response of the inverse helix derivative. VIEW noiz/. antoine2

Figure 6.8 displays $\mathbf{p}$ estimated by least-squares on the left, and by hyperbolic penalty the right. Introducing the hyperbolic penalty has removed most of the isolated bursts. Some ancient shorelines in the western and southern parts of the Sea of Galilee are now easier to identify (shown as AS). We also start to see a valley (or fault?) in the middle of the lake (shown as R). Data acquisition tracks are ~~mostly~~ primarily north-south lines and east-west

lines. They are even more visible after the suppression of the outliers.

6.6.3 Abandoned strategy for eliminating ship tracks

Figure 6.8 shows that vessel tracks could overwhelm fine scale details. Next we investigate a strategy based on the idea that the inconsistency between tracks comes mainly from different human and seasonal conditions during the data acquisition. Since we have no records of the weather and the time of the year the data were acquired we presume that the depth differences between different acquisition tracks must be small and relatively smooth along the super track (track of all tracks).

The unsuccessful strategy to remove the ship tracks was to filter the residual as follows:

$$\begin{array}{rcccl} \mathbf{0} & \approx & \mathbf{r}_d & = & \frac{d}{ds}(\mathbf{G}\mathbf{A}^{-1}\mathbf{p} - \mathbf{d}) \\ \mathbf{0} & \approx & \mathbf{r}_p & = & \epsilon\,\mathbf{p}, \end{array} \tag{6.56}$$

where $\frac{d}{ds}$ is the derivative along the track. The derivative removes the drift (surface elevation?) from the field data (and the modeled data). An unfortunate consequence of the track derivative is that it creates more glitches and spiky noise at the track ends and at the bad data points. Several students struggled with this idea with results like you see in Figure 6.9.

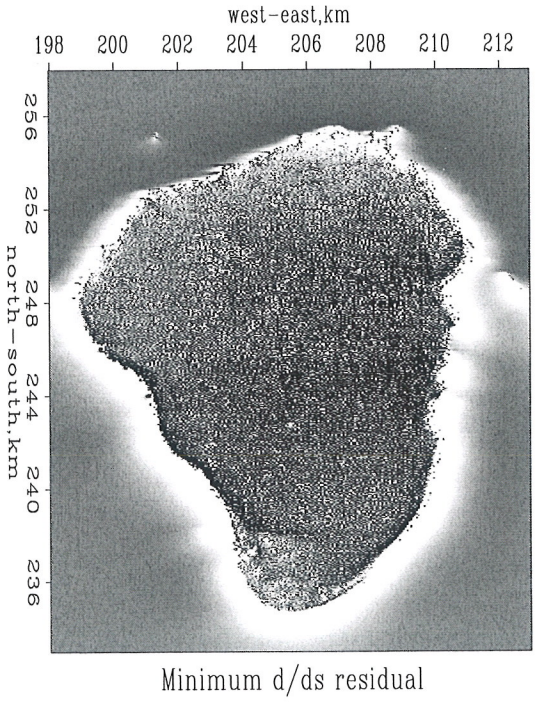

Figure 6.9: The result of minimizing the derivative along the tracks.
VIEW noiz/. antoine8

The operator $\frac{d}{ds}$ is too simple a lowcut filter. We have boosted all the high (spatial) frequencies in the residual when all we really sought to do was to remove the very low frequencies, almost zero frequency. Recall the low-cut filters from Chapter 2. These are filters that would remove only low frequencies leaving higher frequencies alone. Such filters are a positive impulse of unit area accompanied by a long negative blob, also of unit area.

The longer the blob, the narrower the low cut filter. Unfortunately, the longer the blob, the more nasty spikes it will catch. After low-cut filtering, the noise bursts would affect a greater percentage of track.

We are in a dilemma. We need to low cut filter to eliminate the drift from the problem, but we don't dare low cut filter because it will smear spike noise out to a much larger region. The dilemma is resolved by expanding our model space to include the drift.

> When a signal of a sensible spectrum (either signal or noise) contains noise bursts, it cannot be filtered; it must be modeled. Modeled noise can then be subtracted.

6.6.4 Understanding the residuals

Examining the discrepancy between observed data and modeled data offers us an opportunity to discover what our data contains that our model does not. It is important to examine both the residual itself $\mathbf{r}$ and the residual in model space $\mathbf{G}^*\mathbf{r}$. Figure 6.10 shows the fitting residuals brought back into model space $\mathbf{G}^*\mathbf{r}$. We are disappointed to see so much noise around the periphery of the lake, the most likely location of historic disturbance. We would like to understand that. We see more noise in the northern half of the lake. That will be easier to understand.

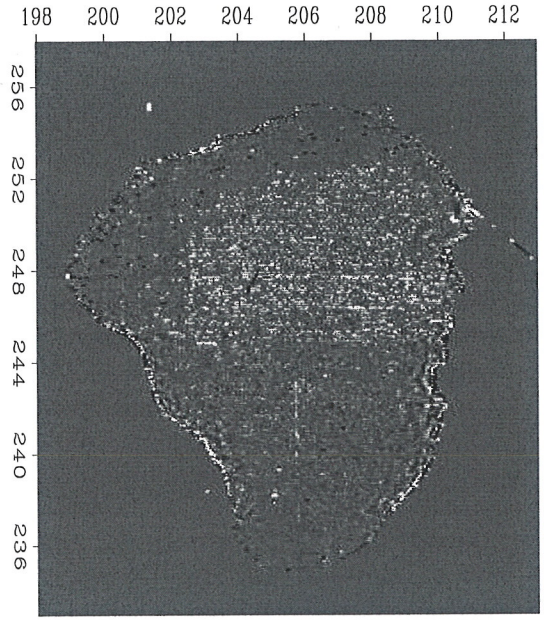

Data residual in model space

Figure 6.10: Fitting residuals brought back into model space $\mathbf{G}^*\mathbf{r}$. Notice short white horizontal streaks in the north in the deep water. VIEW noiz/. antoine7gr

Figures 6.11 and 6.12 show selected segments of data space. In each figure the top plot is the input data $\mathbf{d}$. Next is the estimated noise-free data $\mathbf{GH}^{-1}\mathbf{p}$. Finally the residual $\mathbf{r}_d$ after a suitable number of iterations. The modeled data in Figure 6.11 shows no remaining spikes.

Compare Figure 6.11 showing noise in the south with Figure 6.12 showing noise in the north. Perhaps in the north the depth sounder has insufficient power for deeper water or

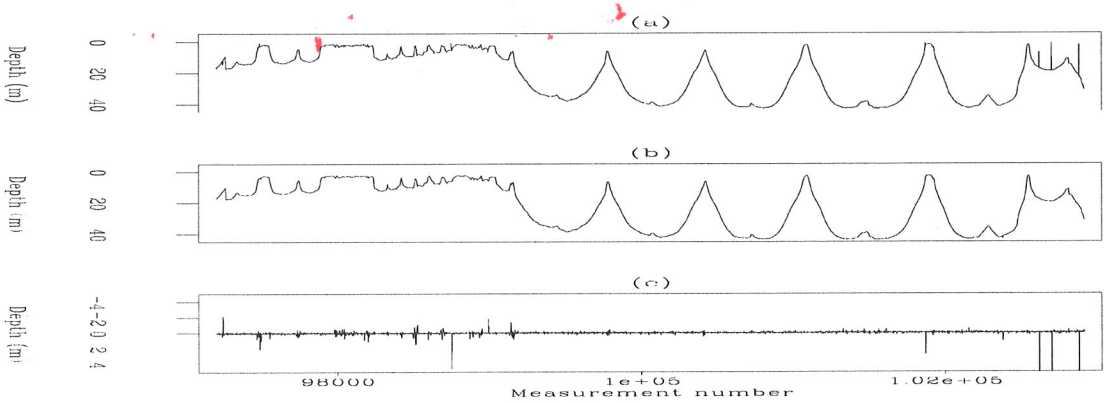

Figure 6.11: Roughly 10% of the complete data space. (a) Track 17 (input data in the south) in Figure 6.6. (b) The estimated noise-free data $\mathbf{GA}^{-1}\mathbf{p}$. (c) Data residual $\mathbf{r}_d$. VIEW noiz/. antoine5abd

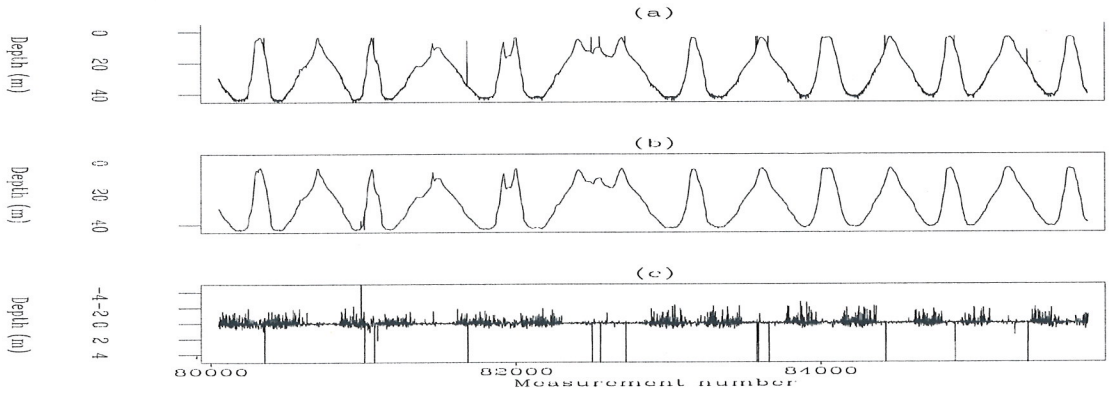

Figure 6.12: Residuals in the north, otherwise like Figure 6.11 VIEW noiz/. antoine6abd

for softer sediments that might be found in northern water. The northern residual (Figure 6.12) is curiously non-symmetric in polarity. This corresponds to the sparse streaks that are white (but not black) in Figure 6.10 in deep water. For Gaussian random noise, there will be equal energy in positive errors as in negative errors. That's clearly not the case here. Since the hyperbolic penalty behaves somewhat like the ℓ_1 norm, we notice that a median can have larger variance on one side of zero than on the other. The plot shows that the larger residuals are up (negative values). If we take the modeled data $\mathbf{Gm}$ to be correct and the observed data wrong, $\mathbf{r} = \mathbf{Gm} - \mathbf{d} < \mathbf{0}$ says the large measured depths $\mathbf{d}$ are exceeding the real depth $\mathbf{Gm}$. Depth is measured from a seismogram by measuring travel time to the first strong return. A good explanation is this: When the outgoing signal is not strong or the water bottom is soft, the first perceived echo return may be later than the weaker first arrival. The instrument, not seeing the signal until later, reports the water deeper than it really is.

We notice the white streaks on east-west traverses only, not the north-south traverses. Perhaps east-west traverses were done with a faster boat causing more noise.

6.6.5 Spikes in the model space!

Looking carefully at Figure 6.12 we discover a spike in the modeled data! Other track regions not shown show many more, some much bigger. Why does the theoretical data contain spikes? The misplaced data tracks outside the lake suggest there may be misplaced tracks inside too. Data values on a misplaced track have a consistent systematic error not as easily dealt with as suppressing isolated spikes. A string of bad data points on a track can locally overwhelm a crossing good track. How can we fight back? When we see a continuous string of high residuals we have evidence of a misplaced track. Those strings of residuals tell us to build a weighting function that is perhaps the inverse of smoothed residuals. This task is being left for a student exercise. Perhaps the smoothing need be only a short window. Perhaps a suitable weighting function would be the inverse of quantity 10 cm plus the residual magnitude.

6.6.6 Dealing with acquisition tracks in the image

Having a preliminary map image of the Galilee water bottom and seeing data acquisition tracks in it, the most obvious hypothesis is that the water surface level was not properly corrected. The data donor assured us it was, but the tracks seem to tell us otherwise. Consumption, irrigation, rain, other factors could play a role in apparent surface level fluctuation during the survey, a survey that took many months, perhaps many seasons. It might have been helpful had the measurements included day and time of day, but they did not.

There are hypotheses other than water level for tracks in the image. Perhaps the speed or the loading of the recording boat is an issue. Perhaps accuracy of navigation is an issue. We seek now to understand the best-fitting surface variation and to model it appropriately in hopes of best removing survey tracks from the bottom image.

We model the water surface elevation by $e(t) = \mathbf{e}$. Physical functions are smooth, both the model map $m(x, y) = \mathbf{m}$ and the surface elevation $\mathbf{e}$. For regularization $\mathbf{m}$ is roughened

with the operator $\mathbf{A}$, typically a helix derivative, and $\mathbf{e}$ is roughened with a low-cut filter, typically $\mathbf{L}^{-1}$ where $\mathbf{L}$ is leaky integration.

$$\mathbf{0} \approx_m \mathbf{Gm} + \mathbf{e} - \mathbf{d} \tag{6.57}$$
$$\mathbf{0} \approx_2 \mathbf{Am} \tag{6.58}$$
$$\mathbf{0} \approx_2 \mathbf{L}^{-1}\mathbf{e} \tag{6.59}$$

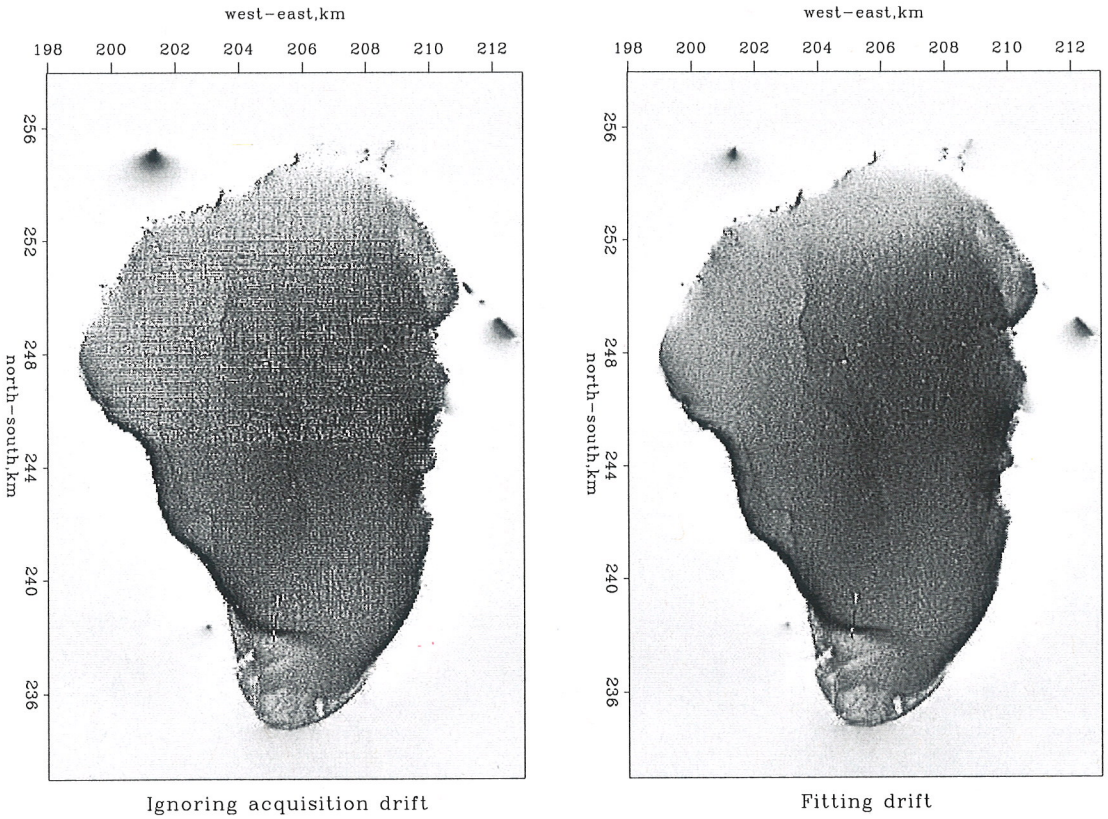

Figure 6.13: LEFT: Estimated $\mathbf{p}$ without track suppression. RIGHT: Estimated $\mathbf{p}$ modeling tracks to eliminate them. VIEW noiz/. antoine4

Next precondition by transforming to rough variables. Let the bottom image be $\mathbf{p} = \mathbf{Am}$. Define a white noise variable $\mathbf{n}$ so that the elevation drift is $\mathbf{e} = \mathbf{Ln}$.

We need two epsilon scale factors for the two regularizations. It matters a lot what their ratio is between the two epsilons because it amounts to the choice of how much of the data to push into $\mathbf{m}$ versus $\mathbf{e}$. Unfortunately the data itself seems not to tell us that. That choice is forced upon us. For convenience we choose both epsilons ϵ the same thus pushing the actual epsilon ratio into a scaling factor λ which we may regard as scaling either $\mathbf{L}$ or $\mathbf{n}$.

$$\mathbf{0} \approx_h \mathbf{GA}^{-1}\mathbf{p} + \lambda\mathbf{Ln} - \mathbf{d} \tag{6.60}$$
$$\mathbf{0} \approx_2 \epsilon\,\mathbf{p} \tag{6.61}$$
$$\mathbf{0} \approx_2 \epsilon\,\mathbf{n} \tag{6.62}$$

Structuring this as a matrix :

$$\mathbf{0} \quad \approx \quad \begin{bmatrix} \mathbf{GA}^{-1} & \lambda\mathbf{L} \\ \epsilon\mathbf{I} & \cdot \\ \cdot & \epsilon\mathbf{I} \end{bmatrix} \begin{bmatrix} \mathbf{p} \\ \mathbf{n} \end{bmatrix} \tag{6.63}$$

we readily recognize the gradient :

$$\begin{bmatrix} \Delta\mathbf{p} \\ \Delta\mathbf{n} \end{bmatrix} \quad = \quad \begin{bmatrix} (\mathbf{GA}^{-1})^T & \epsilon\mathbf{I} & \cdot \\ \lambda\mathbf{L}^T & \cdot & \epsilon\mathbf{I} \end{bmatrix} \begin{bmatrix} h'(\mathbf{r}_d) \\ \epsilon\,\mathbf{p} \\ \epsilon\,\mathbf{n} \end{bmatrix} \tag{6.64}$$

where $h'(\mathbf{r}_d)$ is the soft clipped data residual.

As described at the end of the preconditioning chapter, Chapter 5, we began here with $\epsilon = 0$. We soon had a pleasing image of the water bottom $\mathbf{p}$ without tracks shown in Figure 6.13. Hooray! Figure 6.13 shows this model enhancement leading to a track-free map.

Although we had a good looking map image in Figure 6.13 the two parameters λ and the decay length in the leaky integration operator $\mathbf{L}$ could not be chosen to lead to a plausible elevation $\mathbf{e}$. This cast doubt upon the image. What was unacceptable about $\mathbf{e}$ is that it came out too big, and it strongly mimicked the raw data $\mathbf{d}$. This is bogus. The concept of this bad result is shown in Figure 6.14 while we see it in the data analysis in Figure 6.15. It says the surface water in the middle of the lake is about a meter higher than at the shoreline! The data measures the separation of the bottom of the lake from its top. Most of the data went into the bottom while the remainder went into the top.

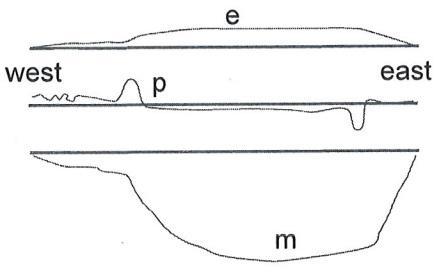

Figure 6.14: For a single lake crossing we see the problem to be overcome that the surface elevation $\mathbf{e}$ falsely grows with the depth $\mathbf{m}$. Some of the data $\mathbf{d}$ that should have gone into $\mathbf{m}$ has gone into $\mathbf{e}$. The depth image is the roughened model $\mathbf{p}$. The image $\mathbf{p}$ is the roughened depth model $\mathbf{m}$. VIEW noiz/. mep

6.6.7 Defeating a null-space with a wise starting guess

After some years of frustration we solved the bulging-surface problem. We first fit the data without a surface model. To do that we used the full-blown theory above, but with $\lambda = 0$. After that we activated λ. This worked. Hooray! The theoretical basis for this technique is

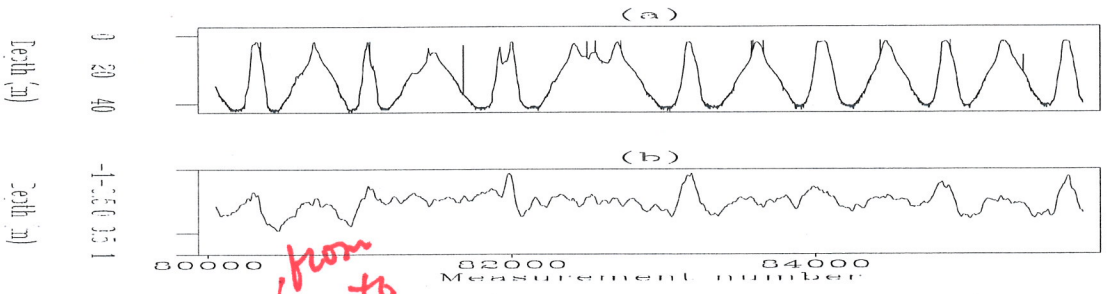

Figure 6.15: Bogus water surface. Water surface curve (b) mimics water depth (a). The water level **e** in the middle of the lake cannot possibly be a meter higher than near the shore. Depth ranges over 0-40m. The surface is mostly negative near shorelines averaging about a half meter. Alternately, the surface is zero on shorelines and positive almost a meter in the middle of the lake. VIEW noiz/. antoine6

explained towards the end of Chapter 5. This useful technique did not evolve from theory but arose from the struggle with this real data!

> Regularization is not the only way to manage a null space. Choosing your initial solution carefully can do it too.

6.6.8 Understanding the derived surface elevation

The water surface **e** was coming out far too rough for realistic water level fluctuations. One way to make it smoother is to lengthen the lag in the leaky integration, but this aggravates the tracks-in-the-image problem. Another way to smooth it is by replacing $\mathbf{L}$ with $\mathbf{L}^*\mathbf{L}$. The impulse response of $\mathbf{L}$ and of its autocorrelation $\mathbf{L}^*\mathbf{L}$ have about the same length implying the same spectrum, but their spectra are very different. The decaying exponential response in $\mathbf{L}$ has a sharp step onset which must have high frequency that the autocorrelation does not. The amplitude spectrum of $\mathbf{L}$ is $1/\sqrt{\omega_0^2+\omega^2}$ while that in $\mathbf{L}^*\mathbf{L}$ is its square. After ω_0 the square drops off much faster. Switching to $\mathbf{L}^*\mathbf{L}$ made the tracks worse, but it had the side benefit that it changed our way of viewing **e**. Serendipity! Formerly we had plotted **e** as on Figure 6.11 but with it being much smoother we were at last inspired to plot it as a single line across the width of the page. It is shown in Figure 6.16.

Figure 6.16 has much to tell us. Before seeing it we had imagined step functions, the boundaries separating the epochs of soundings. Or perhaps the load in the boat being changed or shifted. We do see step discontinuities in Figure 6.16, but the function value between them is far from constant. Some of the blocks are ramp-like. It takes a long time to survey a lake this size. How many days did the survey take, and how much change in water level is reasonable? Let's make some guesses. Depth sounders do not work well from a speeding boat. A reasonable speed would be 8 km/hour. We see hundreds of tracks crossing this 20 km long lake. The ramp-like blocks could correspond to correct water depth calibration somewhere on the block, but with significant water level drift during that surveying epoch.

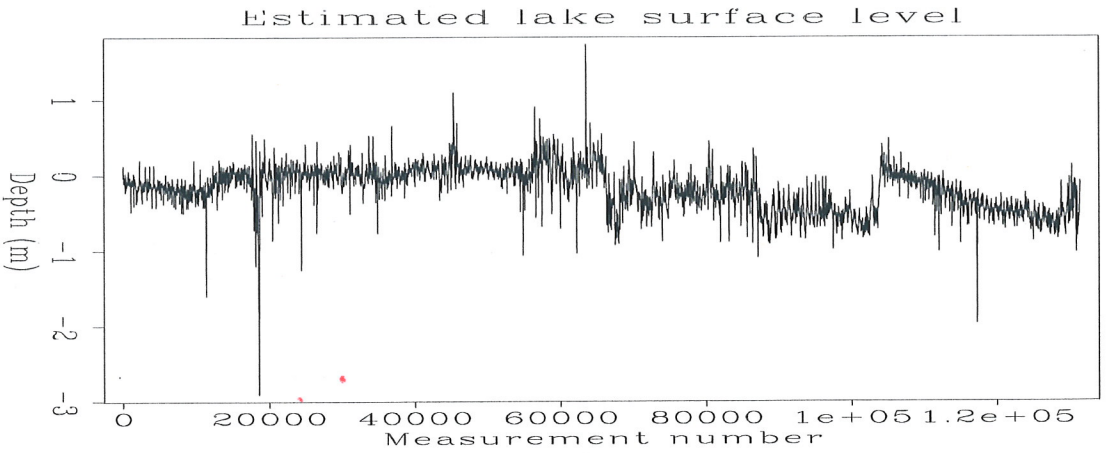

Figure 6.16: Apparent surface elevation of the entire data set. Notice the scale. Recall measurement nominal precision is 10 cm = 1/10 meter. VIEW noiz/. tide

Measurements came in integer multiples of 10 cm. It may seem surprising that we observe **e** apparently at that precision or even better. The many independent measurements may be doing their job in canceling the ±5 cm discretization noise.

Spikes in Figure 6.16 might represent short sections of track that are mispositioned. We are expecting students to fix that by weighting residuals inversely with their variance.

Figure 6.16 also contains short wavelengths. Short on this scale means comparable in length to a lake crossing. Of course this is annoying. These short wavelengths may be the annoying correlation with the geography seen earlier. Their amplitude is only about 20cm which is not large compared with the nominal measurement accuracy of 10cm or the 40 meter depth of the lake.

Wind can move lake water from one shore to the opposite supporting altitude variations on this scale. I do not see how to identify such a model with the available information.

6.6.9 Interpreting model-space residuals and tracks

From an archeological perspective the most interesting part of the lake would be its near shoreline, those locations affected by human habitation. Unfortunately Figure 6.17 shows our greatest measurement difficulties occur along the shoreline. Figure 6.17(left) shows the data residual in model space. We imagine this being random (white) in both data space and model space. The most striking feature is a noisy rim around the lake. I had predicted a systematic surface error elevation error on the shoreline track. Figure 6.17(right) does confirm that error, but the modeling now includes the surface and the depth. Even with both models the shoreline residuals dominate the survey residuals. Perhaps the larger noise on the shoreline is caused the mechanics of slowing, stopping, and turning the vessel. Or maybe the shoreline noise results from irregularity in bottom vegetation.

Additionally we notice the residual is smaller in the southern half of the lake. Perhaps that part of the survey was done with better equipment or in better environmental condi-

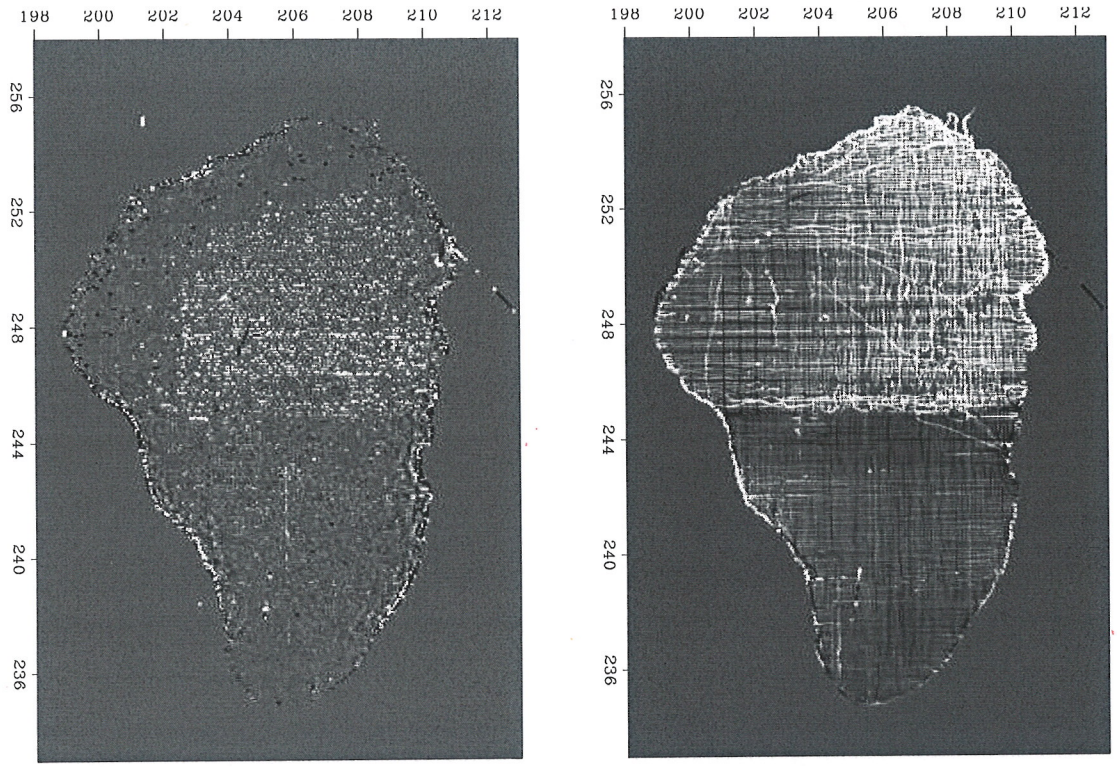

Figure 6.17: LEFT: Data residual brought back into model space $\mathbf{G}^*\mathbf{r}_d$ shows measurement inconsistency near the shoreline and also an interesting haze of white speckles or short horizontal lines. RIGHT: Surface elevation $\mathbf{e}$ brought back into model space $\mathbf{G}^*\mathbf{e}$. Northern and southern lake halves evidently used different equipment. Although much is clear on this fascinating figure, much is without explanation. Especially the large regional elevation, white to the upper right is unexplained. VIEW noiz/. antoine7

tions. An interesting feature of the residual in the northern half of the lake is the haze of short white streaks in the deeper water. The explanation for these was suggested by Figure 6.12. Oddly, they mostly run east-west.

Figure 6.17(right) shows the transformation of elevation $\mathbf{e}$ to model space $\mathbf{G}^*\mathbf{e}$. Mostly what we see is evidently ship tracks. In the northern half of the lake we particularly notice what seems to be a superposition of a sparse survey with a dense one. We do not wish to see hints of geography in this space, and I do not see any. There are prominent geographic features but they should be explainable by surveying operational issues we can only guess at.

Tracks might be explained not only by water level fluctuation but by navigation errors. This data was recorded in the early 1990s before modern GPS navigation. The tracks outside the lake attest to episodic navigation errors. That being so, we must expect episodic track misplacement within the lake. The tiny remaining short tracks in the lake image Figure 6.13 might be explainable that way. This suggests the time has come to cut off our efforts at fully understanding the derived surface model.

A few other miscellaneous things appear to be happening. We plotted the distance between successive measurement locations. Normally this is some reasonable number of tens of meters but it occasionally it is a kilometer or more. This may sometimes have a valid operational explanation, but we have noticed that it is often associated with residual spikes. That is motivation for a weighting function to vanish at such track ends. I believe there is one place in the lake where the boat made many measurements while not moving, but I do not recognize the implications.

6.6.10 Lessons learned from Galilee

It is common for geophysical data to be made up additively from two or more models. For example, two kinds of rock anisotropy imply seismic data affected by two grids, one grid of each kind. The relationship may be nonlinear, but to first order, Taylor series will linearize it. The model-to-data operator $\mathbf{F} = [\mathbf{A}\ \mathbf{B}]$ is a row. What are the general principles teaching us how to estimate those two model images? Is their apparent correlation physical or statistical, real or apparent? We can thank Galilee for delivering us this comprehensible example of a deep, wide-ranging problem, and for teaching us that we do not fully understand it.

It took me twenty years to pull this story together. Any tricks here to help a struggling seismologist? Reflection seismologists are buried in problems even more subtle with much more very high quality data. Better go back, read here again to see if skills and tricks learned in this supposedly easy study might help them.